The University Of Sheffield.

EXPANDING MOLECULAR TOOLS FOR THE METABOLIC ENGINEERING OF *RALSTONIA EUTROPHA* H16

By:

ABAYOMI OLUWANBE JOHNSON

A thesis submitted in partial fulfillment of the requirements for the degree of Doctor of Philosophy

The University of Sheffield
Faculty of Engineering
Department of Chemical and Biological Engineering

July 2018

(This page has been left blank intentionally)

DECLARATION

This thesis is a product of original research conducted by me as a PhD student at the Department of Chemical and Biological Engineering, University of Sheffield. All sources of information herein have been duly referenced. This thesis, in its entirety, has never been previously submitted at this University or any other institution.

This thesis is written in conformance to the rules of Alternative Format Thesis (Code Of Practice For Research Degree Program 2017-18) of the University of Sheffield. Some parts of this thesis have been previously published/submitted as peer-reviewed scientific publications.

ASSOCIATED PUBLICATIONS

- Johnson, A. O., Gonzalez Villanueva, M., & Wong, T. S. (2015). Engineering *Ralstonia eutropha* for chemical production. In Industrial Processes and Nanotechnology (Vol. 10). USA: Studium Press LLC.

- Johnson, A.O., Gonzalez, V.M., Wong, L., Steinbüchel, A., Tee, K.L., Xu, P., Wong, T.S., 2017. Design and application of genetically-encoded malonyl-CoA biosensors for metabolic engineering of microbial cell factories. *Metab. Eng*.

- Johnson, A. O., Gonzalez-Villanueva, M., Tee, K. L. & Wong, T. S. 2018. An Engineered Constitutive Promoter Set with Broad Activity Range for *Cupriavidus necator* H16. *ACS Synthetic Biology*.

ACKNOWLEDGEMENTS

I would like to thank my esteemed supervisor – Dr. Tuck Seng Wong for his invaluable supervision, support and tutelage during the course of my PhD degree. My gratitude extends to the Faculty of Engineering for the funding opportunity to undertake my studies at the Department of Chemical and Biological Engineering, University of Sheffield.

Additionally, I would like to express gratitude to Dr. Kang Lan Tee for her treasured support which was really influential in shaping my experiment methods and critiquing my results. I also thank Dr. David Gonzalez, Dr. Pawel Jajeniak, Dr. Amir Zaki Abdullah Zubir for their mentorship.

I would like to thanks my friends, lab mates, colleagues – Abdulrahman Alessa, Miriam Gonzalez-Villanuva, Inas Al-nuaemi, Jose Avalos, Valeriane Keita, Melvin Mikuzi, Robert Berchtold for a cherished time spent together in the lab, and in social settings.

My appreciation also goes out to my family and friends for their encouragement and support all through my studies.

SUMMARY

Ralstonia eutropha H16 (also known as *Cupriavidus necator* H16) is a non-pathogenic chemolithoautotrophic soil bacterium. It has increasingly gained biotechnological interest for its use as a microbial cell factory for the production of several valuable bio-based chemicals. However the absence of a large repertoire of molecular tools to engineer this organism remains a critical limiting factor to exploiting its full biotechnological potential. Also, adopting established molecular tools applicable to the more notable microbial hosts such as *E. coli* and *Saccharomyces cerevesiae* is severely hampered by chassis-incompatibility and functional variability of essential biological parts. The work detailed in this thesis focuses on the development of key molecular tools crucial to improving the biosynthesis of malonyl-CoA - a precursor metabolite required for the biosynthesis of fatty acids and potentially several valuable bio-products in *Ralstonia eutropha* H16.

All molecular tools developed were based on the broad host range (BHR) plasmid vector backbone of pBBR1MCS1 – a *R. eutropha* H16-compatible vector. Firstly, to facilitate heterologous pathway optimization, a combination of pre-existing and novel methods of genetic modifications were applied to engineer a collection of 42 promoters. Promoter strengths were characterized using a fluorescence-based assay and benchmarked to the dose-dependent activity of an L-arabinose-inducible P_{BAD} promoter. Next, to detect intracellular accumulation of malonyl-CoA, transcriptional factor-based malonyl-CoA-sensing genetic circuits were developed *via* careful selection from the promoter collection. Thirdly, BHR L-arabinose-inducible λ-Red plasmid vectors were developed for mediating λ-Red-based genome editing. These were first tested in *E. coli* BW25113 to confirm their functionality and then subsequently tested in *R. eutropha* H16.

Overall, the collection of engineered promoters yielded a 137-fold range of promoter activity and the malonyl-CoA biosensors responded to changing malonyl-CoA concentrations. The BHR λ-Red plasmids showed high recombination efficiency in *E. coli* BW25113. The molecular tools developed from this work will further facilitate rapid control and regulation of gene expression in *R. eutropha*, particularly for malonyl-CoA engineering.

TABLE OF CONTENT

DECLARATION ..... **I**

ASSOCIATED PUBLICATIONS ..... **II**

ACKNOWLEDGEMENTS ..... **III**

SUMMARY ..... **IV**

TABLE OF CONTENT ..... **V**

TABLE OF FIGURES ..... **X**

TABLE OF TABLES ..... **XIV**

LIST OF ABBREVIATIONS ..... **XVII**

CHAPTER ONE **1**

LITERATURE REVIEW **1**

1 LITERATURE REVIEW **2**

1.1 ENGINEERING MICROBIAL CELL FACTORIES FOR BIO-MANUFACTURING ..... **ERROR! BOOKMARK NOT DEFINED.**

1.2 *R. EUTROPHA* H16 – AN INDUSTRIAL WORK-HORSE FOR CHEMICAL PRODUCTION **ERROR! BOOKMARK NOT DEFINED.**

1.3 ENGINEERING STRATEGIES FOR CHEMICAL PRODUCTION IN *R. EUTROPHA* ..... **ERROR! BOOKMARK NOT DEFINED.**

1.4 METABOLIC ENGINEERING IN *R. EUTROPHA* ..... **ERROR! BOOKMARK NOT DEFINED.**

1.4.1 EVOLUTIONARY ENGINEERING OR ADAPTIVE EVOLUTION **ERROR! BOOKMARK NOT DEFINED.**

1.4.2 RECOMBINANT STRAIN ENGINEERING ..... **ERROR! BOOKMARK NOT DEFINED.**

1.4.3 GENOME EDITING ..... **ERROR! BOOKMARK NOT DEFINED.**

1.5 EXPANDING CARBON SUBSTRATE RANGE OF *R. EUTROPHA* ..... **ERROR! BOOKMARK NOT DEFINED.**

1.5.1 GLUCOSE ..... **ERROR! BOOKMARK NOT DEFINED.**

1.5.2 GLYCEROL ..... **ERROR! BOOKMARK NOT DEFINED.**

1.5.3 SUGARS DERIVED FROM LIGNOCELLULOSIC BIOMASS **ERROR! BOOKMARK NOT DEFINED.**

1.5.4 CARBON DIOXIDE ..... **ERROR! BOOKMARK NOT DEFINED.**

1.6 ENGINEERING STRATEGIES FOR BIOPRODUCT SYNTHESIS IN *R. EUTROPHA* ..... **ERROR! BOOKMARK NOT DEFINED.**

1.6.1 PHA PRODUCTION ..... **ERROR! BOOKMARK NOT DEFINED.**

1.6.2 BIOFUEL PRODUCTION ..... **ERROR! BOOKMARK NOT DEFINED.**

1.6.3 METHYL CITRATE ..... **ERROR! BOOKMARK NOT DEFINED.**

1.6.4 FERULIC ACID ..... **ERROR! BOOKMARK NOT DEFINED.**

1.6.5 CHIRAL SYNTHONS ..... **ERROR! BOOKMARK NOT DEFINED.**

1.6.6 BIOHYDROCARBONS ..... **ERROR! BOOKMARK NOT DEFINED.**

1.6.7 OTHER BIOPOLYMERS .....**ERROR! BOOKMARK NOT DEFINED.**
1.7 EMERGING STRATEGIES TO EXPAND CHEMICAL RANGE .....**ERROR! BOOKMARK NOT DEFINED.**
1.7.1 *IN SILICO* METABOLIC PATHWAY ANALYSIS AND DESIGN**ERROR! BOOKMARK NOT DEFINED.**
1.7.2 PROTEIN ENGINEERING.....**ERROR! BOOKMARK NOT DEFINED.**
1.7.3 SYNTHETIC BIOLOGY.....**ERROR! BOOKMARK NOT DEFINED.**
1.8 BIOPROCESS ENGINEERING STRATEGIES FOR INDUSTRIAL APPLICATIONS OF *R. EUTROPHA* **ERROR! BOOKMARK NOT DEFINED.**
1.8.1 FEEDSTOCK .....**ERROR! BOOKMARK NOT DEFINED.**
1.8.2 BIOREACTOR AND FERMENTATION STRATEGY.....**ERROR! BOOKMARK NOT DEFINED.**
1.9 FUTURE OUTLOOK.....**ERROR! BOOKMARK NOT DEFINED.**
1.10 SCOPE OF RESEARCH 39
1.11 WHY MALONYL-COA? 40
1.12 STRATEGIES FOR MALONYL-COA ENGINEERING IN MODEL MICROBIAL FACTORIES ... 41
1.13 DEVELOPMENT OF CHASSIS-COMPATIBLE EXPRESSION VECTORS 48
1.14 PROMOTER ENGINEERING..... 49
1.15 METABOLITE SENSING GENETIC CIRCUITS 49
1.15.1 MALONYL-COA BIOSENSORS..... 51
1.15.2 MECHANISM OF MALONYL-COA SENSING..... 51
1.15.3 THE ARCHITECTURE OF A MALONYL-COA BIOSENSOR 52
1.15.4 THE DESIGN CRITERIA OF AN EFFECTIVE MALONYL-COA BIOSENSOR 53
1.15.5 APPLICATIONS OF MALONYL-COA BIOSENSORS..... 59
1.15.6 FUTURE PERSPECTIVES..... 69
1.16 GENOME EDITING – A ROBUST MOLECULAR TOOL FOR METABOLIC ENGINEERING IN *R. EUTROPHA* H16..... 70
1.16.1 λ-RED RECOMBINEERING..... 74
1.16.2 MECHANISM..... 74
1.16.3 APPLICATION OF λ-RED RECOMBINEERING IN MICROBIAL SYSTEMS 75
1.16.4 COMPARATIVE ADVANTAGE TO OTHER GENOME EDITING METHODS 82
1.16.5 λ-RED RECOMBINEERING APPLICATION IN *RALSTONIA EUTROPHA*: OPPORTUNITIES AND CHALLENGES..... 85
1.17 ROADMAP FOR THE APPLICATION OF MOLECULAR TOOLS FOR MALONYL-COA ENGINEERING IN *RALSTONIA EUTROPHA* H16..... 86
1.18 AIMS AND OBJECTIVES OF STUDY 89

CHAPTER TWO 90

2 DEVELOPMENT OF BROAD HOST EXPRESSION VECTORS FOR ENGINERING RALSTONIA EUTROPHA-COMPATIBLE MOLECULAR TOOLS 91

2.1 INTRODUCTION 91
2.2 METHODS AND MATERIAL 92
2.2.1 BACTERIAL CULTIVATION..... 92
2.2.2 PLASMID AND LINEAR DSDNA CONSTRUCTION..... 96
2.2.3 PLASMID PROPAGATION AND CIRCULARIZATION 109
2.2.4 BACTERIAL TRANSFORMATION 109
2.2.5 CELL DENSITY MEASUREMENT 110

2.2.6 Plasmid Isolation 110
2.2.7 Colony PCR verification of transforamnts 110
2.2.8 Protein expression: Expression of reporter proteins RFP and eGFP 111
2.2.9 Examining the induction range of the L-arabinose inducible P_{BAD} promoter in *Ralstonia eutropha* H16 111
2.2.10 Protein expression: Expression of the FapR transcriptional regulator in *R. eutropha* H16 and *E. coli* DH5α 112
2.2.11 Protein expression: Expression of the λ-Red genes in *E. coli* BW25113 and *R. eutropha* H16 112
2.2.12 Protein analysis with SDS-PAGE 113
2.3 RESULTS AND DISCUSSION 114
2.3.1 Bacterial transformation 114
2.3.2 Protein expression of RFP and eGFP in *Ralstonia eutropha* H16 114
2.3.3 Induction fold of the P_{BAD} promoter in pBBR1c-RFP in *Ralstonia eutropha* H16 115
2.3.4 Protein expression of FapR 115
2.3.5 Protein expression of λ-Red proteins 117
2.4 CONCLUSION 119

CHAPTER THREE 121

3 AN ENGINEERED CONSTITUTIVE PROMOTER SET WITH BROAD ACTIVITY RANGE FOR *RALSTONIA EUTROPHA* H16 122

3.1 INTRODUCTION 123
3.2 RESULTS AND DISCUSSION 126
3.2.1 Defining a promoter and quantifying its activity 126
3.2.2 Defining the boundaries and architectures of 4 parental promoters 127
3.2.3 Narrow range of promoter activities between the 4 parental promoters 130
3.2.4 Expanding the range of promoter activities through rational engineering 130
3.2.5 Promoter nomenclature 136
3.2.6 Mutations in -35 box tuned transcriptional activity down 136
3.2.7 A minimal P_{PHAC1} promoter with enhanced activity 137
3.2.8 Synthetic RBS and RBS repeat increased promoter activity 138
3.2.9 Repeat of -35 and -10 boxes increased transcriptional activity 138
3.2.10 Operator insertion reduced transcriptional activity drastically 138
3.2.11 Divergent promoters, arranged in back-to-back, increased transcriptional activity 139
3.2.12 Promoter characterization using P_{BAD} as reference scale 140
3.2.13 Summary of rational promoter engineering for *R. eutropha* H16 142
3.2.14 The use of engineered constitutive promoters in *R. eutropha* H16 144
3.3 CONCLUSION 146
3.4 MATERIALS & METHODS 147
3.4.1 Materials 147
3.4.2 Strains 147
3.4.3 Bacterial cultivation and transformation 147
3.4.4 Promoter engineering and sequences 147

3.4.5 PROMOTER ACTIVITY QUANTIFICATION USING FLUORESCENCE ASSAY 147
3.4.6 EFFECTS OF ENGINEERED CONSTITUTIVE PROMOTERS ON BACTERIAL GROWTH AND PROTEIN EXCRETION 148
3.4.7 FOLD CHANGE AND RELATIVE PROMOTER ACTIVITY CHANGE 148
3.5 SUPPLEMENTARY INFORMATION 149
3.5.1 MATERIALS & METHODS 149

CHAPTER FOUR 161

4 MALONYL-COA BIOSENSORS ENGINEERED FOR *RALSTONIA EUTROPHA* H16 162

4.1 INTRODUCTION 163
4.2 RESULTS AND DISCUSSION 166
4.2.1 SINGLE-PLASMID BIMODULAR MALONYL-COA BIOSENSOR 166
4.2.2 CONTROL GENETIC CIRCUITS FOR VALIDATING THE DESIGN OF MALONYL-COA BIOSENSOR 167
4.2.3 CONSTRUCTING A SET OF 6 MALONYL-COA BIOSENSORS BY CAREFUL SELECTION OF CONSTITUTIVE PROMOTER COMBINATIONS 170
4.2.4 RFP EXPRESSION IN ALL 6 BIOSENSORS WAS REPRESSED BY FAPR 172
4.2.5 ALL 6 BIOSENSORS ARE RESPONSIVE TO CHANGES IN INTRACELLULAR MALONYL-COA CONCENTRATION 173
4.2.6 ALL 6 BIOSENSORS DISPLAYED HIGH DEGREE OF ORTHOGONALITY 177
4.2.7 S1 IS THE BEST BIOSENSOR AND WORKS IN *E. COLI* 179
4.3 CONCLUSION 179
4.4 MATERIALS & METHODS 180
4.4.1 MATERIALS 180
4.4.2 STRAINS 180
4.4.3 BIOSENSOR CONSTRUCTION AND FAPR/PROMOTER SEQUENCES 180
4.4.4 BACTERIAL CULTIVATION AND TRANSFORMATION 180
4.4.5 BIOSENSOR CHARACTERIZATION USING FLUORESCENCE ASSAY 180
4.4.6 FOLD REPRESSION, FOLD INDUCTION AND INDUCTION EFFICIENCY 181
4.5 SUPPLEMENTARY INFORMATION 182
4.5.1 METHODS AND MATERIAL 182

CHAPTER FIVE 187

5 DEVELOPING A λ-RED RECOMBINEERING METHOD OF GENOME EDITING IN R. EUTROPHA H16 (PART I) 188

5.1 INTRODUCTION 188
5.2 METHOD 188
5.2.1 LINEAR DSDNA CASSETTES 188
5.2.2 λ-RED RECOMBINATION PROTOCOL 191
5.2.3 VERIFICATION OF GENOMIC INTEGRATION OF LINEAR DSDNA CASSETTE 192
5.2.4 λ-RED RECOMBINEERING IN *E. COLI* BW25113 WITH PKD20 198
5.2.5 λ-RED RECOMBINEERING IN *E. COLI* BW25113 WITH PKD20 AND PBBR1C-RED1 198
5.2.6 λ-RED RECOMBINEERING IN *E. COLI* BW25113 WITH PBBR1C-RED1, PBBR1C-RED2, PBBR1K-RED 198
5.3 RESULTS AND DISCUSSION 200

5.3.1 λ-RED RECOMBINEERING WITH PKD20 200
5.3.2 λ-RED RECOMBINEERING IN *E. COLI* BW25113 WITH PKD20 AND PBBR1C-RED1 201
5.3.3 λ-RED RECOMBINEERING IN *E. COLI* BW25113 WITH PBBR1C-RED1, PBBR1C-RED2, AND PBBR1K-RED 202
5.4 CONCLUSION 207

CHAPTER SIX 208

6 DEVELOPING A λ-RED RECOMBINEERING METHOD OF GENOME EDITING IN R. EUTROPHA H16 (PART II) 209

6.1 INTRODUCTION 209
6.2 METHODS 209
6.2.1 LINEAR DSDNA CASSETTES 209
6.2.2 VERIFICATION OF STABILITY OF PBBR1C-RED1 AND PBBR1C-RED2 IN *RALSTONIA EUTROPHA* H16 221
6.2.3 RECOMBINEERING VIA λ-RED RECOMBINASE PROTEINS IN *RALSTONIA EUTROPHA* H16 222
6.2.4 VERIFICATION OF SUCCESSFUL RECOMBINATION *RALSTONIA EUTROPHA* H16 223
6.2.5 λ-RED RECOMBINEERING WITH PBBR1C-RED2 AND KANR CASSETTES FROM PBBA8K-RFP 223
6.3 RESULTS AND DISCUSSION 228
6.3.1 TRANSFORMATION OF PBBR1C-RED1 AND PBBR1C-RED2 INTO *R. EUTROPHA* H16 228
6.3.2 λ-RED RECOMBINEERING WITH PBBR1C-RED2 AND KANR CASSETTES FROM PBBA8K-RFP 228
6.4 CONCLUSION 233

CHAPTER SEVEN 234

7 CONCLUSION 235

7.1 CONTRIBUTIONS OF THIS WORK 235
7.2 FUTURE WORK 237
7.3 FUTURE PERSPECTIVES 239

REFERENCES 240

TABLE OF FIGURES

Figure 1.1: Key metabolic pathways in *R. eutropha* under heterotrophic and autotrophic conditions. .....**Error! Bookmark not defined.**

Figure 1.2: Some value-added chemicals and chemical products derivable from Polyhydroxybutyrate (PHB). .....**Error! Bookmark not defined.**

Figure 1.3: Key milestones in the understanding of *R. eutropha***Error! Bookmark not defined.**

Figure 1.4: Engineering strategies for chemical production in *R. eutropha* ..... **Error! Bookmark not defined.**

Figure 1.5: Industries that have adopted *R. eutropha* as a microbial cell factory for polyhydroxyalkanoate (PHA) production. .....**Error! Bookmark not defined.**

Figure 1.6 Native PHB synthesis pathway in *R. eutropha* H16.**Error! Bookmark not defined.**

Figure 1.7: A schematic of the engineered biochemical pathway for P(3HB-*co*-3HV) synthesis in mutant strain R3. .....**Error! Bookmark not defined.**

Figure 1.8: Reconstructed metabolic pathway for P(3HB-*co*-3HHx) synthesis from fructose in *R. eutropha.* .....**Error! Bookmark not defined.**

Figure 1.9: Engineered branched chain alcohol production pathway in *R. eutropha*. . **Error! Bookmark not defined.**

Figure 1.10: Native β-oxidation pathway (left part) and the re-engineered pathway for the biosynthesis of methyl ketones (right part, and dotted arrows) in *R. eutropha*. ... **Error! Bookmark not defined.**

Figure 1.11: Compounds derived from malonyl-CoA. Malonyl-CoA, a direct product of acetyl-CoA, can be used as a precursor for the synthesis of fatty acids, flavonoids, bio-polymers, biofuels, and polyketides. 43

Figure 1.12: A summary of metabolic engineering strategies to increase intracellular malonyl-CoA concentration. 44

Figure 1.13: Mechanism of malonyl-CoA sensing. 52

Figure 1.14: Schematic diagram of the architecture of a malonyl-CoA sensor showing its modularity with a repressor module (P1 and FapR gene) and a reporter module (P2, *fapO* and RFP gene). P1 – repressor promoter, P2 – reporter promoter, O – *fapO* operator, T1, T2 – transcriptional terminators. 53

Figure 1.16: A schematic of the key design considerations for crafting an efficient malonyl-CoA biosensor. 55

Figure 1.17: Key biological parts for crafting versatile malonyl-CoA sensors. 56

Figure 1.18: Promoter-regulatory circuits for actuation of malonyl-CoA in *E. coli*. 61

Figure 1.19: Schematic representation of a malonyl-CoA sensor-actuator and a negative feedback regulatory circuit. 63

Figure 1.20: Malonyl-CoA metabolic sensor and switch 65

Figure 1.21: Malonyl-CoA sensor in yeast 68

Figure 1.22: Molecular mechanism of λ-Red recombineering. 75

Figure 1.23: Simplified process of λ-Red recombineering for genomic integration of marker. 78

Figure 1.24: Schematic of λ-Red recombineering with a dsDNA selectable marker. 79

Figure 1.25: Mechanism of λ-Red recombineering with pREDI. 81

Figure 1.26: Proposed application of developed tools for malonyl-CoA engineering in *Ralstonia eutropha* H16. 88

Figure 2.1: Maps of plasmids possessing essential biological parts for constructing vital expression vectors for molecular tool development in *Ralstonia eutropha* H16. 97

Figure 2.2: *In silico* construction of pBBR1c-RFP 99

Figure 2.3: *In silico* construction of pBBR1k-RFP 103

Figure 2.4: *In silico* construction of pBBR1c-eGFP 104

Figure 2.5: *In silico* construction of pBBR1c-FapR 105

Figure 2.6: *In silico* construction of pBBR1c-RED1 106

Figure 2.7: *In silico* construction of pBBR1k-RED 107

Figure 2.8: *In silico* construction of pBBR1c-RED2 108

Figure 2.9: Inducible expression of RFP and eGFP in *Ralstonia eutropha* 114

Figure 2.10: Dose-dependent induction of P_{BAD} promoter, using L-arabinose concentration from 0.001% (w/v) to 0.200% (w/v). (A) Graph of RFU versus L-arabinose concentration. (B) Graph of RFU/OD_{600} versus L-arabinose concentration. 115

Figure 3.11: SDS-PAGE image showing expression of the ~26 kDa FapR transcriptional regulator (green arrow) and RFP (red arrow) in *E. coli* DH5α and *R. eutropha* H16. 116

Figure 2.12: SDS-PAGE showing expression of the λ-Red proteins Bet (~29 kDa, red arrow), Exo (~25 kDa, blue arrow), and Gam (~15 kDa, green arrow) in *E. coli* BW25113. (A) The λ-Red proteins Bet and Exo and Gam are expressed at 0.1% L-arabinose in strain BWRed1, BWRed2c and BWRed2k (B) The λ-Red proteins are more vividly expressed in strains BWRed1, BWRed2c and BWRed2k than in strains BWD20 and BWD46. 118

Figure 3.1: (*A*) Promoter definition used in this study. (*B*) High-throughput characterization of engineered promoters using a fluorescence-based assay. (5'-UTR: 5'-untranslated region; bp: base pair; *CamR*: chloramphenicol resistance gene; *Rep*: replication gene; RFP: red fluorescent protein) 127

Figure 3.2: (*A*) Boundaries and architectures of the 4 parental promoters, P_{phaC1}, P_{rrsC}, P_{j5} and P_{g25}, used in this study. (*B*) Comparison of the 4 parental promoters to an *Escherichia coli* σ^{70} promoter. (*C*) Activities of the 4 parental promoters. 129

Figure 3.3: Architectures of parental promoters and their engineered variants. 132

Figure 3.4: Activities of parental promoters and their engineered variants. 133

Figure 3.5: (*A*) For gene pairs in HH arrangement, promoters that effect divergent transcription can be organized in 3 possible ways: back-to-back, overlapping or face-

to-face. (*B*) Composite promoters engineered using P_{g25} as parental promoter. (*C*) Composite promoters engineered using P_{rrsC} as parental promoter. (*D*) Composite promoters engineered using P_{j5} as parental promoter. (*E*) Composite promoters with P_{phaC1} as secondary promoter. (*F*) Composite promoters with P_{g25} as secondary promoter. (*G*) Composite promoters with $P_{j5[A1C1C2]}$ as secondary promoter. In graphs E to G, red, blue and orange symbols represent primary promoter activity, composite promoter activity and fold change, respectively. 137

Figure 3.6: (*A*) Hierarchical ranking of all 42 constitutive promoters reported in this study. (*B*) The range of promoter activity was expanded from 6 folds to 137 folds, after applying combination of promoter engineering strategies. 141

Figure 3.7: Relative promoter activity change upon application of promoter engineering strategies. 143

Figure 3.8: Growth curves of *R. eutropha* H16 harbouring either pBBR1MCS-1 (control; black line) or plasmids containing various engineered constitutive promoters [P_{g25} (red line), $P_{phaC1[B1d]}$ (blue line), $P_{rrsC[E1D4]}$ (brown line), $P_{g25[E3]}$ (green line), $P_{g25[D1C2]}$ (pink line), $P_{j5[E1A1C1C2]}$ (orange line) and $P_{j5[E2C2]}$ (purple line)]. 144

Figure 3.9: Fluorescence of cell culture (black columns) and of spent medium (grey columns) of *R. eutropha* H16 harbouring either pBBR1MCS-1 (control) or plasmids containing various engineered constitutive promoters (P_{g25}, $P_{phaC1[B1d]}$, $P_{rrsC[E1D4]}$, $P_{g25[E3]}$, $P_{g25[D1C2]}$, $P_{j5[E1A1C1C2]}$ and $P_{j5[E2C2]}$). 145

Figure S3.1: Plasmid map of pBBR1c-RFP 150

Figure S3.2: Alignment of P_{j5} and P_{g25} promoters used in Gruber *et al.* (2014) and those used in this study. 151

Figure S3.3: Rational promoter engineering strategies applied in this study. (*A*) Point mutation. (*B*) Length alteration. (*C*) Incorporation of regulatory genetic element. (*D*) Promoter hybridization. (*E*) Configuration alteration. 151

Figure S3.4: Dose-dependent induction of P_{BAD} promoter, using L-arabinose concentration from 0.001% (w/v) to 0.200% (w/v). 152

Figure S3.5: Fitting of cell culture fluorescence *vs* time data (scattered points) to a 4-parameter dose response curve (red line). 153

Figure S3.6: Fluorescence of cell culture (Figure S3.5) normalized by OD600 value (Figure 3.8). 154

Figure 4.1: (*A*) Bimodular malonyl-CoA biosensor. (*B*) Three negative control genetic circuits constructed for each biosensor (FapR, *fapO*): control A (ΔFapR, *fapO*), control B (FapR, Δ*fapO*) and control C (ΔFapR, Δ*fapO*). (*C*) Promoters used in this study. 167

Figure 4.2: (*A*) Reporter activity from each biosensor (FapR, *fapO*). Promoter P2 of each biosensor is indicated above each data set. (*B*) Reporter activity from control A (ΔFapR, *fapO*) of each biosensor. Promoter P2 of each control genetic circuit is indicated above the respective data set. (*C*) Fold repression of each biosensor, after 12 h cultivation in 96-well deep well plate. Promoter strength is indicated above each data point, written in the format of (Strength of promoter P1, Strength of promoter P2). (*D*) Reporter activity from control B (FapR, Δ*fapO*) and control C (ΔFapR, Δ*fapO*). Promoter P2 of the control genetic circuit is indicated above each data set. 173

Figure 4.4: Reporter activity from biosensor (FapR, *fapO*) S1 to S6 in the presence of increasing cerulenin concentration, measured after 12 h (red line), 18 h (blue line) and 24 h (black line) of cultivation in 96-well microtitre plate. 176

Figure 4.5: Fold repression (black column) and maximal fold induction (grey column) of each biosensor. Promoter strength is indicated above each data point, written in the format of (Strength of promoter P1, Strength of promoter P2). 176

Figure 4.6: Fold induction from biosensor [(FapR, *fapO*); black line], control A [(ΔFapR, *fapO*); blue line] and control B [(FapR, Δ*fapO*); red line] for each design in the presence of increasing cerulenin concentration. 178

Figure S4.2: Effect of cerulenin on the growth of *Ralstonia eutropha* H16..... 183

Figure S4.3: Comparison of reporter activities from biosensor (FapR, *fapO*), control A (ΔFapR, *fapO*) and control B (FapR, Δ*fapO*) of each design, measured after 12 h (black), 18 h (light grey) and 24 h (dark grey) of cultivation in 96-well deep well plate. 184

Figure 5.1: Methods of screening for successful genomic integration of antibiotics resistance marker..... 194

Figure 5.2: Agarose gel electrophoresis image from colony PCR with cassette-specific primers to identify Δ*zwf* BWD20K and BWRed1K strains of *E. coli* BW25113 after λ-Red recombineering. 202

Figure 5.3: Agarose gel electrophoresis from colony PCR screening with upstream-downstream primers to identify Δ*zwf* strains BWRed1K, BWRed2cK and BWRed2kC of *E. coli* BW25113 after λ-Red recombineering. 205

Figure 5.4: Agarose gel electrophoresis of colony PCR screening with upstream-midstream primers to confirm Δ*zwf* strains BWRed2kC *E. coli* BW25113 after λ-Red recombineering..... 206

Figure 6.1. Schematic of experimental set-up of λ-Red recombineering in *Ralstonia eutropha* H16 using several variants of the kanR cassette from pBbA8K-RFP and the strain ReRed2 containing the pBBR1c-RED2 λ-Red plasmid. 226

Figure 6.2: Agarose gel electrophoresis of colony PCR amplicons of *Ralstonia eutropha* with pBBR1c-RED1 (ReRed1), and pBBR1c-RED2 (ReRed2) transformants using appropriate primers for the λ-Red operon. (A) 1.905 kb band shows the *Nde*I-pKD20-*BamH*I amplicon from pBBR1c-RED1, (B) 2.2 kb band shows the *Nde*I-pKD46-*BamH*I amplicon from pBBR1c-RED2. L – 1 kb DNA ladder. 228

Figure 6.3: Agarose gel electrophoresis of colony PCR from selected colonies which grew above OD_{600} after λ-Red recombineering with pBBR1c-RED2 in *R. eutropha* H16. All 8 screened colonies show band at ~2.0 kb showing that the *phaC1* gene is undeleted and that the linear dsDNA cassettes are not integrated into the genome. 232

TABLE OF TABLES

Table 1.1 Engineering strategies for improving acetyl-CoA flux to PHB synthesis. .. **Error! Bookmark not defined.**

Table 1.2 Substrate requirements and engineering strategies for synthesis of some scl-PHAs. ..... **Error! Bookmark not defined.**

Table 1.3 scl-PHA product concentration and productivity from autotrophic and heterotrophic fermentation using various cultivation strategies. **Error! Bookmark not defined.**

Table 1.4: Notable examples of conventional metabolic engineering strategies to increase intracellular malonyl-CoA amount and end chemicals 45

Table 1.5: A summary of reported malonyl-CoA sensors 57

Table 1.6: Notable singleplex genome editing techniques potentially applicable in *Ralstonia eutropha* 72

Table 1.7: Some notable examples of λ-Red recombinase expression vectors and properties 77

Table 1.8: Comparison of λ-Red Recombineering to other notable genome editing methods 84

Table 2.1: Bacteria strains used in this study 93

Table 2.2: Plasmids used in this study 94

Table 2.3: Primers used in this study 95

Table 3.1: Summary of 42 parental promoters and their variants engineered using a combination of promoter engineering strategies (A = point mutation, B = length alteration, C = incorporation of regulatory genetic element, D = promoter hybridization and E = configuration alteration). Numbers in bracket represent promoter digital identifier, in the format of [Activity level – Relative activity to $P_{phaC1[A1]}$ – Promoter length]. 134

Table S3.1: Promoter engineering strategies. 158

Table S3.2: A list of all 42 promoters in ascending order of activity 159

Table S3.3: Growth rates of *R. eutropha* H16 harbouring either pBBR1MCS-1 (control) or plasmids containing various engineered constitutive promoters. 160

Table S3.4: Fitting of cell culture fluorescence *vs* time data to a 4-parameter 160

dose response curve according to the Hill's equation 160

Table 4.1: Promoters used in this study 168

Table 4.2: Six malonyl-CoA biosensors described in this study. 169

Table 4.3: Controls for all six malonyl-CoA biosensors described in this study. Biosensors S1 and S2 share the same promoter P1. Therefore, these two biosensors share the same control B and control C. The same applies to biosensor pairs S3 and S4 as well as S5 and S6. 171

Table S4.1: Fitting of data in Figure S4.4 to a dose-response curve with variable slope (4-parameter) 185

Table S4.2: Induction efficiencies of all 6 biosensors 186

Table 5.1: Description of dsDNA cassettes for λ-Red recombineering in *E. coli* BW25113 189

Table 5.3: PCR protocol for *zwf*-kanR-*zwf* 190

Table 5.4: PCR programme for *zwf*-kanR-*zwf* 190

Table 5.5: PCR protocol for *zwf*-camR-*zwf* 191

Table 5.6: PCR programme for *zwf*-camR-*zwf* 191

Table 5.7: Strains used in this study 192

Table 5.8: Colony PCR protocol with cassette primers 195

Table 5.9: Colony PCR programme with cassette primers 195

Table 5.10: Colony PCR protocol with upstream-downstream Primers 195

Table 5.11: Colony PCR programme with upstream-downstream Primers 196

Table 5.12: Colony PCR protocol with upstream-midstream and midstream-downstream Primers (for checking *zwf*-kanR-*zwf* integration) 196

Table 5.13: Colony PCR Programme for 1181 bp UP*zwf*-kanR amplicon using primers UP*zwf*-for and *zwf*-kanR-rev 196

Table 5.15: Colony PCR protocol with upstream-midstream and midstream-downstream primers (for checking zwf-camR-zwf integration) 197

Table 5.16: Colony PCR programme for 600 bp *zwf*-camR amplicon using upstream-midstream primers: UP*zwf*-for and camR-rev 197

Table 5.17: Colony PCR programme for 500 bp *zwf*-camR amplicon using upstream-midstream primers: UP*zwf*-for and camR-rev 197

Table 5.18: Colony count λ-Red recombineering with pKD20 at different conditions 200

Table 5.19: Colony count from λ-Red recombineering with pKD20 and pBBR1c-RED1 201

Table 5.20: Colony count from λ-Red recombineering with pBBR1c-RED1, pBBR1c-RED2 and pBBR1k-RED 204

Table 6.1: Description of dsDNA cassettes for λ-Red recombineering in *R.eutropha* H16 210

Table 6.2: Primers used in this study 211

Table 6.3: PCR protocol for *phaC1*-nkanR-*phaC1* 216

Table 6.4: PCR programme for *phaC1*-nkanR-*phaC1* 216

Table 6.5: PCR protocol for 100H.*phaC1*-nkanR-100H.*phaC1* 217

Table 6.6: PCR programme for *phaC1*-nkanR-*phaC1* 217

Table 6.7: PCR protocol for 50H.*phaC1*-kanR-50H.*phaC1* 218

Table 6.8: PCR programme for 50H.*phaC1*-kanR-50H.*phaC1* 218

Table 6.9: PCR protocol for 50H.*phaC1*-rckanR-50H.*phaC1* 219
Table 6.10: PCR programme for 50H.*phaC1*-rckanR-50H.*phaC1* 219
Table 6.11: PCR protocol for 100H.*phaC1*-kanR-100H.*phaC1* and 100H.*phaC1*-rckanR-100H.*phaC1* 220
Table 6.12: PCR programme for 100H.*phaC1*-kanR-100H.*phaC1* and and 100H.*phaC1*-rckanR-100H.*phaC1* 220
Table 6.13: PCR protocol for phosphorothiolated cassettes 221
Table 6.14: PCR programme for phosphorothiolated cassettes 221
Table 6.15: Colony PCR protocol for ReRed1 and ReRed2 222
Table 6.16: Colony PCR programme for ReRed1 and ReRed2 222
Table 6.17: Experimental set-up of λ-Red recombineering using different dsDNA cassettes 224
Table 6.18: Negative controls for λ-Red recombineering 224
Table 6.19: Colony PCR protocol for screening for mutant clones 227
Table 6.20: Colony PCR programme for screening for mutant clones 227
Table 6.21: Colony count for λ-Red recombineering in *R. eutropha* H16 230
Table 6.22: OD_{600} of cells of selected colonies screened for cell growth against kanamycin selection pressure. 231

LIST OF ABBREVIATIONS

%	Percentage
°C	Degree Celsius
2-MC	2-Methyl Citrate
5'-UTR	5'-Untranslated Region
α	Alpha
ACC	Acetyl-CoA Carboxylase
ACP	Acyl Carrier Protein
Amp	Ampicillin
AmpR	Ampicillin resistant
aTc	Anhydrotetracycline
ATP	Adenosine Triphosphate
β	Beta
bp	Base pair
C. necator	*Cupriavidus necator*
CA	Carbonic Anhydrase
$CaCl_2$	Calcium Chloride
Cam	Chloramphenicol
camR	Chloramphenicol resistance
Cas9	CRISPR Associated Protein 9
CBB	Calvin-Benson Bassham
CBM	Carbohydrate Binding Motif
CCU	Carbon Capture and Utilization
CDW	Cell Dry weight
CiED	Cipher of Evolutionary Design
CO	Carbon Monoxide
CO_2	Carbon Dioxide
CoA	Coenzyme A
COBRA	Constraint-Based Reconstruction and Analysis
CPT	Carnitine Palmitoyltransferase
CRISPR	Clustered Regularly Interspaced Short Palindromic Repeats
DNA	Deoxyribonucleic Acid
dNTP	Deoxyribonucleotide Trinucleotide
dsDNA	Double stranded DNA
E_m	Emission coefficient
E_x	Excitation coefficient
E. coli	*Escherichia coli*
e.g	Example given
EDP	Entner Doudoroff Pathway

EDTA	Ethylenediamine Tetraacetic Acid
eGFP	Enhanced Green Fluorescence Protein
FACS	Fluorescence Assisted Cell Sorting
fapO	Fatty Acid and Phosplolipid Synthesis Operator
FapR	Fatty Acid and Phospholipid Synthesis Repressor
FAS	Fatty Acid Synthase
for	forward
g	Gram
g/L	Gram per Litre
GenR	Gentamicin Resistance
Gen^r	Gentamicin resistant
GETR	Genome Editing with Targetrons and Recombinases
GFP	Green Fluorescence Protein
h	Hour
H_2	Hydrogen
HB	Hydroxybutyrate
HD	Hydroxydecanoate
HHx	Hydroxyhexanoate
HO	Hydroxyoctanoate
HPLC	High Performance Liquid Chromatography
HV	Hydroxyvalerate
IBS	Intron Binding Site
IEP	Intron-Encoded Protein
Kan	Kanamycin
kanR	Kanamycin resistance
kb	Kiobase
K_D	Dissociation constant
kDa	Kilodaltons
kg	Kilogramme
λ	Lambda
LC	Liquid Chromatography
μ	Micro
Mal-CoA	Malonyl-CoA
MCS	Multiple Cloning Site
MEA	Monoethanolamine
mins	Minutes
μL	Microliter
mL	millimlitre
μm	Micron
mM	millimolar
μM	micromolar

mRNA	Messenger Ribonucleic acid
MS	Mass Spectroscopy
NADH	Nicotinamide Adenine Dinucleotide
NADPH	Nicotinamide Adenine Dinucleotide Phosphate
NB	Nutrient Broth
NCBI	National Centre for Biotechnology Information
NH_4Cl	Ammonium Chloride
nmol	Nanomole
NO_2^-	Nitrite
NO_3^-	Nitrate
nm	Nanometres
nt	Nucleotide
NTG	*N*-methyl-*N'*-nitro-*N*-nitrosoguanidine
O_2	Oxygen
OD	Optical density
OPH	Organophosphohydrolase
PCR	Polymerase Chain Reaction
PDH	Pyruvate dehydrogenase
PGK	Phosphoglycerate Kinase
PHA	Polyhydroxyalkanoate
PHAS	Polyhydroxyalkanoate Synthase
PHB	Polyhydroxybutyrate
PROM	Probabilistic Regulation Of Metabolism
R. eutropha	*Ralstonia eutropha*
RBS	Ribosome Binding Site
Red	Recombination deficient
rev	Reverse
RFP	Red Fluorescence Protein
RFU	Relative Fluorescence unit
RNA	Ribonucleic Acid
RNP	Ribonucleoprotein
RPU	Relative Promoter Unit
RuBisCO	Ribulose-1,5-Bisphosphate Carboxylase/Oxygenase
s	Seconds
S. cerevisiae	*Saccharomyces cerevisiae*
SD	Shine Dalgarno
SDS-PAGE	Sodium Dodecylsulphate Polyacrylamide Gel Electrophoresis
ssDNA	Single stranded DNA
TALENs	Transcription Activator-Like Effectors Nucleases
TCA	Tricarboxylic Acid
U	Unit

UAS	Upstream Activation Sequence
UP	Upsteam element
UV	Ultra-violet
V	Volt
w/v	Weight per volume
WT	Wild type
ZFN	Zinc Finger Nucleases

CHAPTER ONE
LITERATURE REVIEW

Some sections of this chapter have been adapted from the book chapter: Johnson, A. O., Gonzalez Villanueva, M., & Wong, T. S. (2015). Engineering *Ralstonia eutropha* for chemical production. In Industrial Processes and Nanotechnology (Vol. 10). USA: Studium Press LLC, and the Journal publication: Johnson, A. O., Gonzalez-Villanueva, M., Wong, L., Steinbüchel, A., Tee, K. L., Xu, P. & Wong, T. S. 2017. Design and application of genetically-encoded malonyl-CoA biosensors for metabolic engineering of microbial cell factories. *Metab Eng,* 44**,** 253-264.

1 LITERATURE REVIEW

REMOVED FROM THE E-THESIS DUE TO COPYRIGHT

REMOVED FROM THE E-THESIS DUE TO COPYRIGHT

REMOVED FROM THE E-THESIS DUE TO COPYRIGHT

REMOVED FROM THE E-THESIS DUE TO COPYRIGHT

REMOVED FROM THE E-THESIS DUE TO COPYRIGHT

REMOVED FROM THE E-THESIS DUE TO COPYRIGHT

REMOVED FROM THE E-THESIS DUE TO COPYRIGHT

REMOVED FROM THE E-THESIS DUE TO COPYRIGHT

REMOVED FROM THE E-THESIS DUE TO COPYRIGHT

REMOVED FROM THE E-THESIS DUE TO COPYRIGHT

REMOVED FROM THE E-THESIS DUE TO COPYRIGHT

REMOVED FROM THE E-THESIS DUE TO COPYRIGHT

REMOVED FROM THE E-THESIS DUE TO COPYRIGHT

REMOVED FROM THE E-THESIS DUE TO COPYRIGHT

REMOVED FROM THE E-THESIS DUE TO COPYRIGHT

REMOVED FROM THE E-THESIS DUE TO COPYRIGHT

REMOVED FROM THE E-THESIS DUE TO COPYRIGHT

REMOVED FROM THE E-THESIS DUE TO COPYRIGHT

REMOVED FROM THE E-THESIS DUE TO COPYRIGHT

REMOVED FROM THE E-THESIS DUE TO COPYRIGHT

REMOVED FROM THE E-THESIS DUE TO COPYRIGHT

REMOVED FROM THE E-THESIS DUE TO COPYRIGHT

REMOVED FROM THE E-THESIS DUE TO COPYRIGHT

REMOVED FROM THE E-THESIS DUE TO COPYRIGHT

REMOVED FROM THE E-THESIS DUE TO COPYRIGHT

REMOVED FROM THE E-THESIS DUE TO COPYRIGHT

REMOVED FROM THE E-THESIS DUE TO COPYRIGHT

REMOVED FROM THE E-THESIS DUE TO COPYRIGHT

REMOVED FROM THE E-THESIS DUE TO COPYRIGHT

REMOVED FROM THE E-THESIS DUE TO COPYRIGHT

REMOVED FROM THE E-THESIS DUE TO COPYRIGHT

REMOVED FROM THE E-THESIS DUE TO COPYRIGHT

REMOVED FROM THE E-THESIS DUE TO COPYRIGHT

REMOVED FROM THE E-THESIS DUE TO COPYRIGHT

REMOVED FROM THE E-THESIS DUE TO COPYRIGHT

REMOVED FROM THE E-THESIS DUE TO COPYRIGHT

REMOVED FROM THE E-THESIS DUE TO COPYRIGHT

1.10 Scope of research

Rapid advancement in the development of state-of-the-art metabolic engineering tools, and the synergistic application of these tools promises to improve the use of *R. eutropha* H16 as an industrial work strain for chemical production. Overall, regulation of gene expression is a forefront strategy in improving the accumulation of pre-defined chemicals and/or their precursor metabolites. To this end, the research study in this thesis aims to expand the collection of molecular tools available to alter/modify/control/regulate gene expression in *R. eutropha* H16 by focusing on (1) engineering promoters for static and/or dynamic control of gene expression, (2) engineering metabolite-responsive genetic circuits for reporting the accumulation of vital metabolites and for achieving programmable and orthogonal regulation of the biosynthesis of such metabolites, (3) developing a facile genome editing molecular tool to alter gene expression at the genomic level. In particular, the goal is to develop these molecular tools to potentially facilitate metabolic engineering efforts to improve biosynthesis of malonyl-CoA in *R. eutropha* H16. All of these tools will rely on the use of expression vectors that are compatible with the transformation, replication and transcriptional machineries of *R. eutropha* H16.

1.11 Why Malonyl-CoA?

In practically every living system, a portion of the acetyl-CoA flux from the central metabolic pathway is carboxylated into malonyl-CoA, with the aid of acetyl-CoA carboxylase (ACC). This suggests the vital roles that malonyl-CoA plays in cell metabolism and structure. Specifically, malonyl-CoA is a rate limiting substrate for fatty acid synthesis, which in turn, is pivotal for maintaining cell membrane integrity and energy conservation (Schujman et al., 2008, Schujman et al., 2006, Schujman et al., 2003). In mammals, it has been identified as a crucial fatty acid oxidation regulator which inhibits the mitochondrial carnitine palmitoyltransferase (CPT) − an enzyme involved in fatty acid uptake in the heart and skeletal muscle (Folmes and Lopaschuk, 2007, Foster, 2012). This makes it a target molecule for treating diseases caused by poor or excessive fatty acid uptake. This has also attracted medical interest in drug development to control malonyl-CoA metabolism at the enzymatic level (Folmes and Lopaschuk, 2007). More relevant to this review, malonyl-CoA is also the modulatory effector molecule for regulating fatty acid synthesis in many Gram-positive bacteria (Dirusso et al., 1993, James and Cronan, 2003, Magnuson et al., 1993, Marrakchi et al., 2001, Nunn et al., 1977, Schujman et al., 2003, Schujman et al., 2006, Schujman et al., 2008, Yao et al., 2012).

The role of malonyl-CoA as a precursor metabolite for fatty acid biosynthesis has particularly attracted vast industrial biotechnology interest in harnessing intracellular malonyl-CoA flux for the synthesis of both value-added fatty acid based end chemicals, and a wide range of non-fatty acid based end chemicals in notable microbial cell factories, such as *Escherichia coli* and *Saccharomyces cerevesiae*, (James and Cronan, 2003, Schujman et al., 2003, Schujman et al., 2006) (Figure 1.11). These end chemicals are potentially useful as pharmaceutical intermediates, biofuels or other potentially useful chemical products vital to a sustainable bio-economy (Liu et al., 2015b, Xu et al., 2014a, Xu et al., 2014b). However, perpetually low intracellular concentrations of malonyl-CoA in microbial hosts (4 – 90 μM or 0.01 – 0.23 nmol/mg dry weight in *E. coli*) necessitate the use of metabolic engineering approaches to realize its commercial-scale applications (Miyahisa et al., 2005, Takamura et al., 1985, Takamura and Nomura, 1988).

1.12 Strategies for malonyl-CoA engineering in model microbial factories

Early metabolic engineering strategies employed static manipulation of relevant pathway enzymes that are directly or indirectly involved in malonyl-CoA metabolism in conjunction with metabolic pathways to channel the ensuing increase in malonyl-CoA amounts to the synthesis of pre-defined end chemicals. Some of these approaches include increasing expression level and/or enzymatic activity of ACC – the enzyme that converts acetyl-CoA to malonyl-CoA, increasing intracellular availability of acetyl-CoA – a malonyl-CoA precursor, and down-regulating malonyl-CoA sink pathways (Figure 1.12 and Table 1.4). As such, early attempts at malonyl-CoA engineering relied on conventional bio-analytical techniques such as HPLC and LC to quantify increased concentrations of malonyl-CoA and the ensuing end chemicals, and to validate the effectiveness of various strategies.

In addition, the outcomes of static manipulation of relevant pathways have been used in building and validating predictive computational models as a metabolic engineering tool (Fowler et al., 2009, Xu et al., 2011). By studying the entire metabolic network of a biological host, such models nominate target genes for knock out and/or over-expression to improve malonyl-CoA amounts. Besides nominating genes directly related to malonyl-CoA metabolism, computational tools have been applied in highlighting potential impact of targeted genes on cell growth. Further, they have been used to explore the potential roles of genes that are indirectly related to malonyl-CoA metabolism with the aim of improving intracellular malonyl-CoA accumulation. Overall, computational tools have been successfully applied for finding the most promising combination of approaches to achieve an improved malonyl-CoA yield. As an example, Xu *et al.* applied a genome-scale metabolic network model to achieve a balanced carbon flux to the citric acid cycle for cell viability and to the synthesis of naringenin, a flavonoid compound, in *E. coli* (Xu et al., 2011). The model predicted over-expression of ACC, phosphoglycerate kinase (PGK) and pyruvate dehydrogenase (PDH), in addition to double knockout of genes for the citric acid cycle enzymes: succinyl-CoA synthetase (sucC) and fumarase (fumC). The combination of these metabolic adjustments resulted in a 3.7-fold increase in malony-CoA amount and a 5.6-fold increase in naringenin production at 474 mg/L, compared to the wild-type cells. Similarly, Fowler *et al.* demonstrated the use of a computational model known as Cipher of Evolutionary Design (CiED) (Fowler et al., 2009). The tool nominated knockout of citric

acid cycle genes (*sdhCDAB* and *citE*), amino acid transporter (*brnQ*) and pyruvate consumer (alcohol dehydrogenase *adhE*) in engineering an efficient malonyl-CoA producing *E. coli* strain. This deletion strain was subsequently used to overexpress ACC, acetyl-CoA synthetase, biotin ligase and pantothenate kinase to achieve 660% and 420% increase in naringenin and eriotictyol production, respectively.

Beside the use of genetically orchestrated metabolic engineering strategies, fatty acid synthesis inhibiting-chemicals such as cerulenin and triclosan have been shown to induce relatively large increase in intracellular malonyl-CoA amounts (Davis et al., 2000). Cerulenin up-regulates intracellular malonyl-CoA amounts by inhibiting β-ketoacyl-acyl carrier protein synthase enzymes (FabB and FabF), which condense malonyl-ACP with acyl-ACP to extend the fatty acid chain by two carbon atoms (Schujman et al., 2006, Schujman et al., 2008). However, the blockade in fatty acid synthesis under high cerulenin concentrations negatively impacts on cell viability. This and the high cost of cerulenin greatly limit its use for commercial-scale malonyl-CoA production (Davis et al., 2000). Despite its limited commercial application, experimentation with cerulenin concentrations to incite increasing malonyl-CoA concentrations was crucial in establishing malonyl-CoA as the modulatory effector molecule for regulating fatty acid synthesis in Gram- positive bacterial species (Schujman et al., 2006, Schujman et al., 2003).

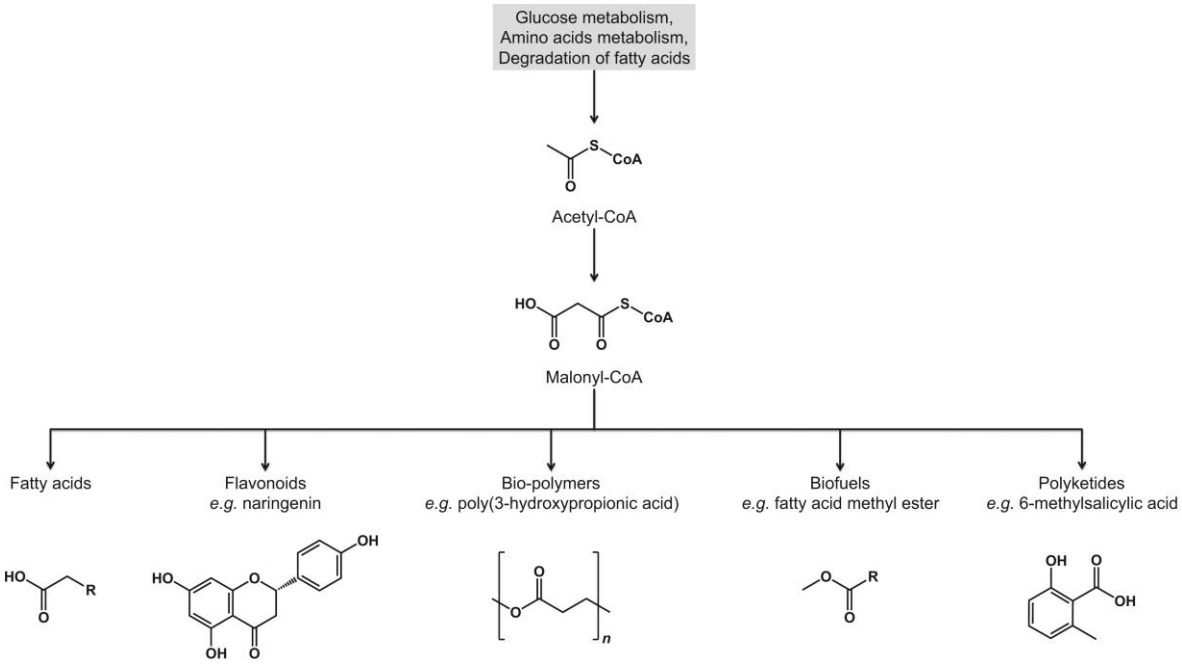

Figure 1.11: Compounds derived from malonyl-CoA. Malonyl-CoA, a direct product of acetyl-CoA, can be used as a precursor for the synthesis of fatty acids, flavonoids, bio-polymers, biofuels, and polyketides.

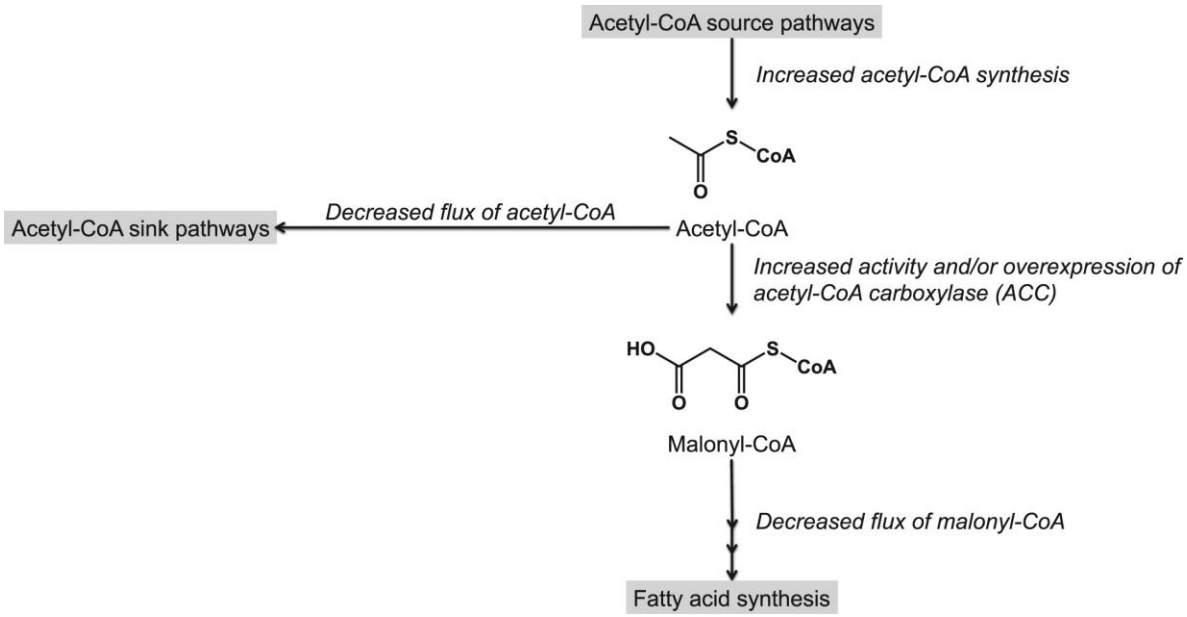

Figure 1.12: A summary of metabolic engineering strategies to increase intracellular malonyl-CoA concentration.
Increasing the pool of acetyl-CoA, decreasing the flux of acetyl-CoA towards non-malonyl-CoA producing acetyl-CoA sink pathways, increasing the expression and/or activity of acetyl-CoA carboxylase and decreasing the flux of malonyl-CoA towards fatty acid synthesis, are direct ways of improving intracellular malonyl-CoA accumulation.

Table 1.4: Notable examples of conventional metabolic engineering strategies to increase intracellular malonyl-CoA amount and end chemicals

Strategy	Mechanism	Microbial host	Malonyl CoA	End chemical	Reference
Increased expression of acetyl-CoA carboxylase (ACC)	Overexpressing the four subunits of *E. coli* acetyl-CoA carboxylase (ACC) in a low copy number plasmid under the control of T7 promoter.	*E. coli*	100-fold increase relative to WT	6-fold increase in free fatty acid synthesis	Davis et al. (2000)
	Overexpression of the two subunits of *Corynebacterium glutamicum* acetyl-CoA carboxylase (ACC) in a high copy number plasmid under the control of T7 promoter.	*E. coli*	Not quantified	60 mg/L yield in flavanones	Miyahisa et al. (2005)
	Changing the promoter of *ACC1* to a strong constitutive promoter TEF1.	*S. cerevisiae*	Not quantified	60% increase in 6-methyl acetyl–salicylic acid	Wattanachaisaereekul et al. (2008)
Increased activity and expression of native acetyl-CoA carboxylase (ACC)	Site-directed mutagenesis of S659 and A1157 to reduce SNF1-mediated phosphorylation of Acc1; overexpression of Acc1 WT and mutants.	*S. cerevisiae*	Not quantified	65% increase in total fatty acid content, 3-fold increase in fatty acid ethyl esters (FAEE), and 3.5-fold increase in 3-hydroxypropionic acid (3-HP)	Shi et al. (2014)

Table continues below

Strategy	Mechanism	Microbial host	Malonyl CoA	End chemical	Reference
Increased acetyl-CoA flux towards malonyl-CoA accumulation	T7 promoter-controlled overexpression of acetyl-CoA carboxylase (ACC), overexpression of acetyl-CoA synthetase, which recycles acetate to acetyl CoA; double knock-out of genes encoding phosphotransacetylase (Pta) and acetate kinase (AckA), which are genes responsible for acetate biosynthesis from acetyl-CoA; deletion of alcohol/aldehyde dehydrogenase (*adhE*).	*E. coli*	15-fold increase relative to WT	4-fold increase in phloroglucinol production	Zha et al. (2009)
	Overexpression of the four subunits of *Photorhabdus luminescens* acetyl-CoA carboxylase (ACC) in a low copy number plasmid and overexpression of *Photorhabdus luminescens* biotin ligase (BirA) in a high copy number episomal vector. Biotin ligase catalyzes the biotinylation of the biotin-dependent BCCP subunit of ACC.	*E. coli*	Not quantified	1166% increase in flavonone synthesis	Leonard et al. (2007)

Table continues below

Strategy	Mechanism	Microbial host	Malonyl CoA	End chemical	Reference
Decreased expression of malonyl-CoA-consuming enzymes	Use of anti-sense RNA to silence the expression of malonyl-CoA transacylase (FabD) – a fatty acid synthesis enzyme.	*E. coli*	4.5-fold increase relative to WT	2.53-, 1.70-, 1.53-fold increase in the production of 4-hydroxycoumarin, resveratrol, and naringenin, respectively	Yang et al. (2015)
Expression of other malonyl-CoA source pathway	Overexpressing the malonate carrier protein (matC), which transports malonate into the cell and malonyl-CoA synthetase (matB), which converts malonate to malonyl-CoA.	*E. coli*	Not quantified	100.64 mg/L of (2*S*)-naringenin	Wu et al. (2014)
Use predictive computational models to select a combination of metabolic engineering approaches for strain optimization	Overexpression of acetyl-CoA carboxylase (ACC), phosphoglycerate kinase (PGK) and pyruvate dehydrogenase (PDH), coupled with double knock-out of fumarase (*fumC)* and succinyl-CoA synthetase (*sucC*) genes.	*E. coli*	3.7-fold increase relative to WT	474 mg/L naringenin production	Xu et al. (2013)
	Overexpression of acetyl-CoA carboxylase (ACC), biotin ligase (BirA), pantothenate kinase in a citric acid cycle genes (*sdhCDAB* and *citE*), amino acid transporter gene (*brnQ*), alcohol dehydrogenase gene (*adhE*) deletion strain.	*E. coli*	2.7-fold increase in relative to WT	660 % fold increase in naringenin synthesis and 420 % fold increase in eriodictyol synthesis	Fowler et al. (2009)

1.13 Development of chassis-compatible expression vectors

Recombinant strain engineering via plasmid-borne expression/overexpression of specific gene(s) has enormous capabilities for genetic manipulation towards desired metabolic phenotypes. By leveraging polished synthetic biology crafts using standardized biological parts; recombinant plasmid vectors have evolved into highly modular expression systems in microbial cell factories. Hence aside heterogeneous over-expression/expression of metabolic genes, recombinant plasmids have also been applied in the design of plasmid modules for (1) mediating genome editing; (2) engineering genetic sensors and circuits for tunable/dynamic protein expression and metabolite biosynthesis. However, beyond function-driven design of plasmid constructs, it is required that the cellular physiology and native machineries of replication and transcription of chosen microbial cell factories is properly understood in order to ensure chassis-compatibility of vectors with the microbial cell factory.

Unlike conventional microbial cell factories like *E. coli* and *Saccharomyces cerevisiae*, the replication and transcriptional machineries for gene expression and regulation in *Ralstonia eutropha* is not totally understood, despite availability of its genetic information (Pohlmann et al., 2006, Cramm, 2009, Schwartz et al., 2003). Expanding the synthetic biology toolbox for efficient genetic manipulation hence begins with the construction of plasmid systems that are compatible with its native replication and transcriptional machineries. Typically, only broad-host range plasmids requiring strand displacement replication mechanism are able to replicate in *Ralstonia eutropha*, for reasons yet to be fully elucidated (Jain and Srivastava, 2013). Narrow range plasmids are transferable into *Ralstonia eutropha* only if they possess a *mob* site from a broad host range plasmid which functions as an origin of transfer. However, the rather cumbersome conjugative transfer is required for bacterial transformation of such plasmids. Additionally, when transformed, these narrow host range plasmids are still unable to replicate, and thus remain as suicide vectors without potential use as expression systems. These constraints immediately limit the choice of plasmid vectors for altering cellular phenotypes to broad host range plasmid and/or recombinant plasmid with broad host range plasmid origin of replication. Electroporation method of bacterial transformation is leveraged on for efficient cellular transfer of these plasmids in order to aid their functions as expression vectors of predefined genes.

Previous studies have focused on leveraging broad host range plasmid for expanding the synthetic biology toolbox for *Ralstonia eutropha*. For example, the broad-host range pBBR1-based vectors are plasmids for have been employed for heterologous gene expression in *Ralstonia eutropha* (Dennis et al., 1998, Kovach et al., 1994, Kovach et al., 1995). Other broad host range plasmids derivatives such as pKT230 (Park et al., 1995), pBHR1 (Solaiman et al., 2010), pCM62 (Bi et al., 2013), have also been employed as expression vectors. Beyond BHR origins, other biological components and properties of suitable plasmid constructs, also inform their suitability for gene expression in *Ralstonia eutropha*. These include vital biological parts for plasmid stability, plasmid mobilization, and host-compatible promoter systems.

1.14 Promoter engineering

Maximal product yield and titre are key requirements in biomanufacturing. To this end, metabolic pathway optimization is vital in eliminating metabolic bottlenecks that compromise cellular productivity and metabolic phenotypes that are detrimental to cell viability (Johnson et al., 2018, Johnson et al., 2017). Proven strategies of tuning gene expression of a metabolic pathway include varying plasmid copy number, gene dosage and promoter strength, among others (Johnson et al., 2018). Inducible promoters are applicable where tunable control of gene expression is required. The L-arabinose inducible P_{BAD} promoter is particularly a choice promoter for controllable gene expression owing to its fast induction rate, its repressibilty, high expression level and tight modulation (Guzman et al., 1995). It has hence been widely utilized as a promoter system in plasmid vectors for inducible expression in *Ralstonia eutropha* (Fukui et al., 2011, Bi et al., 2013). Leveraging on promoter strength of constitutive promoters for pathway optimization however requires proper characterization, standardization of promoters for universal comparison of promoter activity (Johnson et al., 2018). It also requires promoter engineering strategies to tune promoter activity at both transcriptional and translational levels (Johnson et al., 2018).

1.15 Metabolite sensing genetic circuits

The field of metabolic engineering has witnessed rapid advancements, further consolidating it as an enabling technology for engineering biological cell factories for producing value-

added chemicals and bio-products. A key advancement is the application of synthetic biology to construct orthogonal genetic circuits or biosensors for *in vivo* detection of metabolites (Liao and Oh, 1999, Mainguet and Liao, 2010, van der Meer and Belkin, 2010). Such synthetic biosensors are archetypal of naturally evolved biosensors that propagate changing environmental signal or cellular status into a biological actuation or cellular phenotype that promotes either cell viability, survival or metabolic economics (Harrison and Dunlop, 2012, Liu et al., 2015b, Liu et al., 2015a). These biosensors are often made up of two components: metabolite-responsive transcriptional regulator and fluorescence-coupled or fitness-related read-out module (Harrison and Dunlop, 2012, Rogers et al., 2015). This enables metabolic engineers to efficiently quantify varying concentration of cellular metabolites in contrast to the more time consuming and lower throughput bio-analytical methods such as HPLC and LC-MS (Dietrich et al., 2013, Liu et al., 2015b, Liu et al., 2015a). Metabolite-sensing genetic circuits have been reported for sensing various metabolites including macrolides (Mohrle et al., 2007), acetyl phosphate (Farmer and Liao, 2000), farnesyl pyrophosphate (Dahl et al., 2013), 3-hydroxypropanoic acid (Rogers and Church, 2016, Rogers et al., 2015), 1-butanol (Dietrich et al., 2013), and more recently, malonyl-CoA (Ellis and Wolfgang, 2012).

The use of biosensors for *in vivo* detection and/or quantification of metabolite essentially creates an input-output communication platform within biological cells. This platform has predominantly been exploited for real-time monitoring of metabolite or product accumulation, *i.e.*, product formation kinetics, allowing metabolic engineers to study product formation dynamics over a cultivation period. In turn, this enables detection of metabolic pathway bottlenecks and other factors that potentially limit end product titers. That said, biosensors have also found front-end applications as dynamic metabolic pathway regulators and back-end applications as screening devices. When applied for dynamic metabolic pathway regulation, biosensors allow the cell to respond to environmental perturbations or potentially detrimental metabolic phenotypes by adjusting pathway expression towards more effective carbon flux for the desired end products (Xu et al., 2014a). When applied as screening devices, they are used to screen for and select high producer genetic variants, and in some cases, for identifying optimized process conditions for high product titers (Dietrich et al., 2010, Dietrich et al., 2013, Williams et al., 2016). All of these applications potentially help to fast track design-build-test cycles in engineering

synthetic metabolic pathways by facilitating genotype manipulation-phenotype evaluation processes (Rogers et al., 2015, Rogers and Church, 2016). Over all, these applications require that such sensors are well crafted and programmed with the right level of specificity, sensitivity and dynamic range needed for their functionality.

1.15.1 Malonyl-CoA biosensors

Malonyl-CoA biosensors are a synthetic mimicry of the native fatty acid biosynthesis transcriptional regulatory circuits, found naturally in many Gram-positive bacteria such as *Bacillus subtilis*, *Staphylococcus aureus, Bacillus anthracis*, *Listeria monocytogenes and Streptococcus pneumonia* (Fujita et al., 2007, James and Cronan, 2003, Li et al., 2015, Liu et al., 2015b, Xu et al., 2014a). This regulation is modulated by the interaction between transcription factor FapR (Fatty acid and phospholipid Regulator) and its operator *fapO*. FapR represses the fatty acid operon through binding to the 17-bp *cis*-regulatory *fapO* operator localized within or in proximity to the operon's promoter. Malonyl-CoA acts as an inducer of the FapR regulon by impairing the FapR-*fapO* interaction. Through replacing the fatty acid operon with a gene encoding a reporter protein, for instance a fluorescence protein, a biosensor that is transcriptionally regulated by malonyl-CoA is created, where the reporter protein activity reflects the intracellular malonyl-CoA concentration.

1.15.2 Mechanism of malonyl-CoA sensing

The naturally occurring fatty acid biosynthesis regulon consists of an autogenously regulated FapR transcriptional repressor module localized adjacent to a fatty acid synthesis operon whose expression is driven by a hybrid promoter possessing a 17-bp *cis*-regulatory *fapO*-operator (James and Cronan, 2003). FapR mediates the repression of fatty acid synthesis genes via DNA-protein interaction with the *fapO*-operator sequence using its N-terminal regulatory domain (K_D = 0.12 μM) (Xu et al., 2014a). This interaction cascades into a FapR-*fapO* complex that sterically hinders RNA polymerase from inducing transcription of the downstream fatty acid synthesis genes. Intracellular accumulation of malonyl-CoA gradually relieves this FapR-mediated repression through metabolite-protein interaction of malonyl-CoA with the C-terminal ligand-binding domain of FapR (K_D = 2.4 μM) (Ellis and Wolfgang, 2012, Xu et al., 2014a, Schujman et al., 2003, Schujman et al., 2006). This interaction triggers a conformational change at the N-terminal of FapR, which destabilizes the FapR-*fapO* complex and relieves FapR from interacting with *fapO*-operator,

thereby permitting interaction of RNA polymerase with the promoter, and thus transcription (Figure 1.13).

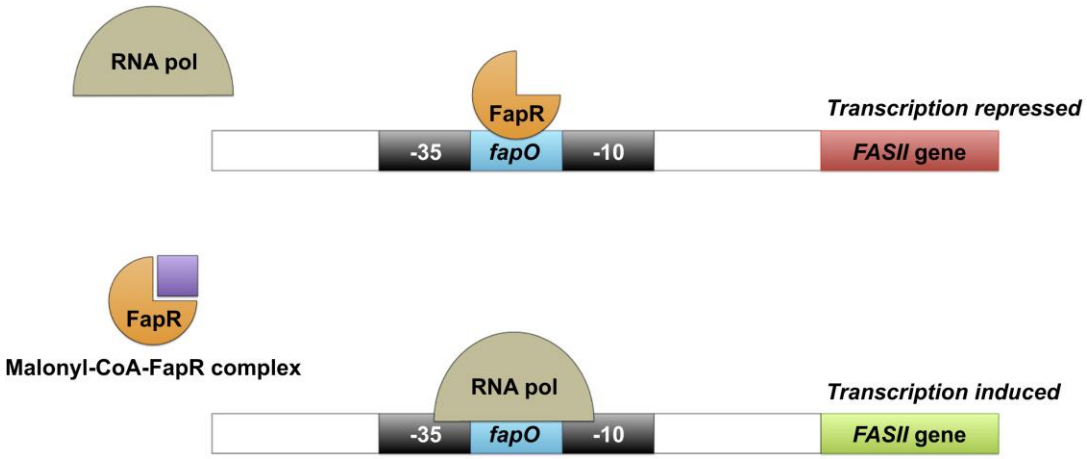

Figure 1.13: Mechanism of malonyl-CoA sensing.
Binding of malonyl-CoA to the C-terminus of FapR cascades into a conformation change at its N-terminus, which destabilizes FapR-fapO interaction. This enables the formation of an RNA polymerase-promoter complex, thus inducing transcription of the downstream fatty acid synthesis gene (FASII).

1.15.3 The architecture of a malonyl-CoA biosensor

The design of a typical malonyl-CoA-sensor (Figure 1.14) requires prototyping its modular architecture after the naturally occurring fatty acid biosynthesis regulon discussed above (Figure 1.13). A repressor module is located on one end of the circuitry, comprising a *fapR* gene and a suitable promoter driving the FapR expression. In the reporter module on the other end, there is a reporter gene typically encoding a fluorescence protein (*e.g.*, *eGFP*, *rfp*, *mCherry* and *tdTomato*); the expression of which is driven by a *fapO*-hybrid promoter with the *cis*-regulatory *fapO*-operator sequence co-located within or adjacent to the reporter promoter. Identical to the naturally occurring regulons, the reporter module translates the increase in intracellular malonyl-CoA concentration (*i.e.*, input) into the expression level of the reporter protein (*i.e.*, output), at a rate that is commensurate with the degree of de-repression of the reporter promoter. Hence, by inciting precise and measurable increase in intracellular concentration of malonyl-CoA (*e.g.*, through the use of cerulenin), the resulting increase in fluorescence signal generates a malonyl-CoA concentration-dependent calibration curve. This, in turn, serves as an input-output model for using such malonyl-

CoA sensors to quantify unknown malonyl-CoA concentrations derived from malonyl-CoA source pathways.

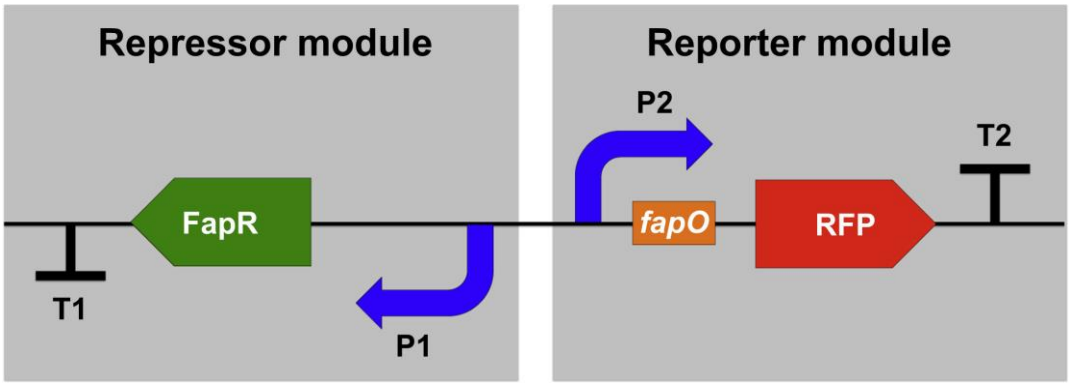

Figure 1.14: Schematic diagram of the architecture of a malonyl-CoA sensor showing its modularity with a repressor module (P1 and FapR gene) and a reporter module (P2, *fapO* and RFP gene). P1 – repressor promoter, P2 – reporter promoter, O – *fapO* operator, T1, T2 – transcriptional terminators.

1.15.4 The design criteria of an effective malonyl-CoA biosensor

Crafting a functionally effective malonyl-CoA sensing genetic circuit for a biological host requires a number of design considerations. Firstly, the biological chassis in question (*i.e.*, the host itself) potentially predetermines the ease of transformation/transfection of the genetic circuit as well as its replication and maintenance within the chassis. This must be duly factored into the structural design of the circuit. In other words, the sensor must have a plasmid backbone with an origin of replication that is compatible with the replication machinery of the host (Li et al., 2015). Moreover, a dual plasmid circuit system with separate vectors for the repressor and reporter modules may be required for some organisms, where a large plasmid may prove difficult to be transformed or transfected. This latter case also requires due consideration of plasmid incompatibility and the choice of selection marker. A fitting example of how these considerations are crucial is seen in the malonyl-CoA biosensors that were developed to investigate fatty acid metabolism in mammalian cells, where carefully selected biological parts facilitated sensor functionality, such as transfection, replication and expression *etc*, in the mammalian host (Ellis and Wolfgang, 2012).

Secondly, a functionally effective sensor requires a fine-tuned balance in expression from both the repressor and reporter modules (Figure 1.16). This is a pre-requisite for a high detection limit and a broad dynamic range of response. The upper detection limit of the sensor is, however, also physically constrained by the maximum possible concentration of malonyl-CoA that does not negatively impact on cellular viability. Additionally, fine-tuning is necessary to achieve optimal sensitivity (*i.e.*, responsive to small changes in intracellular malonyl-CoA concentration), responsivity (*i.e.*, yielding a measurable read-out value), and a high signal-to-noise ratio in response to malonyl-CoA. This intricate balance requires intracellular FapR repressor concentration to be optimal: high enough to achieve high detection limit, but not too high so as to avoid poor sensitivity. Likewise, the expression of the reporter module should be high enough to achieve detectable read-out response, but not too high so as to avoid sub-optimal repression of the reporter module (Figure 1.16).

Despite the importance of a fine-tuned repressor to operator ratio, there is no algorithm to design a well-balanced malonyl-CoA sensor, at least not to our knowledge. In practice, most sensors are achieved by extensive experimentation and trial-and-error. Common strategies are summarized in Figure 1.17, one of which is experimenting with plasmid copy number (low, medium, and high) of the genetic circuit to modulate the expression of both repressor and reporter modules. This parameter is more profound in cases where the repressor and reporter modules of the sensor circuit are expressed from separate plasmids. Alternatively, a wide range of promoters (constitutive or inducible) can be leveraged to tune for the right cellular transcription of the *fapR* gene. The promoter strength can be utilized in conjunction with *cis*-regulatory biological parts such as ribosome binding site (RBS) (Peretti and Bailey, 1987), upstream activation sequence (UAS) (Aiyar et al., 1998) and mRNA stem-loop (Paulus et al., 2004) to attain a desired level of FapR repressor (Figure 1.17). The copy number and location of the *fapO*-operator within the *fapO*-hybrid reporter promoter could significantly influence the degree of FapR-*fapO* interaction (Xu et al., 2014a), thus potentially affecting response to increasing malonyl-CoA amounts. In some cases, the copy number and the precise location of the *fapO*-operator could also influence the response through altering the resultant activity of the *fapO*-hybrid reporter promoter.

Lastly, unlike in naturally occurring regulons where the *fapR* promoter is autogenously regulated, the sensor promoters (both the *fapR* promoter and the reporter promoter excluding *cis*-regulatory *fapO*-operator sequence) in a malonyl-CoA biosensor must show minimal, ideally no, regulatory response to the FapR protein. Also, to ensure sensor orthogonality, the activities of the chosen promoters must not be naturally modulated by acyl-CoAs and/or any other intracellular metabolites. These are particularly crucial requirements to ensure that the sensor's response to increasing malonyl-CoA amounts is exclusively an actuation of malonyl-CoA-FapR-*fapO* interactions. Making due design considerations for these requirements eliminates noise interferences in sensor response and invariably validates the correlation between fluorescence read-out responses and intracellular malonyl-CoA amounts. Examples of how the aforementioned design considerations have been successfully applied are detailed in Table 1.5.

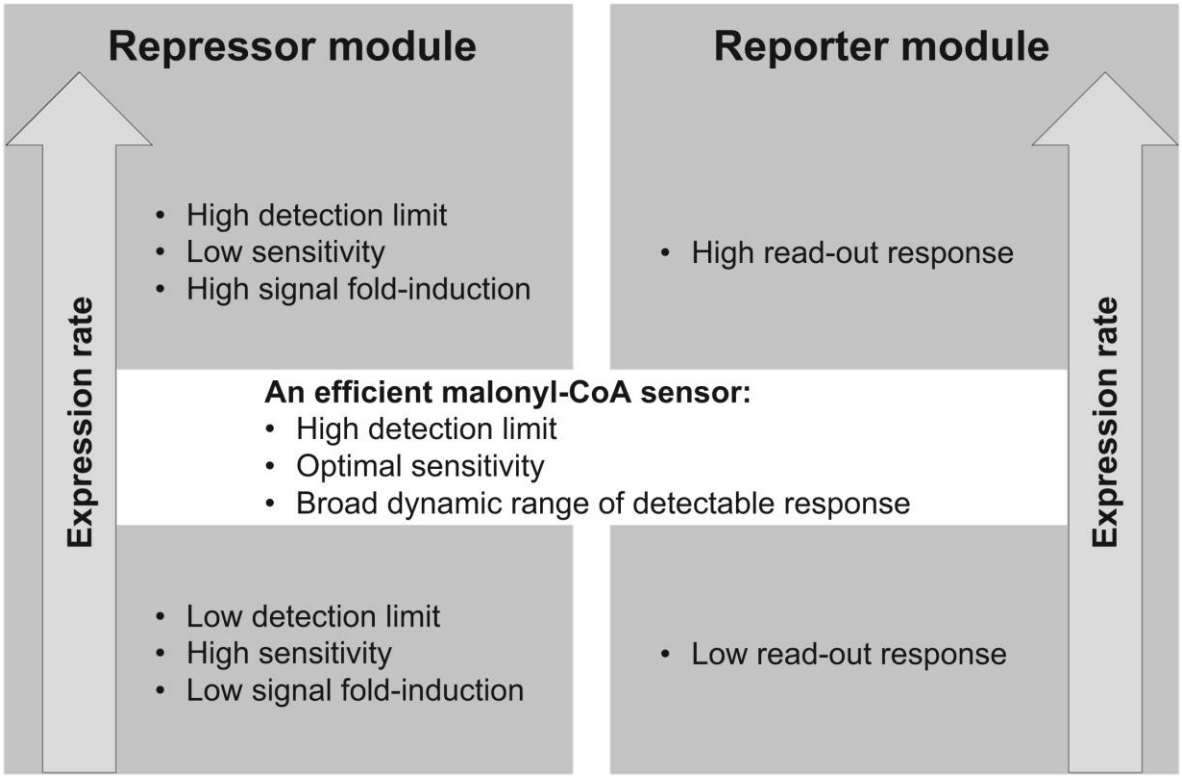

Figure 1.16: A schematic of the key design considerations for crafting an efficient malonyl-CoA biosensor.

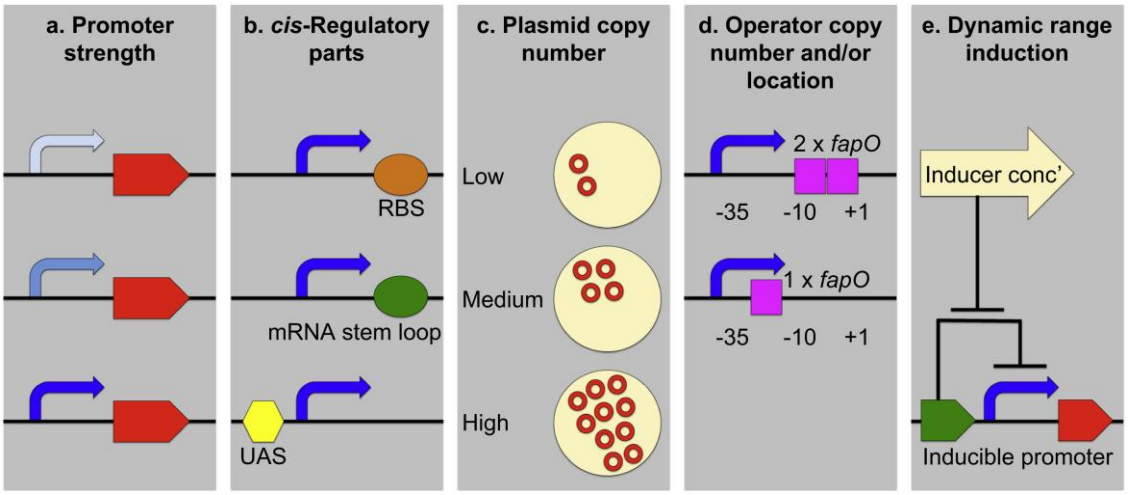

Figure 1.17: Key biological parts for crafting versatile malonyl-CoA sensors.
(a) Choosing a promoter with the right transcriptional activity, (b) Tuning for the right promoter activity with *cis*-regulatory elements such as ribosome binding site (RBS), upstream activation sequence (UAS) or mRNA stem loop, (c) Varying the copy number of plasmid expressing the reporter and/or repressor module, (d) Varying the copy number and/or location of the *fapO*-operator sequence, and (e) Tuning the expression using varying inducer concentration, when an inducible promoter is adopted.

Table 1.5: A summary of reported malonyl-CoA sensors

Microbial Host	Repressor Module		Reporter Module			Regulatory mechanism	Dynamic detection range	Ref.
	Promoter	**Repressor**	**Promoter**	**Operating Site**	**Reporter**			
E. coli	IPTG-inducible T7	FapR	IPTG-inducible T7	*fapO* inserted after the transcriptional start of T7 promoter	*eGFP*	Binding of FapR to the *fapO/ lacO/ fapO.lacO* operator of the T7 *eGFP* promoter thus repressing the expression of *eGFP*	0.1–1.1 nmol/mgDW	(Xu et al., 2014b)
E. coli	*L*-arabinose inducible P_{BAD}	FapR	P_{FR1}	*fapO* inserted into the flanking regions of -10 region of phage P_{A1} promoter resulting in P_{FR1}	*rfp*	Binding of FapR to the *fapO* of P_{FR1} thus repressing the expression of *rfp*	0.14–24.4 μM	Feher et al. (2015), Liu et al. (2015b)

Table continues below

Microbial Host	Repressor Module		Reporter Module			Regulatory mechanism	Dynamic detection range	Ref.
	Promoter	**Promoter**	**Promoter**	**Operating Site**	**Reporter**			
E. coli	pGAP, transcribed by *E. coli* RNA polymerase	FapR	pGAP	*fapO* inserted after the transcriptional start of pGAP.	*eGFP*	Binding of FapR to the UAS of pGAP thus activating the expression of *eGFP*	0.1–1.1 nmol/mgDW	Xu et al. (2014a)
	Constitutive T7 promoter	FapR	Constitutive T7 promoter	*fapO* inserted after the transcriptional start of T7 promoter	*mCherry*	Binding of FapR to the *fapO* of pGAP thus repressing the expression of *mCherry*	0.1–1.1 nmol/mgDW	
S. cerevisiae	TEF1	FapR	GPM1	Inserted before the TATA box of the GPM1 promoter	*tdTomato*	Binding of FapR to the *fapO* of GPM1 thus repressing the expression of *tdTomato*	Malonyl-CoA amount equivalent to 1- 12 mg/L cerulenin	Li et al. (2015)

1.15.5 Applications of malonyl-CoA biosensors

Dynamic quantification of malonyl-CoA has been widely demonstrated in mammalian cells (Ellis and Wolfgang, 2012) and model microbial cell factories (*e.g.*, *E. coli* and *S. cerevisiae*) (Li et al., 2015, Xu et al., 2014b) using chemical agents such as cerulenin and triclosan, known to block the fatty acid biosynthesis thereby inducing intracellular accumulation of malonyl-CoA (Johnson et al., 2017, Zhang et al., 2006). Increased malonyl-CoA concentration resulting from heterologously expressed source pathways has also been quantified (Johnson et al., 2017). Examples include acetyl-CoA carboxylase (ACC), which converts acetyl-CoA into malonyl-CoA, and malonyl-CoA synthetase (MatB), which converts malonate, channeled into the cell via malonate carrier protein (MatC), into malonyl-CoA. Using malonyl-CoA biosensors, malonyl-CoA levels ranging from 0.1–1.1 nmol/mg DW can be detected in the aforementioned hosts.

Other than the detection and quantification of intracellular malonyl-CoA accumulation, malonyl-CoA biosensors have also been modified into more complex genetic circuits, primarily to enhance cellular malonyl-CoA production or to facilitate the selection of high malonyl-CoA-producing strains. This of course requires more complex structural and system design considerations in crafting such circuits with relevant modular functionalities specific to the intended application(s). In this section, we review the design of such circuits and how they were applied for improved cellular production of malonyl-CoA and its end chemicals.

1.15.5.1 Sensor-actuator

The application of malonyl-CoA sensors for *in vivo* detection of malonyl-CoA relies heavily on the linearity between varying malonyl-CoA concentrations and fluorescence read-out responses as well as the orthogonality of the genetic circuit (*i.e.*, elimination of regulatory protein and nonspecific DNA cross-communication). Hence, profiling how cellular fluorescence varies with intracellular malonyl-CoA level (and with time of cultivation in some cases) is a standard procedure in characterizing the biosensor constructed.

To illustrate this, Xu *et al.* reported the construction of two promoter-regulator variants in *E. coli* (Xu et al., 2014a). They exhibited different kinetic response to increasing malonyl-

CoA concentrations induced by increasing cerulenin concentrations. The first circuit (Figure 1.18a) consisted of an IPTG-inducible T7 promoter driving the FapR expression, and an IPTG-inducible *lacO.fapO*-hybrid T7 promoter driving the expression of a downstream *eGFP* reporter gene. The second circuit (Figure 1.18b) had the same circuitry as the former, except that the *eGFP* T7 promoter lacked the *fapO*-operator but had the *lacO*-operator. It was observed that the FapR repressor exhibited cross-communication with the *lacO*-operator, in both the first and second circuits. In other words, *eGFP* T7 promoter could be repressed via either FapR-*fapO* interaction or FapR-*lacO* interaction or both interactions simultaneously. IPTG induction of the T7 promoters in the above two circuits at low malonyl-CoA concentrations (<0.63 nmol/mgDW, induced by addition of <25 μM cerulenin) resulted in a biphasic kinetic response – exhibiting increasing EGFP fluorescence signal in the first phase (t < 300 minutes), and subsequently decreasing EGFP fluorescence in the second phase (t > 300 minutes). The first phase was characterized by constitutive expression of lacI repressor, and IPTG-induced derepression of lacI-mediated repression of the *eGFP* T7 promoter at the *lacO*-operator. The second phase, however, was characterized by IPTG-induced FapR expression and FapR-mediated repression of the *eGFP* T7 promoter (at both *lacO* and *fapO* sites in the first circuit and the *lacO* site in the second circuit). This biphasic response was however gradually abolished at high malonyl-CoA concentration (>0.63 nmol/mgDW, induced by addition of >25 μM cerulenin), as more FapR repressor molecules were antagonized by malonyl-CoA, thus actuating continued increase in fluorescence response beyond 300 minutes of cultivation. The inconsistent response profile at low and high malonyl-CoA concentration meant that the promoter-regulatory systems could not actuate fluorescence signals over time consistent with malonyl-CoA concentration, and as such was unusable for real time monitoring of intracellular malonyl-CoA accumulation or consumption. To solve this problem, the *lacO* site in the *eGFP* T7 promoter in the first circuit was removed yielding a third circuit (Figure 1.18c). This abolished the *lacI*-mediated repression of *eGFP* T7 promoter at the *lacO*-operator and cross-communication of FapR repressor at the *lacO*-operator, thus correcting the biphasic response due to *lacO*-operator. The modification effectively improved the circuit's linear response to increasing malonyl-CoA concentrations up to 1 nmol/mgDW.

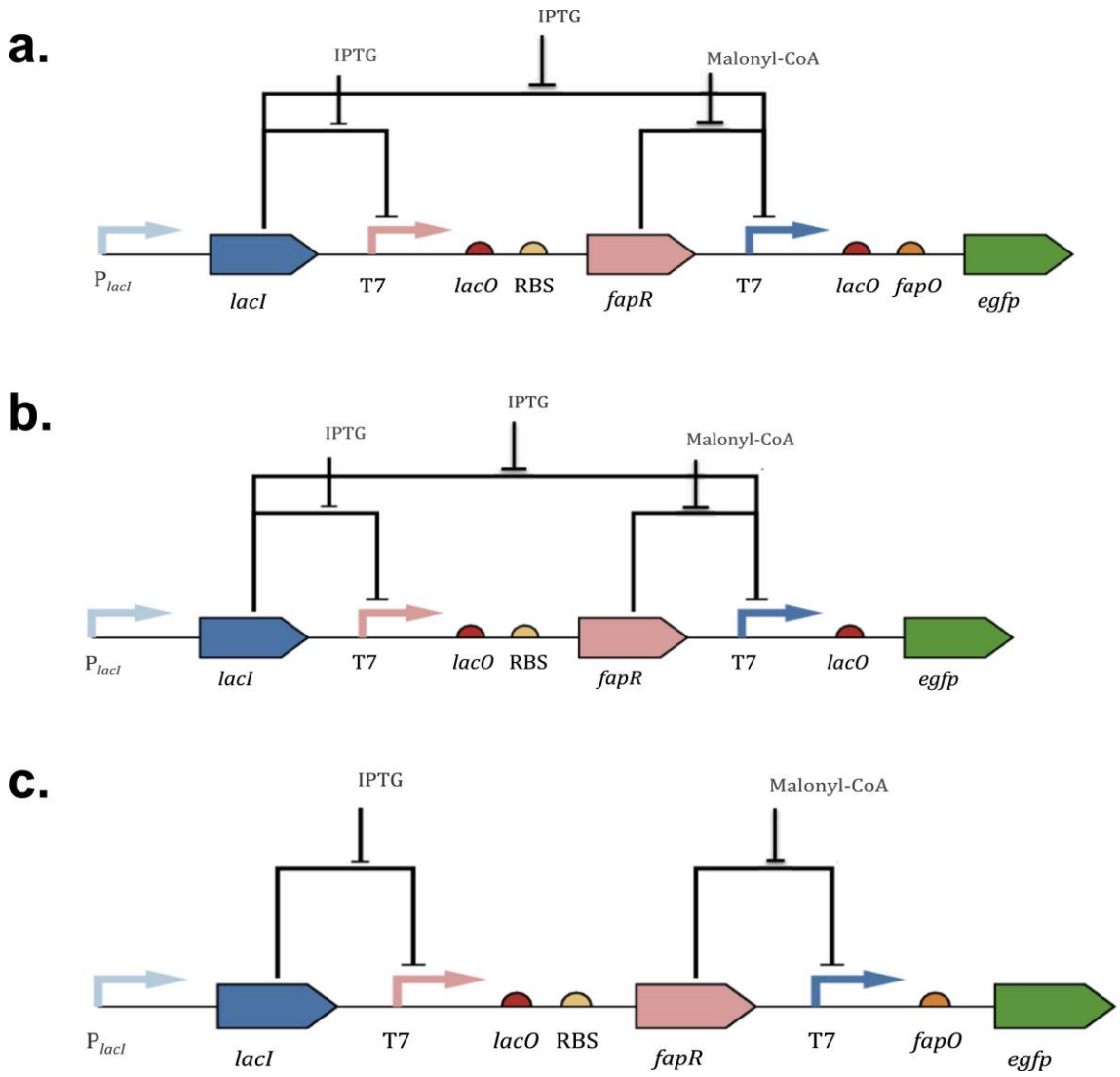

Figure 1.18: Promoter-regulatory circuits for actuation of malonyl-CoA in *E. coli*. (a) A circuit with a *fapO.lacO*-hybrid T7 reporter promoter, (b) A circuit with a *lacO*-hybrid T7 promoter, and (c) A circuit with a *fapO*-hybrid T7 promoter.

1.15.5.2 Sensor-inverter

Liu *et al.* described the development of a sensor-invertor for negative feedback regulation of fatty acid synthesis in *E. coli* by modifying a malonyl-CoA-based sensor-actuator circuit (Liu et al., 2015b). The original sensor-actuator circuit (Figure 1.19a) had a L-arabinose-inducible P_{BAD} promoter driving the expression of FapR repressor, and this repressor module was grafted onto low copy number plasmid. Inserting the *fapO*-operator sequence into two DNA regions flanking the -10 region of a P_{A1} phage promoter resulted in the FapR-repressed *fapO*-hybrid reporter promoter P_{FR1}, which drove the expression of an *rfp* reporter gene from a second plasmid. Varied intracellular malonyl-CoA concentrations

were achieved via IPTG-inducible expression of the acetyl-CoA carboxylase gene (*acc*)-based malonyl-CoA source pathway, placed under the control of the LacI-repressed T7 promoter from a third plasmid. At an optimal expression of FapR repressor [with 0.01% (w/v) L-arabinose], a 4-fold increase in the fluorescence signal from the reporter module was achieved, when cellular malonyl-CoA amount was varied by induction with 0 mM to 1 mM IPTG. This increase in fluorescence signal correlated with the measured increase in malonyl-CoA concentration, resulting in fluorescence versus malonyl-CoA concentration calibration curve for rapid fluorescence-based quantification of cellular malonyl-CoA concentrations (Liu et al., 2015b). Subsequently, this sensor-actuator was modified into a sensor-invertor (Figure 1.19b) to alleviate *acc*-overexpression-mediated cellular toxicity and for dynamic regulation of malonyl-CoA source and sink pathways towards increased fatty acid production. By replacing the *rfp* reporter gene with a *lacI* gene, increasing malonyl-CoA concentrations (achieved with 0–40 μM IPTG) was actuated into increasing expression of LacI repressor. This, in turn, would repress the expression of *acc* at unfavorably high malonyl-CoA concentrations, thus gradually decreasing malonyl-CoA synthesis. Additionally, when a cytosolic thioesterase (*tesA*)-based fatty acid synthesis pathway under the control of an aTc-inducible P_{Tet} promoter was co-transformed with the sensor-invertor (Figure 1.19b), 34% and 33% increases in fatty acid titre and productivity, respectively, were achieved, relative to when it was co-transformed with just the sensor-actuator.

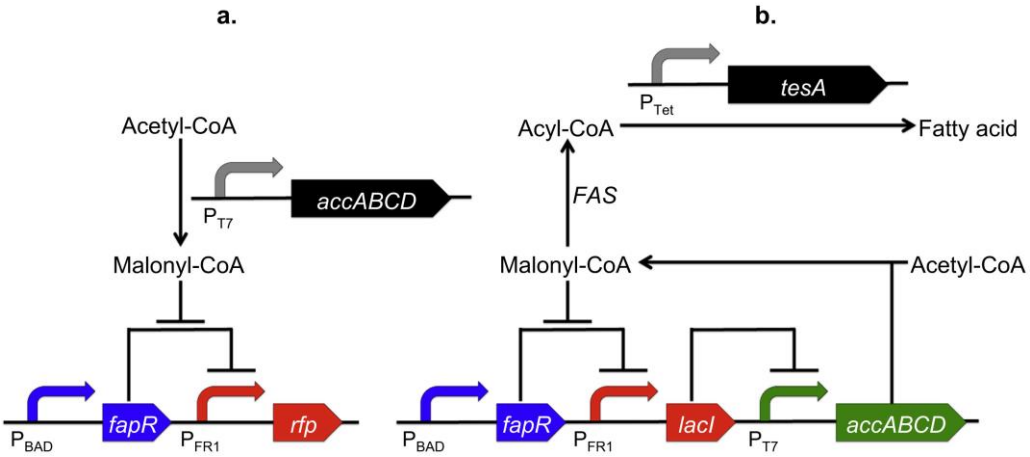

Figure 1.19: Schematic representation of a malonyl-CoA sensor-actuator and a negative feedback regulatory circuit.
(a) The malonyl-CoA sensor-actuator comprises the P_{BAD}-driven FapR repressor module, the PFR1-driven reporter module and the P_{T7}-driven malonyl-CoA source pathway (accABCD). (b). The circuit comprises P_{Tet}-driven cytoplasmic thioesterasse gene (tesA), the LacI-repressed, P_{T7}-driven malonyl-CoA source pathway (accABCD), the FapR-repressed, PFR1 –driven lacI gene and the P_{BAD}-driven FapR. The biosensor turns on lacI expression at excessively high malonyl-CoA amount thereby down-regulating acc expression and alleviating its cellular toxicity.

1.15.5.3 Metabolic switch for autonomous metabolism control

Xu *et al.* described a metabolic switch that reported the malonyl-CoA metabolic state of the cell by distinct on/off fluorescence signals (Xu et al., 2014a). In this sensor (Figure 1.20a), an *E. coli* σ70-based pGAP promoter was used to drive the expression of eGFP reporter protein. However, FapR repressor expression resulted in a 7-fold increase in the pGAP-driven *eGFP* expression. This clearly suggested that FapR exhibited promoter activity-influencing protein-protein interaction with RNAP-pGAP complex, rendering it a transcriptional activator instead of a repressor on the pGAP promoter. Also, at malonyl-CoA concentrations above 1 nmol/mgDW, eGFP fluorescence signals were comparable to the control construct lacking the sensor presumably because malonyl-CoA-FapR interaction annulled the activating FapR-RNAP-pGAP interaction. Further investigation with Surface Plasmon Resonance (SPR) analysis confirmed that the activating effect of FapR on the pGAP promoter was exerted on an upstream activating sequence (UAS), but not on the *fapO*-operator. A sensor variant without the *fapO*-operator reported higher fluorescence signal than the sensor with one *fapO*-operator placed after the transcriptional start of the pGAP promoter. Also, on creating a second sensor variant by replacing the pGAP promoter with a FapR-repressed *fapO*-hybrid T7 promoter and replacing eGFP reporter with

mCherry reporter, and co-transforming this sensor variant with the FapR-activated pGAP-based malonyl-CoA sensor, they achieved a malonyl-CoA metabolic switch that responded to both high and low intracellular malonyl-CoA concentrations (Figure 1.20a). At low malonyl-CoA concentrations, the pGAP-based malonyl-CoA sensor was turned on – actuating a green fluorescence signal while the T7-*fapO*-based sensor was turned off. Conversely, at high malonyl-CoA concentration, the FapR-repressed T7-*fapO* hybrid promoter was turned on – actuating a red fluorescence while the FapR-activated pGAP-based malonyl-CoA sensor was turned off. This metabolic switch thus reported the malonyl-CoA metabolic state of the cell by actuating distinct flip-flop states of green and red fluorescence signals. Additionally, as increasing the copy number of *fapO*-units in the FapR-activated pGAP-based malonyl-CoA sensor gradually decreased the promoter activity of the pGAP promoter, a series of finely tuned sensors with varying response range to increasing malonyl-CoA-concentrations were derived. Varying the number of *fapO*-units in the metabolic switch was also leveraged to regulate the on-off flip-flop frequency of the metabolic switch.

The authors then replaced the *eGFP* and m*Cherry* reporter genes with acetyl-CoA carboxylase (*accADBC*) malonyl-CoA-source pathway and the fatty acid synthetase (*fabADGI* and *tesA*') malonyl-CoA-sink pathway, respectively (Figure 1.20b). The oscillatory pattern of the metabolic switch was used to regulate expression in both pathways to achieve 15.7- and 2.1-fold improvement in fatty acid titer compared to the wild type strain and the strain expressing both pathways without the metabolic switch, respectively. In this metabolic switch, when malonyl-CoA amounts from the source-pathway increased above a threshold range, derepressive malonyl-CoA-FapR interaction turned on the sink pathway to convert the malonyl-CoA into fatty acid products. Conversely, when the malonyl-CoA amount reached a critically low value, FapR-RNAP-pGAP interaction up-regulated malonyl-CoA amounts from the source-pathway (Figure 1.20b and 1.20c). Interestingly, it was shown that variants with only one *fapO*-unit in the FapR-activated pGAP promoter showed a more favorable oscillatory pattern in the on state of both sink and source pathways compared to the switch variants with no *fapO* unit or with three *fapO* units. This optimal oscillatory pattern, characterized by a sink-source oscillation faster than the oscillation in the zero *fapO*-unit variant but slower than the oscillation in the three *fapO*-unit variant, resulted in the highest titer of fatty acid (Xu et al., 2014a)

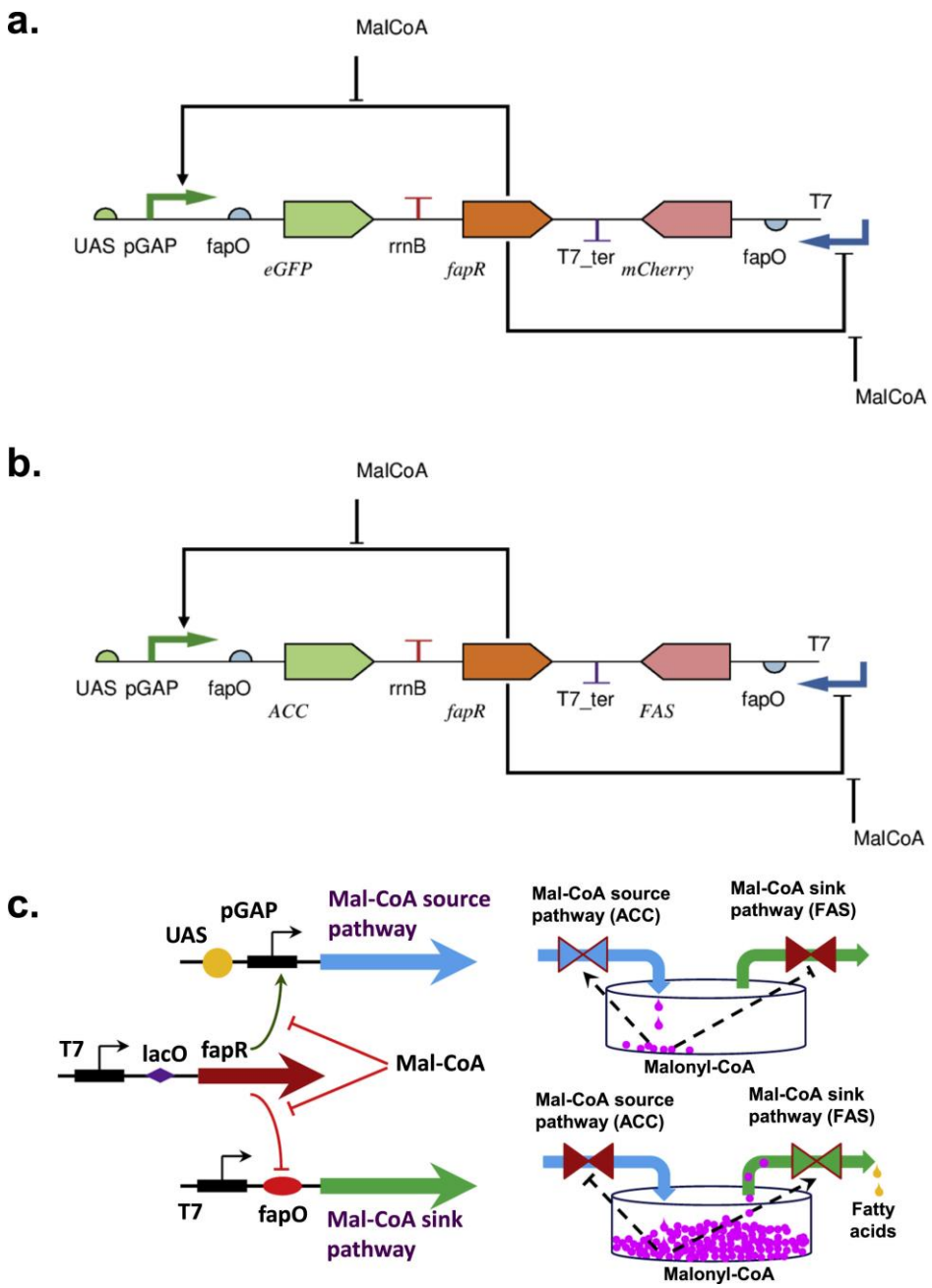

Figure 1.20: Malonyl-CoA metabolic sensor and switch
(a) Schematic representation of malonyl-CoA metabolic sensor. The sensor comprises the FapR-activated, pGAP-driven eGFP gene, and the FapR-repressed, T7-driven mCherry gene. Both promoters possess a *fapO* operator site after their transcriptional start. The sensor gives green fluorescence signal at excess cellular malonyl-CoA amount, and mCherry fluorescence signal at low cellular malonyl-CoA amount. (b) Schematic representation of a malonyl-CoA metabolic switch. The metabolic switch is archetypal of the sensor with the eGFP and mCherry genes replaced with a malonyl-CoA source pathway (ACC) and a malonyl-CoA sink pathway (FAS), respectively. (c) The metabolic switch turns on the expression of the malonyl-CoA source pathway (ACC) and turns off the sink pathway (FAS) at low cellular malonyl-CoA amount. At high cellular malonyl-CoA amount, the switch turns on the sink pathway and turns off the source pathway.

1.15.5.4 Malonyl-CoA producer screening tool

S. cerevisiae, a widely utilized biological cell factory, is known to require biological parts and expression systems uniquely different from other eukaryotic systems and yet more complex than prokaryotic hosts, owing to its rather complex transcriptional and regulatory networks (Li et al., 2015). This, in turn, has limited the development of genetically encoded circuits for metabolite sensing and allied applications. However, by optimizing the functionality of carefully selected biological parts to bolster their compatibility with the host's regulatory requirements, Li *et al.* reported the development of the first ever malonyl-CoA biosensor for *S. cerevisiae* (Li et al., 2015). In this dual plasmid sensor system, a strong constitutive *TEF1* promoter drove the transcription of a codon-optimized *fapR* gene, which had a strong SV40 nuclear localization sequence at its C-terminus to enhance nuclear import and an *ADH1* terminator to terminate transcription. The tdTomato reporter protein was expressed from a separate plasmid under the control of an engineered GPM1 promoter, which had the *fapO*-operator inserted immediately upstream of the TATA box. To tune for a broad dynamic range of sensor responsiveness and optimal sensitivity, the authors varied the sensor FapR-*fapO* ratios. Single copy plasmid and multi-copy plasmids were used to adjust the FapR repressor expression, while the reporter expression was varied by using either a single *fapO*-unit or a double *fapO*-unit operator. By varying the intracellular concentration of malonyl-CoA through media supplementation with varying cerulenin concentrations ranging from 0–12 mg/L, malonyl-CoA-dependent response curves were derived for all sensor variants. Eventually, the sensor design comprising multi-copy plasmid expressing FapR and a reporter module with a single *fapO*-unit resulted in the broadest dynamic range of response to increasing cellular malonyl-CoA concentrations induced by cerulenin concentrations ranging from 0–8 mg/L. Other sensor variants had detection limits of less than 8 mg/L owing either to poor FapR repressor expression (as in the single copy plasmid) or low FapR-*fapO* ratio (as in the sensor variant with a double *fapO*-unit).

The malonyl-CoA sensor with the broadest dynamic response range was subsequently used to screen for high malonyl-CoA producers from a yeast library, co-transformed with the sensor and plasmid carrying genome-wide overexpression cassette. By identifying transformant colonies with the highest fluorescence intensity using three rounds of FACS,

genes enhancing malonyl-CoA synthesis were identified from 11 different clones, which elicited 2-fold higher fluorescence signals. The genes *PMP1* and *TP1*, encoding the plasma membrane proteolipid protein and triose-phosphate isomerase, respectively, were identified as genes which individually or collectively unregulated malonyl-CoA synthesis in yeast strain CEN.PK2 (Figure 1.21) (Li et al., 2015). The genes were subsequently individually expressed in yeast and the ensuing improved malonyl-CoA synthesis was subsequently leveraged on to achieve 120% increase in the titre of 3-hydroxypropanoic acid – a value-added compound and important basic chemical derived from malonyl-CoA. While the attachment of SV40 nuclear localization signal on C-terminal ligand-binding domain facilitated the import of FapR inside the nucleus, this, however, may negatively interfere with the malonyl-CoA-FapR interaction and change the transcriptional activity of the FapR protein.

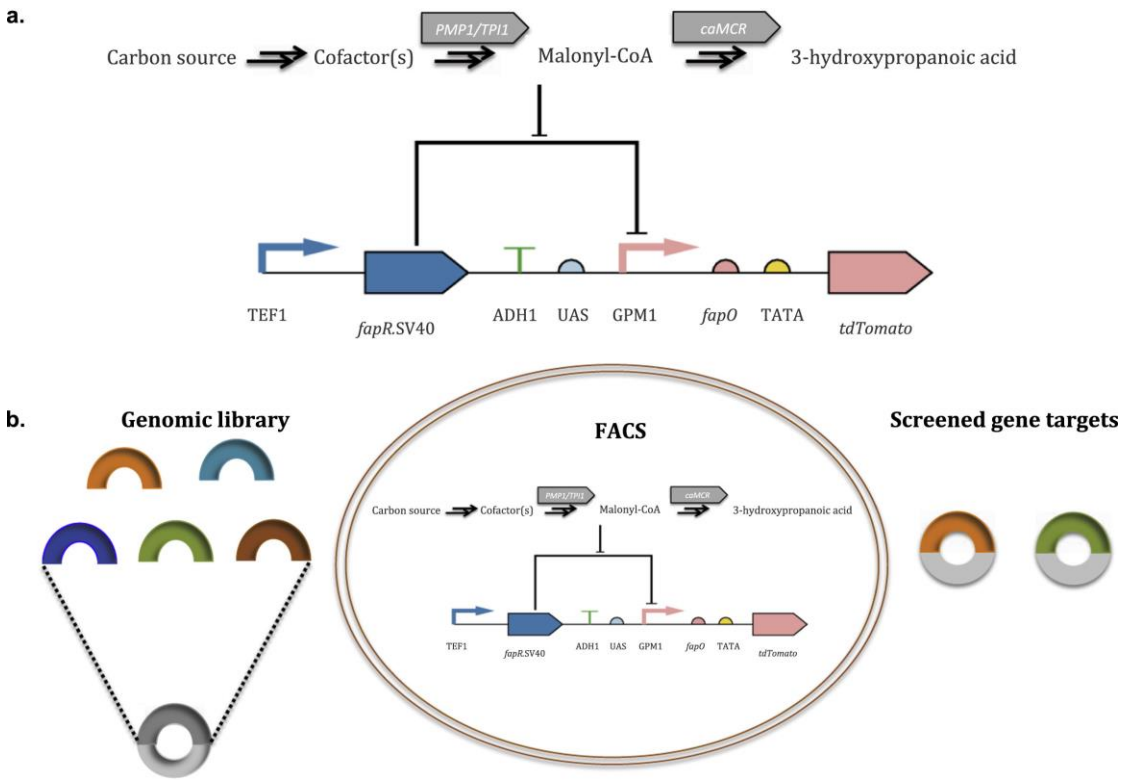

Figure 1.21: Malonyl-CoA sensor in yeast
(a) The sensor comprises the TEF1 promoter-driven fapR gene possessing a strong SV40 nuclear localization sequence at its C-terminus, an ADH1 terminator and the FapR-repressed GPM1 promoter-driven tdTomato reporter gene. The GPM1 promoter has an upstream activation to prevent native transcriptional regulation and a *fapO*-operator sequence located before the TATA sequence. (b) Schematic representation of the application of the sensor for screening malonyl-CoA producers. Fluorescence actuation from the sensor was used to detect improved cellular synthesis of malonyl-CoA due to the plasma membrane proteolipid (PMP1) and the triose-phosphate isomerase gene (TPI1).

1.15.6 Future perspectives

Malonyl-CoA genetic sensors allow real-time monitoring of the intracellular malonyl-CoA concentration, hence complementing analytical techniques like HPLC and LC-MS. Despite being able to conduct direct metabolite quantification, these analytical techniques are generally more time consuming and of relatively lower throughput, often entailing laborious pre-treatment requirements. Analytical technique, however, remains a *sine qua non* for generating malonyl-CoA concentration-response calibration curve from which malonyl-CoA amounts may be deduced. Yet the diverse applications of malonyl-CoA biosensors, as discussed in this review, form a compelling rationale to justify their design and subsequent use in the metabolic engineering of microbial hosts for malony-CoA production. Some of these applications include regulating malonyl-CoA sink/source pathways, screening for high malonyl-CoA producing strains and identifying high malonyl-CoA-producing process conditions.

Thus far, *E. coli* and *S. cerevisiae* are the two main microbial hosts that have been extensively engineered for improved cellular synthesis of malonyl-CoA and chemicals derived from it. This is largely owing to the ample availability of chassis-specific molecular biology and synthetic biology toolbox, robustness and our more comprehensive understanding of these two production hosts. As more biological hosts are successfully engineered for improved malonyl-CoA production, we envisage that the current design of malonyl-CoA biosensor will be adapted for use in such hosts. These may well include notable Gram-negative microbial hosts, such as *Pseudomonas* spp. and *Ralstonia eutropha* H16, and eukaryotic hosts such as *Pichia pastoris,* which are potentially promising for industrial-scale biomanufacturing.

The success of expanding the range of hosts in which malonyl-CoA biosensors are applicable would depend on whether the engineered malonyl-CoA sensing circuits are compatible with chassis-specific biological parts. This could be primarily ascribed to intrinsic biological differences in the replication, transcription, translation, post-translational modification and nuclear transport architectural network of different hosts. All these factors should be considered to design and engineer an effective malonyl-CoA sensor. Additionally, there is a need to ensure that the design of malonyl-CoA biosensors in such

hosts is robust and efficient, with optimal sensitivity, broad dynamic range of response and high detection limit. This is potentially achievable by leveraging the successes in engineering effective malonyl-CoA biosensors in model microbial hosts as a vantage point for achieving similar design successes in other potential microbial hosts, as summarized in this review. Moreover, we see the possibility of mathematically modeling existing experimental data to further polish the design and behavior of malonyl-CoA sensors and regulatory networks for more advanced applications (Liu et al., 2015b).

1.16 Genome editing – a robust molecular tool for metabolic engineering in *R. eutropha* H16

Cellular phenotypes requiring non-expression of certain genes require manipulation at the genomic level. Genome engineering techniques allow us not only to delete undesired genes from the genome, but also to insert desired genes into the genome, or replace undesired genes with desired genes, amongst many other options. More so, mutants created via genome engineering have permanent cellular phenotypes as against cellular phenotypes created via plasmid-borne recombinant strain engineering, which only last as long the stability of the plasmid vector in question. Several considerations have to be made in judging what genome engineering techniques are efficient for specific microbial cell factories. Amongst several other qualities, efficient techniques must be fast, robust, non-complicated, and above all, should allow for relatively easy screening for successful mutants. Also, such a technique should have limited drawbacks in comparison to other promising techniques, and must show prospects for process improvements and optimizations, in terms of its capabilities.

The diversity of genome engineering techniques and strategies has been critically reviewed by Song et al. (2015), Nakashima and Miyazaki (2014), Esvelt and Wang (2013). Some popular methods of genome editing, including those that have been demonstrated in *Ralstonia eutropha*, and those that potentially could also be used but have not been reported are summarized in Table 1.6. Allelic exchange (Lindenkamp et al., 2012, Brigham et al., 2010), transposon mutagenesis (Braemer and Steinbuechel, 2001), using suicide vectors such as pJQ200 (Quandt and Hynes, 1993) have all been adopted for genome engineering in *Ralstonia eutropha.* Till date, the only expression system-based genome engineering

method reported for *Ralstonia eutropha* is the Group II introns retrohoming method (Zhong et al., 2003) using the pBBR1MCS2 broad host range plasmid as an expression vector for Group II introns (Park et al., 2010). An obvious major reason is the rather limited synthetic biology toolbox for efficient expression systems in *Ralstonia eutrop*ha, as described earlier. Expanding the options of techniques for genome engineering in *Ralstonia eutropha* will thus rely heavily on the development of robust expression systems that are both compatible with its transcriptional machinery, and also function efficiently for intracellular delivery of genome engineering modules/elements. Recombineering is a classical example of a promising genome editing technique that has continued to witness optimizations, making it a genome editing technique for rapid manipulation of metabolic/cellular phenotypes. However, till date, there has been no report of this technique being used for genome-level genetic manipulation in *Ralstonia eutropha.*

Table 1.6: Notable singleplex genome editing techniques potentially applicable in *Ralstonia eutropha*

Genome Editing Tool	Advantages	Plasmid vector requirement	Editing-effector Module	Sequence specificity Module
Allelic Exchange	Scarless genome editing	Suicide plasmids (pJQ200, pCVD441, pDS132, pKOK4, pKAS32, pCVD442), temperature-sensitive plasmids (pKO3, pSC101) with homology arms of target genes for knock-out/replacement/ knock-in	Endogenous RecA/Rad51	Target gene homology arms (>500 bp)
Retrohoming with Group II Introns	Offer efficiencies of 0.1 to 25 %	Expression vector for retargeted group II intron	Llt lariat Intron Encoded Protein (IEP)	Retargeted introns
Transposition Mutagenesis		Expression vector for Transposase, Suicide vector for Transposon	Transposase	
TALEN[a] technology	Programmable, scarless and efficient genome editing	Expression vectors for repair construct and TALEN	Heterodimeric *Fok*I restriction endonuclease	TALE DNA-binding domains
ZFNs[b] technology	Programmable, scarless and efficient genome editing genome editing	Expression vectors for repair construct and ZFN	Heterodimeric *Fok*I restriction endonuclease	Zinc finger motifs
CRISPR-Cas[c]	Offer 65-100% efficiencies. Programmable genome editing	Expression vectors for sgRNA, Cas9 nuclease, and repair construct	Cas9 endonuclease	Single guide RNA

Table continues below

Genome Editing Tool	**Advantages**	**Plasmid vector requirement**	**Editing-effector Module**	**Sequence specificity Module**
GETR[d]	Does not require selection markers. Offers 100% efficiencies. Allows for gene deletion, insertion, inversion, and tranversions of larger genomic/genetic fragments	Expression vector retargeted group II intron with *lox* sites Delivery plasmid for gene insert with lox sites Expression vector for Cre/*lox*-recombinase	Cre recombinase	Retargeted introns (Ll.Ltrb and EcoI5 introns) with *lox* sites containing retargeted introns. *lox* sites on gene insert
λ-Beta Recombineering	Relatively easier transformation of ssDNA compared to dsDNA and plasmids allows for multiplex genome editing with higher chances genomic integration	Expression vector for beta protein	λ-Beta recombinase	Optimally matching ssDNA (~70-nt)
λ-Red Recombineering		Expression vector for λ-Red proteins Helper vectors for flippase protein.	λ-Red recombinase	Selection marker with flanking >35 bps homology arms

a – Transcription Activator-Like Effectors Nucleases (TALENs)
b – Zinc Finger Nucleases (ZFN)
c – Clustered Regularly Interspaced Short Palindromic Repeats (CRISPR)
d – Genome Editing with Targetrons and Recombinases (GETR)

1.16.1 λ-Red Recombineering

λ-Red Recombineering or recombination-mediated genetic engineering employs homologous recombination between a linear dsDNA cassette and targeted genome to orchestrate modification of chromosomal genes. It is required that the dsDNA cassette possesses 30-70 flanking nucleotide sequences (homology arms) homologous to sequences flanking, the targeted genomic region (Yu et al., 2000). In addition, site-specific recombinase proteins such as the RecET *rac* prophage or λ-Red prophage proteins are required to mediate recombination event. Use of the RecE/T proteins from the *rac* prophage for recombineering in the *E. coli* chromosome was first reported by Zhang et al. (1998). Similarly, recombineering with λ-Red proteins was demonstrated in *E. coli* for inactivation of chromosomal genes using a defective λ-prophage, and later with the use of specially designed plasmid systems for expressing the λ-Red proteins (Datsenko and Wanner, 2000, Murphy, 1998).

1.16.2 Mechanism

λ-Red recombinase proteins are Exo, Beta and Gam. Exo is an exonuclease which just like RecE in the RecET prophage systems, degrades linear dsDNA in the 5'-3' direction into a ssDNA intermediate (Carter and Radding, 1971, Cassuto et al., 1971a). Beta, aided by Exo binds to the ssDNA intermediate thus stabilizing it from further degradation by endogenous exonucleases (Cassuto et al., 1971b). RecT is known to serve the same function as Beta in the Rec E/T system. Gam inhibits RecBCD and SbcCD endogenous exonucleases from degrading the dsDNA (Cassuto et al., 1971a, Murphy, 1991, Poteete, 2001). The recombination activities of the recombinase proteins in both systems, however occurs independently of the endogenous RecA-mediated homologous recombination responsible for natural recombinogenicity in some microbial systems (Yu et al., 2000, Poteete, 2001).

It has been proposed that recombinase-mediated homologous recombination occurs through a strand annealing mechanism, wherein the ssDNA intermediate anneals as an Okazaki fragment at the replication fork preferentially to the lagging strand of the host genome (Lim et al., 2008, Mosberg et al., 2010, Li et al., 1998, Karakousis et al., 1998).

This mechanism invariably culminates in the integration of the ssDNA intermediate into

targeted genomic region (Mosberg et al., 2010, Boyle et al., 2013), (Figure 1.22).

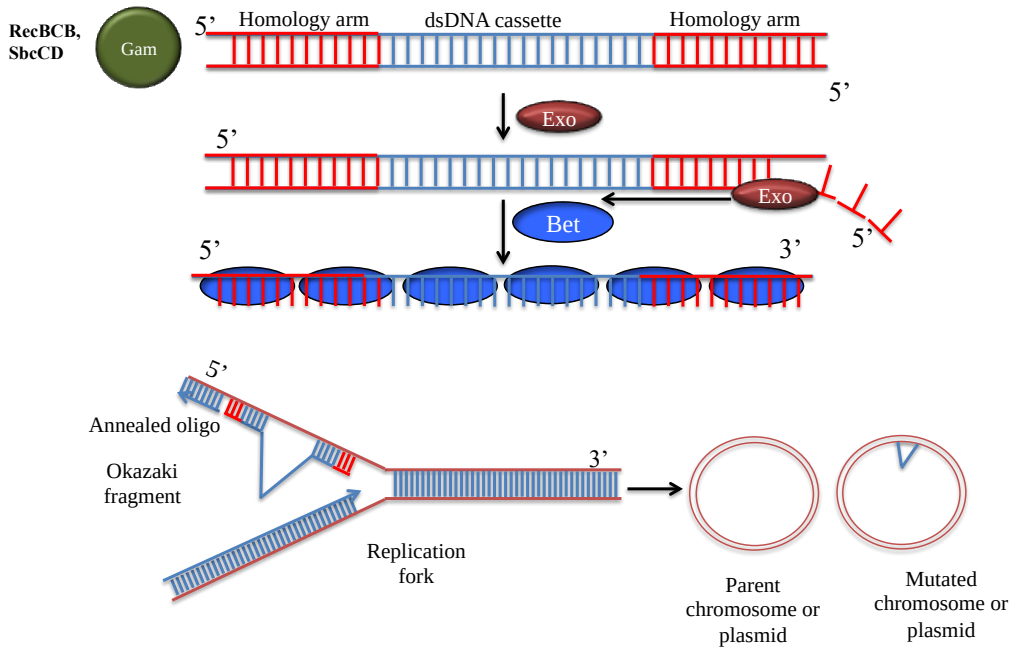

Figure 1.22: Molecular mechanism of λ-Red recombineering.
Gam inhibits endogenous RecBCB and SbcCB from degrading the dsDNA cassette, Exo degrades it in the 5'-3' direction into a ssDNA intermediate, while Bet aided by Exo binds tightly to the ssDNA and mediates preferential strand annealing at the replication fork to the lagging strands, thus displacing an endogenous Okazaki fragment. Replication of the annealed ssDNA leads to integration to targeted region or either plasmid or chromosome.

1.16.3 Application of λ-Red recombineering in microbial systems

Beyond its application in *E. coli* by Datsenko and Warner, λ-Red recombineering has been adopted for genome editing in a number of microbial systems (Song et al., 2015). This is largely owing to its ease, efficiency and versatility allowing for genomic modifications to suit specific microbial systems. Examples of such microbial systems include *Pseudomonas aeruginosa* (Lesic and Rahme, 2008), *Salmonella enterica* (Datta et al., 2006, Blank et al., 2011), *Yersinia enterocolitica* (Derbise et al., 2003), *Aspergillus nigulans* (Chaveroche et al., 2000). In addition to inactivation of chromosomal genes, λ-Red recombineering employed for making gene replacement, chromosomal insertion of large genomic fragments, and point mutations.

1.16.3.1 λ-Red recombinase plasmids

λ-Red recombinase plasmids are designed with inducible promoter systems for regulated expression of the λ-Red proteins to control the onset of homologous recombination Table

1.7. pKD20 and pKD46 λ-Red recombinase plasmids developed for recombineering utilize the P_{BAD} promoter system for strong expression of the λ-Red proteins (Datsenko and Wanner, 2000). pKD46 is known to offer better recombination efficiencies than pKD20 for reasons yet unclear (Datsenko and Wanner, 2000). Construction of a set of pSIM recombinase plasmids from a λ-prophage strain using both Red-catalyzed gap reaction and λ-Red recombineering has also been reported (Datta et al., 2006). These plasmids utilize the temperature-sensitive λ *CI857* repressor for the induction of protein expression via temperature shift to 42°C. The constructed plasmids were shown be useful for λ-Red recombineering both *E. coli* and *S. enterica*, yielding 10^4 recombinants/10^8 viable cells in *E. coli*, offering 10-fold higher recombination efficiency when compared to pKD20/pKD46 recombinase plasmids (Datta et al., 2006). A number of λ-Red vectors recombinase vector, possess a temperature-sensitive (ts) origin of replication, which functions optimally at 30°C, and abrogates replication at temperatures from 37°C. Thus after cultivating cells at 30°C for the recombination event, recombinant cells are re-cultivated at 42°C to cure the plasmid. Non-temperature sensitivity-based plasmid curing has been achieved by cloning the *Bacillus subtilis sacB* counter-selection marker into λ-Red recombinase plasmids. *sacB* gene encodes levansucrose (SacB), an enzyme that produces the toxic levan from sucrose. Accumulation of levan in the periplasm of Gram-negative bacteria causes cellular toxicity via cell lysis (Gay et al., 1985). Thus sucrose-induced cell death serves to impose a selection pressure for the propagation of recombinants whose recombinase plasmids have been lost due to plasmid instability. With the *sacB* system, plasmids are cured by plating cultures of recombinant cells on agar plates with 5% sucrose to select for recombinants with cured plasmids. pUCP18-RedS (Lesic and Rahme, 2008) and pKOBEG-*sacB* (Derbise et al., 2003) are two typical *sacB*-counter selection plasmids.

Table 1.7: Some notable examples of λ-Red recombinase expression vectors and properties

Recombinase Plasmid	Origin	Host range	Drug marker	Promoter	Reference
pSIM2	pBR322	Narrow	Chloramphenicol	λ P_L	Datta et al. (2006)
pSIM4	pBR322	Narrow	Ampicillin	λ P_L	Datta et al. (2006)
pSIM5	$pSC101^{ts}$	Narrow	Chloramphenicol	λ P_L	Datta et al. (2006)
pSIM6	$pSC101^{ts}$	Narrow	Ampicillin	λ P_L	Datta et al. (2006)
pSIM7	pBBR1	Broad	Chloramphenicol	λ P_L	Datta et al. (2006)
pSIM8	pBBR1	Broad	Ampicillin	λ P_L	Datta et al. (2006)
pSIM9	$RK2^{ts}$	Broad	Chloramphenicol	λ P_L	Datta et al. (2006)
pSIM18	$pSC101^{ts}$	Narrow	Hygromycin	λ P_L	Datta et al. (2006)
pSIM19	$pSC101^{ts}$	Narrow	Spectinomycin	λ P_L	Datta et al. (2006)
pKM208	$pSC101^{ts}$	Narrow	Ampicillin	P_{tac}	Murphy and Campellone (2003)
pKD20	$pSC101^{ts}$	Narrow	Ampicillin	P_{BAD}	Datsenko and Wanner (2000)
pKD46	$pSC101^{ts}$	Narrow	Ampicillin	P_{BAD}	Datsenko and Wanner (2000)
pREDI	$pSC101^{ts}$	Narrow	Ampicillin	P_{BAD}	Yu et al. (2008)
pUCP18-RedS	pMB1 ori	Broad	Ampicillin	P_{BAD}	Lesic and Rahme (2008)
pKOBEG	$pSC101^{ts}$	Narrow	Chloramphenicol	P_{BAD}	Chaveroche et al. (2000)
pKOBEG-*sacB*	$pSC101^{ts}$	Narrow	Chloramphenicol	P_{BAD}	Derbise et al. (2003)

1.16.3.2 Design of dsDNA cassette

dsDNA cassette for gene inactivation are often designed as antibiotics selection markers flanked by 36-100 nucleotide sequences (homology arms) homologous to sequences upstream and downstream to the genomic region targeted for inactivation (Figure 1.23). Although 50-nt is often optimal for homologous recombination, some studies have shown that lengthy homology arms (>500-nt) are required for efficient recombination (Chaveroche et al., 2000, Derbise et al., 2003, Lesic and Rahme, 2008). Generally, lengthy homology arms increase the chances of recombination leading to higher recombination efficiencies (Chaveroche et al., 2000). To allow for excision of the antibiotics selection marker via a second recombination event, inverted repeats such as flippase recognition target (FRT) sites are placed in between the each homology arm and the antibiotics selection marker (Figure 1.24). *loxP* sites are also usable in place FRT sites. Marker excision using the FRT sites is mediated by FLP recombinase, while Cre-recombinase is mediated via *loxP*-based recombination.

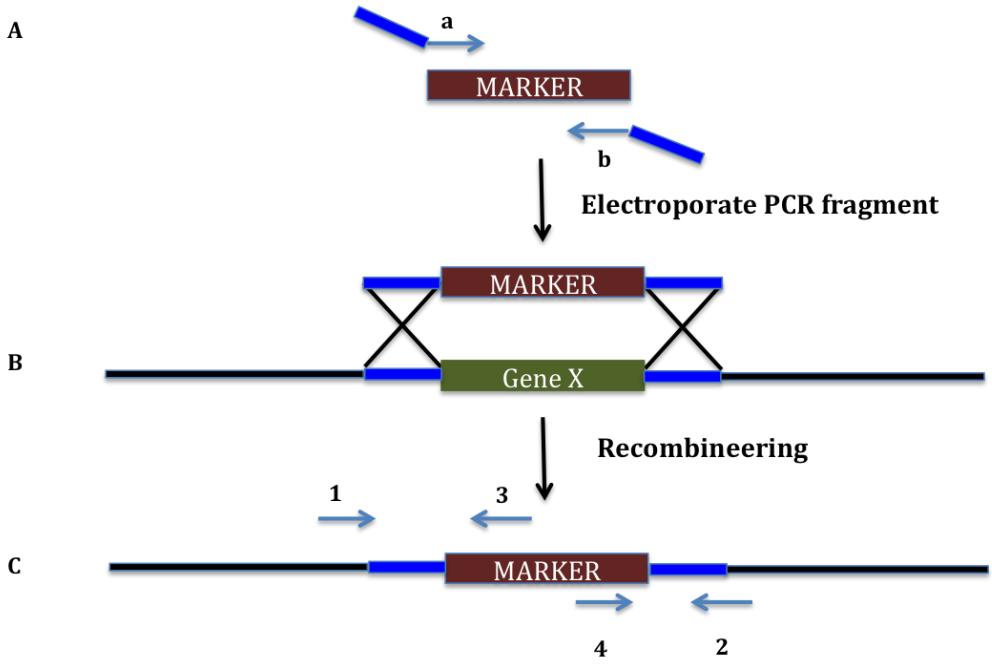

Figure 1.23: Simplified process of λ-Red recombineering for genomic integration of marker.
The marker is amplified with a set of primers a and b, which possess 5' flanking regions bearing targeting sequences homologous to the genomic regions upstream and downstream to the target Gene X. Electroporated PCR amplicon of marker undergoes homologous recombination with target sites leading to genomic insertion of the marker. Genomic insertion is confirmed by using a set of primers pairs (1, 2), (1, 3), (2,4) and (3,4).

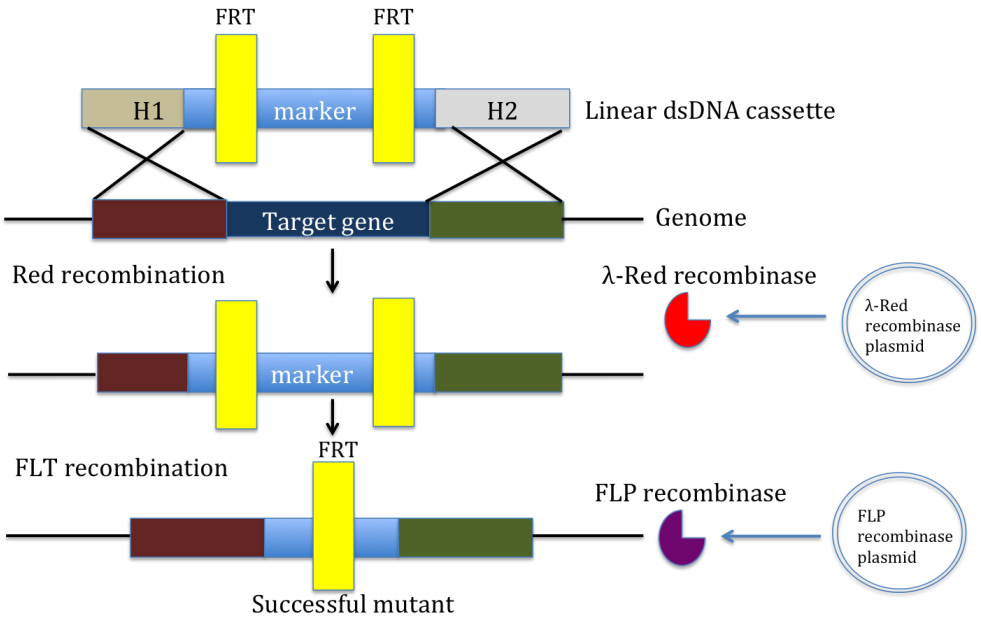

Figure 1.24: Schematic of λ-Red recombineering with a dsDNA selectable marker. ssDNA intermediate from dsDNA cassette binds complementarily to genomic region flanking target gene using its flanking homology arms (H1 and H2). λ-Red recombinase proteins expressed from a λ-Red plasmid system mediate homologous recombination between target gene and linear dsDNA cassette. A second recombination event mediated by FLP recombinase expressed from FLP recombinase plasmid removes one of the FLT scars leaving behind one.

1.16.3.3 Improving λ-Red recombineering methods and strategies in microbial systems

Several intrinsic drawbacks exist in the use of the above traditional form of recombineering for genome editing. One of these drawbacks is the lengthy turnaround period for a single deletion experiment. The dependency of the process on plasmid vectors requires an extra plasmid curing stage to eliminate the recombinase plasmids from recombinant cells. Antibiotics selection marker excision stages and plasmid curing stages, requiring colony-screening steps, thus increasing the turnaround time of the experimental protocol to up to a week or more, depending on the host organism. Another major drawback is the presence of an unwanted FRT scar (81-85 base pairs) left behind in the genome after the marker excision stage (Datsenko and Wanner, 2000). This culminates in unintended genomic disruption thus compromising the precision of genome editing, especially when more than

one round of genomic modification is intended (Blank et al., 2011, Nakashima and Miyazaki, 2014).

An improved system of λ-Red recombineering was achieved by Yu et al. (2008), involving a more robust recombinase plasmid system cohosting the λ-Red and the I-SceI recombination modules. The robust plasmid pREDI, which was constructed from pKD46, has two independent inducible promoter systems for the expression of the λ-Red proteins, and an I-SceI endonuclease (Yu et al., 2008). As with the pKD20 and pKD46 plasmid systems, the λ-Red proteins are expressed with the P_{BAD} promoter system, while the I-SceI endonuclease is expressed under control of a rhamnose-inducible promoter system. In this novel system, scarless excision of genome integrated antibiotics selection marker was achieved *via* homologous recombination via an I-SceI endonuclease-mediated double-stranded break at an I-SceI site located in the dsDNA cassette (Figure 1.25). The dsDNA cassette was designed to have an extra homology arm (H3) possessing sequences further downstream of the genomic loci scheduled for gene inactivation. Screening of mutants with excised cassette was facilitated by the presence of *sacB* counter-selection marker between the antibiotic selection marker and the I-SceI site. This design ensured that mutants with successful excision of the antibiotics selection marker are selected by replica plating on agar plates supplemented with 5% sucrose (Gay et al., 1985). This system obviates the need for *FRT* or *loxP* sites in the design of the dsDNA. Also, unlike the use of *FRT* or *loxP* sites, use of the I-SceI endonuclease system for excising the antibiotics from the mutant does not leave behind unwanted scars in the genome, thus allowing for limitless number of gene inactivation. Additionally, the combined knock-in and knockout function of the pREDI plasmid reduces the time frame for a single gene inactivation experiment from a week to days. Reported recombination efficiencies at 70% and 100% for knock-in and knock-out of the linear dsDNA, respectively, trumps reported efficiencies in previous methods of λ-Red recombineering (Yu et al., 2008). This system was used for simultaneous deletion of two far apart genomic loci in *E. coli* K-12 strain MG1655.

Another strategy for scarless excision of antibiotics selection marker after gene deletion is the use of a selection/counterselection dsDNA cassette in a two-step recombination process using the same λ-Red recombinase vector for both stages. This method is originally suitable

for the insertion of non-selectable genes, or the replacement of specific gene in the genome with non-selectable genes. An example of this is the use of a cat-*sacB* cassette (Thomason et al., 2014, Ellis et al., 2001). In this method, recombinants with chloramphenicol resistance and sucrose sensitivity are subjected to a second recombination event to introduce the non-selectable gene while excising the cat-*sacB* cassette. Successful recombination event is confirmed by screening for sucrose-resistance and chloramphenicol-sensitivity from colonies that had previously shown chloramphenicol resistance and sucrose sensitivity.

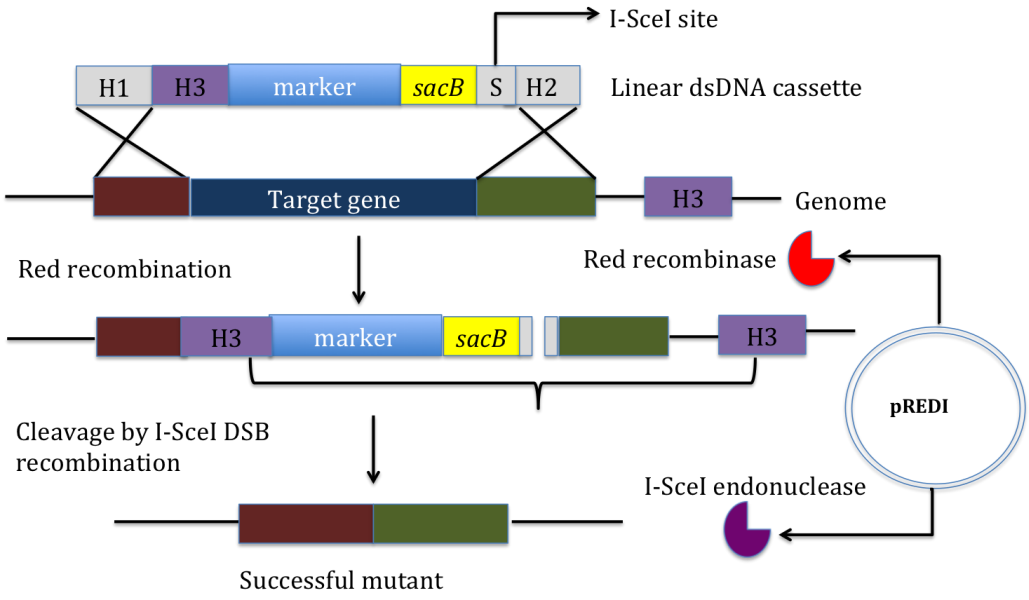

Figure 1.25: Mechanism of λ-Red recombineering with pREDI.
λ-Red proteins expressed from pREDI mediate a first homologous recombination, which replaces target gene with marker, using the H1 and H2 homology arms. I-SceI endonuclease expressed from pREDI cleaves the I-SceI site via a double strand break mechanism (DSB). This initiates a second homologous recombination event at the H3 sites, thus removing the marker, the sacB counterselection marker and the H3 homology sites. Successful mutant possesses no marker or scar.

1.16.4 Comparative advantage to other genome editing methods

λ-Red recombineering compares well with other notable genome editing methods (Table 1.8), especially due to the aforementioned technical improvisations. Aside not having some of the major drawbacks of these notable methods, the improved methods of λ-Red recombineering also possess some of the most vital advantages of notable methods, typically improved efficiencies. For example, genome editing with CRISPR-Cas is particularly known to offer one of the highest efficiencies (Nakashima and Miyazaki, 2014), owing to the fact that unedited cells are killed off by the cytotoxicity of the Cas9 endonuclease. The efficiency of the CRISPR-Cas system has thus been leveraged on in improving the efficiency of λ-Red recombineering to as much as 100% in *S. pneumoniae* and 65% in *E. coli* (Jiang et al., 2013). However, the method suffers the typical drawback of unprecedented off-target mutagenesis causing death of mutant cells as well. Another method that offers high efficiencies and versatility in the types of genome editing options is the recent GETR method, with 100% efficiencies reported in *E. coli* (Enyeart et al., 2014). This method, which leverages Cre/lox-based recombineering and mobile group II retrohoming, requires three different plasmid systems for a each genome editing round. It utilizes one plasmid for expressing the retargeted intron, a delivery plasmid for genomic integration of gene insert, and a third plasmid vector for expressing the Cre-lox recombinase. Aside the complex plasmid requirement, a major drawback is unwanted genomic introduction of lox scars. However, major comparative advantages of this method over other notable genome editing techniques, are the potential for editing large genomic fragment (up to 1.5 megabases) and its independence selection markers, and hence antibiotics selection.

Another crucial method of recombineering is the use of ssDNA oligos (~70-nt oligos), and hence only λ-Beta in mediating homologous recombination event (Yu et al., 2000, Oppenheim et al., 2004, Ellis et al., 2001). ssDNA cassettes have also been shown to offer better recombination efficiencies than dsDNA, at about 10^5 recombinants/10^8 viable cells (Costantino and Court, 2003). This figure sometimes reaches 25% of viable cells where small changes or point mutation are required, especially when the methyl-directed mismatch repair mechanism is mutated (Thomason et al., 2014, Mosberg et al., 2010, Boyle et al., 2013). The prospects of λ-beta recombineering as a high throughput genome editing

technique has also been leveraged for multiplex genome-scale manipulation techniques such as Multiplex Genome Engineering and Accelerated Evolution (MAGE) (Boyle et al., 2013, Wang et al., 2009, Wang and Church, 2011). Although conventional λ-Beta recombineering with dsDNA offers 0.1 - 0.2% recombination efficiency (Yu et al., 2000, Thomason et al., 2014), it is still relatively preferred for making large chromosomal deletions and genomic insertion of up to several thousand bases. These applications include the creating of the Keio collection (Baba et al., 2006), which is a library of single-gene knockout of *E. coli* strains (Baba et al., 2006, Mosberg et al., 2010), chromosomal insertion of a complete heterologous pathway into an *E. coli* strain (Zhang et al., 1998), and the removal of up to 15% of the genome of an *E. coli* strain (Mosberg et al., 2010, Posfai et al., 2006). Additionally, λ-Red recombineering has also been leveraged for combinatorial genome-scale techniques such as Trackable Multiplex Recombineering (Warner et al., 2010).

Overall, leveraging the most recent improvements, such as achieved with pREDI (Yu et al., 2008) and pUCP18-RedS (Lesic and Rahme, 2008), λ-Red recombineering promises to compare well with other promising genome editing techniques (Table 1.8), with a number of comparative advantages.

Table 1.8: Comparison of λ-Red Recombineering to other notable genome editing methods

Drawback of genome editing methods	Comparative advantages of λ-Red Recombineering
Allelic exchange versus λ-Red Recombineering	
Require large homology arms (>500 base pairs) for homologous recombination	Requires only 35-70 base pairs homology arms for homologous recombination
Require suicide vectors to introduce selection/counter-selection markers	Linear dsDNA cassette is introduced via electroporation of electrocompetent cells
Endogenous RecA/Rad51-mediated Homologous recombination has low probability	Induction of λ-Red expression initiates homologous recognition
Non-selectional homologous recombination makes screening of successful mutant more tedious	Intended homologous recombination is selected for making screening easier
Reversal of mutants to wild type	No reversal of mutants to wild type
Causes polar effects to neighbouring genes	Design of cassette Reduce s occurrence of polar effects
Transposon mutagenesis versus λ-Red Recombineering	
Bias for sequence integration	No bias for sequence integration
Indefinite manipulation of target sequence	Specific manipulation of target genomic region
Retrohoming versus λ-Red Recombineering	
Susceptible to bias in intron insertion	No bias in cassette integration
TALENS & ZFN versus λ-Red Recombineering	
Sequence homology-dependent off-targeting, and cytotoxicity	Design of dsDNA eliminates changes of off targeting. No cytotoxicity
Laborious and expensive target-specific protein engineering requirement of the nuclease proteins	No protein engineering requirement
RNA interference versus λ-Red Recombineering	
Off-targeting	No off-targeting
Incomplete and temporary knock-out	Permanent knock-out event
CRISPR-Cas versus λ-Red Recombineering	
Sequence homology dependent off-targeting	No off targeting
Cellular toxicity	No cellular toxicity
Requires extra deep sequencing verification step to check for off-target mutagenesis	Does not require deep sequencing. Colony PCR of region around genomic alteration is the major verification step
GETR versus λ-Red Recombineering	
Unwanted scar formation of *lox* sites Cre recombination	Latter methods do not require Cre recombination, hence scarless genomic modification is possible
Susceptible to bias in intron insertion	No bias in cassette integration
λ-Red (Beta) versus λ-Red Recombineering	
Insertion/Deletion inefficiency for large DNA fragment	Relatively for suitable for insertion/deletion of large DNA fragment
Requires mutation of the methyl-directed mismatch repair system (MMR) for better efficiencies	Does not require MMR mutation

1.16.5 λ-Red Recombineering application in *Ralstonia eutropha*: Opportunities and Challenges

Transformation of *R. eutropha* with plasmid vectors is a significant milestone for genetic manipulation, especially for metabolic engineering strategies. The highly efficient transformation technique *via* electroporation has been utilized and optimized to harness the genetic tractability of *R. eutropha* (Park et al., 1995, Tee et al., 2017). However, despite high transformation efficiencies, a major uncertainty in the use of this method of genome editing is the question of if the Gam protein is able to effectively protect electroporated dsDNA from endogenous RecBCD nuclease attack in *Ralstonia eutropha*, as is the case in several bacteria. Studies by Mosberg et al. (2012) have shown that 5'-phosphorothiated dsDNA cassettes are relatively better protected from endogenous RecBCD nuclease attack and thus afford higher recombination efficiencies. Thus the use of 5'-phosphorothiated dsDNA cassettes might be good way to further improve recombination event in *R. eutropha.*

On the other hand, it is uncertain if the λ-Red proteins when expressed are compatible with endogenous enzymes in *Ralstonia eutropha*. Some studies report cellular toxicity from expression of the λ-Red proteins, particularly high expression of Gam (Copeland et al., 2001, Sergueev et al., 2001) and Exo (Katashkina et al., 2009) in some bacterial species. The potential effect this might have on λ-Red recombineering in *Ralstonia eutropha* is currently unknown, and thus worthy of investigation.

Amongst the listed plasmid in Table 1.7, pUCP18-RedS (Lesic and Rahme, 2008), is by its functionality the most fitting recombinase expression system applicable to *R. eutropha.* This is largely owing to the fact that, aside being a broad host range plasmid; it uses the non-temperature dependent P_{BAD} inducible promoter system for λ-Red expression, as well as the non-temperature-dependent *sacB*-counter-selection system. Temperature-sensitive/dependent BHR λ-Red recombinase plasmids, such as pSIM9, may not be ideal as expression induction and plasmid-curing temperatures at 37°C and 42°C, respectively are not supportive of optimal cell growth in *Ralstonia eutropha,* which is known to grow optimally at 30°C (Park et al., 2011). More so, *sacB* counter-selection has previously been shown to be compatible with *Ralstonia eutropha* (Lindenkamp et al., 2012, Boyle et al.,

2013), as much as the P_{BAD} promoter is a choice promoter for inducible gene expression in *R. eutropha.*

Additionally, narrow host range λ-Red recombinase plasmids could be reconstructed into fitting recombinant broad host range λ-Red recombinase plasmids, using broad host range plasmids as plasmid backbones. Typically, the plasmid backbone template of pBBR1MCS with a BBR1 replicon could potentially be used as a plasmid backbone for constructing such recombinant plasmids from pKD20, pKD46, pREDI, and the narrow host range pSIM plasmids.

1.17 Roadmap for the application of molecular tools for malonyl-CoA engineering in *Ralstonia eutropha* H16

The natural ability of *R. eutropha* to utilize diverse carbon sources for growth and accumulation of bio-plastics essentially makes it a fitting microbial cell factory for the production of valuable chemicals using vital cellular metabolites such as malonyl-CoA as precursor intermediates. Although, the ease of readily enhancing acetyl-CoA accumulation for bioproduct synthesis in *R. eutropha* has been well studied (Table 1.1), the sheer lack of identified acetyl-CoA-responsive transcriptional regulators makes it rather difficult to develop genetic circuits to sense and/or to regulate acetyl-CoA accumulation, specifically.

As malonyl-CoA is a product of the carboxylation of acetyl-CoA, established strategies for the up-regulation of acetyl-CoA for PHB production in *R. eutropha* H16 could potentially be leveraged on improve carbon flux towards malonyl-CoA accumulation. However, this will also require the deletion of the PHB operon - a non-essential acetyl-CoA sink pathway to ensure that increased acetyl-CoA flux is channeled into malonyl-CoA accumulation. These strategies could be applied synergistically with reported methods to improve malonyl-CoA accumulation in *E. coli* and *S. cerevisiae.* Identification of target genes to improve malonyl CoA biosynthesis will rely heavily on reported literature indicating crucial target genes in these model microbial cell factories. Target genes, which are potentially linked to malonyl-CoA production, are identified, primarily based on demonstrated impact on malonyl-CoA phenotype in microbial host such as *E. coli* and *Saccharomyces cerevisiae.*

Figure 1.26 describes how these may be applied synergistically. It is decided if these gene(s) should be expressed *via* heterologous pathways or deleted from the genome to achieve improved malonyl-CoA phenotypes. Genes from heterologous pathways will require the use of expression vectors with promoters that possess appropriate activities to achieve desired malonyl-CoA pheonotype. Malonyl-CoA sensors will be used to detect malonyl-CoA phenotypes, to validate the roles of target genes in malonyl-CoA production and/or to evaluate the effectiveness of gene expression/genome editing molecular tools in improving malonyl-CoA phenotype. The ensuing malonyl-CoA phenotype could be made permanent *via* the use of plasmid addiction sytems (Kroll et al., 2010) to maintain the plasmids in the cell. Genes meant to be deleted (knockout) to achieve malonyl-CoA phenotype are deleted from the genome using the developed genome editing tool, and with concomitant use of the sensors to detect improved malonyl-CoA phenotype. Finally, after rounds of pathway optimization to achieve a mutant strain with the desired malonyl-CoA phenotype, plasmid-curing procedures are performed to eliminate the expression vectors of the genome editing tool from cell.

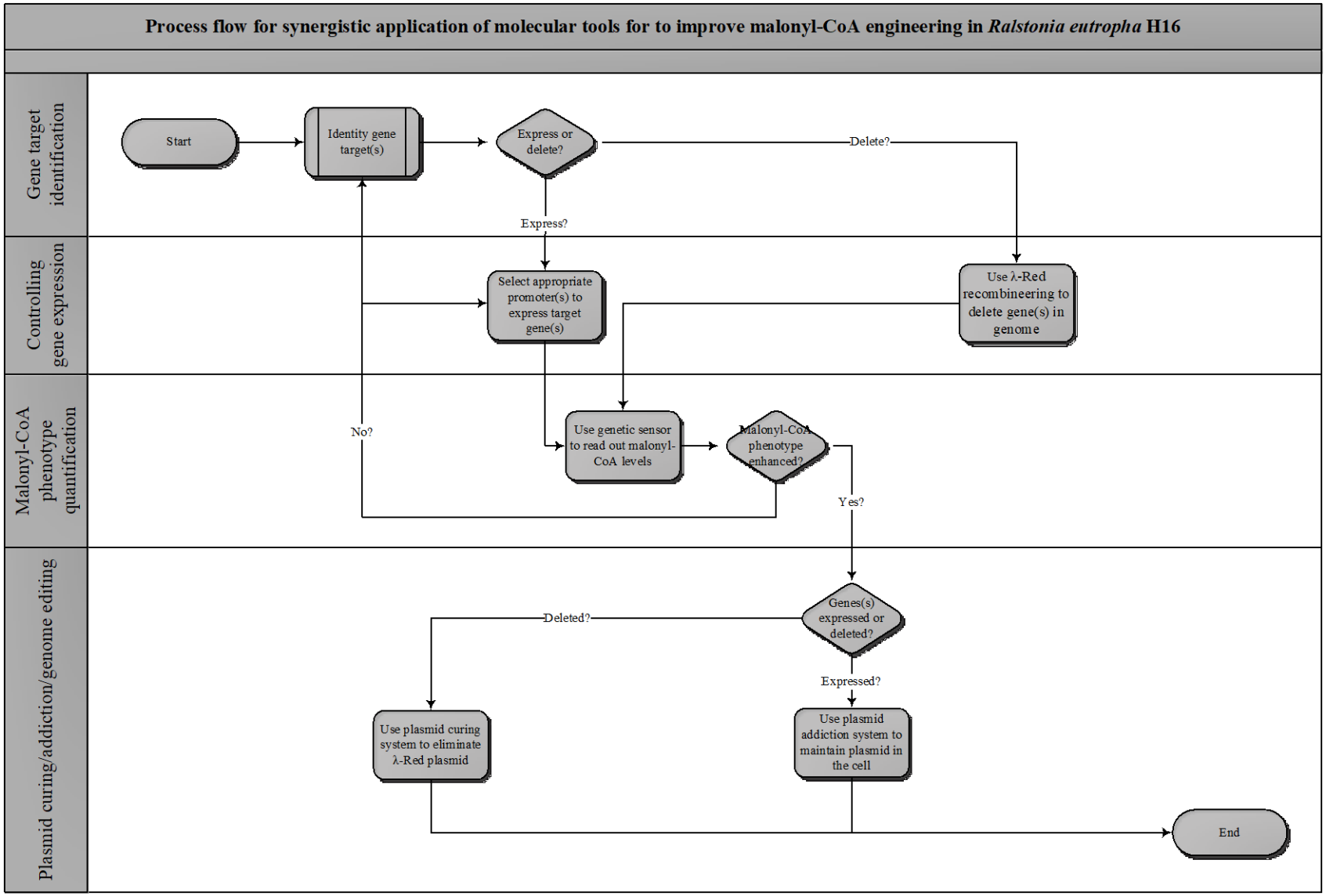

Figure 1.26: Proposed application of developed tools for malonyl-CoA engineering in *Ralstonia eutropha* H16.

1.18 Aims and objectives of study

Overall, synergistic application of the aforementioned molecular tools *viz* a toolbox of promoters, malonyl-CoA-responsive genetic circuits, and a facile genome editing method are required for malonyl-CoA engineering in *Ralstonia eutropha* H16.

To this end, Chapter Two describes the construction of broad host range chassis-compatible expression vectors required to develop molecular tools for malonyl-CoA engineering in *Ralstonia eutropha*. These vectors were used to (1) study the induction range of the L-arabinose inducible promoter using the red fluorescence protein, (2) to observe inducible expression the FapR repressor, and (3) to observe expression of the λ-Red genes in *Ralstonia eutropha*. Chapter Three describes the development of an engineered set of constitutive promoters for tunable gene expression in using *Ralstonia eutropha* within ~137-fold range of activity. Chapter Four describes the selection and application of some of these promoters to engineer six functional malonyl-CoA-responsive genetic circuits for sensing varying intracellular concentrations of malonyl-CoA accumulation in *Ralstonia eutropha*. Chapter Five validates the functionality of a *Ralstonia eutropha*-compatible genome editing molecular tool in *E. coli* BW25113. Chapter Six describes the attempt to use this genome editing molecular tool for actual genome editing in *Ralstonia eutropha*. Chapter Seven concludes the thesis and highlights the novelty of the research findings, provides a critical discussion of the aforementioned chapters and also details future work required to further achieve the research objectives.

CHAPTER TWO

2 DEVELOPMENT OF BROAD HOST EXPRESSION VECTORS FOR ENGINERING RALSTONIA EUTROPHA-COMPATIBLE MOLECULAR TOOLS

2.1 INTRODUCTION

Three essential molecular tools previously identified for regulating gene expression in *R. eutropha* H16 include a toolbox of promoters, a set of malonyl-CoA-responsive genetic cricuits and a λ-Red recombineering toolbox. These tools all require expression vectors that are compatible with the native transcriptional and replication machineries in *R. eutropha* H16. This is achieved by incorporating essential genetic elements and biological parts into the pBBR1 backbone of the broad host range, medium copy number plasmid pBBR1MCS-1 (Kovach et al., 1994). Firstly, a broad host range expression vector was constructed by incorporating the P_{BAD} promoter part (together with the araC gene) and the red fluorescence protein (RFP) gene from pBbA8k-RFP – a narrow range plasmid (Lee et al., 2011) into pBBR1MCS-1. The resultant plasmid vector, pBBR1c-RFP, was designed to evaluate the induction range of the P_{BAD} promoter in *R. eutropha* and to explore its use for tunable expression of heterologous pathways in *R. eutropha* H16.

The FapR transcriptional regulator protein has been identified as a crucial protein for regulating gene expression in synthetic malonyl-CoA genetic circuits in model biological factories like *E. coli* and *Saccharomyces cerevisiae* (Johnson et al., 2017). FapR expression was investigated in *E. coli* DH5α and *Ralstonia eutropha* H16 using the plasmid pBBR1c-FapR (derived by replacing *rfp* with *fapR*) in order to evaluate its potential use for regulating gene expression in heterologous malonyl-CoA genetic circuits in *Ralstonia eutropha* H16.

To develop a λ-Red recombineering in *Ralstonia eutropha*, the λ-Red proteins operon from the low copy number narrow host range λ-Red plasmids, pKD20 and pKD46 were incorporated into pBBR1c-RFP vector, hence replacing the *rfp* gene. The ensuing broad host range λ-Red expression vectors pBBR1c-RED1, pBBR1k-RED and pBBR1c-RED2 were subsequently used to observe expression of the λ-Red proteins in *E. coli* BW25113 and *Ralstonia eutropha* H16.

2.2 METHODS AND MATERIAL

2.2.1 Bacterial Cultivation

Ralstonia eutropha H16 (Gen^r) was grown in nutrient broth (NB) media supplemented with gentamicin (10 mg/L) and cultivated at 30°C, 500 rpm. *E. coli* DH5α and *E. coli* BW25113 were grown in 2XYT media at 37°C, 500 rpm except otherwise stated. All media are prepared by dissolving components in deionized water followed by autoclave sterilization. NB media was made up of 1 g/L beef extract, 2 g/L yeast extract, 5 g/L peptone, 5 g/L sodium chloride. 2XYT media contained 16 g/L tryptone, 10 g/L yeast extract, 5 g/L sodium chloride. All inoculation and preparation of all reagents used for cultivation were performed under sterile condition. All cultivation was done in an incubator mini shaker (VWR, Germany). Kanamycin (50 mg/L for *E. coli* and 200-300 mg/L for *Ralstonia eutropha*), chloramphenicol (25 mg/L), ampicillin (100 mg/L) were used as selection antibiotics as appropriate. All antibiotics stock solutions were prepared under sterile conditions and filtered with the 0.2 μm Whatman syringe filter. Overnight cultures of *Ralstonia eutropha* (wild-type or mutant) were set by inoculating 5 mL of nutrient broth supplemented with gentamicin with glycerol stock of *Ralstonia eutropha* H16 in a falcon tube. The culture was cultivated at 30°C for 40 h. Overnight cultures of *E. coli* strains were set by inoculating 5 mL of 2XYT media supplemented with appropriate inoculum of *E. coli*.

Table 2.1: Bacteria strains used in this study

Strain	Description	Reference
E. coli DH5α	F^-, φ80dlacZΔM15, Δ(*lacZYA-argF*) U169, *deoR*, *recA*1, endA1, *hsdR*17(rk^-, mk^+), *phoA*, *supE*44, λ^-, thi-1, *gyrA*96, *relA*1	Invitrogen
E. coli BW25113	$lacI^q$ $rrnB_{T14}$ $\Delta lacZ_{WJ16}$ *hsdR514* $\Delta araBAD_{AH33}$ $\Delta rhaBAD_{LD78}$	Invitrogen
Ralstonia eutropha H16	Gen^r, DSM-428	DSMZ, Braunschweig, Germany
EcRFP	*E. coli* DH5α with pBBR1c-RFP	This study
EcGFP	*E. coli* DH5α with pBBR1c-eGFP	This study
EcFapR	*E. coli* DH5α with pBBR1c-FapR	This study
ReRFP	*E. coli* DH5α with pBBR1c-RFP	This study
ReGFP	*Ralstonia eutropha* H16 with pBBR1c-GFP	This study
Re-null	*Ralstonia eutropha* H16 with pBBR1MCS-1	This study
ReFapR	*Ralstonia eutropha* H16 with pBBR1c-FapR	This study
BWD20	*E. coli* BW25113 with pKD20	This study
BWD46	*E. coli* BW25113 with pKD46	This study
BWRed1	*E. coli* BW25113 with pBBR1c-RED1	This study
BWRed2c	*E. coli* BW25113 with pBBR1c-RED2	This study
BWRed2k	*E. coli* BW25113 with pBBR1k-RED	This study
ReRed1	*Ralstonia eutropha* H16 with pBBR1c-RED1	This study
ReRed2	*Ralstonia eutropha* H16 with pBBR1c-RED2	This study

Table 2.2: Plasmids used in this study

Plasmid	Origin	Description	Reference
pBBR1MCS1	BBR1 OriV	Broad host range, medium copy number plasmid compatible with IncQ, IncP, IncW, and colE1, *camR*	Kovach et al. (1994)
pBbA8k-RFP	p15A	Narrow host range, 1ow copy number $P_{araC\mathit{BAD}}$-RFP plasmid, *kanR*	Lee et al. (2011)
pKD20	pSC101	Narrow host range, 1ow copy number λ-Red recombinase vector, *ampR*	Datsenko and Wanner (2000)
pKD46	pSC101	Narrow host range, 1ow copy number λ-Red recombinase vector, *ampR*	Datsenko and Wanner (2000)
pEGFP	pUC	eGFP plasmid, *ampR*	BD Biosciences Clontech
pBBR1c-RFP	BBR1 OriV	Broad host range RFP plasmid construct, *camR*	This study
pBBR1c-EGFP	BBR1 OriV	Broad host range EGFP plasmid construct, *camR*	This study
pBBR1c-FapR	BBR1 OriV	Broad host range FapR plasmid construct, *camR*	This study
pBBR1k-RFP	BBR1 OriV	Broad host range EGFP plasmid construct, *kanR*	This study
pBBR1c-RED1	BBR1 OriV	Broad host range λ-Red plasmid construct, *camR*	This study
pBBR1c-RED2	BBR1 OriV	Broad host range λ-Red plasmid construct, *camR*	This study
pBBR1k-RED	BBR1 OriV	Broad host range λ-Red plasmid construct, *camR*	This study

Table 2.3: Primers used in this study

Primer Name	Direction	Sequence (5'-3')
Primers for 4.3 kb AvrII-pBBR1-camR-PstI amplicon		
AvrII-Cam-pBBR1	Forward	GATCCCTAGGATTGTTATCCGCTCACA ATTCCACACAACATAC
pBBR1MCS1-*PstI*	Reverse	GATCCTGCAGAAATTGTAAGCGTTAAT ATTTTGTTAAAATTCGCGTTAAATTTT TG
Primers for 3.3 kb AvrII-pBBR1-SacI amplicon		
AvrII-pBBR1MCS1	Forward	GATCCCTAGGGAAGACGAAAGGGCCTC GTGATACG
pBBR1MCS1-*SacI*	Reverse	GATCGAGCTCAAATTGTAAGCGTTAAT ATTTTGTTAAAATTCGCGTTAAATTTT TG
Primers for 0.74 kb NdeI-eGFP-BamHI amplicon		
NdeI-EGFP-*for*	Forward	GATCCATATGATGGTGAGCAAGGGCGA GG
BamHI-EGFP-*rev*	Reverse	GATCGGATCCTTACTTGTACAGCTCGT CCATGCC
Primers for 1.9 kb NdeI-pKD20-BamHI amplicon		
NdeI-Gam-*for*	Forward	GATCCATATGATGGATATTAATACTGA AACTGAGATCAAGCAAAAGC
BamHI-Exo-*rev*	Reverse	GATCGGATCCTCATCGCCATTGCTCCC CA
Primers for 2.2 kb NdeI-pKD46-λLt-BamHI amplicon		
NdeI-Gam-*for*	Forward	GATCCATATGATGGATATTAATACTGA AACTGAGATCAAGCAAAAGC
BamHI-λLt-Exo-*rev*	Reverse	GATCGGATCCCTACTGGTATTGGCACA AACCTGATT
Primers for 579 bp pBBR1 NdeI-FapR-BamHI amplicon		
NdeI-FapR-*for*	Forward	GATCCATATGCGCCGCAACAAG
BamHI-FapR-*rev*	Reverse	GATCGGATCCTTATCAGCTATGCTTG

* Underlined nucleotides are restriction sites

2.2.2 Plasmid and linear dsDNA construction

Plasmid construction was performed using ligase dependent restriction-based cloning. All polymerases (Pfu Turbo, Pfu Ultra, Q5, Phusion, Taq, OneTaq polymerases) used for PCR, restriction enzymes for restrictive digestion were obtained from the New England Biolabs together with associated reagents, and used according to the manufacturer's protocol. All PCR reactions were performed using the Eppendorf Mastercycler Personal (Eppendorf, Germany) according to the manufacturer's instructions. T4 ligase from New England Biolabs was used for ligation reactions, and used according to the manufacturer's protocol. Where necessary, PCR with insert primers were used to verify presence and molecular size of inserts in constructed plasmids. Agarose gel electrophoresis (100 V, 70 minutes) was carried out with the Bio-Rad Mini-Sub Cell GT, using 0.6-1.0% agarose solution, 1.0 kb DNA ladder, 2-3 μL of ethidium bromide to verify bands of PCR amplified inserts and linear dsDNA cassette where necessary. DNA on agarose gel was extracted using the QIAquick Gel extraction kit (Qiagen, Germany). All PCR products were purified using the QIAquick PCR purification kit (Qiagen, Germany) after 2-3 hours digestion with *DpnI* to remove template plasmid. DNA concentration was measured with Versawave Expedeon (Cambridge, UK) while DNA band imaging was performed with Genosmart2 (VWR, Europe).

Correct construction of all plasmids was confirmed by restrictive analysis/DNA sequencing. All DNA products were stored temporarily or permanently at -20°C in the refrigerator (Liebherr). All plasmids and linear dsDNA were *a priori* constructed *in silico* using SnapGene software (from GSL Biotech; available at snapgene.com).

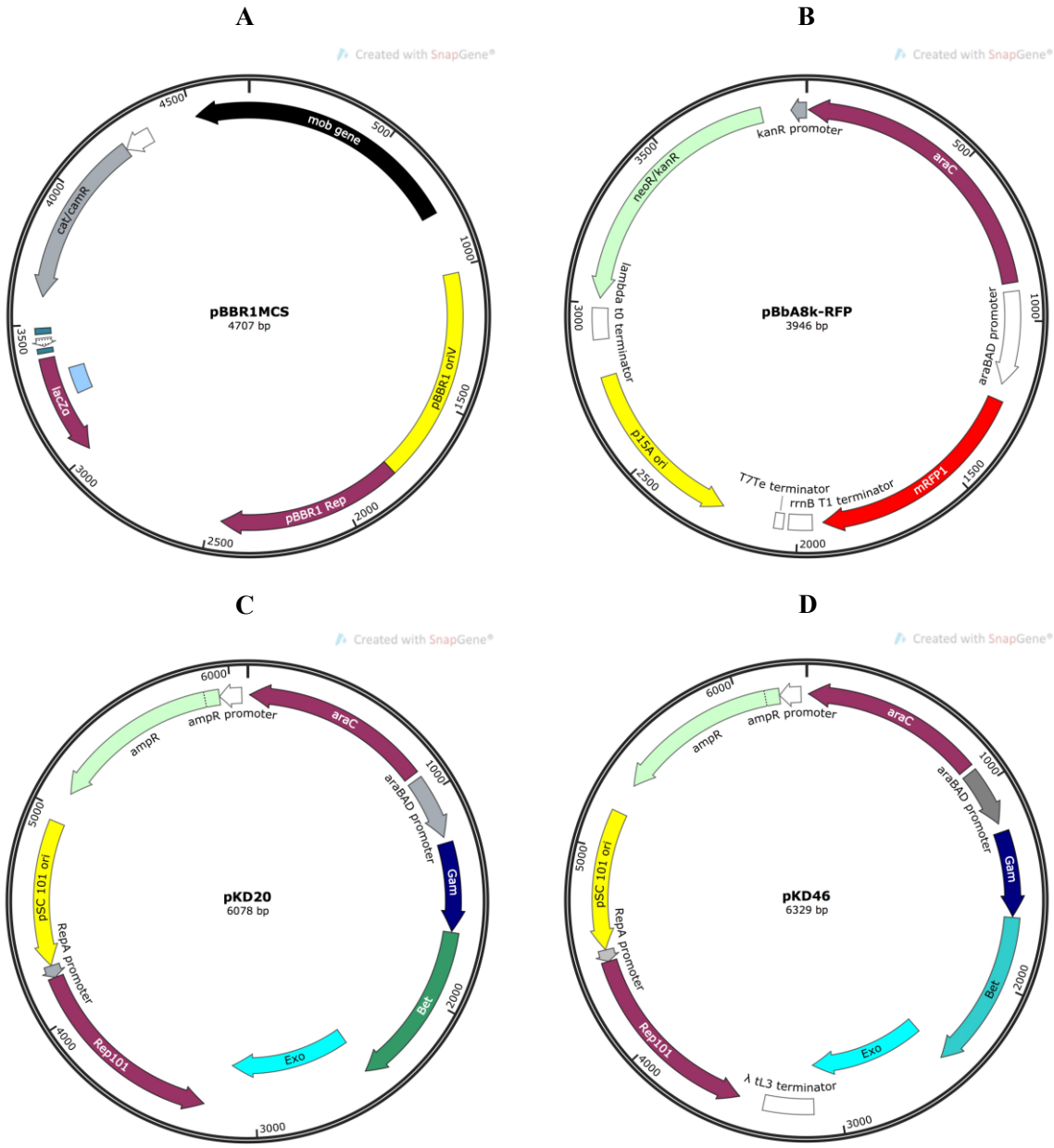

Figure 2.1: Maps of plasmids possessing essential biological parts for constructing vital expression vectors for molecular tool development in *Ralstonia eutropha* H16.
(A) pBBR1MCS is a broad host range plasmid possessing a *mob* gene for plasmid mobilization (*mob*), and the BBR1 origin of replication (pBBR1 oriV), and a chloramphenicol resistance gene (P_{cat}-camR). (B) pBbA8k-RFP is a narrow host range plasmid possessing the P_{BAD} promoter (*araC* gene and the araBAD promoter), the *rfp* gene (mRFP1), and the double transcriptional terminators (rrnB T1 and T7). (C) pKD20 is a narrow host range λ-Red recombinase plasmid possessing the P_{BAD} promoter (*araC* gene and the araBAD promoter) and the genes for Gam, Bet and Exo. (D) pKD46 is basically the pKD20 plasmid with a tL3 transcriptional terminator at the end of the λ-Red genes.

2.2.2.1 pBBR1c-RFP

The recombinant BHR plasmid pBBR1c-RFP was constructed from the BHR pBBR1MCS-1 and the synthetic plasmid pBbA8k-RFP, (Figure 2.1). A 4.3 kb AvrII-pBBR1-*camR*-PstI amplicon containing the chloramphenicol resistance, P_{cat}-*camR* gene for chloramphenicol resistance, the *mob* gene for plasmid mobilization, the BBR1 origin of replication was cloned from pBBR1MCS using forward and reverse primers AvrII-Cam-pBBR1MCS and pBBR1MCS-*PstI*, respectively. The PCR product was incubated with 1 μL *DpnI* to remove plasmid template of pBBR1MCS, and subsequently purified. The purified product was then double digested with the enzymes AvrII and PstI, and re-purified. pBbA8k-rfp synthetic plasmid was double digested with both enzymes AvrII and PstI to obtain a 2.4 kb AvrII-$P_{araCBAD}$-RFP-PstI product which was gel extracted. PCR product from pBBR1MCS and the restrictive digest product from pBbA8k-RFP were then ligated to obtain the 6.7 kb recombinant broad host range plasmid pBBR1c-RFP, (Figure 2.2).

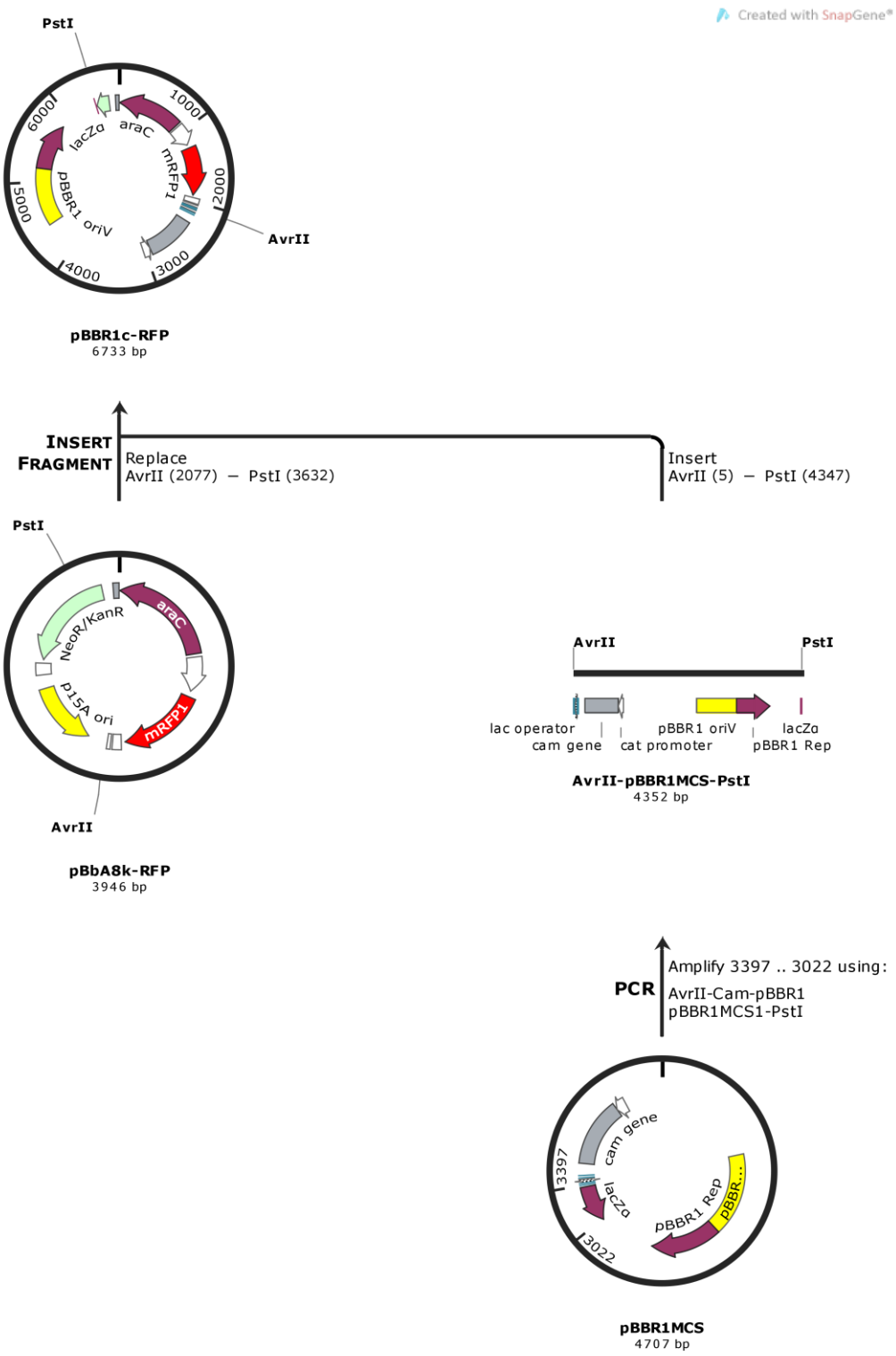

Figure 2.2: *In silico* construction of pBBR1c-RFP

2.2.2.2 pBBR1k-RFP

The recombinant BHR plasmid pBBR1k-RFP was constructed from the BHR pBBR1MCS-1 and the synthetic plasmid pBbA8k-RFP, (Figure 2.1). A 3.3 kb AvrII-pBBR1-SacI amplicon containing the *mob* gene for plasmid mobilization, the BBR1 origin of replication was cloned from pBBR1MCS using forward and reverse primers AvrII-pBBR1 and pBBR1MCS-SacI, respectively, and *pfu* turbo polymerase. The PCR product was incubated with 1 µl *DpnI* to remove the plasmid template of pBBR1MCS-1, and subsequently purified. The purified product was then double digested with the enzymes AvrII and SacI, and re-purified. pBbA8k-rfp synthetic plasmid was double digested with both enzymes AvrII and SacI to obtain a 3.0 kb AvrII-$P_{araCBAD}$-RFP-SacI product with the P_{neokan}-kanR gene for resistance to kanamycin. The digest was gel extracted. The 3.3 kb PCR product from pBBR1MCS and the 3.0 kb restrictive digest product from pBbA8k-RFP were then ligated to obtain the 6.3 kb recombinant broad host range plasmid pBBR1k-RFP, (Figure 2.3).

2.2.2.3 pBBR1c-eGFP

The chloramphenicol resistant broad host range EGFP plasmid, pBBR1c-EGFP was constructed from the plasmids pBBR1c-RFP and pEGFP, (Figure 2.4). pBBR1c-RFP was double digested with the restrictive enzymes NdeI and BamHI, to obtain a 6.0 kb NdeI-pBBR1c-BamHI linear DNA without the *rfp* gene. The product was gel extracted. The *eGFP* gene was amplified from pEGFP with *pfu* turbo polymerase, using the forward primer *NdeI*-EGFP-*for* and reverse primer BamHI-EGFP-*rev* to obtain a 0.74 kb NdeI-eGFP-BamHI PCR product. The PCR product was incubated with 1µl *DpnI* to remove the pEGFP plasmid template, and subsequently purified. The purified product was then double digested with NdeI and BamHI, and re-purified using the same kit. The 6.0 kb restrictive digest from pBBR1c-RFP, and the 0.74 kb PCR product from pEFGP were then ligated to obtain the 6.7 kb recombinant broad host range plasmid pBBR1c-eGFP, (Figure 2.4).

2.2.2.4 pBBR1c-FapR

The plasmid pBBR1c-FapR containing the *fapR* gene was constructed from the pBBR1c-RFP plasmid as vector. The *fapR* gene was synthesized and codon-optimized for gene expression in *R. eutropha* H16 by GenScripts HK Limited. The *fapR* gene was amplified from the pUC57 plasmid containing the gene using primers NdeI-FapR-*for* and BamHI-FapR-*rev* to generate 579 bp NdeI-FapR-BamHI amplicon where in the *fapR* gene is

flanked by NdeI and BamHI restriction sites. NdeI-FapR-BamHI was doule digested with NdeI and BamHI restriction enzymes and the product was purified. The purified 6.0 kb NdeI-pBBR1c-BamHI linear DNA was ligated with the purified NdeI-FapR-BamHI digest to yield the plasmid pBBR1c-FapR, (Figure 2.5).

Protein sequence of codon-optimzed FapR

MRRNKRERQELLQQTIQATPFITDEELAGKFGVSIQTIRLDRLELSIPELRERIKNVAEK
TLEDEVKSLSLDEVIGEIIDLELDDQAISILEIKQEHVFSRNQIARGHHLFAQANSLAVA
VIDDELALTASADIRFTRQVKQGERVVAKAKVTAVEKEKGRTVVEVNSYVGEEIVFSGRF
DMYRSKHS

DNA sequence of codon-optimzed *fapR* gene

ATGCGCCGCAACAAGCGCGAACGCCAGGAGCTCCTCCAGCAGACGATCCAGGCCACCCCGTTCATCACGGACG
AAGAACTGGCGGGCAAGTTCGGCGTGTCGATCCAGACCATCCGCCTGGACCGCCTGGAGCTGAGCATCCCGGA
GCTGCGCGAGCGCATCAAGAACGTGGCCGAGAAGACCCTGGAGGACGAGGTGAAGTCGCTGAGCCTGGACGAG
GTGATCGGCGAGATCATCGACCTGGAGCTGGACGACCAGGCCATCTCGATCCTGGAGATCAAGCAGGAGCACG
TGTTCAGCCGCAACCAGATCGCACGCGGCCACCACCTGTTCGCCCAGGCGAACTCGCTGGCGGTGGCCGTGAT
CGACGACGAGCTGGCCCTGACCGCCAGCGCGGACATCCGCTTCACCCGCCAGGTGAAGCAGGGCGAGCGCGTG
GTGGCCAAGGCCAAGGTGACCGCGGTGGAGAAGGAGAAGGGCCGCACCGTGGTGGAAGTGAACTCGTACGTGG
GCGAGGAAATCGTGTTCTCGGGCCGCTTCGACATGTACCGCAGCAAGCATAGC

2.2.2.5 pBBR1c-RED1

The chloramphenicol resistant broad host range λ-Red plasmid, pBBR1c-RED was constructed from the plasmids pBBR1c-RFP and pKD20, (Figure 2.6). pBBR1c-RFP was double digested with the restrictive enzymes NdeI and BamHI, to obtain a 6.0 kb NdeI-pBBR1c-BamHI linear DNA without the *rfp* gene. The product was gel extracted. The gene operon for the λ-Red proteins (Gam, Exo and Bet) was amplified with Q5 polymerase from pKD20 using forward primer NdeI-Gam-*for* and reverse primer BamHI-Exo-*rev* to obtain the 1.9 kb NdeI-pKD20-BamHI PCR product. The PCR product was incubated with 1 μL *DpnI* to remove pKD20 plasmid template, and subsequently purified. The purified product was then double digested with NdeI and BamHI, and repurified using the same kit. The 6.0 kb restrictive digest from pBBR1c-RFP, and the purified digest of the 1.9 kb NdeI-pKD20-BamHI PCR product from pKD20 were then ligated to obtain the 7.9 kb recombinant broad host range plasmid pBBR1c-RED1.

2.2.2.6 pBBR1c-RED2 and pBBR1k-RED

The kanamycin resistant broad host range λ-Red plasmid, pBBR1k-RED and the chloramphenicol resistant broad host range λ-Red plasmid were constructed from the plasmids pBBR1k-RFP and pBBR1c-RFP and pKD46, respectively, (Figure 2.7 and 2.8). pBBR1k-RFP and pBBR1k-RFP was double digested with the restrictive enzymes NdeI and BamHI, to obtain the 5.63 kb NdeI-pBBR1k-BamHI and the 6.06 kb NdeI-pBBR1c-BamHI the linear vectors. The product was gel extracted. The gene operon for the λ-Red proteins was amplified with Q5 polymerase from pKD46 using forward primer NdeI-Gam-*for* and reverse primer BamHI-tL3-Exo-*rev* to obtain the 2.147 kb NdeI-pKD46-BamHI PCR product. The PCR products were incubated with 1 μL *DpnI* to remove pKD46 plasmid template, and subsequently purified. The purified product were then double digested with NdeI and BamHI, and repurified using the same kit. The restrictive digest of the linear vectors and the purified digest of the 2.147 kb NdeI-pKD46-BamHI PCR product were then ligated to obtain the 7.8 kb pBBR1k-RED and the 8.2 kb pBBR1c-RED2 recombinant broad host range plasmids.

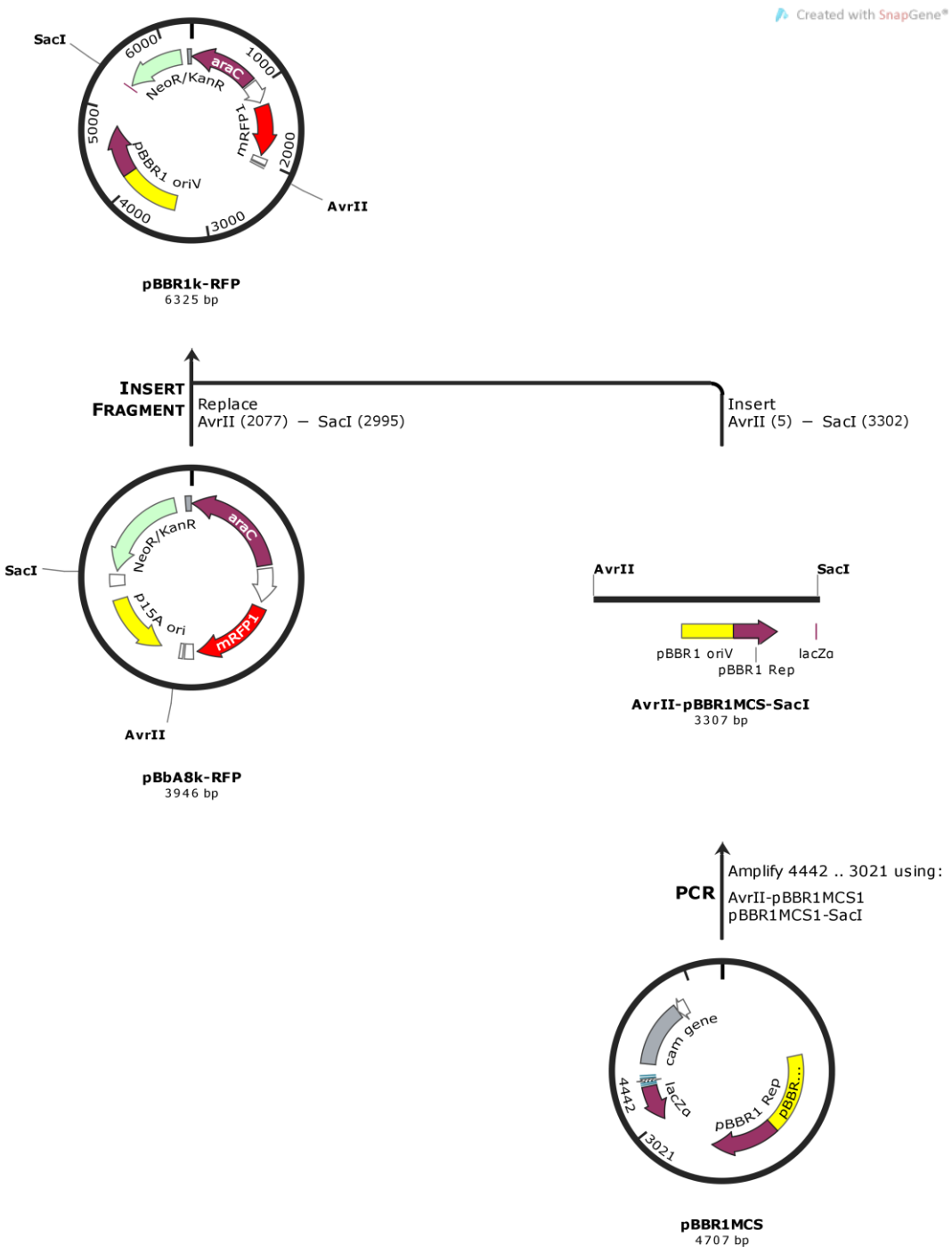

Figure 2.3: *In silico* construction of pBBR1k-RFP

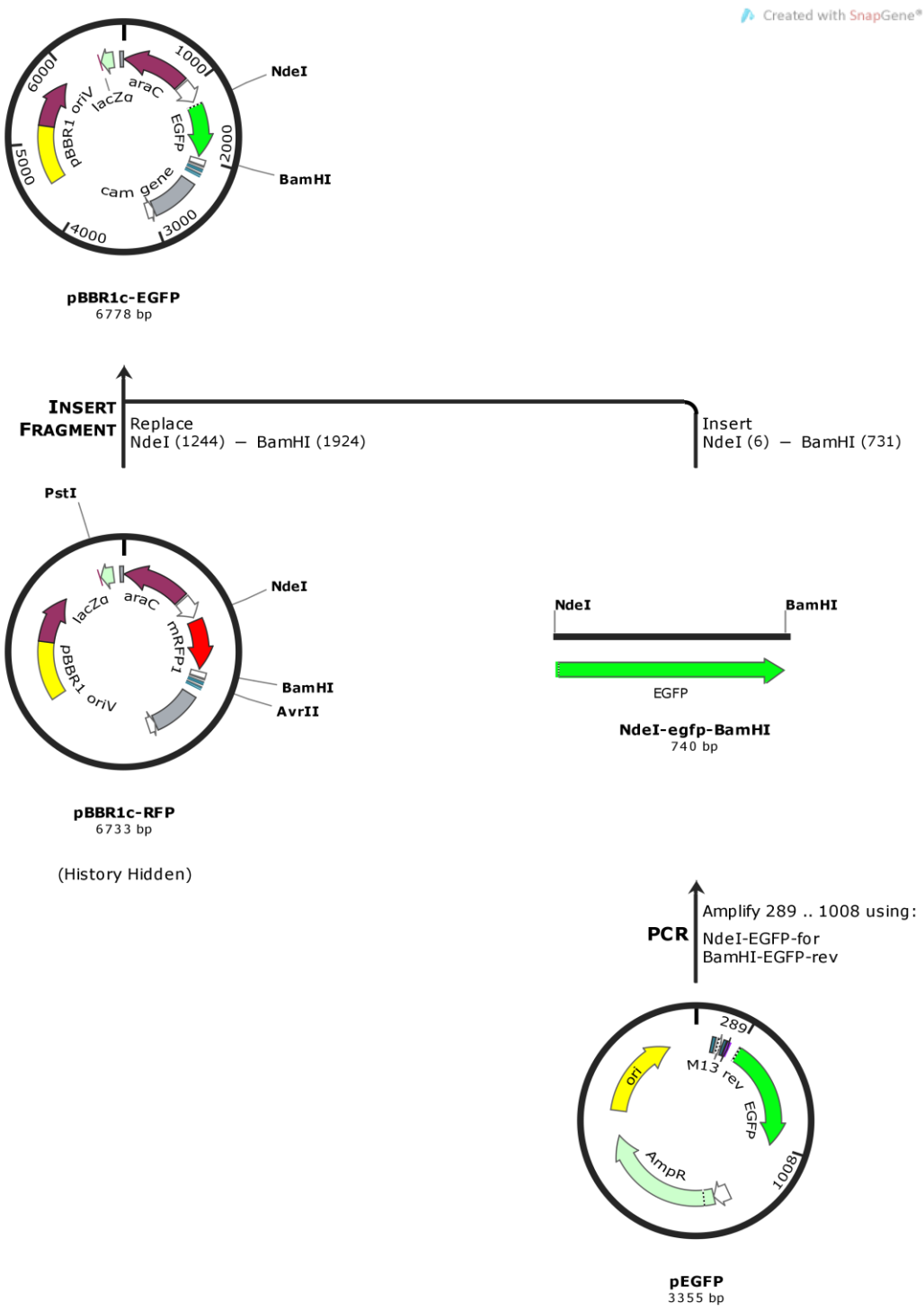

Figure 2.4: *In silico* construction of pBBR1c-eGFP

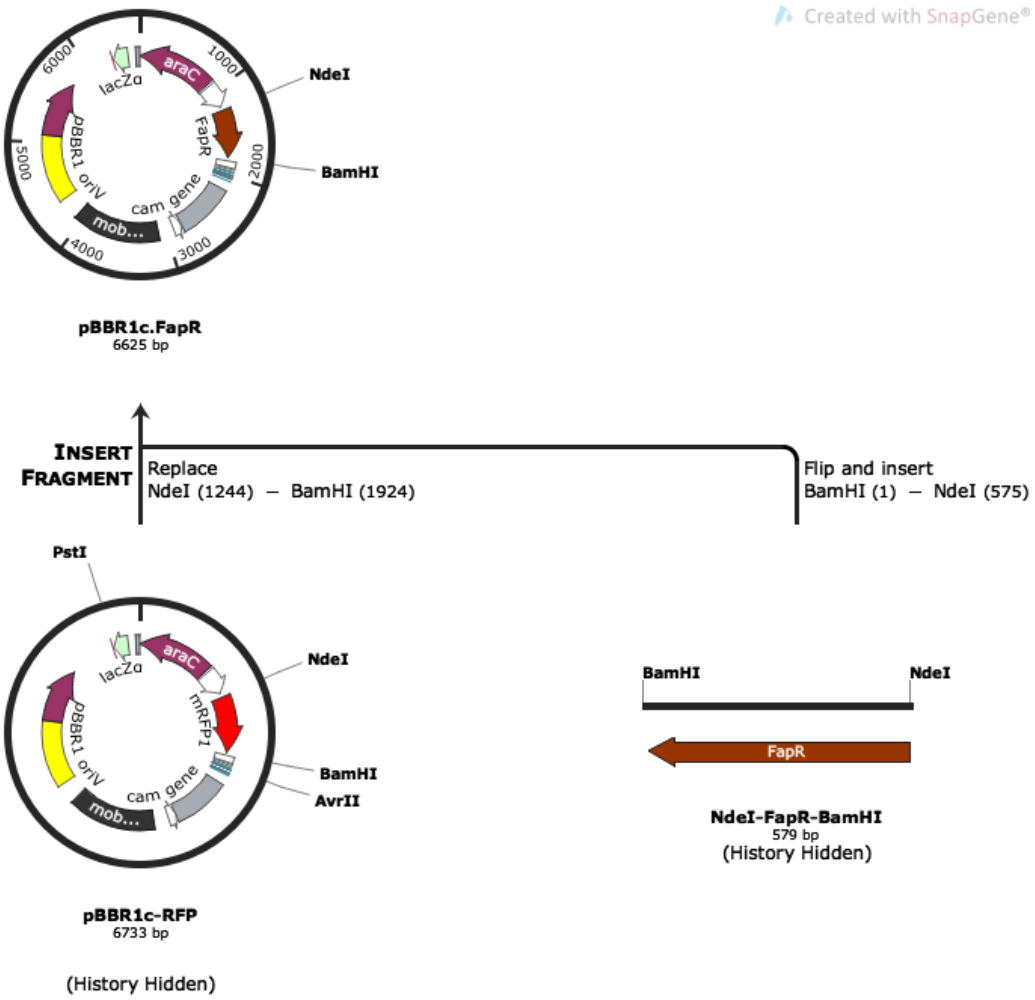

Figure 2.5: *In silico* construction of pBBR1c-FapR

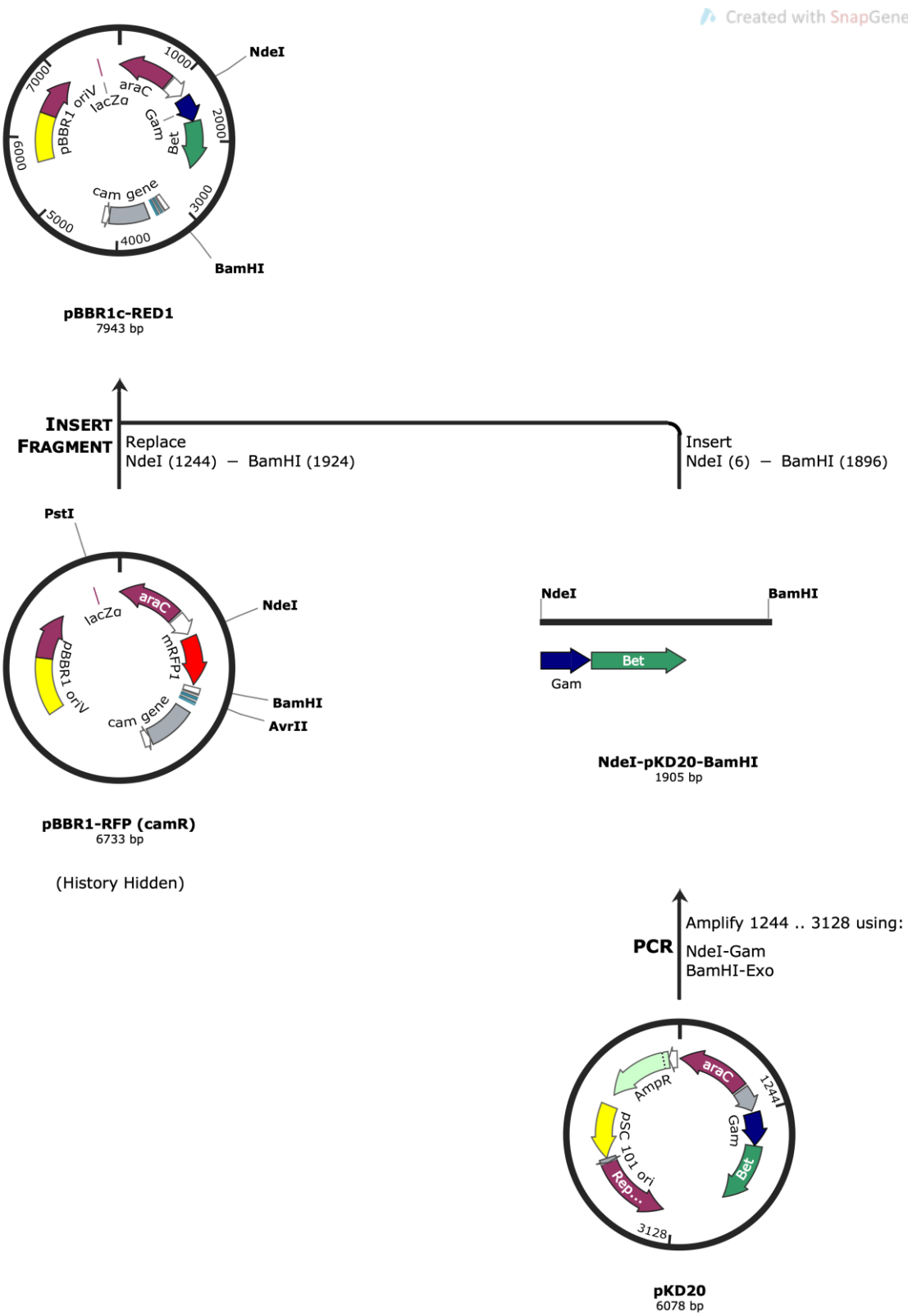

Figure 2.6: *In silico* construction of pBBR1c-RED1

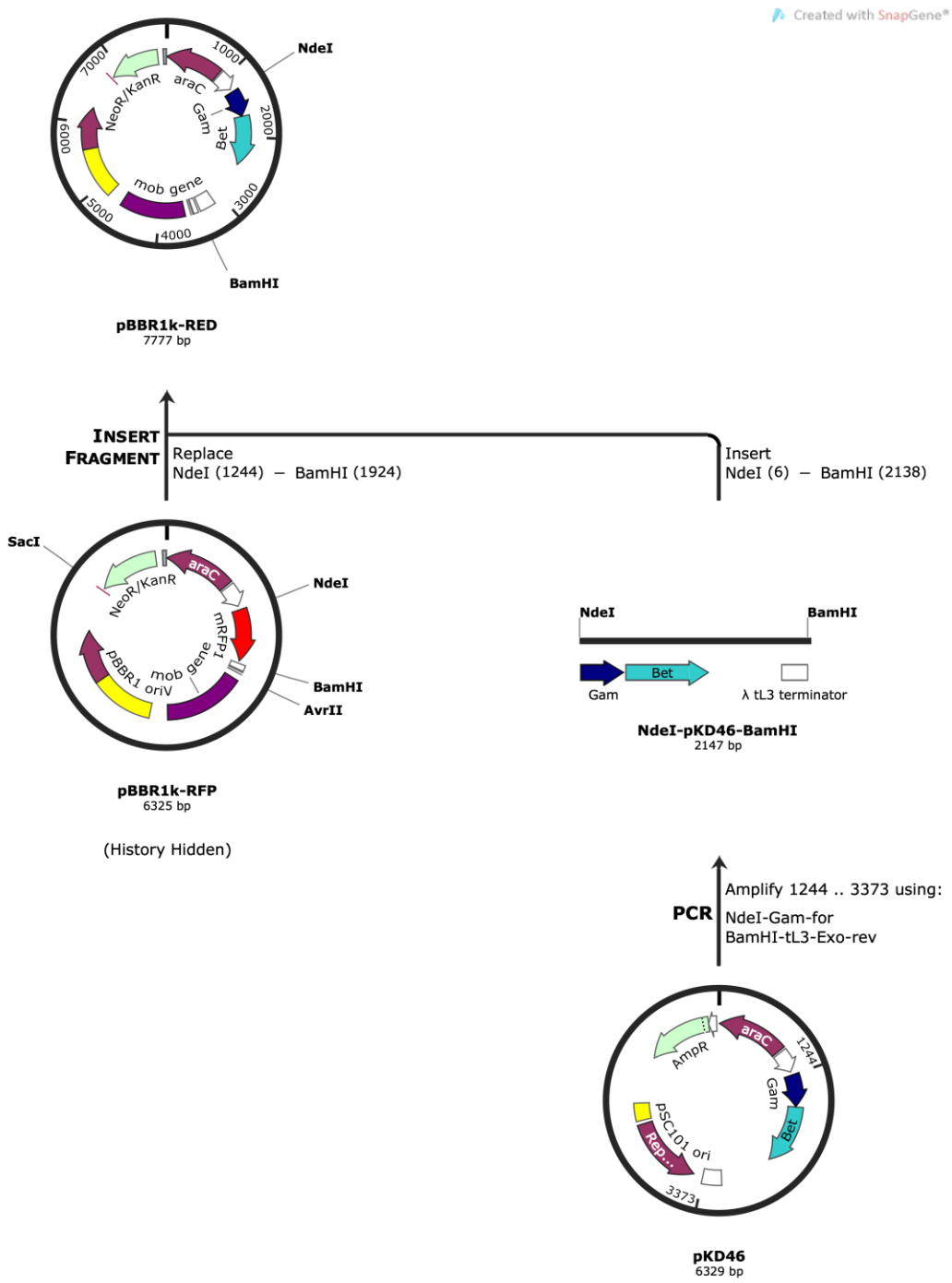

Figure 2.7: *In silico* construction of pBBR1k-RED

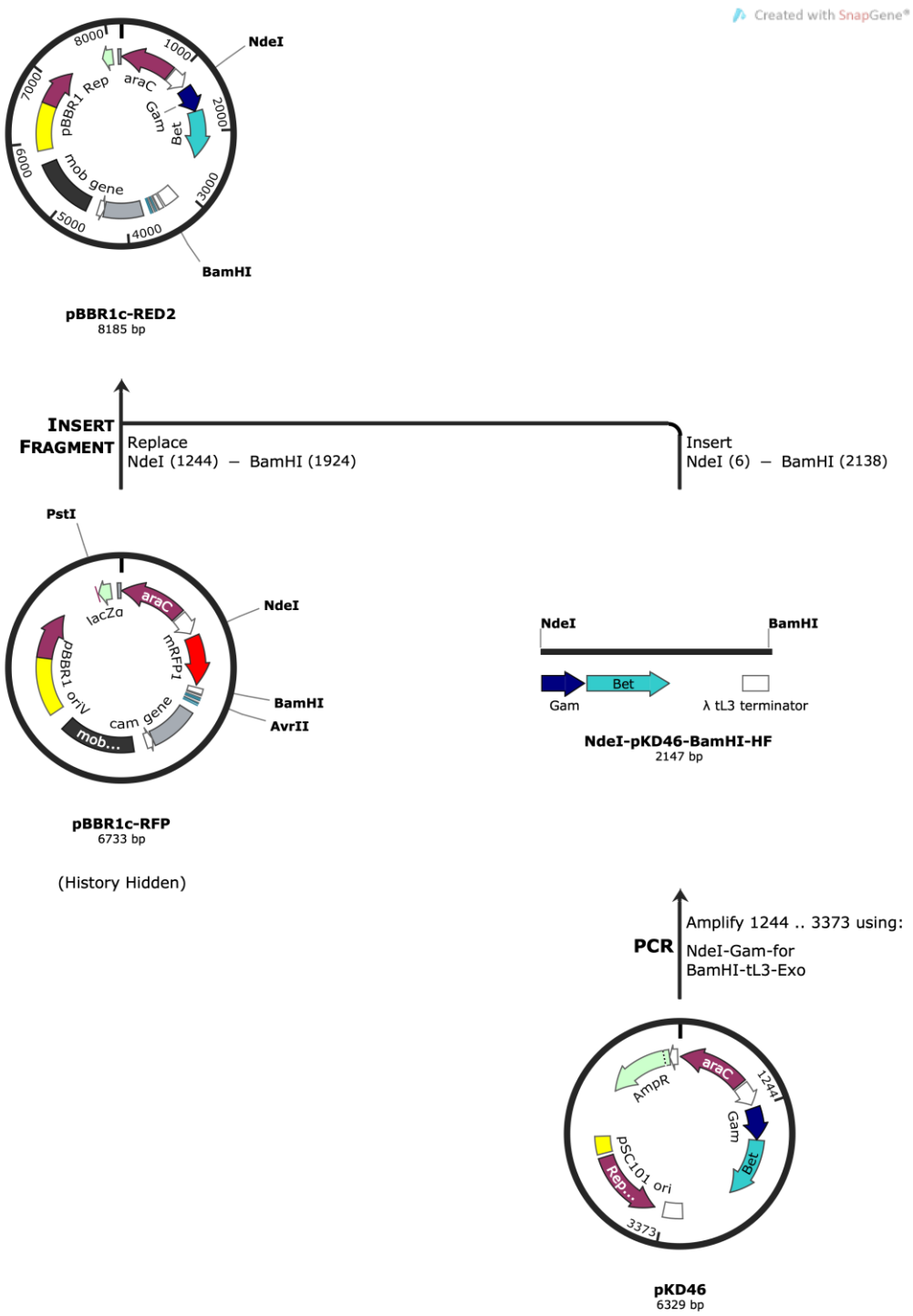

Figure 2.8: *In silico* construction of pBBR1c-RED2

2.2.3 Plasmid propagation and circularization

Ligation mixtures of all plasmids constructed were initially transformed into *E. coli* DH5α for intact plasmid circularization and plasmid propagation. 5 µl of ligation mixture was used for transformation into *E. coli* DH5α.

2.2.4 Bacterial Transformation

Bacterial transformation in *E. coli* was done using heat shock with the Eppendorf Thermomixer C preset at 42°C. 5 mL of 2XYT media was inoculated with fresh overnight cultures of *E. coli* in a 1:50 ratio. The culture was grown for 2 h to an OD_{600} value 0.5–0.6. The samples were then aliquoted into 1.5 mL microfuge tubes and centrifuged at 2,800 rpm to obtain cell pellets. Cell pellets were then washed with 500 µL of pre-chilled 500 mM $CaCl_2$ solution. Washed cells were resuspended in 500 µL of prechilled 500 mM $CaCl_2$ solution and cooled in wet ice for 30 minutes. 100 ng of plasmid DNA was added into the cooled cell suspension as appropriate. The cell suspension was again cooled in wet-ice for 10-30 minutes, after which the cell suspension was heat shocked at 42°C for 1 min, and immediately incubated in wet-ice for 2 minutes. 1 mL of 2XYT media was added to this cell suspension, and the mixture was immediately cultivated at 37°C for 1 h. The outgrowth culture was then centrifuged at 2,800 rpm, 1 mL of the supernatant was discarded and the cell suspension was resuspended before plating on Tryptone-Yeast (TYE) agar plates supplemented with appropriate antibiotics and incubated overnight in the VWR INCU-Line Incubator (Germany). As an exception, transformation of the plasmids pKD20 and pKD46 into *E. coli* required cultivation/ incubation at 30°C to prevent plasmid curing.

Electroporation with the Eppendorf Eporator (Eppendorf AG, Hamaburg, Germany) was used for bacterial transformation of the broad host range plasmids pBBR1MCS1, into *Ralstonia eutropha* H16 the transformation protocol according to Tee et al. (2017). Briefly, fresh NB supplemented with gentamicn (10 mg/L) is inculated with overight culture of *Ralstonia eutropha* H16 in a 1:50 ratio. The culture is grown to OD_{600} of ~0.6 and cooled in ice briefly for up to 3 minutes. Competent cells are created by first resuspending and incubating the cells in 50 mM $CaCl_2$ at a voume one-half the volume of cell culture. The cell suspension is incubated in ice for up to 15 minutes. Subsequently, the cells are washed twice in 0.2M sucrose at a volume one-half the volume of initial cell culture. The

competent cells are resuspended in 200 μL of 0.2 M sucrose and 100 ng – 1 μg of DNA is added to the cell suspension. The cells suspension is transferred to the pre-chilled electropration cuvettes and the cells is electroporated at 2.3 kV. 1 mL of NB supplemented with gentamicin (10 mg/L) is immediately added to the electroporated cells and the mixture is transferred into 2 mL microfuge tubes to create and outgrowth culture. The outgrwoh culture is cultivated at 30°C, 250 rpm for between 2 hours to overnight. The outgrowth is afterwards centrifuged to decant 1 mL of the supernatant. The cell pellet is re-suspended in the remaining 100–200 μL of supernatant and plated on NB agar plate supplemented with appropriate antibiotics.

2.2.5 Cell density measurement

Cell density at OD_{600} was measured using the Eppendorf Biophotometer (Eppendorf AG, Hamburg, Germany) when cells were cultivated in falcon tubes or conical flasks. When cells are cultured in 96-well micro-titre plates, cell density measured at OD_{595} using the MultiSkan^{TM} FC Microplate Photometer (Thermo Fisher Scientific) or at OD_{600} using the SpectraMax M2e microplate/cuvette reader [Molecular Devices (Wokingham, UK)].

2.2.6 Plasmid Isolation

After plasmid construction plasmids were isolated from *E. coli* DH5α transformant colonies for gene/protein expression in *Ralstonia eutropha* or *E. coli*. Plasmids were isolated from overnight cultures of *E. coli* DH5α using the QIAprep miniprep kit (Qiagen) according to the manufacturer's protocol. Isolated plasmids were verified *via* restrictive analysis and/or DNA sequencing. Plasmids were stored at -20°C before being used for bacterial transformation and gene expression.

2.2.7 Colony PCR verification of transforamnts

Where applicable colony PCR using *OneTaq* or *Taq* polymerase from New England Biolabs according to the manufacturer's protocol was used to verify correct transformation of plasmids into *Ralstonia eutropha* H16. Forward and reverse Primers specific to the inserts present in the plasmids were used for the colony PCR verification. Amplicons were

checked using agarose gel electrophoresis (0.6-1% agarose). Transformant strains of *E. coli* and *Ralstonia eutropha* H16 are listed in Table 3.1.

2.2.8 Protein expression: Expression of reporter proteins RFP and eGFP

Fresh pBBR1c-RFP and pBBR1c-eGFP-transformant colonies of *R. eutropha* H16 (*i.e.* strains ReRFP and ReGFP) were inoculated into 5 mL of nutrient broth (NB) supplemented to 10 mg/L gentamicin and 25 mg/L chloramphenicol. Each inoculum was cultivated at 30°C, 500 rpm for up to 48 h to create overnight cultures. 100 mL of fresh NB media in 500 mL cultivation flasks supplemented with aforementioned antibiotics was inoculated with 500 µl of each seed culture. A 20% (w/v) stock solution of L-arabinose was prepared by dissolving 5 g of L-arabinose (Sigma Aldrich) in 25 mL of triple-filtered de-ionized water and filtered using the 0.2 µm Whatman syringe filter. The new cultures were cultivated up to OD_{600} 0.5–0.6, after which protein expression was induced with L-arabinose solution at 0.1% (w/v). Control cultures were not induced for protein expression. All cultures were cultivated for 48 hours in the incubator shaker (New Brunswick Scientific Excella E24) at 30°C, 250 rpm for up to 30 h. Expression cultures were collected in 50 mL falcon tubes and centrifuged at maximum speed to collect cell pellets with expressed proteins. Cell pellets were stored at -20°C for further analyses of expressed proteins.

2.2.9 Examining the induction range of the L-arabinose inducible P_{BAD} promoter in *Ralstonia eutropha* H16

Fresh media supplemented with gentamicin and chloramphenicol was inoculated in 1:50 ratio with overnight cultures of *R. eutropha* H16 with pBBR1c-RFP and pBBR1MCS-1 (*i.e.* strains ReRFP and Re-null). 200 µL of each culture was aliquoted into fresh clear-bottom 96-well microtitre plates [Greiner Bio-One (Stonehouse, UK)]. The cultures were supplemented with L-arabinose of final concentrations between 0 and 0.2 % (w/v). All cultures were cultivated at 30°C, 1050 rpm for up to 48 h. OD_{600} and fluorescence (E_x 584 nm, E_m 607 nm; bottom read) were measured using SpectraMax M2e microplate/cuvette reader [Molecular Devices (Wokingham, UK)] after 12 h of cultivation and repeated at 12 h intervals. Relative fluorescence unit (RFU) was calculated by normalizing fluorescence value with the fluorescence value of *R. eutropha* H16 carrying the pBBR1MCS-1 RFP-null vector (negative control). RFU/OD_{600} value was then calculated as the ratio of RFU and

OD_{600} value of the respective strain. The ratio was used to account for potential metabolic burden due to high protein expression level, affecting bacterial growth. Promoter activity (PA) was defined as the RFU/OD_{600} value after 48 h of cultivation. All experiments were done in triplicate.

2.2.10 Protein expression: Expression of the FapR transcriptional regulator in *R. eutropha* H16 and *E. coli* DH5α

Overnight cultures of *R. eutropha* H16 and *E. coli* DH5α transformed with pBBR1c-FapR (*i.e.* ReFapR and EcFapR, respectively) were cultivated as already described. Fresh 5 mL cultures in 50 mL falcon tubes were inoculated in a 1:50 ratio with the overnight cultures, cultivated to OD_{600} 0.5-0.6, and induced with L-arabinose at final concentrations of 0.01% and 0.1% L-arabinose. Control cultures were not induced. All cultures of ReFapR and EcFapR were then cultivated at 30°C, 250 rpm for 36 h, and 37°C, 250 rpm for 24 h, respectively. 2 mL of each expression cultures were collected in 2 mL falcon tubes and cell pellets were stored at -20°C for further analyses of expressed proteins.

2.2.11 Protein expression: Expression of the λ-Red genes in *E. coli* BW25113 and *R. eutropha* H16

The λ-Red plasmids pKD20 and pKD46 are low copy number, narrow host range plasmids (Datsenko and Wanner, 2000). pBBR1c-RED1 possseses the pKD20 λ-Red operon (containing the three genes Gam, Exo and Bet) while pBBR1c-RED2 and pBBR1k-RED possess the pKD46 λ-Red operon (containing the three genes Gam, Exo, Bet and the tL3 transciptional terminator), (Figure 2.1). Expression of the λ-Red proteins was examined in *E. coli* BW25113 using all the λ-Red plasmids in order to observe if the differences in copy number and components of λ-Red operon might affect expression of the the proteins.

Overnight cultures of respective strains were cultivated in 5 mL 2XYT media. Fresh 5 mL 2XYT media in 50 mL falcon tubes were inoculated with overnight cultures. Test cultures were induced with L-arabinose at final concentration of 0.1%. Control cultures were not induced. The cultures were cultivated at 30°C (for BWD20 and BWD46) and 37°C (for BWRed1, BWRed2c, and BWRed2k) at 500 rpm for 24 hours. Protein expression was

similarly examined in *R. eutropha* H16 (with ReRed1, ReRed2c) was performed in 5 mL nutrient broth (NB) in 50 mL falcon tubes at 30°C, 500 rpm for 30 hours. 2 mL of each expression cultures were collected in 2 mL falcon tubes and cell pellets were stored at -20°C for further analyses of expressed proteins.

2.2.12 Protein analysis with SDS-PAGE

Sodium Dodecyl Sulphate-Polyacrylamide Gel Electrophoresis (SDS-PAGE) with 2X SDS-reducing buffer (5% β-mercaptoethanol) and 10-15% acrylamide-SDS gel was used to detect expressed proteins in protein fractions. Protein samples were treated with denatured with SDS-reducing buffer contaiining 5% β-mercaptoethanol. 15% SDS-polyacrylamide gels were prepared from resolving and stalking gels. Resolving gel contained: 2.05 mL DDI water, 1.65 mL of 30 % acrylamide, 1.25 mL of 1.5 M Tris-HCl (pH 8.8), 0.05 mL SDS, 2.5 µL TEMED, 25 µL APS. Stalking gel contained: 2.05 mL DDI water, 1.65 mL of 30 % acrylamide, 1.25 mL of 0.5 M Tris-HCl (pH 6.8), 0.05 mL SDS, 5.0 µL TEMED, 25 µL APS. 5 µl of PageRuler^{TM} unstained protein ladder was used as marker to detect the sizes of protein bands. Commassie Brillaint Blue staining dye was used as the protein gel staining solution followed by counter-staining with de-staining solution.

2.3 RESULTS AND DISCUSSION

2.3.1 Bacterial transformation

All plasmids were successfully constructed and transformed into *E. coli* DH5α and *E. coli* BW25113. Transformations into *Ralstonia eutropha* following the protocol by Tee et al. 2017 had transformation efficiencies of (3.86±0.29) x 10^5 cfu/μg (Tee et al., 2017). Transformant strains of *E. coli* and *Ralstonia eutropha* H16 are listed in Table 2.1.

2.3.2 Protein expression of RFP and eGFP in *Ralstonia eutropha* H16

Cell pellets of the cultures from L-arabinose-induced expression of the RFP and eGFP from pBBR1c-RFP and pBBR1c-eGFP in *R. eutropha* H16 (*i.e.* ReRFP and ReGFP, respectively) indeed were red and green, (Figure 2.9). This is in wide contrast to pellets from the un-induced culture of ReRFP, which only had an orange colour, which is quite typical of pellets of wild type *R. eutropha* H16, (Figure 2.9). This confirmed that the red and green fluorescence proteins were successfully expressed in *R. eutropha* from the plasmids pBBR1c-RFP and pBBR1c-eGFP, respectively following protein expression with 0.1% L-arabinose. It also indicates that the P_{BAD} promoter in pBBR1c-RFP and pBBR1c-eGFP is tightly repressed under un-induced conditions thus validating potential use for tightly regulated gene expression, (Figure 2.9).

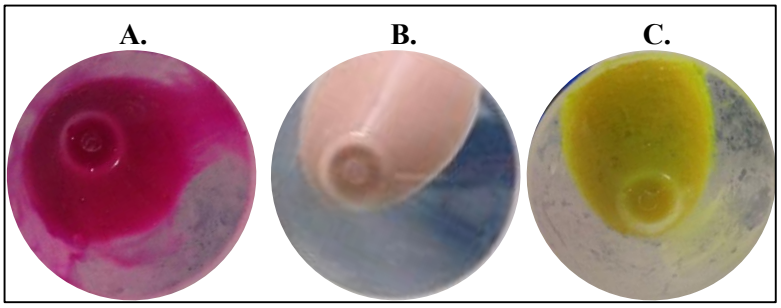

Figure 2.9: Inducible expression of RFP and eGFP in *Ralstonia eutropha*
A - Cell pellet of *R. eutropha* with pBBR1c-RFP (ReRFP) with inducible expression the RFP protein. B - Cell pellet of *R. eutropha* with pBBR1c-RFP (ReRFP) without L-arabinose induction. C - Cell pellet of *R. eutropha* with pBBR1c-eGFP (ReGFP) with inducible expression the eGFP protein.

2.3.3 Induction fold of the P_{BAD} promoter in pBBR1c-RFP in *Ralstonia eutropha* H16

RFP fluorescence value of strain ReRFP at zero concentration of L-arabinose (92.84±25.19 a.u.) was comparable to the activity of Re-null at 90±7 a.u. This very negiglible basal expression when not induced confirms that the araC repressor tightly represses the P_{BAD} promoter in pBBR1c-RFP. RFU (*i.e.* relative fluorescence unit) values of 43.39±3.90-8671.89±46.45 were obtained between 0.01-0.200% final concentrations of L-arabinose after 48 h of cultivation. A 162-fold of activity was detected between activities of the promoter upon induction with final concentrations of 0.001-0.200% L-arabinose, (Figure 2.10B).

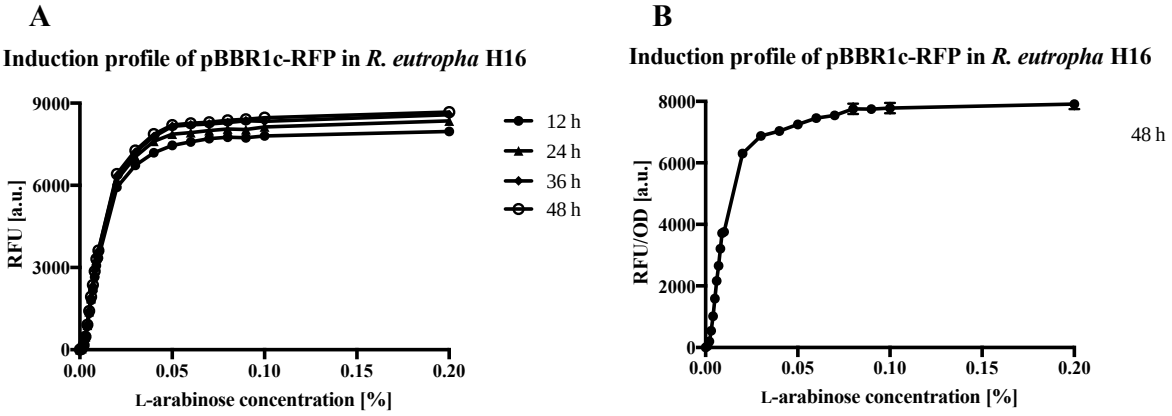

Figure 2.10: Dose-dependent induction of P_{BAD} promoter, using L-arabinose concentration from 0.001% (w/v) to 0.200% (w/v). (A) Graph of RFU versus L-arabinose concentration. (B) Graph of RFU/OD_{600} versus L-arabinose concentration.

2.3.4 Protein expression of FapR

SDS-PAGE analysis of the total protein fraction from L-arabinose induced cultures of EcFapR show a unique protein band at ~26 kDa, (Figure 2.11A). This band corresponds to the size of the FapR transcriptional regulator confirming that the protein is well expressed in *E. coli* DH5α particularly under induction with 0.1% L-arabinose. Only a faint band of the ~26 kDa FapR protein was observed from cultures induced with 0.01% L-arabinose suggesting that the protein was not well expressed at 0.01% L-arabinose induction in *E. coli* DH5α, (Figure 3.11A). Additionally, the intensity of the ~26 kDa FapR protein band from EcFapR is relatively weaker compared to the intensity of RFP band (~30 kDa) from EcRFP

when both cultures were induced at 0.1% L-arabinose concentration, (Figure 2.11A). This suggested that the FapR protein was either not as well expressed as the RFP protein or not as freely available as the RFP protein in the intracellular space of *E. coli* DH5α.

In *R. eutropha* H16, SDS-PAGE analysis of the total protein fraction show that the ~26 kDa FapR protein is well expressed from ReFapR when cultures were induced with both 0.01% and 0.1% L-arabinose, (Figure 2.11B). However as was the case in *E. coli* DH5α, the ~30 kDa RFP band was more intense than of the ~26 kDa FapR band. This also suggested that the FapR protein was also not as well expressed as was the RFP protein or not as freely available as the RFP protein in the intracellular space in *R. eutropha* H16.

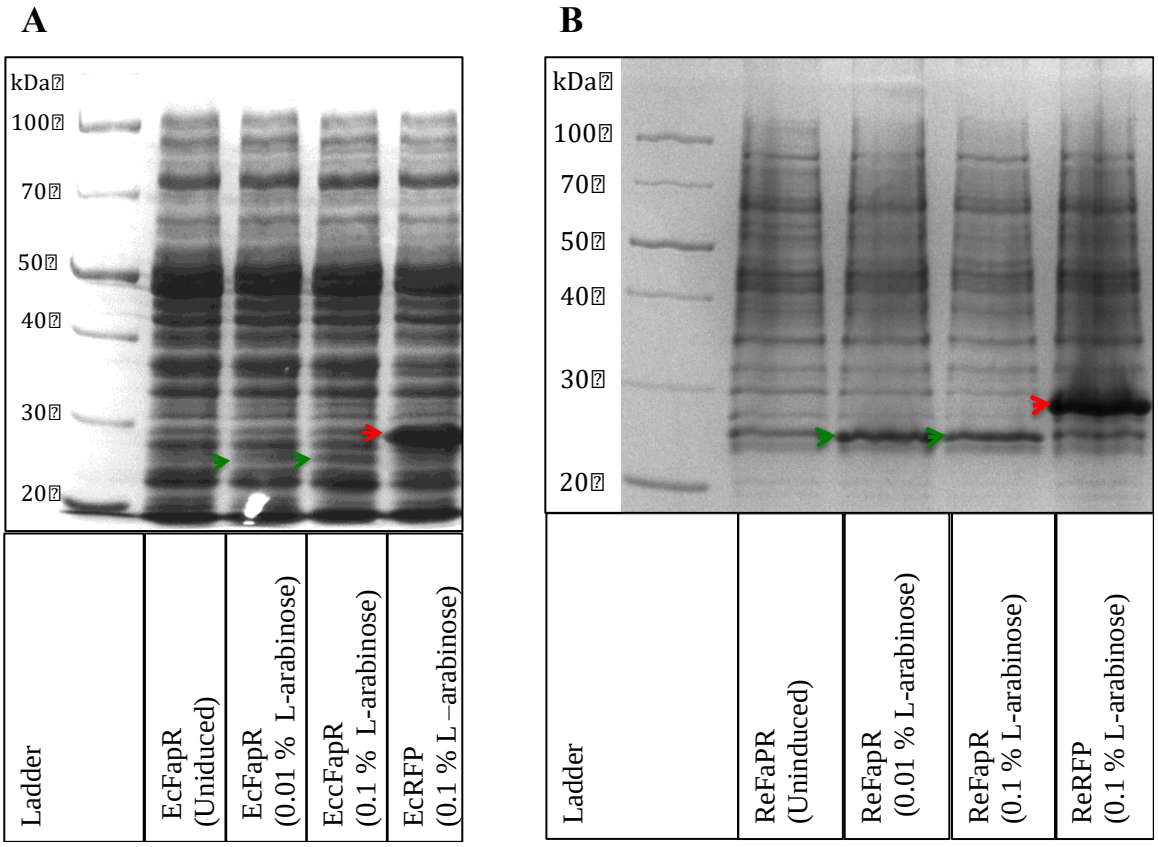

Figure 3.11: SDS-PAGE image showing expression of the ~26 kDa FapR transcriptional regulator (green arrow) and RFP (red arrow) in *E. coli* DH5α and *R. eutropha* H16.
(A) SDS-PAGE image showing expression of total protein expressed EcFapR under 0.01% L-arabinose, EcFapR under 0.1% L-arabinose (4) EcRFP under 0.1% L-arabinose. (B) SDS-PAGE image showing expression of total protein expressed from (1) ReFapR, uninduced (2) ReFapR, under 0.01% L-arabinose (3) ReFapR under 0.1% L-arabinose (4) ReRFP under 0.1% L-arabinose. Ladder – 10 - 250 Protein Ladder.

2.3.5 Protein expression of λ-Red proteins

SDS-PAGE analysis of expression of the λ-Red proteins in induced cultures of *E. coli* BW25113 strains BWRed1, BWRed2c, BWRed2k showed unique protein bands at ~15, ~25 and ~29 kDa, (Figure 3.12A). These bands correspond to the λ-Red proteins Gam (~15 kDa), Exo (~25 kDa) and Bet (~29 kDa), (Figure 2.12A). This indicates that the proteins are well expressed in *E. coli* BW25113 from the three broad host range plasmids (pBBR1c-RED1, pBBR1k-RED, pBBR1c-RED2) at 0.1% L-arabinose induction, (Figure 2.12A).

SDS-PAGE analysis of expression of the three λ-Red proteins from *E. coli* BW25113 possessing the plasmids pKD20 and pKD46 (BWD20 and BWD46) barely revealed bands of the proteins despite induction with 0.1% L-arabinose, (Figure 2.12B). This suggested that the broad host range plasmids pBBR1c-RED1, pBBR1k-RED, pBBR1c-RED2 are better expression vectors of the λ-Red proteins than the pKD20 and pKD46 plasmids in *E. coli* BW25113. This might be due to the fact that the former are medium copy number plasmids while the later are low copy number plasmids. It also indicates that lack of identifiable expression bands of the λ-Red proteins from pKD20 and pKD46 does not entirely define the performance of these plasmids as they have reportedly been well utilized for λ-Red recombineering in *E. coli*.

In *R. eutropha* H16, expression bands of λ-Red proteins from pBBR1c-RED1 and pBBR1c-RED2 were not detected *via* SDS-PAGE analysis. This is in wide contrast to marked expression of the proteins from these plasmids in *E. coli* BW25113. It is also in wide contrast to the observed vivid expression of FapR and RFP observed from the plasmids pBBR1c-FapR and pBBR1c-RFP, respectively. This suggested that the proteins might not be well expressed in *R. eutropha* H16. The poor yield of protein expression may be attributed to possible proteolytic degradation of the proteins as a native cellular defense mechanism to protect the cell from potential detrimental effects the recombinase proteins might have on cell viability. On the other hand, expression of the proteins in *R. eutropha* H16 may be repressed by the action of native global transcriptional regulator on the L-arabinose inducible P_{BAD} promoter. It is also possible that due to these cellular responses, the proteins are expressed in only very amounts too little to be detected by the SDS-PAGE procedure.

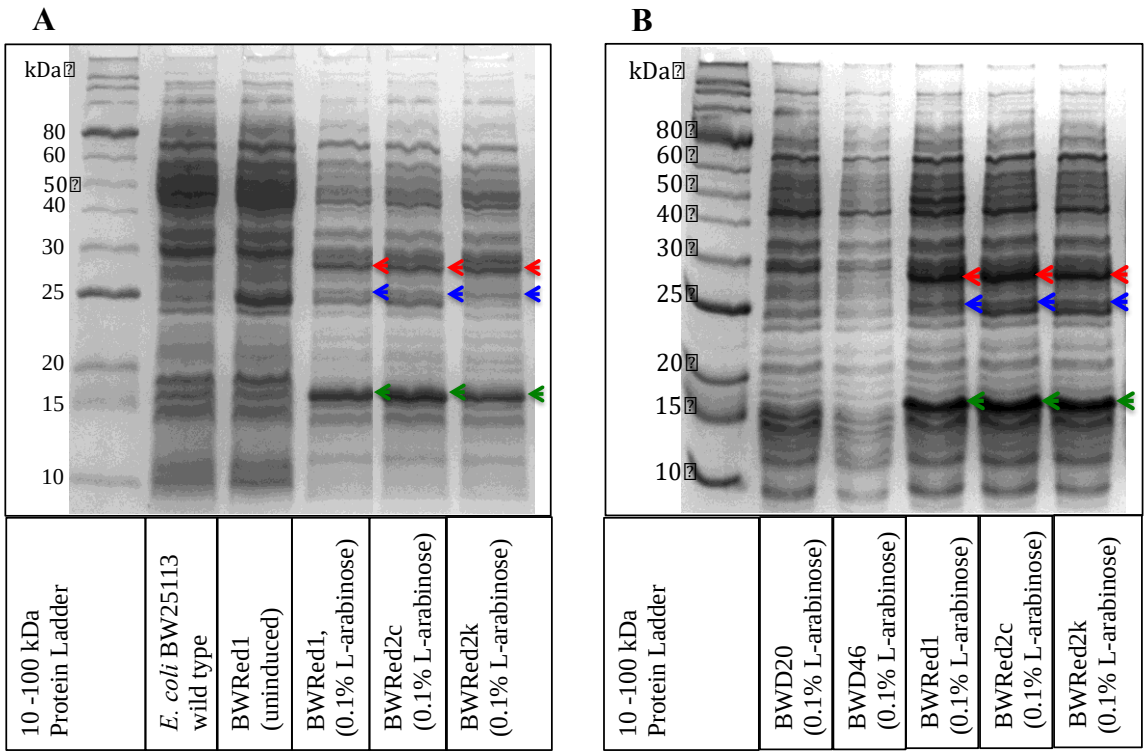

Figure 2.12: SDS-PAGE showing expression of the λ-Red proteins Bet (~29 kDa, red arrow), Exo (~25 kDa, blue arrow), and Gam (~15 kDa, green arrow) in *E. coli* BW25113. (A) The λ-Red proteins Bet and Exo and Gam are expressed at 0.1% L-arabinose in strain BWRed1, BWRed2c and BWRed2k (B) The λ-Red proteins are more vividly expressed in strains BWRed1, BWRed2c and BWRed2k than in strains BWD20 and BWD46.

2.4 CONCLUSION

The plasmid pBBR1c-RFP is a viable expression vector for tunable protein expression in *R. eutropha* H16 as confirmed by red fluorescent protein expression studies. The dose-dependent induction of the P_{BAD} promoter in this plasmid revealed a ~160 fold of activity between 0.01-0.200% L-arabinose induction concentrations. However, the rather costly concomitant need for an inducer to achieve this activity spectrum, especially in large-scale fermentation, necessitates a compilation of constitutive promoters that span the breadth of activity of the L-arabinose inducible P_{BAD} promoter. Benchmarking the activities of such promoters to the activity spectrum of the P_{BAD} promoter will definitely help to identify constitutive promoter substitutes to achieve the varied activities within and beyond the activity spectrum of the P_{BAD} promoter. Additionally, the size of the P_{BAD} promoter (1238 bp together with the *araC* repressor gene and other genetic elements) is a potential limiting factor where compact modularity is required in designing complex heterologous pathways. This again accentuates the need for properly characterized constitutive promoters with easily adjustable lengths to suit the design of complex expression circuitries.

Expression of the FapR repressor from the P_{BAD} promoter in pBBR1c-FapR was confirmed in *R. eutropha* H16 at 0.01% and 0.10% L-arabinose induction concentrations, thus demonstrating that the protein could potentially be applied in the design of malonyl-CoA-responsive genetic circuits in *R. eutropha* H16. As carefully tuning expression of the FapR repressor is highly crucial in optimizing the functionality of such circuits, properly characterized constitutive promoters are required in the design-test-build cycles required to optimize the performance of such genetic circuits in *R. eutropha* H16.

The broad host range λ-Red plasmids (pBBR1c-RED1, pBBR1c-RED2 and pBBR1k-RED) were especially designed to mediate λ-Red recombineering in *Ralstonia eutropha* H16. Poor λ-Red protein expression presumably might severely compromise chances of successful recombineering events or recombineering efficiency in *Ralstonia eutropha* H16. Nonetheless, validating the functionality of these vectors *E. coli* BW25113 in place of the conventional pKD20/pKD46 vectors is required to test the general effectiveness of the λ-Red vectors in microbial chassis where they are compatible.

The constructed expression vectors can thus be used to engineer promoters, metabolite-sensitive genetic circuits, and λ-red genome editing methods for the metabolic engineering of *R. eutropha* H16.

CHAPTER THREE

3 AN ENGINEERED CONSTITUTIVE PROMOTER SET WITH BROAD ACTIVITY RANGE FOR *RALSTONIA EUTROPHA* H16

Abstract

Well-characterized promoters with variable strength form the foundation of heterologous pathway optimization. It is also a key element that bolsters the success of microbial engineering and facilitates the development of biological tools like biosensors. In comparison to microbial hosts such as *Escherichia coli* and *Saccharomyces cerevisiae,* the promoter repertoire of *Ralstonia eutropha* H16 is highly limited. This limited number of characterized promoters poses a significant challenge during the engineering of *R. eutropha* H16 for biomanufacturing and biotechnological applications. In this article, we first examined the architecture and genetic elements of the 4 most widely used constitutive promoters of *R. eutropha* H16 (*i.e.*, P_{phaC1}, P_{rrsC}, P_{j5} and P_{g25}), and established a narrow 6-fold difference in their promoter activities. Next, using these 4 promoters as starting points and applying a range of genetic modifications (including point mutation, length alteration, incorporation of regulatory genetic element, promoter hybridization and configuration alteration), we created a library of 42 constitutive promoters; all of which are functional in *R. eutropha* H16. Although these promoters are also functional in *E. coli*, they show different promoter strength and hierarchical rank of promoter activity. Subsequently, the activity of each promoter was individually characterized, using L-arabinose-inducible P_{BAD} promoter as a benchmark. This study has extended the range of constitutive promoter activities to 137 folds, with some promoter variants exceeding the L-arabinose-inducible range of P_{BAD} promoter. Not only has the work enhanced our flexibility in engineering *R. eutropha* H16, it presented novel strategies in adjusting promoter activity in *R. eutropha* H16 and highlighted similarities and differences in transcriptional activity between this organism and *E. coli*.

Keywords: *Ralstonia eutropha* H16, *Cupriavidus necator* H16, gene expression, constitutive promoter, synthetic biology, metabolic engineering

3.1 INTRODUCTION

Ralstonia eutropha H16 (or *Cupriavidus necator* H16) is a chemolithoautotrophic soil bacterium, most widely known for its ability to accumulate polyhydroxyalkanoates (PHA) (Pohlmann et al., 2006). This metabolically versatile organism is capable of utilizing a wide range of energy and carbon sources (including H_2 and CO_2) to support growth and achieving high cell density (Volodina et al., 2016). These intrinsic properties have cemented its potential applications in biological CO_2 capture and utilization (Jajesniak et al., 2014, Peplow, 2015) as well as commercial-scale production of diverse bio-products (Brigham et al., 2012) including polymers (Lutke-Eversloh and Steinbüchel, 2003, Steinbüchel and Pieper, 1992, Voss and Steinbuchel, 2006, Valentin et al., 1995) hydrocarbons (Chen et al., 2015, Crépin et al., 2016, Marc et al., 2017, Bi et al., 2013, Lu et al., 2012) and amino acids (Luette et al., 2012). Its potential will rapidly come into fruition, aided by the development of molecular tools. These include genome engineering methods to permanently alter its metabolic phenotype (Park et al., 2010), expression vectors to assemble heterologous pathway (Voss and Steinbuchel, 2006, Gruber et al., 2014) transposon-based random mutagenesis (Raberg et al., 2015) and transformation method to introduce recombinant plasmids (Tee et al., 2017).

Maximal product yield and titre are key requirements in biomanufacturing. To this end, metabolic pathway optimization is vital in eliminating metabolic bottlenecks that compromise cellular productivity and metabolic phenotypes that are detrimental to cell viability. Proven strategies of tuning gene expression of a metabolic pathway include varying plasmid copy number, gene dosage and promoter strength, among others. Leveraging on promoter strength for pathway optimization is the most straightforward strategy, which involves tuning promoter activity at both transcriptional and translational levels.

L-arabinose-inducible P_{BAD} promoter and anhydrotetracycline-inducible P_{tet} promoter are most widely applied to tune expression of genes, gene clusters or operons in *R. eutropha* H16 (Bi et al., 2013, Fukui et al., 2011, Guzman et al., 1995b, Li and Liao, 2015). With a P_{BAD} promoter, high inducer concentration (up to 1 g/L) is required to achieve high expression yield. The leaky P_{tet} promoter, on the other hand, is induced by a weak antibiotic

that is undesirable and its promoter strength is comparatively weaker. These factors greatly limit the use of these two promoters for large-scale fermentation. The more recently developed 3-hydroxypropionic acid-inducible systems (Hanko et al., 2017) and the *p*-cumate- and IPTG-inducible P_{j5} promoters (Gruber et al., 2016) are promising alternatives. Nonetheless, achieving scalable and tunable gene expression of a multi-gene pathway by solely relying on inducible expression systems is severely limited by the poor modularity of inducer-based systems (or potential risk of unwanted inducer crosstalk) and limited number of *R. eutropha* H16-compatible inducible promoters. Further, the use of inducers such as L-arabinose or anhydrotetracycline on a large scale is commercially uneconomical.

In this regard, engineering constitutive promoters with a broad range of activities is a more facile means to modularly adjust gene expressions of a multi-gene pathway to the desired levels or ratios. In addition to facilitating static metabolic control, constitutive promoters are used to engineer more efficient inducible promoters (Li and Liao, 2015) and to construct metabolite-sensing genetic circuits that in turn facilitate dynamic metabolic control in microorganisms (Johnson et al., 2017). Examples of constitutive promoters for use in *R. eutropha* H16 include P_{lac} and P_{tac} promoters, native *R. eutropha* H16 promoters such as P_{phaC1} promoter and coliphage T5 promoter and its variants such as P_{j5}, P_{g25}, P_{n25} and P_{n26} promoters (Arikawa and Matsumoto, 2016, Fukui et al., 2011, Gruber et al., 2014). Despite these precedent studies, there are knowledge gaps that hinder constitutive promoter utilization and engineering for *R. eutropha* H16, which are (1) lack of a universal definition of promoter architecture, (2) lack of a universal reference scale for hierarchical ranking of constitutive promoter activities and (3) limited examples of rational promoter engineering. The latter is in stark contrast to promoter engineering reported for *E. coli* and yeast.

In this study, we first examined the architecture of four notable *R. eutropha* H16-compatible constitutive promoters: the native P_{phaC1} promoter, a semi-synthetic P_{rrsC} promoter, and two coliphage T5 promoters P_{j5} and P_{g25}. We then evaluated their activities using *in vivo* fluorescence measurement of red fluorescent protein (RFP) expression to establish an understanding of the relationship between promoter architecture and activity. Guided by these structure-function relationships, we next proceeded to rational engineering of these 4 parental promoters. Our engineering strategies include combinations of point mutation, length alteration, incorporation of regulatory genetic element, promoter

hybridization and configuration alteration. This resulted in a collection of 42 promoters displaying a range of promoter activities. Of these there are composite promoter variants that are stronger than the P_{j5} promoter; the latter has previously been acclaimed to be the strongest known constitutive promoter for gene expression in *R. eutropha* H16 (Gruber et al., 2014). This new promoter library is envisaged to further propel the biotechnological applications of *R. eutropha* H16.

3.2 RESULTS AND DISCUSSION

3.2.1 Defining a promoter and quantifying its activity

Standardizing the definition of a promoter is deemed necessary and particularly relevant to this study for 4 obvious reasons: (1) to objectively benchmark the activities of wild-type and engineered promoters, (2) to critically assess promoter structure-function relationships, (3) to measure the effectiveness of various promoter engineering strategies, and (4) to compare promoters reported by various research groups. In this study, we describe a promoter as a constellation of three distinct genetic elements as shown in Figure 3.1A: (Part 1) a core promoter sequence comprising -35 box, -10 box (or the Pribnow box), +1 transcriptional start, spacer of 16-18 bp between the -35 and the -10 boxes as well as the spacer between the -10 box and +1 site, (Part 2) an upstream element (UP) that refers to the entire DNA sequence upstream of the core promoter sequence, and (Part 3) a downstream element spanning the nucleotide after the +1 transcriptional start and the nucleotide before the translation initiation codon. Therefore, the 5'-untranslated region (5'-UTR) consists of the +1 transcriptional start and the downstream element, with the latter typically containing *cis*-acting regulatory elements such as the ribosome binding site (RBS). Putting it simply, a promoter is a defined stretch of sequence upstream of the translational start. This definition is not uncommon in genome annotation, particularly when the promoter boundary is unclear or ambiguous. This definition also pre-supposes that the functional characteristics of a given promoter are composite effect of all genetic elements within the pre-defined promoter architecture. To quantify promoter activity in *R. eutropha* H16, RFP was used as a reporter protein (Figure 3.1B). Briefly, DNA fragments corresponding to a promoter and *rfp* gene were cloned, in tandem, into a broad host range pBBR1MCS plasmid backbone harbouring a chloramphenicol resistance gene (Figures 3.1B & S3.1).

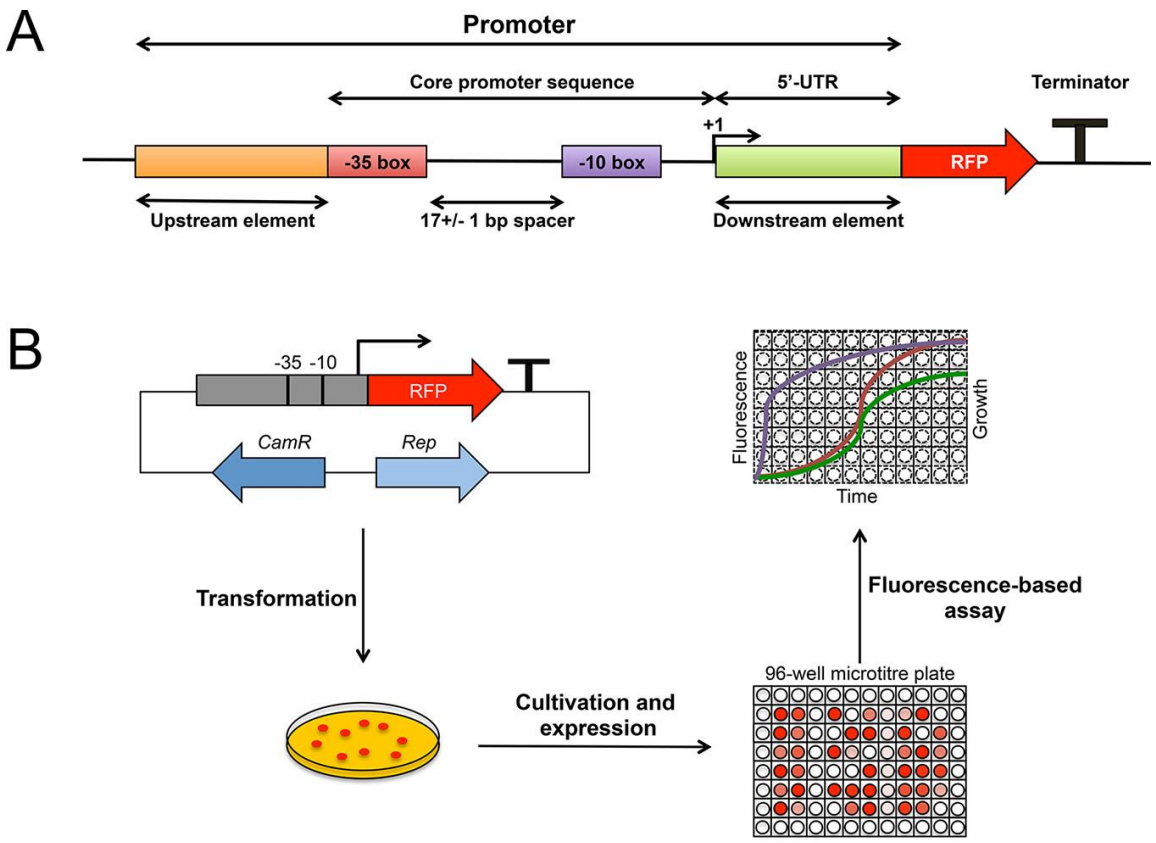

Figure 3.1: (*A*) Promoter definition used in this study. (*B*) High-throughput characterization of engineered promoters using a fluorescence-based assay. (5'-UTR: 5'-untranslated region; bp: base pair; *CamR*: chloramphenicol resistance gene; *Rep*: replication gene; RFP: red fluorescent protein)

3.2.2 Defining the boundaries and architectures of 4 parental promoters

Since the 4 parental promoters, P_{phaC1}, P_{rrsC}, P_{j5} and P_{g25}, form the basis of this entire study, clearly defining their boundaries and examining their architectures are essential, such that all subsequently engineered promoters can be compared against these 4 'standards'. All 4 parental promoters contain -35 box and -10 box that are almost identical to the hexameric promoter consensus sequences recognized by the *E. coli* housekeeping sigma factor σ^{70} (Figures 3.2A & 3.2B) (Kutuzova et al., 1997). P_{phaC1} is known to be a relatively strong native promoter (Arikawa and Matsumoto, 2016, Fukui et al., 2011, Li and Liao, 2015). It has been widely studied and applied for improved PHA-based biopolymer production in *R. eutropha* H16 (Arikawa and Matsumoto, 2016, Fukui et al., 2011). However, P_{phaC1} promoters of different lengths are used in various studies, making objective comparison impossible. In this study, P_{phaC1} promoter is defined as a 466-bp DNA sequence upstream of the translation start of the *phaC1* gene. Previous studies of this promoter affirmed the

presence of a 7-bp “AGAGAGA” Shine-Dalgarno (SD) sequence within its 5’-UTR. This native RBS is located 11 bp upstream of the translational start (Arikawa and Matsumoto, 2016). The P_{rrsC} promoter used in this study is a combination of a 210-bp DNA sequence upstream of the +1 transcriptional start of the native *rrsC* gene, the first 5 bp of the native 5’-UTR and a 26-bp synthetic genetic element. The latter comprises a 20-bp RBS found in the pBBR1c-RFP P_{BAD} promoter (see Supplementary Information) flanked by an upstream 6-bp *Bgl*II restriction site. The synthetic RBS contains a purine-rich 5-bp “AGGAG” SD sequence known to markedly improve translation efficiency. Finally, the P_{g25} and P_{j5} promoters used in this study are both 75-bp DNA sequences, identical to those previously reported by Gentz and Bujard (Gentz and Bujard, 1985).

A

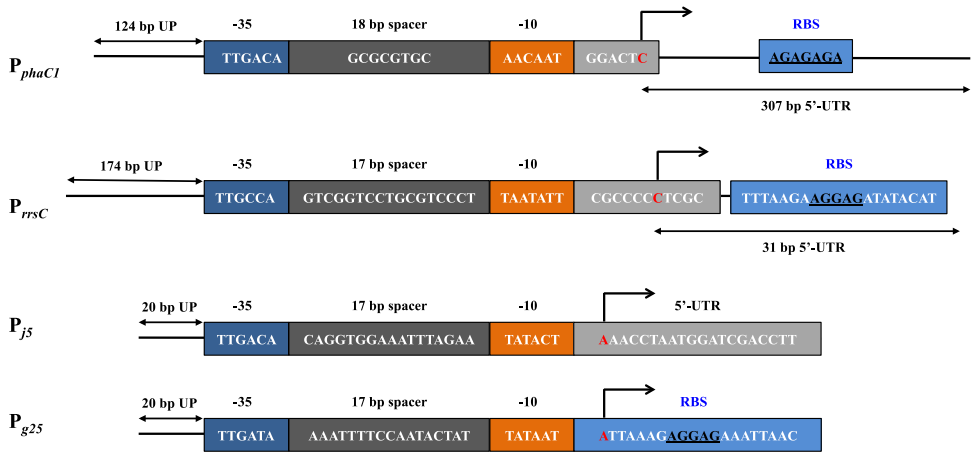

B

Promoter	Origin	-35 box	-10 box	Length [bp]	AT content of upstream element [%]
σ^{70}	*E. coli*	TTGACA	TATAAT	Variable	Variable
P_{phaC1}	*C. necator* H16	TTGACA	AACAAT	466	40
P_{rrsC}	*C. necator* H16	TTGCCA	TAATATT	241	43
P_{j5}	Coliphage T5	TTGACA	TATACT	75	65
P_{g25}	Coliphage T5	TTGATA	TATAAT	75	86

C

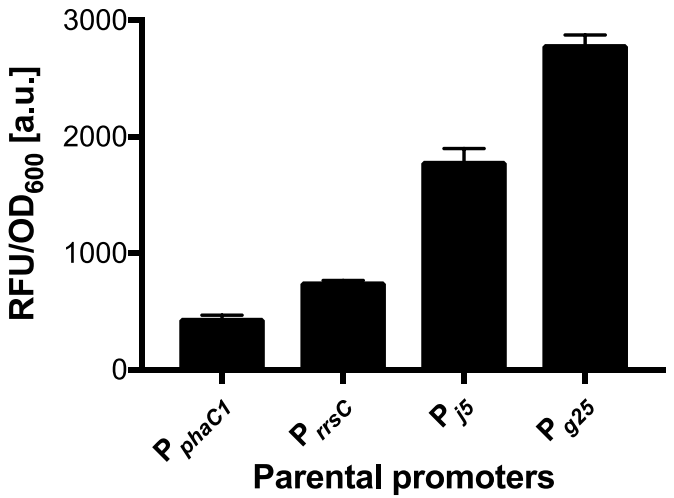

Figure 3.2: (*A*) Boundaries and architectures of the 4 parental promoters, P_{phaC1}, P_{rrsC}, P_{j5} and P_{g25}, used in this study. (*B*) Comparison of the 4 parental promoters to an *Escherichia coli* σ^{70} promoter. (*C*) Activities of the 4 parental promoters.

3.2.3 Narrow range of promoter activities between the 4 parental promoters

Fluorescence measurement of RFP expression revealed a narrow range of promoter activities (defined as relative fluorescence unit normalized by optical density; see Methods & Materials) between the 4 parental promoters (Figure 3.2C). The ratio of promoter activities between the strongest (P_{g25}) and the weakest (P_{phaC1}) is only 6.3. The promoter activity of P_{rrsC} is 1.7-fold higher than that of P_{phaC1}. This difference may be attributed to the synthetic RBS in P_{rrsC} being more effective in promoting translation compared to the native RBS in P_{phaC1}. The coliphage T5 promoters, P_{j5} (75 bp) and P_{g25} (75 bp), are much shorter in length compared to P_{phaC1} (466 bp) and P_{rrsC} (241 bp). They have previously been reported as some of the strongest constitutive promoters in *E. coli* (Gentz and Bujard, 1985). The strong transcriptional activity was also verified in *R. eutropha* H16 (Gruber et al., 2014). The A/T rich sequence of many coliphage T5 promoters, particularly in their upstream elements, has been implicated in accounting for their high transcriptional activity (Gentz and Bujard, 1985). Indeed, the upstream elements of both P_{j5} and P_{g25} promoters show high A/T contents (65% for P_{j5} and 85% for P_{g25}), and the difference in the A/T content may partly be responsible for the higher activity of P_{g25} relative to P_{j5} (Figure 3.2B). In addition, P_{g25} possesses within its 5'-UTR the purine-rich 5-bp SD sequence used in most commercially available pET and pBAD vectors, which is lacking in P_{j5} (Figure 3.2A). This initial examination highlighted two critical points which guided our subsequent promoter engineering: (1) conservation of -35 and -10 boxes is important for maintaining high transcriptional activity in *R. eutropha* H16, (2) promoter length or A/T content or *cis*-acting genetic regulatory element (such as a synthetic RBS) could potentially influence promoter activity in *R. eutropha* H16 significantly.

3.2.4 Expanding the range of promoter activities through rational engineering

Informed by our understanding of the 4 'standard" promoters, we proceed to increase the range of promoter activities beyond the existing 6.3 folds between P_{phaC1}, P_{rrsC}, P_{j5} and P_{g25}. Our objectives are 3-fold: (1) creating both weaker ('tuning down') and stronger ('tuning up') promoter variants to further expand the promoter activity range, (2) generating promoter variants that exceed or at least cover the entire L-arabinose inducible range of P_{BAD} promoter, and (3) developing a set of promoters with gradual increase in activity (*i.e.*,

having promoters with activities evenly distributed across the entire promoter activity scale).

To this end, we applied a range of rational engineering approaches. These strategies, summarized in Table S4.1 and Figure S4.3, can be loosely classified into 5 categories: (A) point mutation, (B) length alteration, (C) incorporation of regulatory genetic element, (D) promoter hybridization and (E) configuration alteration. Category A, point mutation, includes base substitution, single-base insertion and single-base deletion. Category B, length alteration, refers to truncation or extension of a promoter from either terminus and insertion or deletion of a stretch of random DNA sequence. Incorporating *cis*-acting translational regulatory elements such as T7 stem-loop and RBS are grouped within category C. Category D, promoter hybridization, encompasses both creating hybrid promoters and incorporating *cis*-acting transcriptional regulatory element such as an operator. Category E, configuration alteration, involves transcriptional amplification using a secondary promoter that is placed in divergent configuration to a primary promoter. In other words, composite promoters are placed in category E. Each category is further divided into sub-categories (*e.g.*, C1 for T7 stem-loop and C2 for RBS in Category C) and sub-sub-categories (*e.g.*, B1a for truncation of 25 bp upstream of -35 box and B1b for truncation of 50 bp upstream of -35 box in Category B) to pinpoint specific modification made. Using a combination of the aforementioned strategies, we created in total 38 promoter variants as summarized in Table 3.1.

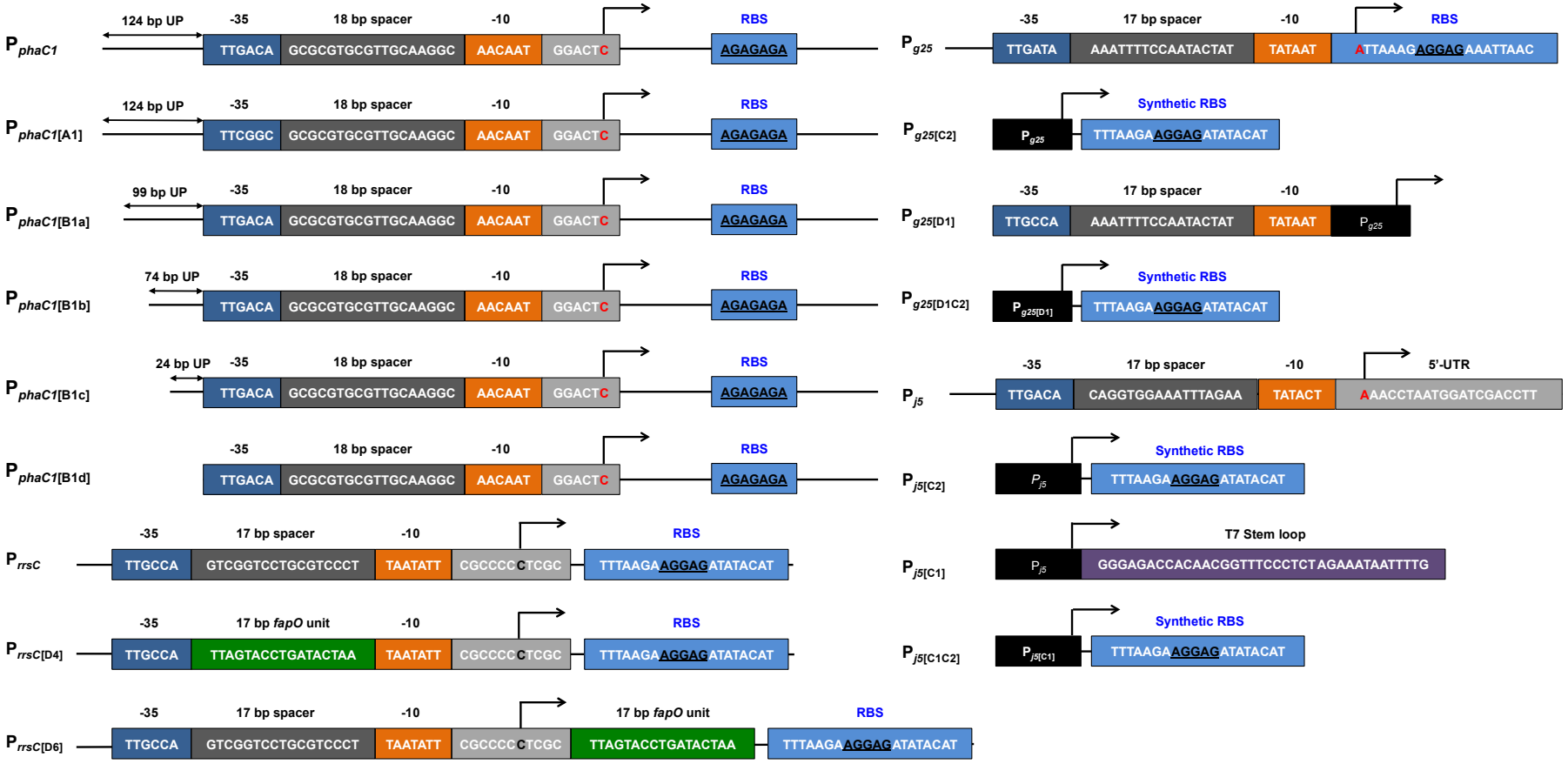

Figure 3.3: Architectures of parental promoters and their engineered variants.

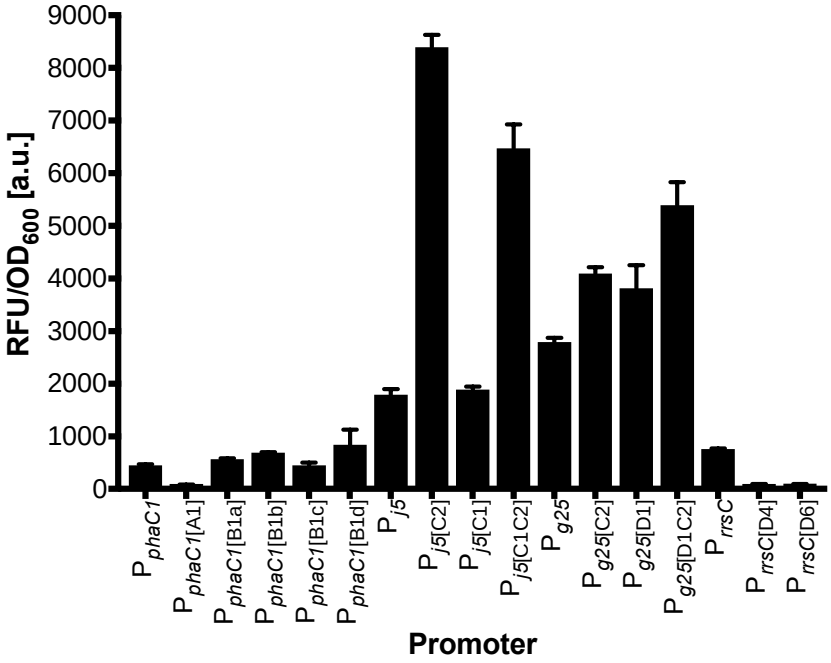

Figure 3.4: Activities of parental promoters and their engineered variants.

Table 3.1: Summary of 42 parental promoters and their variants engineered using a combination of promoter engineering strategies (A = point mutation, B = length alteration, C = incorporation of regulatory genetic element, D = promoter hybridization and E = configuration alteration). Numbers in bracket represent promoter digital identifier, in the format of [Activity level – Relative activity to P_{phaC1}[A1] – Promoter length].

Parental promoter	**A**	**B**	**C**	**D**	**E**		
					Transcriptional amplifier (Secondary promoter)		
					P_{phaC1}	**P_{g25}**	**$P_{j5[A1C1C2]}$**
P_{phaC1} [1-6-466]	P_{phaC1}[A1] [1-1-466]	P_{phaC1}[B1a] [1-8-441]					
		P_{phaC1}[B1b] [1-10-416]					
		P_{phaC1}[B1c] [1-6-366]					
		P_{phaC1}[B1d] [1-12-342]					
P_{rrsC} [1-11-241]					P_{rrsC}[E1] [2-34-713]		P_{rrsC}[E3] [1-22-434]
				P_{rrsC}[D6] [1-1-258]	P_{rrsC}[E1D6] [2-31-730]		P_{rrsC}[E3D6] [1-21-451]
				P_{rrsC}[D4] [1-1-241]	P_{rrsC}[E1D4] [1-14-713]		P_{rrsC}[E3D4] [1-9-434]

Table continues below

Parental promoter	A	B	C	D	E		
					Transcriptional amplifier (Secondary promoter)		
					P_{phaC1}	P_{phaC1}	P_{phaC1}
P_{j5} [1-25-75]			$P_{j5[C1]}$ [1-26-136]				
			$P_{j5[C1C2]}$ [4-91-162]		$P_{j5[E1C1C2]}$ [5-120-634]	$P_{j5[E2C1C2]}$ [4-106-268]	
			$P_{j5[A1C1C2]}$ [3-64-162]		$P_{j5[E1A1C1C2]}$ [4-104-634]	$P_{j5[E2A1C1C2]}$ [4-84-268]	
			$P_{j5[A1D6aC1C2]}$ [3-70-179]		$P_{j5[E1A1D6aC1C2]}$ [4-112-651]	$P_{j5[E2A1D6aC1C2]}$ [4-90-285]	
			$P_{j5[A1D6bC1C2]}$ [3-68-196]		$P_{j5[E1A1D6bC1C2]}$ [4-111-668]	$P_{j5[E2A1D6bC1C2]}$ [4-87-302]	
			$P_{j5[C2]}$ [5-117-101]		$P_{j5[E1C2]}$ [5-134-573]	$P_{j5[E2C2]}$ [5-125-207]	
			$P_{j5[A3C2]}$ [5-116-100]		$P_{j5[E1A3C2]}$ [5-137-572]	$P_{j5[E2A3C2]}$ [5-128-206]	
P_{g25} [2-39-75]					$P_{g25[E1]}$ [3-61-547]	$P_{g25[E2]}$ [2-46-181]	$P_{g25[E3]}$ [2-45-268]
				$P_{g25[D1]}$ [2-53-130]			
			$P_{g25[C2]}$ [2-57-101]				
			$P_{g25[D1C2]}$ [3-75-156]				

3.2.5 Promoter nomenclature

Based on the classification of our promoter engineering strategies, we devised a promoter nomenclature system to systematically name all 38 engineered promoters (Table 3.1). The system is designed to provide 3 pieces of key information: parental promoter, modifications made and promoter architecture, using the standard format of $P_{parent[M1M2M3\ldots]}$. In this nomenclature system, capital P signifies a promoter. Italic subscript $_{parent}$ indicates the parental promoter from which the engineered promoter is derived. All modifications made are summarized in bracketed subscript $_{[M1M2M3\ldots]}$, with the modifications arranged in sequence of appearance to reflect the engineered promoter architecture. As an example, $P_{j5[C1C2]}$ is a promoter variant engineered from the parental promoter P_{j5} by inserting a T7-stem loop (denoted by $_{C1}$) as well as an RBS (denoted by $_{C2}$) in its 5'-UTR. The T7-stem loop was placed upstream of the RBS, as indicated by $_{C1}$ that comes before $_{C2}$.

3.2.6 Mutations in -35 box tuned transcriptional activity down

Li and Liao previously reported $P_{phaC1\text{-}G3}$ promoter, in which its -35 box was mutated from "TTGACA" to "TTCGGC" (Figure 4.3A) (Li and Liao, 2015). This promoter variant was shown to retain 15% of the activity of its P_{phaC1} parent, when characterized using enhanced green fluorescent protein (eGFP) as a reporter (Li and Liao, 2015). To validate our initial hypothesis that conserved -35 and -10 boxes are necessary in maintaining high transcriptional activity in *R. eutropha* H16, we recreated $P_{phaC1\text{-}G3}$ and this variant was named $P_{phaC1[A1]}$ in our nomenclature system. RFP fluorescence measurement ascertained that $P_{phaC1[A1]}$ retains 16% of the activity of P_{phaC1} (Figure 3.4B). This data also indicated that both reporter proteins, RFP and eGFP, give similar outcome in transcriptional activity quantification. RFP and eGFP are commonly used in synthetic biology for characterization of biological parts (*e.g.*, promoter, terminator) (Guo et al., 2015, Phelan et al., 2017). Li and Liao also created a promoter library with mutated -35 box (TTNNNN). All promoter variants screened showed lower activity in comparison to the wild type promoter (Li and Liao, 2015). Therefore, mutations in -35 box likely tune the transcriptional activity down.

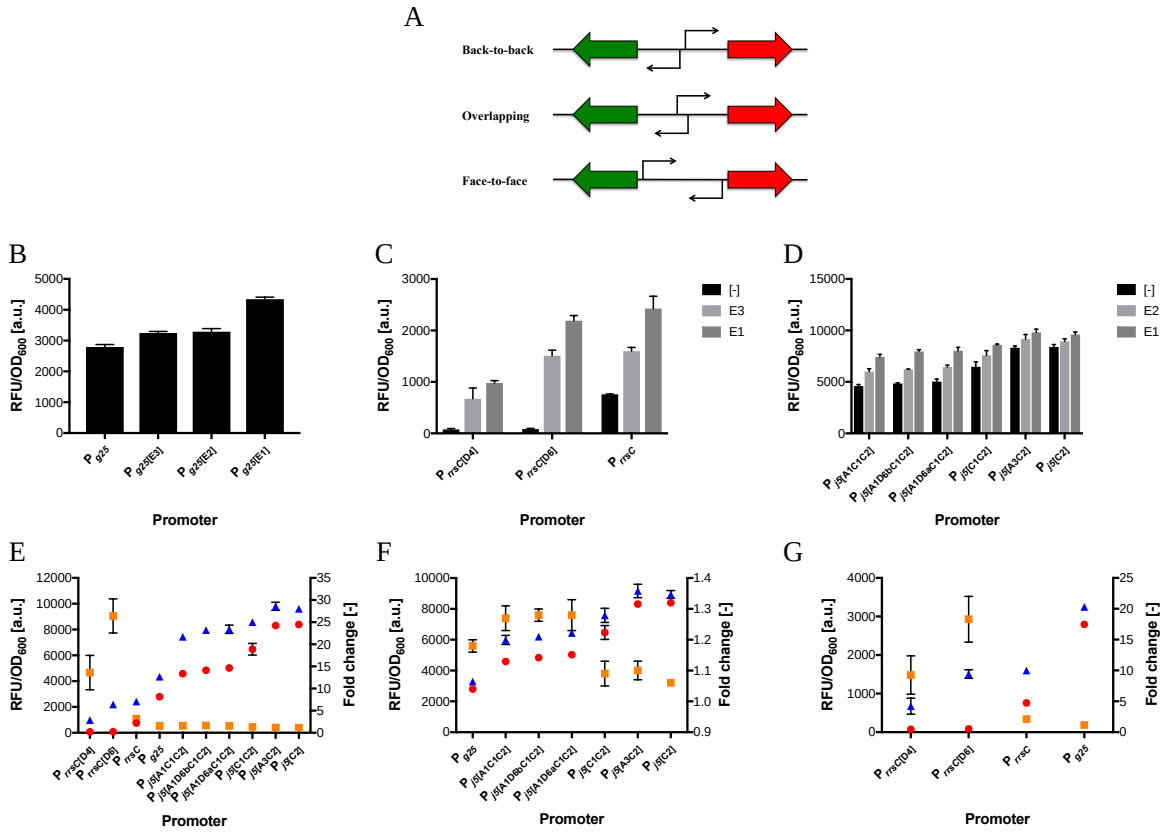

Figure 3.5: (*A*) For gene pairs in HH arrangement, promoters that effect divergent transcription can be organized in 3 possible ways: back-to-back, overlapping or face-to-face. (*B*) Composite promoters engineered using P_{g25} as parental promoter. (*C*) Composite promoters engineered using P_{rrsC} as parental promoter. (*D*) Composite promoters engineered using P_{j5} as parental promoter. (*E*) Composite promoters with P_{phaC1} as secondary promoter. (*F*) Composite promoters with P_{g25} as secondary promoter. (*G*) Composite promoters with $P_{j5[A1C1C2]}$ as secondary promoter. In graphs E to G, red, blue and orange symbols represent primary promoter activity, composite promoter activity and fold change, respectively.

3.2.7 A minimal P_{phaC1} promoter with enhanced activity

P_{phaC1} (466 bp) is the longest promoter among the 4 parental promoters. To find the minimal functional sequence, we created 5'→3' truncated variants of P_{phaC1}: 25 bp truncation in $P_{phaC1[B1a]}$, 50 bp in $P_{phaC1[B1b]}$, 100 bp in $P_{phaC1[B1c]}$, and 124 bp in $P_{phaC1[B1d]}$ (Figure 3.3). Interestingly, removing the entire upstream element (124 bp) in $P_{phaC1[B1d]}$ resulted in highest promoter activity, which is 2-fold higher compared to that of its P_{phaC1} parent (Figure 3.4). This suggested that *cis*-acting elements exist within the upstream element of P_{phaC1} and contribute to transcriptional suppression.

3.2.8 Synthetic RBS and RBS repeat increased promoter activity

Our initial study with the 4 parental promoters, along with a previous study conducted by Bi et al. (2013) motivated us to further investigate the effects of *cis*-acting translational regulatory elements on promoter activity. We focused specifically on the 26-bp synthetic genetic element derived from P_{rrsC} (containing a 20-bp RBS found in the pBBR1c-RFP P_{BAD} promoter flanked by an upstream 6-bp *Bgl*II restriction site; herein denoted as synthetic RBS) and the 37-bp T7 stem-loop reported by Bi et al. (2013). We observed a 4.7-fold increase in promoter activity when a synthetic RBS was added to P_{j5} (the $P_{j5[C2]}$ variant) (Figure 3.4). On the contrary, there was no significant change in promoter activity when a T7 stem-loop was added to P_{j5} (the $P_{j5[C1]}$ variant). A drop in promoter activity was observed when a T7 stem-loop was added to $P_{j5[C2]}$ (the $P_{j5[C1C2]}$ variant). As such, synthetic RBS is an effective means to amplify promoter activity. We then added the same synthetic RBS to P_{g25} and created a variant $P_{g25[C2]}$ that also showed ~50% increase in promoter activity. A smaller promoter activity increase in $P_{g25[C2]}$ could be attributed to a pre-existing effective SD sequence ("AGGAG") in P_{g25}.

3.2.9 Repeat of -35 and -10 boxes increased transcriptional activity

-35 and -10 boxes are highly conserved regions in prokaryotic promoters, essential for the binding of RNA polymerases. To test if creating more binding sites for RNA polymerase would further increase transcriptional activity, we created $P_{g25[D1]}$ variant. In this variant, we duplicated the DNA sequence spanning -35 box and -10 box. In essence, this hybrid promoter is a tandem repeat of two P_{g25} promoters and we observed ~40% increase in promoter activity (Figure 3.3 & 3.4). Again, incorporating a synthetic RBS ($P_{g25[D1C2]}$) gave an additive effect, resulting in further increase in promoter activity.

3.2.10 Operator insertion reduced transcriptional activity drastically

Hybrid promoters are crucial genetic elements in the construction of biosensors. Using a malonyl-CoA biosensor (Johnson et al., 2017) as an example, we inserted the *fapO* operator sequence "TTAGTACCTGATACTAA" in P_{rrsC} promoter to create two variants: $P_{rrsC[D4]}$ (*fapO* inserted between -35 and -10 boxes) and $P_{rrsC[D6]}$ (*fapO* inserted within the 5'-UTR) (Figure 3.3). *fapO* operator is conserved in Gram-positive bacteria such as *Bacillus subtilis* and acts as a *cis*-regulatory unit for transcriptional regulation of fatty acid biosynthesis. For

both promoter variants, we observed a drastic activity reduction to ~10% of their P_{rrsC} parent (Figure 3.4). The position of operator and the copy number of operator could therefore significantly change the transcriptional activity of the resultant hybrid promoters. Our data corroborated a previous study by Li and Liao, where *tetO* operators were inserted to create P_{rrsC} hybrid promoters (Li and Liao, 2015).

3.2.11 Divergent promoters, arranged in back-to-back, increased transcriptional activity

The distance between and the relative transcriptional directions of adjacent genes are known to be important in some organisms. Neighbouring genes arranged in head-to-head (HH) orientation, for instance, could be co-regulated and this has been proven experimentally (Gherman et al., 2009). For gene pairs in HH arrangement, promoters that effect divergent transcription can be organized in 3 possible ways: back-to-back, overlapping or face-to-face (Figure 3.5) (Beck and Warren, 1988). In a recent attempt to construct a malonyl-CoA biosensor for *R. eutropha* H16 (publication in preparation), we discovered the significance of divergent transcription in this organism. Therefore, we created 21 composite promoters to systematically investigate divergent transcription in *R. eutropha* H16. Each composite promoter is made up of two promoters arranged in back-to-back (or divergent to each other). The promoter driving the RFP expression is termed the primary promoter, while the counterpart is called the secondary promoter.

When P_{phaC1} (denoted as modification $_{E1}$), P_{g25} (modification $_{E2}$) and $P_{j5[A1C1C2]}$ (modification $_{E3}$) was applied individually as secondary promoters, they generally served as transcriptional amplifiers, increasing the transcriptional activity of the primary promoters (Figures 3.5B-G). The promoter activities of these three secondary promoters follow the order of $P_{j5[A1C1C2]} > P_{g25} > P_{phaC1}$ (eq. $_{E3} > _{E2} > _{E1}$). Interestingly, transcriptional amplification depends on the transcriptional activities of both the primary and the secondary promoters. For the same primary promoter, activity enhancement typically decreases with the increased activity of the secondary promoter (Figures 3.5B-D; herein described as secondary promoter effect).

Also, for the same secondary promoter, activity enhancement decreases with the increased activity of the primary promoter (Figures 3.5E-G; herein described as primary promoter effect). We postulate that secondary promoter effect is attributed to the fact that weaker secondary promoter competes less with the primary promoter for transcriptional machinery or factors. If a secondary promoter of very high activity is used, the competition is so strong that it diminishes the activity of the primary promoter (data not shown). The primary promoter effect observed is perhaps more intuitive and easier to comprehend. If the primary promoter displays high activity, it is more difficult to further improve its activity using an amplifier. Important to point out, transcriptional enhancement resulted from divergent promoters is not universal to all prokaryotic systems. Generally, we did not observe such behaviours when we tested our composite promoters in *E. coli* (data not shown).

3.2.12 Promoter characterization using P_{BAD} as reference scale

This study resulted in a set of 42 constitutive promoters, including the 4 parental promoters. The ratio of promoter activities between the strongest ($P_{j5[E1A3C2]}$) and the weakest ($P_{phaC1[A1]}$, eq. $P_{phaC1\text{-}G3}$ reported by Li and Liao (Li and Liao, 2015)) is 137. These promoters showed gradual increase in activity across the entire scale (Figure 3.6A). To promote the widespread use of these promoters, we benchmarked each of them using L-arabinose inducible P_{BAD} promoter as a reference scale. Figure S3.4 illustrates the dose-dependent induction of P_{BAD} promoter, using L-arabinose concentration from 0.001% (w/v) to 0.200% (w/v). Expression maxima was reached at 0.200% (w/v) L-arabinose. As depicted in Figure 3.6B, our engineered promoters covered the entire L-arabinose inducible range (indicated by scattered data points). We categorized all promoters into 5 activity levels to aid promoter selection: Level 1 (with promoter activity between 0 a.u. – 2000 a.u.), Level 2 (2000 a.u. – 4000 a.u.), Level 3 (4000 a.u. - 6000 a.u.), Level 4 (6000 a.u. – 8000 a.u.) and Level 5 (> 8000 a.u.). With a P_{BAD} promoter, one could only achieve expression levels between 1 – 4. Through promoter engineering, we obtained seven Level 5 variants ($P_{j5[A3C2]}$, $P_{j5[C2]}$, $P_{j5[E1C1C2]}$, $P_{j5[E2C2]}$, $P_{j5[E2A3C2]}$, $P_{j5[E1C2]}$ and $P_{j5[E1A3C2]}$) with promoter activities exceeding that of P_{BAD} (Table S3.2). For easy classification of all engineered promoters, we developed a numerical coding system (Table 3.1) and assigned a digital identifier to each promoter. This will allow us to develop a *R. eutropha* H16-specific promoter database (work in progress). Each promoter code is in the format of [X-Y-Z],

with X representing activity level, Y representing relative activity to $P_{phaC1[A1]}$ and Z representing promoter length. While conceptualizing our engineered promoter nomenclature and coding systems, we have endeavoured to make them universal such that they can be applied to other promoters yet to be developed.

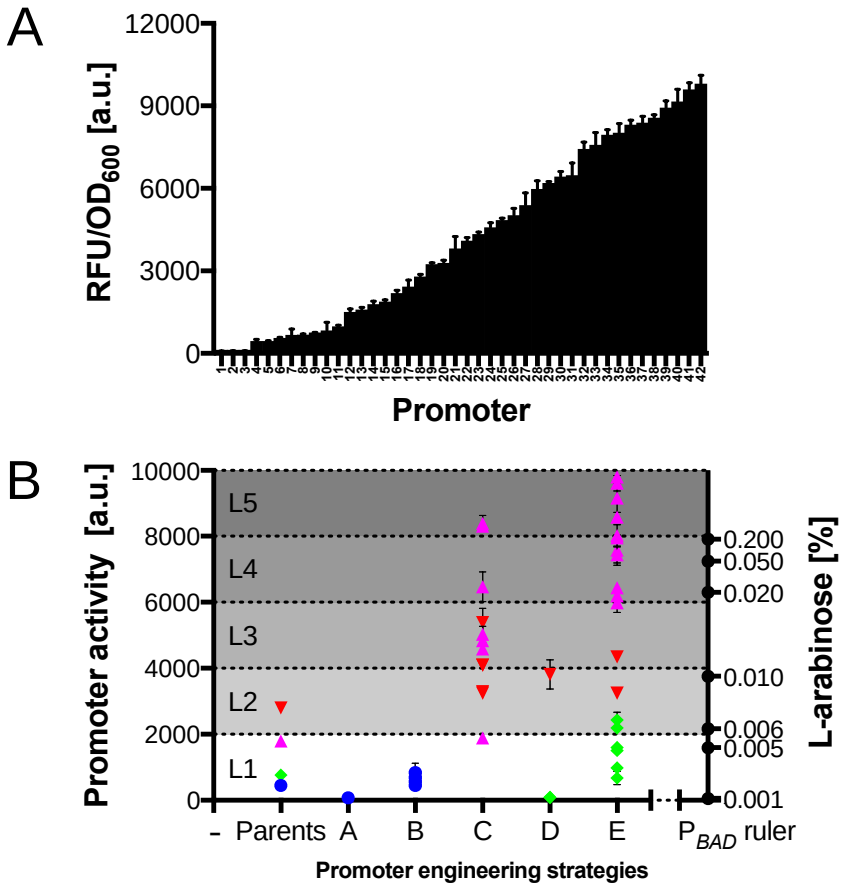

Figure 3.6: (*A*) Hierarchical ranking of all 42 constitutive promoters reported in this study. (*B*) The range of promoter activity was expanded from 6 folds to 137 folds, after applying combination of promoter engineering strategies.
(A = point mutation, B = length alteration, C = incorporation of regulatory genetic element, D = promoter hybridization and E = configuration alteration). Promoters derived from P_{phaC1}, P_{rrsC}, P_{j5} and P_{g25} were coloured in blue, green, pink and red, respectively. Promoters were categorized into 5 activity levels: Level 1 (with promoter activity between 0 a.u. – 2000 a.u.), Level 2 (2000 a.u. – 4000 a.u.), Level 3 (4000 a.u. - 6000 a.u.), Level 4 (6000 a.u. – 8000 a.u.) and Level 5 (> 8000 a.u.). Each promoter was benchmarked against P_{BAD} promoter, induced using various concentrations of L-arabinose, from 0.001% (w/v) to 0.200% (w/v).

3.2.13 Summary of rational promoter engineering for *R. eutropha* H16

Figure 3.7 provides an overview of the rational promoter engineering strategies discussed in this article. It shows the effect of a specific modification by looking at the promoter activity difference before and after that particular modification. Creating mutation(s) within -35 box and inserting operator sequence(s) resulted in drastic reduction in promoter activity (represented by red data points), while inserting a T7 stem-loop caused almost no change in promoter activity. On the contrary, inserting a synthetic RBS and applying a transcriptional amplifier (specifically P_{phaC1} or $P_{j5[A1C1C2]}$) gave the highest increase in promoter activity (>100%). In fact, those promoters that are stronger than P_{BAD} promoter (indicated as blue data points) were mostly created using either one of these strategies or combination of them. All the other strategies provided marginal promoter activity increase (from 10% to 50%). Also clearly reflected in Figure 3.6B, creating divergent promoters is the most effective way of broadening the range of promoter activity. Worthy of note, relative promoter activity change is dependent on the parental promoter, judging on the work presented in this article.

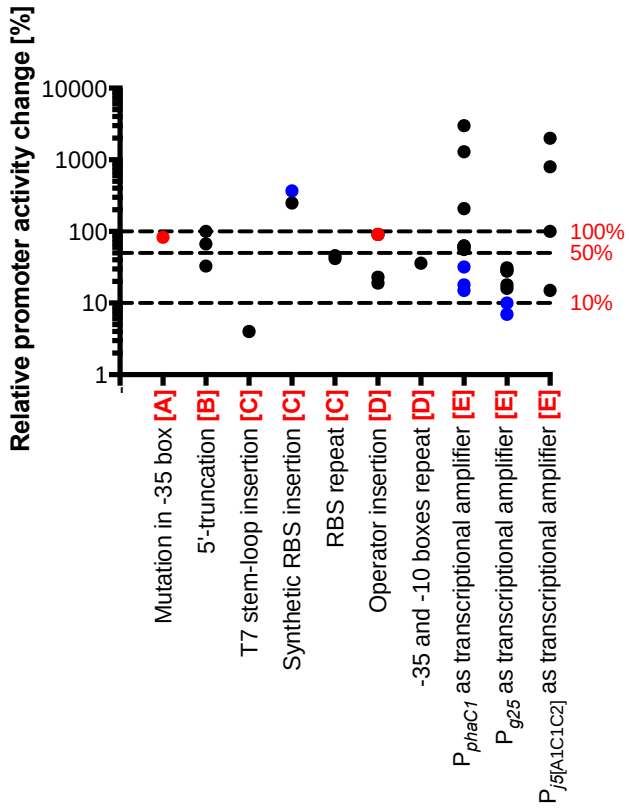

Figure 3.7: Relative promoter activity change upon application of promoter engineering strategies.
(A = point mutation, B = length alteration, C = incorporation of regulatory genetic element, D = promoter hybridization and E = configuration alteration). Modifications that resulted in loss of promoter activity were indicated as red data points. Promoters with activities higher than P_{BAD} promoter were indicated as blue data points.

3.2.14 The use of engineered constitutive promoters in *R. eutropha* H16

The use of strong constitutive promoters could potentially result in (a) bacterial growth impairment due to high metabolic burden and/or (b) protein excretion/leakage due to high protein expression level. To study these effects, we selected representative promoters from each activity level (Table S3.3) and conducted further characterization. We observed similar growth for most of the strains (Figure 3.8), with growth rates (μ_{max}) falling between 0.21 h^{-1} and 0.24 h^{-1} (Table S4.3). For promoter $P_{j5[E2C2]}$, which is a Level 5 promoter, we noticed a slight drop in growth rate with μ_{max} of 0.18 h^{-1} (Table S3.3). Comparing fluorescence of cell culture and of spent medium (Figure 3.9) confirmed that there was no protein excretion/leakage. Fluorescence of spent medium was maintained at the level of ~1000 a.u, throughout the bacterial cultivation. This value was almost identical to that of the control (*R. eutropha* H16 harbouring pBBR1MCS-1). To study the time-dependent increase in fluorescence signal, we fitted the cell culture fluorescence *vs* time data to a 4-parameter dose-response curve (Figure S3.5 and Table S3.4) for all promoters from Level 2 and above. The fluorescence increase was mainly caused by bacterial growth. If we divided the fluorescence measured (Figure 3.9) by the OD_{600} (Figure 3.8), the ratio was kept almost constant at cultivation times above 12 h (Figure S3.6), further verifying our approach in promoter activity quantification in 96-well plate by taking the RFU/OD_{600} at t = 48 h.

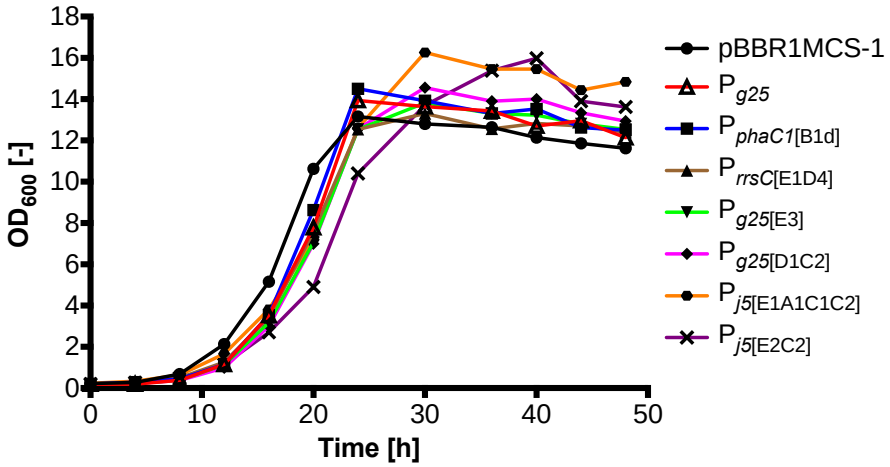

Figure 3.8: Growth curves of *R. eutropha* H16 harbouring either pBBR1MCS-1 (control; black line) or plasmids containing various engineered constitutive promoters [P_{g25} (red line), $P_{phaC1[B1d]}$ (blue line), $P_{rrsC[E1D4]}$ (brown line), $P_{g25[E3]}$ (green line), $P_{g25[D1C2]}$ (pink line), $P_{j5[E1A1C1C2]}$ (orange line) and $P_{j5[E2C2]}$ (purple line)].

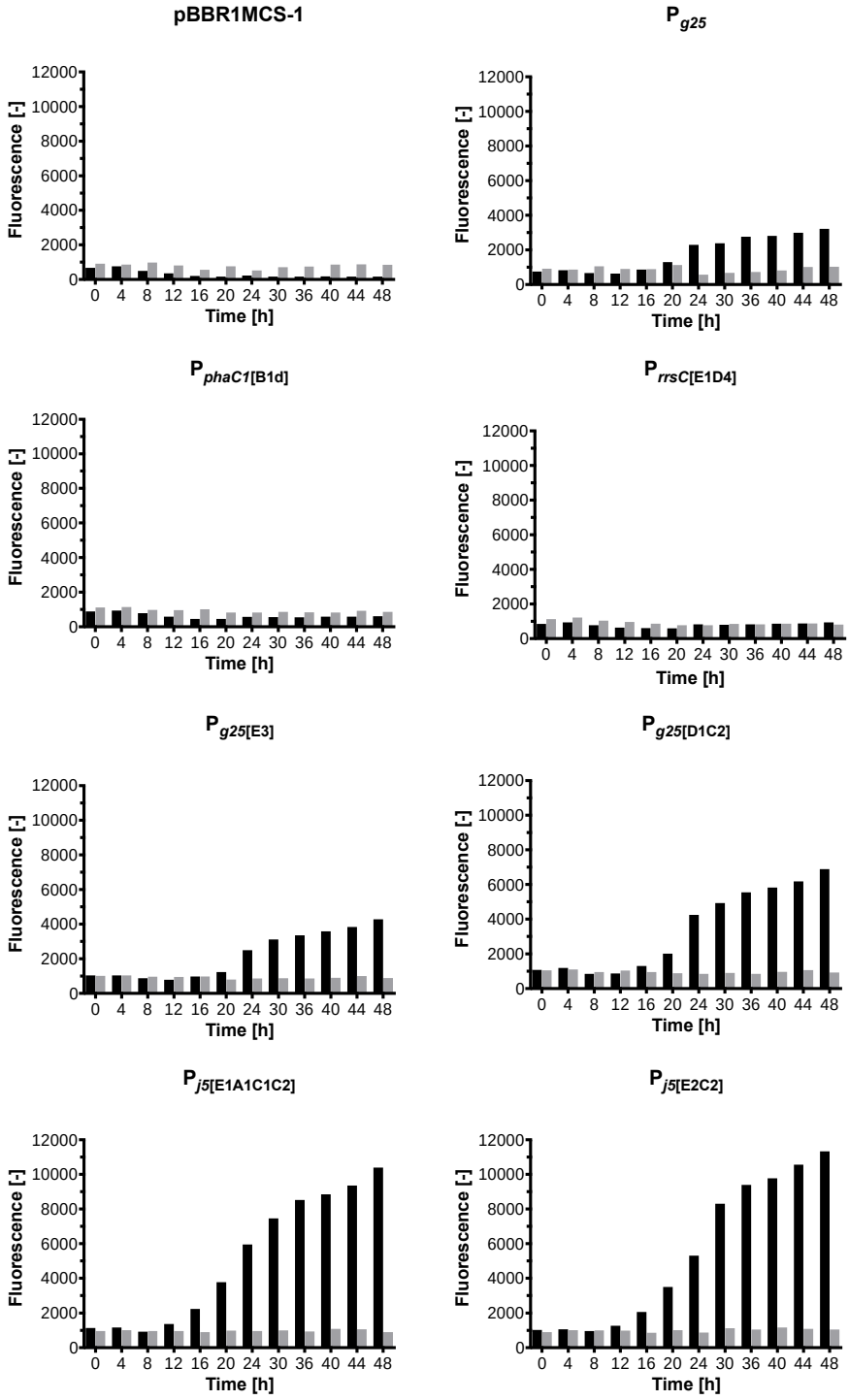

Figure 3.9: Fluorescence of cell culture (black columns) and of spent medium (grey columns) of *R. eutropha* H16 harbouring either pBBR1MCS-1 (control) or plasmids containing various engineered constitutive promoters (P_{g25}, P_{phaC1}[B1d], P_{rrsC}[E1D4], P_{g25}[E3], P_{g25}[D1C2], P_{j5}[E1A1C1C2] and P_{j5}[E2C2]).

3.3 CONCLUSION

This article (1) reported and characterized a set of 42 constitutive promoters with a broad range of promoter activity, which are derived from the 4 most widely used constitutive promoters for *R. eutropha* H16 (P_{phaC1}, P_{rrsC}, P_{j5} and P_{g25}), (2) introduced a nomenclature system and a coding system for engineered promoters, (3) sketched out the relationship between promoter architecture and its resultant activity, (4) highlighted similarities (conservation of -35 and -10 boxes) and differences (composite promoters) in transcriptional activity between *R. eutropha* H16 and *E. coli*, and (5) provided guidelines for rational promoter engineering. We strongly believe our constitutive promoter toolbox that exceeds the activity range of the inducible P_{BAD} promoter will serve the biotechnology community working on *R. eutropha* H16, be it strain engineering for industrial biomanufacturing or developing advanced molecular biology tools for this organism.

3.4 MATERIALS & METHODS

3.4.1 Materials

All DNA modifying enzymes were purchased from either New England Biolabs (Hitchin, UK) or Agilent (Craven Arms, UK). Nucleic acid purification kits were purchased from Qiagen (Manchester, UK). All oligonucleotides were synthesized by Eurofins (Ebersberg, Germany).

3.4.2 Strains

Escherichia coli DH5α was used for all molecular cloning, plasmid propagation and maintenance. *Ralstonia eutropha* H16 (DSM-428, purchased from DSMZ, Braunschweig, Germany) was used for all experiments described in this article.

3.4.3 Bacterial cultivation and transformation

R. eutropha H16 was cultivated at 30°C in nutrient broth (NB: 5 g/L peptone, 1 g/L beef extract, 2 g/L yeast extract, 5 g/L NaCl; pH 7.0 ± 0.2 @ 25°C) supplemented with 10 μg/mL of gentamicin. Cells were transformed with plasmids using the electroporation protocol described by Tee et al. (2017) plated on NB agar supplemented with 10 μg/mL of gentamicin and 25 μg/mL of chloramphenicol, and incubated at 30°C for 40–60 h. *E. coli* DH5α was transformed with plasmids using the standard $CaCl_2$ method, plated on TYE agar (10 g/L tryptone, 5 g/L yeast extract, 8 g/L NaCl, 15 g/L agar) supplemented with 25 μg/mL of chloramphenicol and incubated overnight at 37°C.

3.4.4 Promoter engineering and sequences

All plasmids were derived from pBBR1c-RFP (see Supplementary Information) and constructed using standard molecular biology techniques. All engineered promoters were verified by restrictive analysis and/or DNA sequencing and their sequences were provided in the Supplementary Information.

3.4.5 Promoter activity quantification using fluorescence assay

Transformants of *R. eutropha* H16, carrying either an RFP-null or an RFP-expressing vector, were pre-cultured in 96-well microtitre plate containing 200 μL/well of NB supplemented with 10 μg/mL of gentamicin and 25 μg/mL of chloramphenicol at 30°C for 40 h. This pre-culture was used to inoculate a fresh clear-bottom 96-well microtitre plate [Greiner Bio-One (Stonehouse, UK)] containing 200 μL/well of NB supplemented with 10

μg/mL of gentamicin, 25 μg/mL of chloramphenicol as well as 0–0.2% (w/v) L-arabinose (when required) to induce RFP expression. The plate was cultivated at 30°C for a total of 48 h. OD_{600} and fluorescence (E_x 584 nm, E_m 607 nm; bottom read) were measured using SpectraMax M2e microplate/cuvette reader [Molecular Devices (Wokingham, UK)] after 12 h of cultivation and repeated at 6 h intervals. Relative fluorescence unit (RFU) was calculated by normalizing fluorescence value with the fluorescence value of *R. eutropha* H16 carrying an RFP-null vector (negative control). The RFU value therefore represents the fluorescence fold increase owing to RFP expression. RFU/OD_{600} value was then calculated as the ratio of RFU and OD_{600} value of the respective strain. The ratio was used to account for potential metabolic burden due to high protein expression level, affecting bacterial growth. Promoter activity (PA) was defined as the RFU/OD_{600} value after 48 h of cultivation. The ratio of RFU/OD_{600} was more or less a constant at cultivation time more than 12 h. All experiments were done in triplicate.

3.4.6 Effects of engineered constitutive promoters on bacterial growth and protein excretion

Selected plasmids were freshly transformed into *R. eutropha* H16 and single colonies were picked to prepare overnight cultures. Falcon tubes, containing 6 mL of fresh mineral salts medium (MSM) (Schlegel et al., 1961) supplemented with 10 g/L sodium gluconate (carbon source), 10 μg/mL gentamicin and 25 μg/mL chloramphenicol, were inoculated at a starting OD_{600} of 0.2. Cells were cultivated at 30°C and sampled at regular time intervals. OD_{600} of each sample was measured using BioPhotometer Plus [Eppendorf (Stevenage, UK)]. For all samples collected, the fluorescence (E_x 584 nm, E_m 607 nm; bottom read) of the cell culture (90 μL) and of the spent medium (90 μL) was measured using SpectraMax M2e microplate/cuvette reader [Molecular Devices (Wokingham, UK)].

3.4.7 Fold change and relative promoter activity change

Fold change and relative promoter activity change were calculated using the formulae below:

$$Fold\ change = \frac{PA_2}{PA_1}$$

$$Relative\ promoter\ activity\ change = \frac{\left|PA_{after} - PA_{before}\right|}{PA_{before}} \times 100\%$$

The cell culture fluorescence versus time data was according to the 4-parameter dose-response model:

$$Expected\ Flourescence = Bottom + (Top - Bottom)/[1 + \left(\frac{T50}{Time}\right)^{Hillscope}]$$

3.5 SUPPLEMENTARY INFORMATION

3.5.1 Materials & Methods

3.5.1.1 Construction of pBBR1c-RFP

pBBR1c-RFP plasmid (6733 bp; Figure S1) was constructed from both the broad-host-range plasmid pBBR1MCS1 (Kovach et al., 1994) and the pBbA8k-RFP (Lee et al., 2011) that carries an *rfp* gene whose expression is driven by an L-arabinose-inducible promoter system (P_{BAD} and *araC*). A 4.3-kb fragment containing the chloramphenicol resistance cassette, the *mob* gene which enables plasmid mobilization and the BBR1 origin of replication was amplified from pBBR1MCS and digested with restriction enzymes AvrII and PstI. A 2.4-kb fragment containing the *rfp* gene and its promoter system (P_{BAD} and *araC*) was excised from pBbA8k-RFP using restriction enzymes AvrII and PstI. Both fragments were subsequently ligated to form the 6.7-kb pBBR1c-RFP plasmid.

3.5.1.2 Reporter plasmids harbouring either a parental or an engineered constitutive promoter

All reporter plasmids harbouring either a parental or an engineered constitutive promoter were constructed from pBBR1c-RFP (Figure S4.1), by replacing the L-arabinose-inducible promoter system (P_{BAD} and *araC*) with the respective promoter (see Promoter List).

Figure S3.1: Plasmid map of pBBR1c-RFP

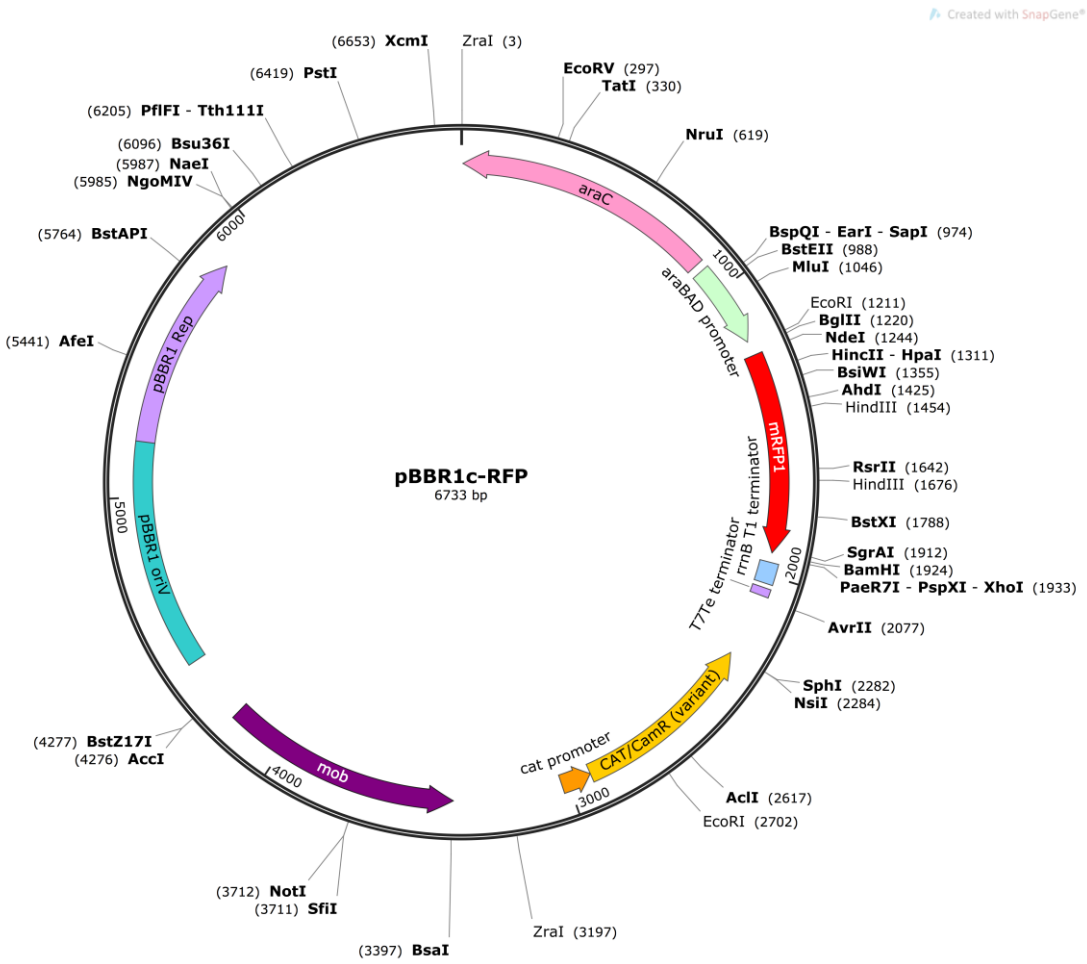

Figure S3.2: Alignment of P_{j5} and P_{g25} promoters used in Gruber *et al.* (2014) and those used in this study.

```
Gruber_Pj5_partial      -gcggccgcaaaaaccgttattgacacaggtggaaatttagaatatactgaattcgagct    59
Johnson_Pj5             agcggatataaaaaccgttattgacacaggtggaaatttagaatatactgttagtaaacc    60
                         ****    ****************************************      * *

Gruber_Pj5_partial      c-------------- 60
Johnson_Pj5             taatggatcgacctt 75

Gruber_Pg25_partial      gcggccgcaaataaaaatttcttgataaaattttccaatactattataatagaattcgag   60
Johnson_Pg25             -tatggaaaaataaaaatttcttgataaaattttccaatactattataattgttatta   59
                                ****************************************   **

Gruber_Pg25_partial      ----------------       60
Johnson_Pg25             aagaggagaaattaac       75
```

XbaI
EcoRI
-35 box
-10 box

Figure S3.3: Rational promoter engineering strategies applied in this study. (*A*) Point mutation. (*B*) Length alteration. (*C*) Incorporation of regulatory genetic element. (*D*) Promoter hybridization. (*E*) Configuration alteration.

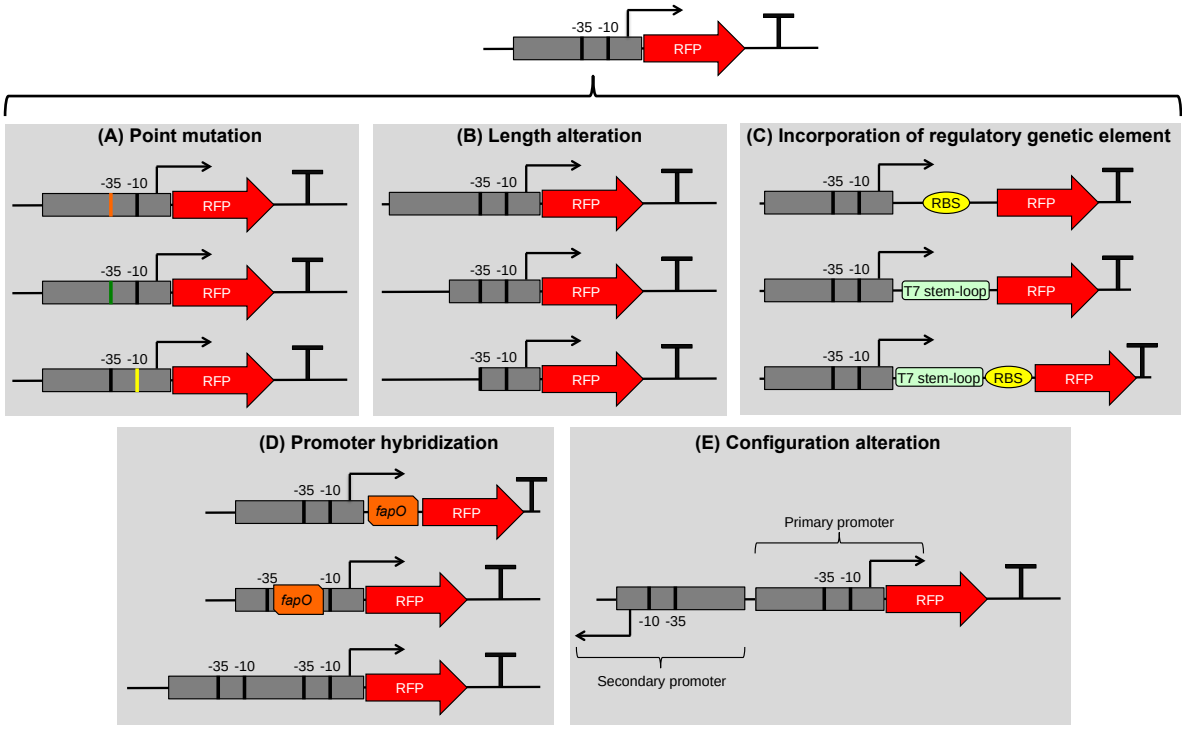

Figure S3.4: Dose-dependent induction of P_{BAD} promoter, using L-arabinose concentration from 0.001% (w/v) to 0.200% (w/v).

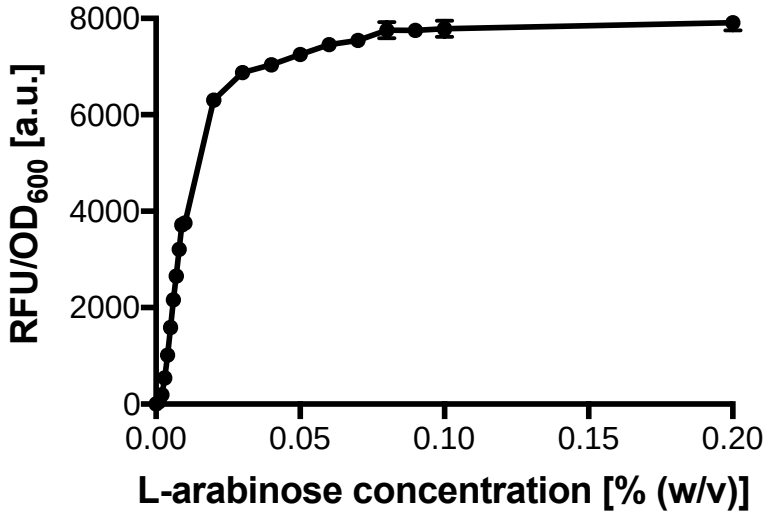

Figure S3.5: Fitting of cell culture fluorescence *vs* time data (scattered points) to a 4-parameter dose response curve (red line).

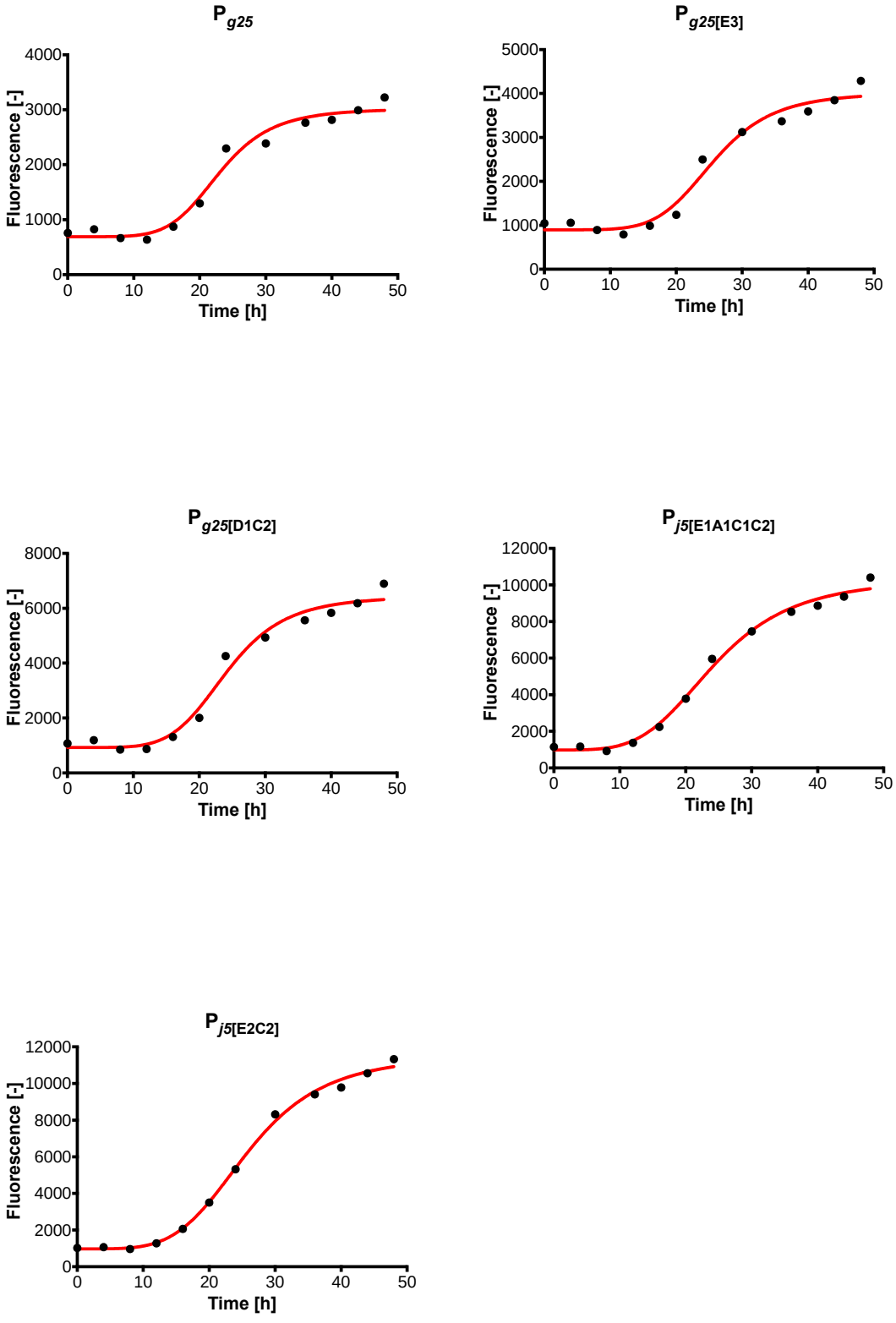

Figure S3.6: Fluorescence of cell culture (Figure S3.5) normalized by OD600 value (Figure 3.8).

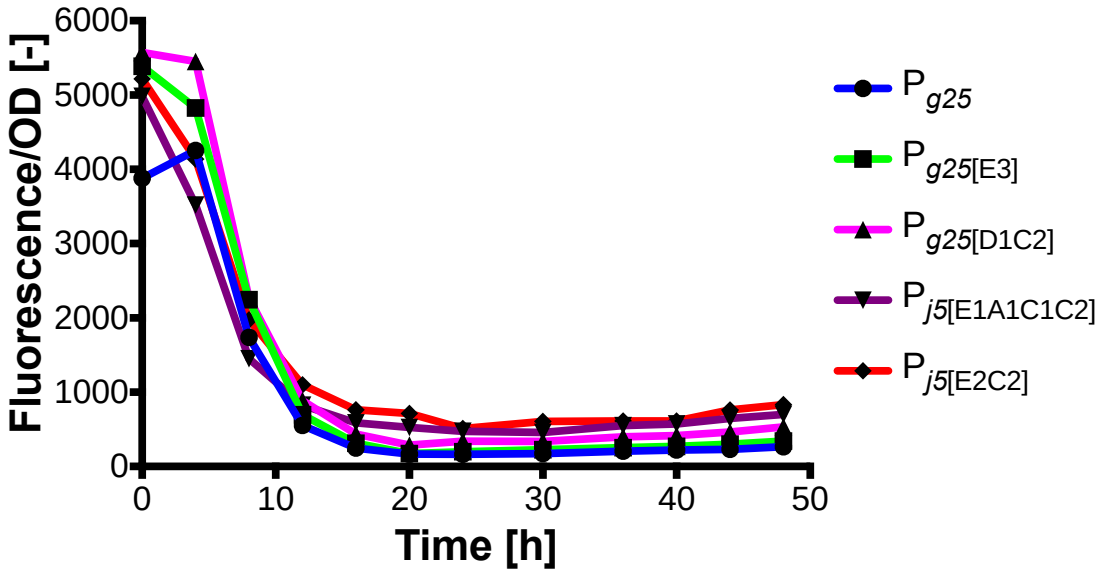

3.5.1.3 Promoter list

Colour code

Colour	Genetic element
Dark orange	Upstream element
Red	-35 box
Purple	-10 box
Light pink	Spacer between the -35 and -10 boxes
Green	5'-untranslated region
Green (upper case)	TRANSCRIPTIONAL START
Light brown	Synthetic or native ribosome binding site
Dark blue	*fapO* sequence
Grey	T7 stem-loop
Black	Region between -10 box and transcriptional start
Cyan (underlined)	Spacer between the P_{phaC1}-based secondary promoter and its primary promoter
Cyan	Spacer between the $P_{j5[A1C1C2]}$-based secondary promoter or the P_{g25}-based secondary promoter and its primary promoter

P_{phaC1}

caatggccacgatgtacatcaaaaattcatccttctcgcctatgctctggggcctcggcagatgcgagcgctgcataccgtcc
ggtaggtcgggaagcgtgcagtgccgaggcggattcccgcattgacagcgcgtgcgttgcaaggcaacaatggactCaa
atgtctcggaatcgctgacgattcccaggtttctccggcaagcatagcgcatggcgtctccatgcgagaatgtcgcgcttgcc
ggataaaaggggagccgctatcggaatggacgcaagccacggccgcagcaggtgcggtcgagggcttccagccagttcc
agggcagatgtgccggcagaccctcccgctttgggggaggcgcaagccgggtccattcggatagcatctccccatgcaaa
gtgccggccagggcaatgcccggagccggttcgaatagtgacggcagagagacaatcaaatc

$P_{phaC1[A1]}$

caatggccacgatgtacatcaaaaattcatccttctcgcctatgctctggggcctcggcagatgcgagcgctgcataccgtcc
ggtaggtcgggaagcgtgcagtgccgaggcggattcccgcattcggcgcgcgtgcgttgcaaggcaacaatggactCaa
atgtctcggaatcgctgacgattcccaggtttctccggcaagcatagcgcatggcgtctccatgcgagaatgtcgcgcttgcc
ggataaaaggggagccgctatcggaatggacgcaagccacggccgcagcaggtgcggtcgagggcttccagccagttcc
agggcagatgtgccggcagaccctcccgctttgggggaggcgcaagccgggtccattcggatagcatctccccatgcaaa
gtgccggccagggcaatgcccggagccggttcgaatagtgacggcagagagacaatcaaatc

P_{rrsC}

ccttcaactgctctgcttggcattcgacgtctatatataaagaggacgtctcgggttgggccgacgcccacggtctcagctta
agccgaggcgccgctggatgctgtcaccaccgcgacatttgagcctcgtgcgccgcttttacgggggttcgaattatttcgc
gaaatcgcttgccagtcggtcctgcgtcccttaatattcgccccCtcgcagatctttaagaaggagatatacat

$P_{rrsC[D6]}$

ccttcaactgctctgcttggcattcgacgtctatatataaagaggacgtctcgggttgggccgacgcccacggtctcagctta
agccgaggcgccgctggatgctgtcaccaccgcgacatttgagcctcgtgcgccgcttttacgggggttcgaattatttcgc
gaaatcgcttgccagtcggtcctgcgtcccttaatattcgccccCtcgcttagtacctgatactaaagatctttaagaagga
gatatacat

$P_{rrsC[D4]}$

ccttcaactgctctgcttggcattcgacgtctatatataaagaggacgtctcgggttgggccgacgcccacggtctcagctta
agccgaggcgccgctggatgctgtcaccaccgcgacatttgagcctcgtgcgccgcttttacgggggttcgaattatttcgc
gaaatcgcttgccattagtacctgatactaataatattcgccccCtcgcagatctttaagaaggagatatacat

P_{j5}

agcggatataaaaaccgttattgacacaggtggaaatttagaatatactgttagtAaacctaatggatcgacctt

$P_{j5[C2]}$

agcggatataaaaaccgttattgacacaggtggaaatttagaatatactgttagtAaacctaatggatcgaccttagatctt
ttaagaaggagatatacat

$P_{j5[A3C2]}$

agcggatataaaaaccgttattgacacaggtggaaatttagaatatactgttagtAaacctaatggatcgacctagatcttt
taagaaggagatatacat

$P_{j5[C1]}$

agcggatataaaaaccgttattgacacaggtggaaatttagaatatactgttagtAaacctaatggatcgaccttgaattca
aaagatctgggagaccacaacggtttccctctagaaataattttggaattcaaa

$P_{j5[C1C2]}$

agcggatataaaaaccgttattgacacaggtggaaatttagaatatactgttagtAaacctaatggatcgaccttgaattca
aaagatctgggagaccacaacggtttccctctagaaataattttggaattcaaaagatctttaagaaggagatatacat

$P_{j5[A1C1C2]}$

agcggatataaaaaccgttattgacacaggtggaaatttaaaatatactgttagtAaacctaatggatcgaccttgaattca
aaagatctgggagaccacaacggtttccctctagaaataattttggaattcaaaagatctttaagaaggagatatacat

$P_{j5[A1D6aC1C2]}$

agcggatataaaaaccgttattgacacaggtggaaatttaaaatatactgttagtAaacctaatggatcgacctttttagtac
ctgatactaagaattcaaaagatctgggagaccacaacggtttccctctagaaataattttggaattcaaaagatctttaag
aaggagatatacat

$P_{j5[A1D6bC1C2]}$

agcggatataaaaaccgttattgacacaggtggaaatttaaaatatactgttagtAaacctaatggatcgacctttttagtac
ctgatactaattagtacctgatactaagaattcaaaagatctgggagaccacaacggtttccctctagaaataattttggaat
tcaaaagatctttaagaaggagatatacat

P_{g25}

tatggaaaaataaaaatttcttgataaaattttccaatactattataattattgttAttaaaggaggagaaattaac

$P_{g25[C2]}$

tatggaaaaataaaaatttcttgataaaattttccaatactattataattattgttAttaaaggaggagaaattaacagatctttt
aagaaggagatatacat

$P_{g25[D1]}$

tatggaaaaataaaaatttcttgataaaattttccaatactattataattattgtttatggaaaaataaaaatttcttgataaaat
tttccaatactattataattattgttAttaaaggaggagaaattaac

$P_{g25[D1C2]}$

tatggaaaaataaaaatttcttgataaaattttccaatactattataattattgtttatggaaaaataaaaatttcttgataaaat
tttccaatactattataattattgttAttaaaggaggagaaattaacagatctttaagaaggagatatacat

Spacer between the P_{phaC1}-based secondary promoter and its primary promoter

ctgcag

Spacer between the $P_{j5[A1C1C2]}$-based secondary promoter or P_{g25}-based secondary promoter and its primary promoter

gactcaaggatgctagtgtaagcatctgcag

Table S3.1: Promoter engineering strategies.

Strategy	Description
A	**Point mutation**
A1	Base substitution
A2	Base insertion
A3	Base deletion
B	**Length alteration**
B1	Truncation of DNA sequence upstream of -35 box
B2	Truncation of DNA sequence downstream of +1 transcriptional start
B3	Extension of DNA sequence upstream of -35 box
B4	Extension of DNA sequence downstream of +1 transcriptional start
B5	Deletion of DNA sequence upstream of -35 box
B6	Deletion of DNA sequence between -35 and -10 boxes
B7	Deletion of DNA sequence between -10 box and +1 transcriptional start
B8	Deletion of DNA sequence in the 5'-UTR
B9	Insertion of DNA sequence upstream of -35 box
B10	Insertion of DNA sequence between -35 and -10 boxes
B11	Insertion of DNA sequence between -10 box and +1 transcriptional start
B12	Insertion of DNA sequence in the 5'-UTR
C	**Incorporation of regulatory genetic element**
C1	T7 stem-loop
C2	Ribosome binding site
D	**Promoter hybridization**
D1	Hybrid promoter comprises DNA sequences derived from two identical promoters
D2	Hybrid promoter comprises DNA sequences derived from two different promoters
D3	Incorporating *ci*s-acting transcriptional regulatory element upstream of -35 box
D4	Incorporating *ci*s-acting transcriptional regulatory element between -35 and -10 boxes
D5	Incorporating *ci*s-acting transcriptional regulatory element between -10 box and +1 transcriptional start
D6	Incorporating *ci*s-acting transcriptional regulatory element in the 5'-UTR
E	**Configuration alteration**
E1	Placing P_{phaC1} promoter divergent to the primary promoter
E2	Placing P_{g25} promoter divergent to the primary promoter
E3	Placing $P_{j5[A1C1C2]}$ promoter divergent to the primary promoter
E4	Placing $P_{phaC1[A1]}$ promoter divergent to the primary promoter

Table S3.2: A list of all 42 promoters in ascending order of activity

Promoter	Activity ranking	Serial number	P_{BAD} ranking	Level
$P_{phaC1[A1]}$	1	1	0.001 – 0.006 % (w/v)	Level One
$P_{rrsC[D4]}$	1	2		
$P_{rrsC[D6]}$	1	3		
$P_{phaC1[B1c]}$	6	4		
P_{phaC1}	6	5		
$P_{phaC1[B1a]}$	8	6		
$P_{rrsC[E3D4]}$	9	7		
$P_{phaC1[B1b]}$	10	8		
P_{rrsC}	11	9		
$P_{phaC1[B1d]}$	12	10		
$P_{rrsC[E1D4]}$	14	11		
$P_{rrsC[E3D6]}$	21	12		
$P_{rrsC[E3]}$	22	13		
P_{j5}	25	14		
$P_{j5[C1]}$	26	15		
$P_{rrsC[E1D6]}$	31	16	0.006 – 0.010 % (w/v)	Level Two
$P_{rrsC[E1]}$	34	17		
P_{g25}	39	18		
$P_{g25[E3]}$	45	19		
$P_{g25[E2]}$	46	20		
$P_{g25[D1]}$	53	21		
$P_{g25[C2]}$	57	22		
$P_{g25[E1]}$	61	23	0.010 – 0.020 % (w/v)	Level Three
$P_{j5[A1C1C2]}$	64	24		
$P_{j5[A1D6bC1C2]}$	68	25		
$P_{j5[A1D6aC1C2]}$	70	26		
$P_{g25[D1C2]}$	75	27		
$P_{j5[E2A1C1C2]}$	84	28		
$P_{j5[E2A1D6bC1C2]}$	87	29	0.020 – 0.200 % (w/v)	Level Four
$P_{j5[E2A1D6aC1C2]}$	90	30		
$P_{j5[C1C2]}$	91	31		
$P_{j5[E1A1C1C2]}$	104	32		
$P_{j5[E2C1C2]}$	106	33		
$P_{j5[E1A1D6bC1C2]}$	111	34		
$P_{j5[E1A1D6aC1C2]}$	112	35		
$P_{j5[A3C2]}$	116	36		Level Five
$P_{j5[C2]}$	117	37		
$P_{j5[E1C1C2]}$	120	38		
$P_{j5[E2C2]}$	125	39		
$P_{j5[E2A3C2]}$	128	40		
$P_{j5[E1C2]}$	134	41		

$P_{j5[E1A3C2]}$	137	42		

Table S3.3: Growth rates of *R. eutropha* H16 harbouring either pBBR1MCS-1 (control) or plasmids containing various engineered constitutive promoters.

Engineered constitutive promoter	μ_{max} [h^{-1}]	Promoter activity level
pBBR1MCS-1 (control)	0.2342	N/A
$P_{phaC1[B1d]}$	0.2357	1
$P_{rrsC[E1D4]}$	0.2120	1
P_{g25} (parental promoter)	0.2194	2
$P_{g25[E3]}$	0.2160	2
$P_{g25[D1C2]}$	0.2269	3
$P_{j5[E1A1C1C2]}$	0.2147	4
$P_{j5[E2C2]}$	0.1796	5

Table S3.4: Fitting of cell culture fluorescence *vs* time data to a 4-parameter dose response curve according to the Hill's equation

Engineered constitutive promoter	Promoter activity level	Bottom	Hillslope	Top	T_{50}	R^2
P_{g25} (parental promoter)	2	691	5.737	3023	23.01	0.9772
$P_{g25[E3]}$	2	897	5.652	4023	25.69	0.9754
$P_{g25[D1C2]}$	3	926	5.450	6445	24.19	0.9803
$P_{j5[E1A1C1C2]}$	4	982	4.011	10384	24.46	0.9937
$P_{j5[E2C2]}$	5	972	4.428	11569	25.89	0.9971

CHAPTER FOUR

This chapter has been adapted from the manuscript: Johnson, A. O.; Tee, K. L.; Wong, T. S., Malonyl-CoA biosensors engineered for *Cupriavidus necator* H16, *Submitted*. **2018.**

4 MALONYL-COA BIOSENSORS ENGINEERED FOR *RALSTONIA EUTROPHA* H16

Abstract

Knallgas bacterium, *Ralstonia eutropha* H16, has increasingly been used for biomanufacturing, owing to the rapid expansion of the synthetic biology toolbox available for this microbial host. That being said, transcription factor-based genetic circuit has not been applied for detecting, quantifying and regulating metabolite accumulation in *R. eutropha* H16. This is primarily due to chassis-specific complexity in constructing such a metabolite-sensing biological device (or a biosensor). In this article, we reported a set of 6 malonyl-CoA biosensors for *R. eutropha* H16. These single-plasmid bimodular biosensors are designed based upon the naturally existing fatty acid metabolism regulon found in Gram-positive bacteria. Using cerulenin as a fatty acid biosynthesis inhibitor, we showed that all 6 biosensors were responsive to changes in intracellular malonyl-CoA concentration and displayed a high degree of orthogonality. The biosensor performance was optimized through careful selection of constitutive promoter combination to give a broad dynamic range and sensitivity. We envisage that this biosensor set will propel more advanced metabolic engineering of *R. eutropha* H16 in the near future.

Keywords

Ralstonia eutropha H16, *Cupriavidus necator* H16, malonyl-CoA, FapR, cerulenin

4.1 INTRODUCTION

Ralstonia eutropha H16 (or *Cupriavidus necator* H16) is a non-pathogenic Gram-negative bacterium, widely known for its natural ability to accumulate polyhydroxyalkanoate (PHA) (Pohlmann et al., 2006). This has informed its use as a microbial host for commercial scale production of bio-plastics. Its intrinsic capability to sense, adapt to, assimilate and conserve carbon supply from a broad range of carbon sources (Volodina et al., 2016) has also expanded its potential industrial applications (Brigham et al., 2012) in the synthesis of value-added chemicals, such as polymers (Arikawa and Matsumoto, 2016, Lutke-Eversloh and Steinbüchel, 2003, Steinbüchel and Pieper, 1992, Valentin et al., 1995, Voss and Steinbuchel, 2006) hydrocarbons of various chain lengths and functional groups (Chen et al., 2015, Crépin et al., 2016, Marc et al., 2017, Bi et al., 2013) as well as amino acids (Luette et al., 2012).

Engineering *R. eutropha* for biomanufacturing requires introduction and optimization of a heterologous pathway to produce a target chemical from precursor molecule(s). However, as is the case in several other microbial cell factories, a synthetic metabolic pathway often perturbs the host's metabolic network and cellular phenotypes, potentially imposing metabolic bottlenecks thereby limiting product yield and titre (Keasling, 2012). To work around this challenge, metabolic engineers endeavour to achieve a dynamic regulation of heterologous pathway to provide a systemic metabolic control over intracellular accumulation of precursor metabolite(s) and downstream metabolism into target chemical, whilst forging for a win-win between cell viability and product yield (Brockman and Prather, 2015, Cress et al., 2015, Holtz and Keasling, 2010, Keasling, 2012, McNerney et al., 2015, Nielsen and Keasling, 2016).

Achieving systemic metabolic control requires efficient quantification of intracellular concentration and accumulation of precursor metabolite, under defined growth and environmental conditions (Dekker and Polizzi, 2017, Johnson et al., 2017, Rogers et al., 2016, Schallmey et al., 2014, Zhang et al., 2015). Malonyl-CoA is one of the most vital precursor metabolites for a myriad of commercially valuable molecules such as fatty acids, flavonoids, bio-polymers, bio-fuels and polyketides (Johnson et al., 2017). It is also a rate-limiting central metabolite in the fatty acid biosynthesis. Conventional analytical techniques for malonyl-CoA quantification (*e.g.*, HPLC/MS, HPLC and capillary

electrophoresis with UV detection) are laborious. As such, malonyl-CoA-responsive biological devices (or biosensors) have been constructed to report intracellular malonyl-CoA concentration (Johnson et al., 2017). Malonyl-CoA biosensor is a synthetic mimicry of the transcriptional regulon of fatty acid biosynthesis found naturally in Gram-positive bacteria such as *Bacillus subtilis*. This regulation is modulated by the interaction between transcription factor FapR (Fatty acid and phospholipid Regulator) and its operator *fapO*. FapR represses the fatty acid operon through binding to the 17-bp *cis*-regulatory *fapO* operator localized within or in proximity to the operon's promoter. Malonyl-CoA acts as an inducer of the FapR regulon by impairing the FapR-*fapO* interaction. Through replacing the fatty acid operon with a gene encoding a reporter protein, for instance a fluorescence protein, a biosensor that is transcriptionally regulated by malonyl-CoA is created, where the reporter protein activity reflects the intracellular malonyl-CoA concentration.

Dynamic quantification of malonyl-CoA has been widely demonstrated in mammalian cells (Ellis and Wolfgang, 2012) and model microbial cell factories (*e.g.*, *E. coli* and *S. cerevisiae*) (Li et al., 2015, Xu et al., 2014b) using chemical agents such as cerulenin and triclosan, known to block the fatty acid biosynthesis thereby inducing intracellular accumulation of malonyl-CoA (Johnson et al., 2017, Zhang et al., 2006). Increased malonyl-CoA concentration resulting from heterologously expressed source pathways has also been quantified (Johnson et al., 2017). Examples include acetyl-CoA carboxylase (ACC), which converts acetyl-CoA into malonyl-CoA, and malonyl-CoA synthetase (MatB), which converts malonate, channeled into the cell *via* malonate carrier protein (MatC), into malonyl-CoA. Using malonyl-CoA biosensors, malonyl-CoA levels ranging from 0.1–1.1 nmol/mg DW can be detected in the aforementioned hosts. Some of these biosensors have in fact been applied as a negative feedback loop (Liu et al., 2015b) and a metabolic switch (Xu et al., 2014b) for dynamic regulation of malonyl-CoA to improve product titre and yield of various metabolites (*e.g.*, 3-hydroxypropionic acid) (Rogers and Church, 2016).

In this article, we reported the design and engineering of a set of genetically-encoded malonyl-CoA biosensors that are compatible with *R. eutropha* H16. To our best knowledge, these are the first malonyl-CoA biosensors engineered for this industrially promising microbial host. We also looked at the application of this sensor set for the dynamic

quantification of intracellular malonyl-CoA concentration. We envisage that this biosensor set will be of high relevance to the dynamic regulation of malonyl-CoA source and sink pathways in *R. eutropha* H16, as well as other applications previously reported for *E. coli* and *S. cerevisiae*.

4.2 RESULTS AND DISCUSSION

4.2.1 Single-plasmid bimodular malonyl-CoA biosensor

The design of a functional malonyl-CoA biosensor for a microbial cell factory requires the contextual knowledge of both DNA replication and gene transcription of the chassis in question (Johnson et al., 2017). We have adapted the bacterial FapR transcriptional regulatory system to generate a malonyl-CoA biosensor that can be used to detect malonyl-CoA changes in R. eutropha H16. To achieve a compact and flexible design, we modified pBBR1c-RFP developed in-house (Figure S1) that was originally derived from the broad-host-range pBBR1MCS plasmid (Kovach et al., 1994). pBBR1MCS is compatible with IncQ, IncP, IncW, and colE1. This medium-copy-number plasmid (<40 copies per cell)(Bi et al., 2013) carries a chloramphenicol resistance gene and is the most widely used plasmid system for *R. eutropha* H16. Each of our biosensor has two modules working in tandem, a repressor module and a reporter module as depicted in Figure 4.1A. The repressor module consists of a gene encoding *Bacillus* transcription factor FapR (NCBI reference sequence WP_003232044.1) and its promoter termed P1 henceforth. The gene sequence of FapR was codon-optimized for expression in *R. eutropha* H16. The reporter module, on the other hand, consists of a gene encoding a monomeric DsRed protein variant (GenBank BAD52341.1) and its promoter termed P2 henceforth. P2 is a *fapO*-hybrid promoter, containing one or more units of the 17 bp-*fapO* operator sequence (5'-TTAGTACCTGATACTAA-3'). The two neighbouring genes (*fapR* and *rfp*) are arranged in head-to-head orientation with their promoters, P1 and P2, in back-to-back configuration (or divergent to one another). Important to note, by having both modules on the same plasmid, the relative ratio of repressor activity to reporter activity is governed by the relative strengths of P1 and P2 promoters, the interaction between FapR and *fapO*, and the number of *fapO* units. Variability due to plasmid copy number, plasmid compatibility and plasmid stability is therefore removed to simplify the design and subsequent optimization. Also worthy of mention, the repressor and reporter modules are flanked by restriction sites Bsu36I|PstI and PstI|XhoI, respectively. This enables flexible exchange of each module (*i.e.*, changing P1 and P2 combination) to optimize the performance of the resultant biosensor.

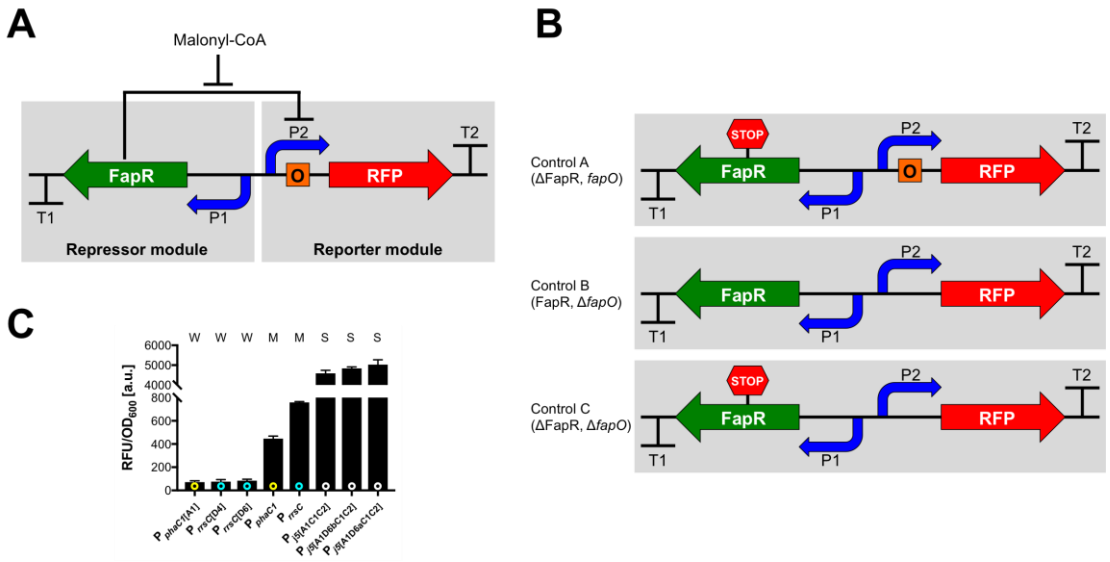

Figure 4.1: (*A*) Bimodular malonyl-CoA biosensor. (*B*) Three negative control genetic circuits constructed for each biosensor (FapR, *fapO*): control A (ΔFapR, *fapO*), control B (FapR, Δ*fapO*) and control C (ΔFapR, Δ*fapO*). (*C*) Promoters used in this study. P_{j5}-, P_{phaC1}- and P_{rrsC}-derived promoters are indicated by white circles, yellow circles and cyan circles, respectively. The letters 'S', 'M' and 'W' are used to indicate strong, medium and weak promoter, respectively. Data was obtained from a previous study.(Johnson et al., 2018).

4.2.2 Control genetic circuits for validating the design of malonyl-CoA biosensor

A malonyl-CoA-responsive biosensor requires the simultaneous presence of two essential genetic elements, *i.e.*, FapR repressor and *fapO* operator [(FapR, *fapO*) was used to indicate the presence of both elements]. To validate our design, we also constructed three control genetic circuits (controls A to C in Figure 4.1B). In control A (ΔFapR, *fapO*) and control B (FapR, Δ*fapO*), one of these genetic elements was either non-functional (a 5'-TAATGA-3' double stop codon was introduced in the *fapR* gene resulting in pre-mature truncation of FapR) or removed (*fapO* was deleted). In control C (ΔFapR, Δ*fapO*), both genetic elements were 'absent'. Ideally, all control circuits should not respond to changes in malonyl-CoA concentration (*i.e.*, negative controls). If a constitutive promoter is applied for P2 (which is the case in our designs; Tables 4.1 & 4.2), RFP expression is not repressed and is therefore permanently turned on. These three control genetic circuits are essential to fully comprehend our biosensor design: (1) By comparing biosensor with its control A, one could determine the level of *rfp* gene repression owing to FapR, (2) By comparing controls A and B or controls A and C, one would know the effect of introducing *fapO* unit(s) on P2

promoter strength, (3) By comparing controls B and C, one could verify if FapR binds non-specifically to P2, and (4) By comparing biosensor with its control A or control B or control C in increasing concentration of chemical that induces malonyl-CoA accumulation (*e.g.*, cerulenin), one could demonstrate biosensor orthogonality.

Table 4.1: Promoters used in this study

Promoter	Description
P_{phaC1}	466-bp native promoter of the *R. eutropha* H16 *phaC1* gene
$P_{phaC1[A1]}$	P_{phaC1} variant with mutations in -35 box
P_{rrsC}	Semi-synthetic promoter of *R. eutropha* H16 *rrsC* gene
$P_{rrsC[D6]}$	P_{rrsC} variant containing one 17-bp *fapO* unit within its downstream element
$P_{rrsC[D4]}$	P_{rrsC} variant containing one 17-bp *fapO* unit between its -35 and -10 boxes
$P_{j5[A1C1C2]}$	Coliphage T5 P_{j5} variant containing a T7 stem-loop and a synthetic RBS in its 5'-UTR
$P_{j5[A1D6aC1C2]}$	$P_{j5[A1C1C2]}$ variant containing one 17-bp *fapO* unit within its downstream element
$P_{j5[A1D6bC1C2]}$	$P_{j5[A1C1C2]}$ variant containing two tandem 17-bp *fapO* units within its downstream element

Table 4.2: Six malonyl-CoA biosensors described in this study

Biosensor	Repressor module			Reporter module			
	Promoter P1	**Promoter strength**	**Repressor**	**Promoter P2**	**Promoter strength**	**Number of *fapO* unit(s)**	**Reporter**
S1	P_{phaC1}	M	FapR	$P_{rrsC[D6]}$	W	1	RFP
S2	P_{phaC1}	M	FapR	$P_{rrsC[D4]}$	W	1	RFP
S3	$P_{phaC1[A1]}$	W	FapR	$P_{rrsC[D6]}$	W	1	RFP
S4	$P_{phaC1[A1]}$	W	FapR	$P_{rrsC[D4]}$	W	1	RFP
S5	P_{phaC1}	M	FapR	$P_{j5[A1D6aC1C2]}$	S	1	RFP
S6	P_{phaC1}	M	FapR	$P_{j5[A1D6bC1C2]}$	S	2	RFP

4.2.3 Constructing a set of 6 malonyl-CoA biosensors by careful selection of constitutive promoter combinations

Although single-plasmid bimodular design (Figure 4.1A) is comparatively simpler than having FapR and *fapO* on separate plasmids, judicious choice of P1 and P2 promoter combination remains crucial. It determines a biosensor's dynamic range and sensitivity. Since we did not modify the gene sequence of FapR and the DNA sequence of *fapO* operator (*i.e.*, K_D between FapR-*fapO* interaction is kept constant), we focused our attention on the relative strength between P1 and P2 promoters. Of course, the strength of *fapO*-hybrid promoter P2 depends also on the location and the number of *fapO* units. We have previously constructed and comprehensively characterized a set of broad-activity-range constitutive promoters for *R. eutropha* H16 (Johnson et al., 2018). Based on this prior knowledge, we selected 8 promoters and they were derived from either promoter P_{phaC1} (indicated by yellow circles), P_{rrsC} (cyan circles) or P_{j5} (white circles) (Table 4.1, Figure 4.1C). Of these 8 promoters, those three P_{j5}-based promoters are comparatively stronger (indicated by an 'S'), compared to P_{phaC1}- or P_{rrsC}-based promoters. Using different combinations of these promoters, we constructed a set of 6 malonyl-CoA biosensors (S1–S6; Table 2) and their respective negative controls (Table 4.3). Important to highlight, promoters P1 and P2 are not independent to one another in *R. eutropha* H16. When placed in back-to-back configuration, they form a composite promoter with the secondary promoter serving as a transcriptional amplifier of the primary promoter. If we use RFP as a reference point, the activity of primary promoter P2 is amplified by the presence of the secondary promoter P1, as we have previously demonstrated (Johnson et al., 2018). This factor needs to be taken into consideration when analysing the performance of a biosensor.

Table 4.3: Controls for all six malonyl-CoA biosensors described in this study. Biosensors S1 and S2 share the same promoter P1. Therefore, these two biosensors share the same control B and control C. The same applies to biosensor pairs S3 and S4 as well as S5 and S6.

Biosensor	Control A			Control B			Control C		
	Repressor	**Promoter P2**	**Promoter strength**	**Repressor**	**Promoter P2**	**Promoter strength**	**Repressor**	**Promoter P2**	**Promoter strength**
S1	Truncated FapR	$P_{rrsC[D6]}$	W	FapR	P_{rrsC}	M	Truncated FapR	P_{rrsC}	M
S2	Truncated FapR	$P_{rrsC[D4]}$	W						
S3	Truncated FapR	$P_{rrsC[D6]}$	W	FapR	P_{rrsC}	M	Truncated FapR	P_{rrsC}	M
S4	Truncated FapR	$P_{rrsC[D4]}$	W						
S5	Truncated FapR	$P_{j5[A1D6aC1C2]}$	S	FapR	$P_{j5[A1C1C2]}$	S	Truncated FapR	$P_{j5[A1C1C2]}$	S
S6	Truncated FapR	$P_{j5[A1D6bC1C2]}$	S						

4.2.4 RFP expression in all 6 biosensors was repressed by FapR

Repression of RFP expression by FapR is the first and foremost criterion of a functional biosensor. The level of repression is quantitatively described by fold repression, which is the ratio of the reporter activity from control A (ΔFapR, *fapO*) to the reporter activity from biosensor (FapR, *fapO*). Another characteristic of a good biosensor is low basal RFP expression when placing the biosensor in a "repressed" or an "un-induced" state (*i.e.*, low noise level). Measurement of reporter activity from all biosensors (Figure 4.2A) and their control As (Figure 4.2B) revealed a 2–15-fold repression (Figure 4.2C) between the 6 designs (S1–S6). Reporter activity is predominantly governed by the strength of P2. When strong promoters ($P_{j5[A1D6aC1C2]}$ and $P_{j5[A1D6bC1C2]}$) were used in biosensors S5 and S6 as P2, we observed a high basal RFP expression (Figure 4.2A) and a low repression of 2–3 folds (Figure 4.2C). In other words, the promoters P2 in S5 and S6 are leaky. Further, this "leaky" RFP expression in P_{j5}-based promoters increases with cultivation time (Figure 4.2A). RFP expression from biosensor S1, on the contrary, is most effectively repressed by FapR, judging on its highest ~15-fold repression. This is achieved via the right level of FapR expression (driven by a promoter of medium strength 'M') and of RFP expression (driven by a weak promoter 'W'). Even though $P_{rrsC[D6]}$ (P2 of biosensor S1) is a weak promoter when characterized independently, it was transcriptionally amplified when placed in back-to-back with P_{phaC1} (P1 of biosensor S1) to achieve a more balanced ratio of repressor to reporter activity. Likewise, the FapR expression driven by the P_{phaC1} could also be amplified by the presence of neighbouring $P_{rrsC[D6]}$, which in turn, contributed to the more optimal repressor to reporter ratio in biosensor S1. Comparing biosensors S1 and S2 also revealed the importance of the location of *fapO* operator in achieving an appropriate level of repression. In biosensor S1, *fapO* unit was placed within the downstream element of P_{rrsC}, whereas in biosensor S2, the same unit was located between -35 and -10 boxes of P_{rrsC}. We then proceeded to measuring the reporter activity from control Bs and control Cs. As indicated in Figure 4.2D, both controls B and C gave almost identical RFP expression level. This proves that there is no non-specific FapR-binding site within the chosen P2 promoters. In other words, RFP repression is a direct consequence of FapR-*fapO* interaction.

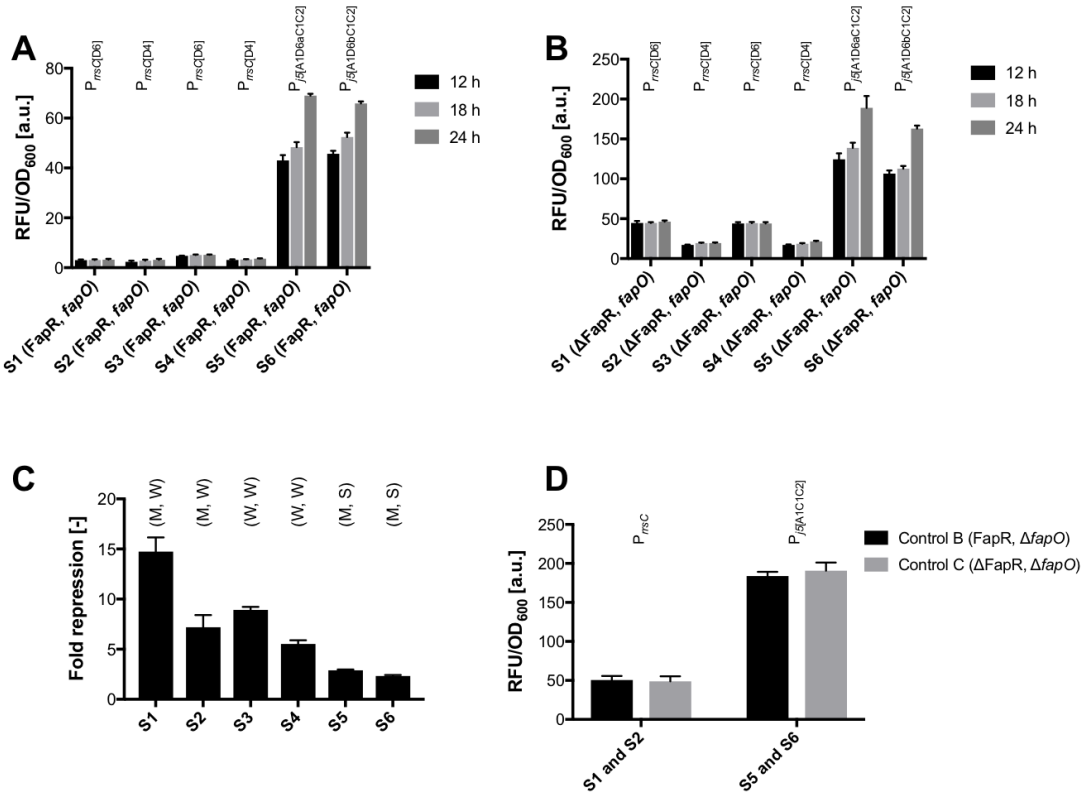

Figure 4.2: (*A*) Reporter activity from each biosensor (FapR, *fapO*). Promoter P2 of each biosensor is indicated above each data set. (*B*) Reporter activity from control A (ΔFapR, *fapO*) of each biosensor. Promoter P2 of each control genetic circuit is indicated above the respective data set. (*C*) Fold repression of each biosensor, after 12 h cultivation in 96-well deep well plate. Promoter strength is indicated above each data point, written in the format of (Strength of promoter P1, Strength of promoter P2). (*D*) Reporter activity from control B (FapR, Δ*fapO*) and control C (ΔFapR, Δ*fapO*). Promoter P2 of the control genetic circuit is indicated above each data set.

4.2.5 All 6 biosensors are responsive to changes in intracellular malonyl-CoA concentration

To show that our biosensors can be applied to detect changes in intracellular malonyl-CoA concentration, we cultivated *R. eutropha* H16 in 96-well deep well plate with varying concentration of cerulenin ([C]) from 0 to 20 μM (Figure 4.3). Cerulenin is a known inhibitor of β-ketoacyl-ACP synthase I/II (FabB/F); addition of which into microbial culture medium results in intracellular accumulation of malonyl-CoA (Zhang et al., 2006). The cerulenin concentration range that we tested did not affect the growth of *R. eutropha* H16 significantly. We observed only a 20 % drop in OD_{595} at 20 μM cerulenin (Figure S4.2). As shown in Figure 5.4, reporter activity correlated with cerulenin concentration for

all 6 biosensors. Important qualities of a good response (R) from a biosensor include broad dynamic range (*i.e.*, high $[C]_{max}/[C]_{min}$, in which $[C]_{max}$ is the highest non-saturating cerulenin concentration and $[C]_{min}$ is the lowest cerulenin concentration that still gives a detectable response) and high sensitivity (*i.e.*, high $\Delta R/\Delta[C]$). To examine these qualities more closely, each data set in Figure 4.4 was fit to a dose-response curve with a variable slope. Each curve fitting therefore returned 4 parameters: top value, bottom value, half maximal effective concentration (EC_{50}) and Hillslope. Broad dynamic range is typically characterized by a large EC_{50} along with a gentle slope. On the other hand, high sensitivity is reflected by a large span (top value minus bottom value). Biosensor S1 gave the largest dynamic range as indicated by its EC_{50} of ~4.5 μM (Table S4.1), which is the highest among the 6 designs, and a gentle slope. Biosensor S2 showed a similar dynamic range compared to S1, but with a lower sensitivity as indicated by a smaller span (~40 for S1 and ~10 for S2). Interestingly, at 20 μM cerulenin, the reporter activity of biosensor S1 was almost identical to that of its control A (Figure S4.3). This showed that FapR was almost completely relieved from binding to *fapO* operator, when 20 μM cerulenin was used. In other words, we observed similar fold repression and maximal fold induction (Figure 4.5). The fold induction is defined as the reporter activity at X μM cerulenin divided by the reporter activity at 0 μM cerulenin. Hence, the maximal fold induction is the maximum fold induction value measured at $[C] = [C]_{max}$. For all biosensors, we achieved induction efficiency between 74–99% (Table S4.2). Also apparent from Figure S4.3, introducing a *fapO* unit between -35 and -10 boxes of P_{rrsC} resulted in loss of promoter activity, as indicated by the obvious difference in reporter activity from controls A and B of both biosensors S4.2 and S4.4.

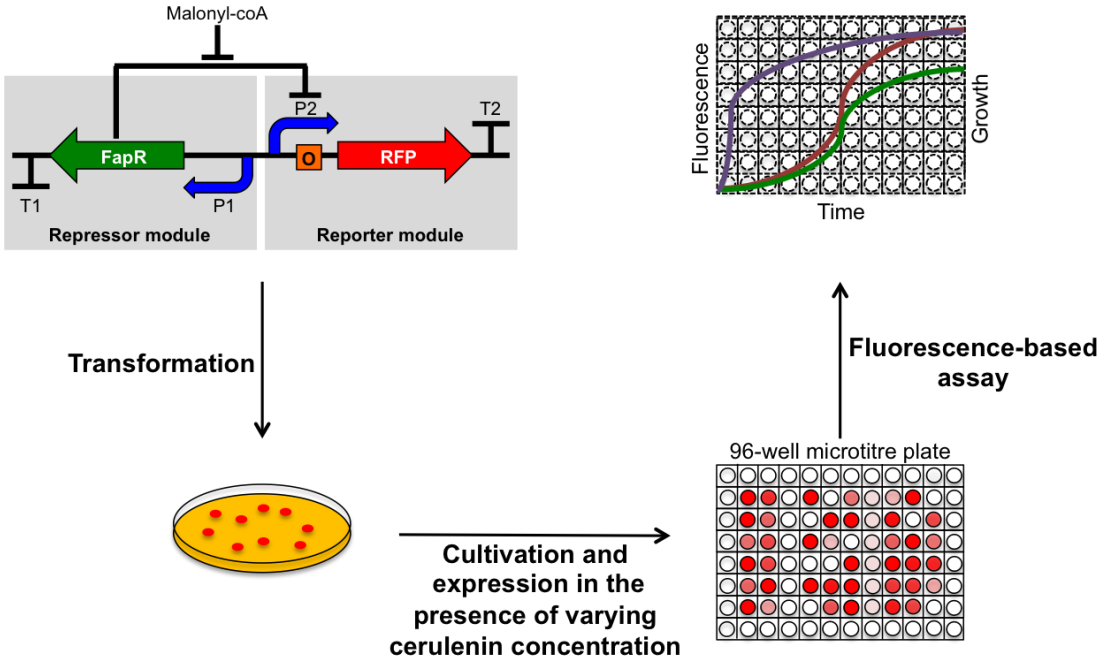

Figure 4.3: High-throughput characterization of malonyl-CoA biosensors using a fluorescence-based assay.

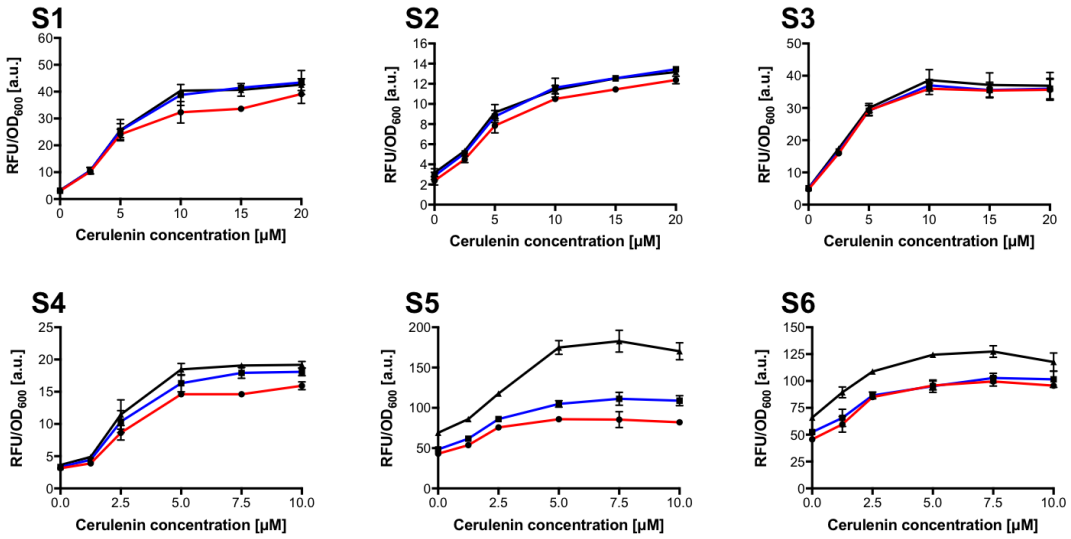

Figure 4.4: Reporter activity from biosensor (FapR, *fapO*) S1 to S6 in the presence of increasing cerulenin concentration, measured after 12 h (red line), 18 h (blue line) and 24 h (black line) of cultivation in 96-well microtitre plate.

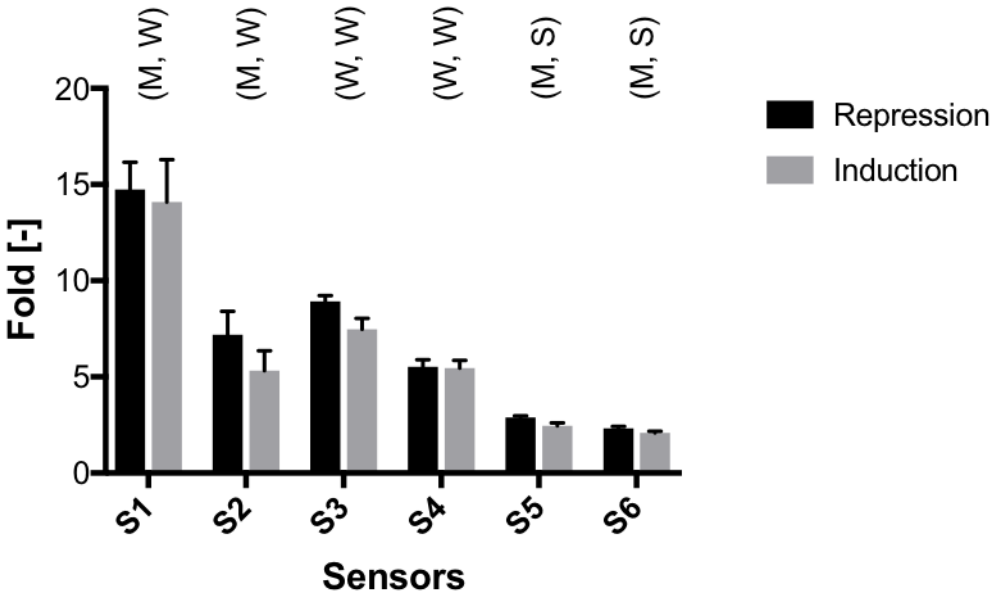

Figure 4.5: Fold repression (black column) and maximal fold induction (grey column) of each biosensor. Promoter strength is indicated above each data point, written in the format of (Strength of promoter P1, Strength of promoter P2).

4.2.6 All 6 biosensors displayed high degree of orthogonality

We also measured the reporter activity from controls A and B of each biosensor, in the presence of identical range of cerulenin concentration. In Figure 4.6, data was reported as cerulenin concentration *vs* fold induction of each sensor and its respective controls A and B. For all biosensors, reporter activity from control A or from control B did not change with increase in cerulenin concentration (*i.e.*, fold induction close to value 1). Figure 4.6 clearly verified the orthogonality of our biosensors. Cerulenin-induced de-repression of reporter module was indeed a direct result of FapR being relieved from binding to *fapO* operator.

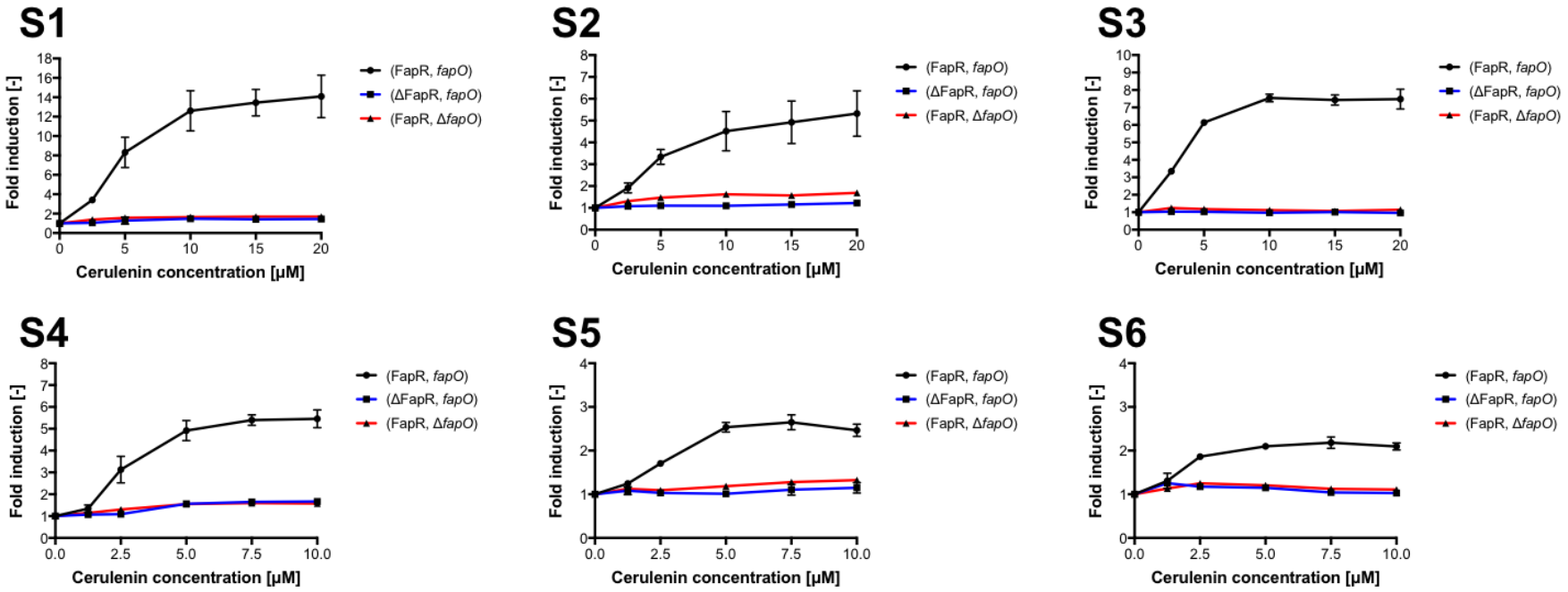

Figure 4.6: Fold induction from biosensor [(FapR, *fapO*); black line], control A [(ΔFapR, *fapO*); blue line] and control B [(FapR, Δ*fapO*); red line] for each design in the presence of increasing cerulenin concentration.

4.2.7 S1 is the best biosensor and works in *E. coli*

Of the 6 biosensors described, S1 showed the best performance, judging on its low basal RFP expression (low 'leakiness' or low noise level), broad dynamic range ([C] from 0 to 20 μM), high fold repression (14.7×), high fold induction (14.1×) and high induction efficiency (96%). S5, on the other hand, is the most sensitive biosensor (high ΔR/Δ[C]) at low range of cerulenin concentration (0 to 5 μM), even though its response is cultivation time-dependent. Therefore, this set of 6 biosensors provides us with the flexibility in choosing the most appropriate sensing device depending on the application and the range of malonyl-CoA concentration to be quantified. All 6 biosensor constructs are also functional in *E. coli* (data not shown), although the response curves differ significantly. This is largely due to the fact that the promoters we have chosen showed very different relative strengths in *E. coli* (Johnson et al., 2018). This particular fact further supported the need to design chassis-specific biosensor. In essence, there is no one size fits all, when it comes to designing transcription-based genetic devices.

4.3 CONCLUSION

In constructing malonyl-CoA biosensors, as described in this article, we considered chassis-specific design constraints, which include promoter combination, relative promoter strength, promoter strength amplification by neighbouring promoter, intracellular malonyl-CoA concentration and cerulenin tolerance, among others. All biosensors presented in this study were functional and responsive to changes in malonyl-CoA concentration in *R. eutropha* H16 induced by cerulenin addition. This was achieved via careful balancing of all chassis-specific design constraints. We strongly believe this set of malonyl-CoA biosensors would be useful for future quantification of malonyl-CoA source/sink pathways and for dynamic regulation of intracellular malonyl-CoA pool in *R. eutropha* H16.

4.4 MATERIALS & METHODS

4.4.1 Materials

All DNA modifying enzymes were purchased from either New England Biolabs or Agilent. Nucleic acid purification kits were purchased from Qiagen. All oligonucleotides were synthesized by Eurofins.

4.4.2 Strains

Escherichia coli DH5α was used for all molecular cloning, plasmid propagation and maintenance. *Ralstonia eutropha* H16 was used for all experiments described in this article.

4.4.3 Biosensor construction and FapR/promoter sequences

All plasmids harbouring a genetic circuit for a malonyl-CoA biosensor were derived from pBBR1c-RFP (see Supplementary Information) and constructed using standard molecular biology techniques. All genetic circuits were verified by restrictive analysis and/or DNA sequencing. FapR and promoter sequences were provided in the Supplementary Information.

4.4.4 Bacterial cultivation and transformation

R. eutropha H16 was cultivated at 30°C in nutrient broth (NB) supplemented with 10 μg/mL of gentamicin. Cells were transformed with plasmids using the electroporation protocol described by Tee et al. (2017) plated on NB agar supplemented with 10 μg/mL of gentamicin and 25 μg/mL of chloramphenicol, and incubated at 30°C for 40–60 h. *E. coli* DH5α was transformed with plasmids using the standard $CaCl_2$ method, plated on TYE agar supplemented with 25 μg/mL of chloramphenicol and incubated overnight at 37°C.

4.4.5 Biosensor characterization using fluorescence assay

Fresh NB, supplemented with 10 μg/mL of gentamicin and 25 μg/mL of chloramphenicol, was inoculated with overnight culture of *R. eutropha* H16 (transformants carrying either a biosensor plasmid or a negative control plasmid) at a dilution factor of 1:50 and was grown at 30°C. When OD_{595} reached ~0.2, the culture was aliquoted to a fresh clear-

bottom 96-well deep well plate (Thermo Fisher Scientific) at 500 μL per well. Cerulenin of final concentration ranging from 0 μM to 20 μM was added at this point. The plate was cultivated at 30°C for a further 24 h. OD_{595} and fluorescence (E_x 589 nm, E_m 604 nm) were measured using MultiSkan™ FC Microplate Photometer (Thermo Fisher Scientific) and Fluoroskan Ascent™ Microplate Fluorometer (Thermo Fisher Scientific), respectively, after 12 h, 18 h and 24 h of cultivation in 96-well microtitre plate. Relative fluorescence unit (RFU) was calculated by normalizing fluorescence value with the fluorescence value of *R. eutropha* H16 carrying no plasmid. RFU/OD_{595} value was then calculated as the ratio of RFU and OD_{595} values. All experiments were done in triplicate.

4.4.6 Fold repression, fold induction and induction efficiency

Fold repression, fold induction and induction efficiency were calculated using the formulae below:

$$Fold\ repression = \frac{\left(\frac{RFU}{OD_{595}}\right)_{control\ A}}{\left(\frac{RFU}{OD_{595}}\right)_{biosensor}}$$

$$Fold\ induction = \frac{\left(\frac{RFU}{OD_{595}}\right)_{biosensor\ at\ [cerulenin]=\ x\ \mu M}}{\left(\frac{RFU}{OD_{595}}\right)_{biosensor\ at\ [cerulenin]=\ 0\ \mu M}}$$

$$Induction\ efficiency = \frac{Maximal\ fold\ induction}{Fold\ repression} \times 100\%$$

4.5 SUPPLEMENTARY INFORMATION

4.5.1 Methods and Material

4.5.1.1 FapR

The gene sequence encoding *Bacillus subtilis* FapR (NCBI reference sequence WP_003232044.1) was codon optimized for expression in *Ralstonia eutropha* H16. The sequence containing P_{phaC1} and *fapR* gene was synthesized by GenScript. The optimized *fapR* sequence is provided below:

```
atgcgccgcaacaagcgcgaacgccaggagctcctccagcagacgatccaggccacccc
gttcatcacggacgaagaactggcgggcaagttcggcgtgtcgatccagaccatccgcc
tggaccgcctggagctgagcatcccggagctgcgcgagcgcatcaagaacgtggccgag
aagaccctggaggacgaggtgaagtcgctgagcctggacgaggtgatcggcgagatcat
cgacctggagctggacgaccaggccatctcgatcctggagatcaagcaggagcacgtgt
tcagccgcaaccagatcgcacgcggccaccacctgttcgcccaggcgaactcgctggcg
gtggccgtgatcgacgacgagctggccctgaccgccagcgcggacatccgcttcacccg
ccaggtgaagcagggcgagcgcgtggtggccaaggccaaggtgaccgcggtggagaagg
agaagggccgcaccgtggtggaagtgaactcgtacgtgggcgaggaaatcgtgttctcg
ggccgcttcgacatgtaccgcagcaagcatagc
```

4.5.1.2 Construction of pBBR1c-P2-RFP

All pBBR1c-P2-RFP plasmids were derived from pBBR1c-RFP. To construct pBBR1c-P_{rrsC}-RFP, DNA fragment containing the L-arabinose-inducible promoter system (P_{BAD} and *araC*) was first excised from pBBR1c-RFP using restriction enzymes PstI and NdeI. This fragment was subsequently replaced by a fragment containing P_{rrsC} promoter. To construct pBBR1c-$P_{j5[A1C1C2]}$-RFP, DNA fragment containing the L-arabinose-inducible promoter system (P_{BAD} and *araC*) and *rfp* gene was first excised from pBBR1c-RFP using restriction enzymes PstI and XhoI. This fragment was subsequently replaced by a fragment containing $P_{j5[A1C1C2]}$ promoter and *rfp* gene. pBBR1c-$P_{rrsC[D6]}$-RFP and pBBR1c-$P_{rrsC[D4]}$-RFP were created from pBBR1c-P_{rrsC}-RFP using the recommended NEBaseChanger protocol. Similarly, pBBR1c-$P_{j5[A1D6aC1C2]}$-RFP and pBBR1c-$P_{j5[A1D6bC1C2]}$-RFP were created from pBBR1c-$P_{j5[A1C1C2]}$-RFP using the same protocol.

4.5.1.3 Construction of pBBR1c-P1-FapR-P2-RFP

P_{phaC1}-*fapR* or $P_{phaC1[A1]}$-*fapR* was amplified and digested with restriction enzymes Bsu36I and PstI. The fragment was subsequently ligated to pBBR1c-P2-RFP plasmid that was pre-digested with the same restriction enzymes set to generate pBBR1c-P1-FapR-P2-RFP (*i.e.*, the sensor).

4.5.1.4 Effect of cerulenin on cell growth

Five mL NB was inoculated with an overnight culture at a dilution factor of 1:50 and grown at 30°C. When OD_{595} reached 0.2–0.3, the culture was aliquoted to a 96-well deep well plate and cerelenin of final concentration from 0 to 20 μM was added to give a total volume of 500 μL per well. The plate was cultivated at 30°C for additional 12 h. Each experiment was done in triplicate.

Figure S4.2: Effect of cerulenin on the growth of *Ralstonia eutropha* H16

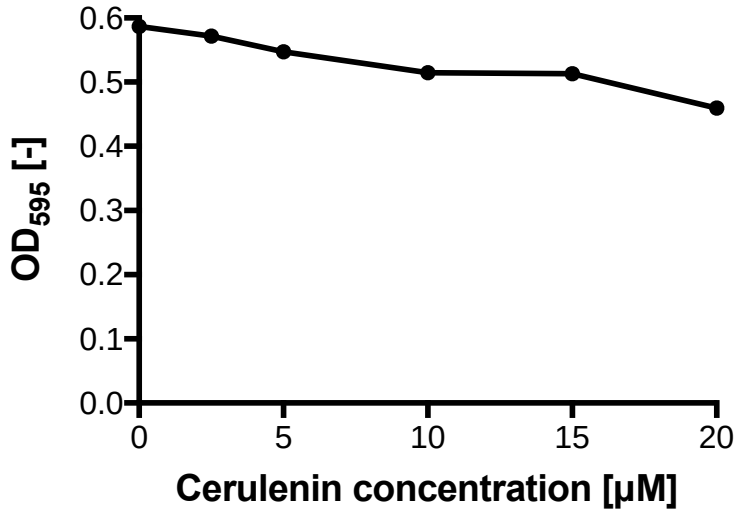

Figure S4.3: Comparison of reporter activities from biosensor (FapR, *fapO*), control A (ΔFapR, *fapO*) and control B (FapR, Δ*fapO*) of each design, measured after 12 h (black), 18 h (light grey) and 24 h (dark grey) of cultivation in 96-well deep well plate.

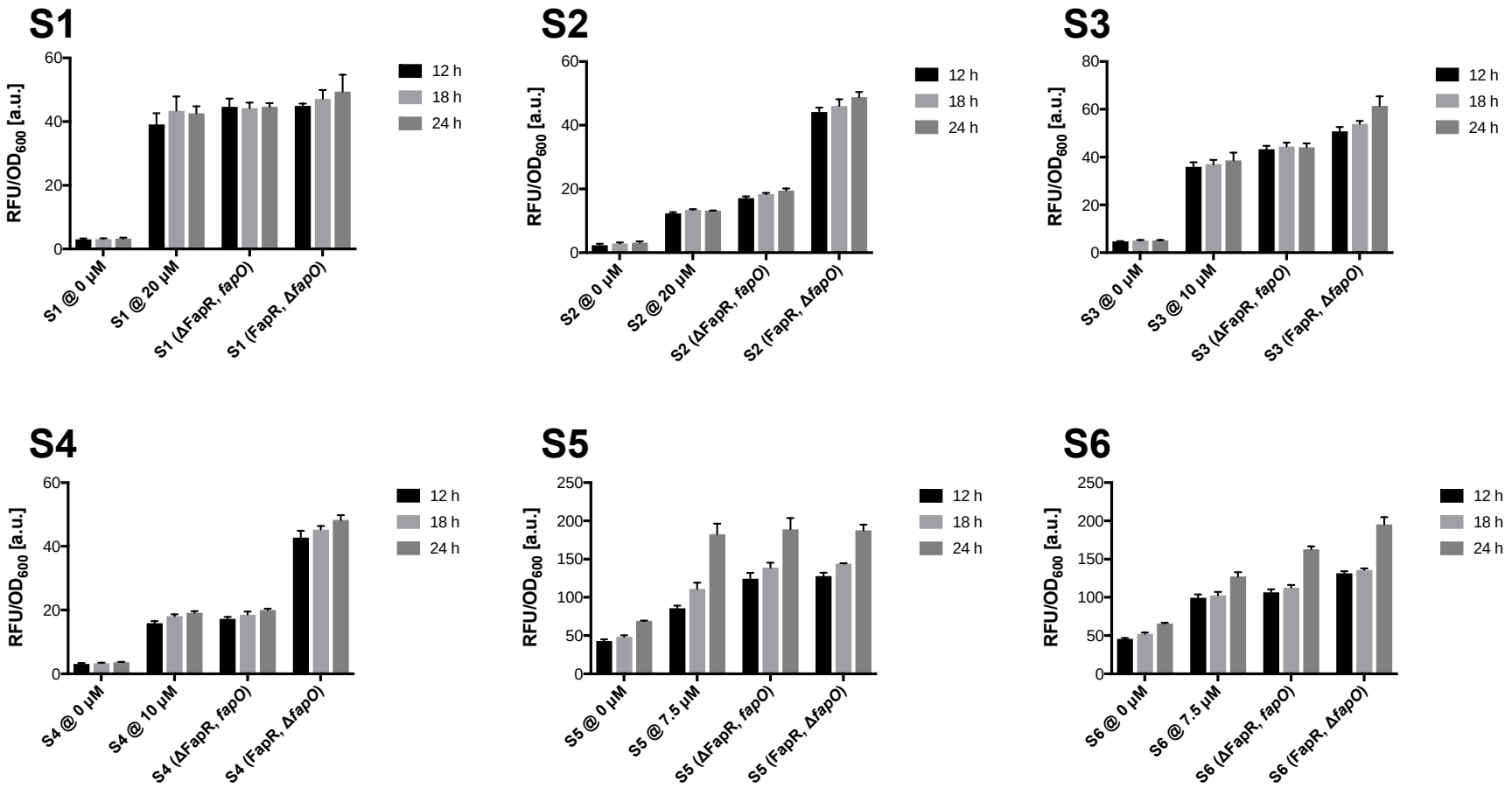

Table S4.1: Fitting of data in Figure S4.4 to a dose-response curve with variable slope (4-parameter)

12 h

	S1	**S2**	**S3**	**S4**	**S5**	**S6**
Bottom	2.77	2.337	4.797	3.132	43.11	45.72
Hillslope	2.111	1.854	2.79	3.658	3.55	3.1
Top	38.31	12.88	36.18	15.54	84.71	97.86
EC_{50}	4.4	4.966	3.112	2.652	1.705	1.735
Span	35.54	10.55	31.38	12.41	41.6	52.15
R^2	0.9881	0.9977	0.9984	0.9958	0.9928	0.9965

18 h

	S1	**S2**	**S3**	**S4**	**S5**	**S6**
Bottom	3.086	2.818	5.163	3.223	48.48	52.28
Hillslope	2.409	1.964	2.681	3.097	2.515	2.296
Top	44.25	13.82	36.72	18.33	111.8	102.8
EC_{50}	4.646	4.774	3.13	2.617	2.136	1.901
Span	41.17	11.01	31.55	15.1	63.33	50.55
R^2	0.9997	0.9981	0.9954	0.9995	0.998	0.9936

24 h

	S1	**S2**	**S3**	**S4**	**S5**	**S6**
Bottom	3.455	3.107	5.248	3.724	74.64	66.11
Hillslope	2.749	2.043	2.605	3.835	4.098	2.404
Top	43.11	13.4	38.14	19.33	178.7	124.4
EC_{50}	4.483	4.455	3.105	2.499	2.663	1.514
Span	39.65	10.29	32.89	15.61	104.1	58.25
R^2	0.9979	0.9965	0.9935	0.9998	0.9841	0.9748

Table S4.2: Induction efficiencies of all 6 biosensors

Biosensors	Induction efficiency [%]
S1	96
S2	74
S3	84
S4	99
S5	85
S6	90

CHAPTER FIVE

5 DEVELOPING A λ-RED RECOMBINEERING METHOD OF GENOME EDITING IN R. EUTROPHA H16 (PART I)

5.1 INTRODUCTION

The absence of fast, efficient and reliable singleplex genome engineering techniques limits the metabolic engineering strategies to further enhance the chemical biomanufacturing applications of *R. eutropha* H16. The work presented here explores a promising genome engineering technique, λ-Red recombineering, and its potentials and immediate applications for facilitating metabolic engineering in *Ralstonia eutropha*. To validate the effectiveness of the broad host range plasmids pBBR1c-RED1, pBBR1c-RED2 and pBBR1k-RED, we used them to mediate non-lethal deletion of the *zwf* gene which encodes the glucose-6-phosphate dehydrogenase protein in *E. coli* BW25113 (NCBI reference sequence (WP_000301727.1). The *zwf* gene (1476 bp) spans position 1929096 and 1930571 of the genome of *E. coli* BW25113. This was achieved using kanamycin or chloramphenicol resistance dsDNA cassettes as the gene targeting selectable markers. Successful integration was confirmed via colony PCR of the ensuing mutant strains. The phenotype of identified mutant was verified by examining their resistance to the antibiotics corresponding to the antibiotics resistance markers used in design of corresponding dsDNA cassettes.

5.2 METHOD

5.2.1 Linear dsDNA cassettes

The linear dsDNA cassettes *zwf*-kanR-*zwf* and *zwf*-camR-*zwf* carrying kanamycin and chloramphenicol resistance genes, respectively were designed to target the *zwf* gene encoding the glucose-6-phosphate dehydrogenase protein in *E. coli* BW25113. The kanR dsDNA cassette contained the neokan promoter (P_{neokan}) and the kanR gene whilst the camR dsDNA cassette contained the chloramphenicol acetyl transferase (cat) promoter (P_{cat}) and camR gene. PCR products of linear dsDNA cassette were incubated with 1 µl *Dpn*I to remove plasmid template where there were no PCR side products. In the presence of PCR side products, the intended PCR products were gel extracted.

Table 5.1: Description of dsDNA cassettes for λ-Red recombineering in *E. coli* BW25113

dsDNA cassette	Antibiotics resistance marker	Template for antibiotics resistance marker	Length of cassette (bp)	Length of each homology arm (bp)	Targeted gene
zwf-kanR-*zwf*	kanR	pBbA8K-RFP	1031	50	*zwf*
zwf-camR-*zwf*	camR	pBBR1MCS1	836	50	*zwf*

Table 5.2: Primers used in thus study

dsDNA Cassette	Primer name	Sequence
1.031 kb *zwf*-kanR-*zwf*	*zwf*-kanR-*for*	5′-**GCGCAAGATCATGTTACCGGTAAAATAACCATAAAGGATAAGCGCAGATA**TCAGAAGAACTCGTCAAGAAGGCG-3′
	zwf-kanR-*rev*	5′-**CAAGTATACCCTGGCTTAAGTACCGGGTTAGTTAACTTAAGGAGAATGA**CGGAATTGCCAGCTGGGGC-3′
0.836 kb *zwf-camR-zwf*	*zwf*-camR-*for*	5′-**GCGCAAGATCATGTTACCGGTAAAATAACCATAAAGGATAAGCGCAGATA**AAACTGTTGTAATTCATTAAGCATTCTGC-3′
	zwf-camR-*rev*	5′-**CAAGTATACCCTGGCTTAAGTACCGGGTTAGTTAACTTAAGGAGAATGAC**TGATCGGCACGTAAGAGGTTCC-3′
1331 bp UP*zwf*-kanR-DOWN*zwf* OR 1136 bp UP*zwf*-camR-DOWN*zwf* OR 1876 bp U*Pzwf-zwf*-DOWN*zwf*	UP*zwf-for*	5′-GATTCACAACGCGTTTCATTCAG-3′
	DOWN*zwf-rev*	5′-TCAGTGTCAGATTTTTACCCAATG-3′
-	camR-*for*	5′-AGACGGTGAGCTGGTGATATGG-3′
	camR-*rev*	5′-AGGCGGGCAAGAATGTGAATAAAG-3′

**Nucleotides in bold represent 50 bp homology arm*

5.2.1.1 *zwf*-kanR-*zwf*

A 1.031 kb *zwf*-kanR-*zwf* amplicon was amplified using pBbA8k-RFP plasmid template as a source of the P_{neokan}-kanR gene. Forward primer: zwf-kanR-for and reverse primer: zwf-kanR-rev possessed 50 nucleotide sequences at their 5'-ends corresponding to the 5'-upstream and 5'-downstream sequences flanking the *zwf* gene in *E. coli* BW25113, respectively.

Table 5.3: PCR protocol for *zwf*-kanR-*zwf*

PCR Mixture components	Volume (μL)	Final concentration
Nuclease free water	37	
10X *pfu* turbo buffer	5	1X
dNTP (10 mM)	2	0.2 mM
zwf-kanR-*for* (20 mM)	1.5	0.5 μM
zwf-kanR-*rev* (20 mM)	1.5	0.5 μM
pBbA8K-RFP	1	variable
Pfu turbo polymerase (2.5 U/μL)	2	2.5U/ 50μL

Table 5.4: PCR programme for *zwf*-kanR-*zwf*

Step	Temperature	Time
Initial denaturation	95°C	2 minutes
30X	95°C 65°C (Anneal) 72°C (Extend)	30 s 30 s 1min/kb *i.e.* 58 s
Final Extension	72°C	10 minutes
Hold	8°C	-

5.2.1.2 *zwf*-camR-*zwf*

A 0.836 kb zwf-*camR*-*zwf* amplicon was amplified using pBBR1MCS-1 plasmid template as a source of the P_{cat}-camR cassette. Forward primer: *zwf*-camR-*for* and reverse primer *zwf*-camR-*rev* possessed 50 nucleotide sequences at their 5'-ends corresponding to the 5'-upstream and 5'-downstream sequences flanking the *zwf* gene in *E. coli* BW25113, respectively.

Table 5.5: PCR protocol for *zwf*-camR-*zwf*

PCR Mixture components	Volume (μL)	Final concentration
Nuclease free Water	35.7	
5X Q5 HF Buffer	10	1X
dNTPs (10 mM)	1	0.2 mM
zwf-camR-for (20 μM)	1.25	0.5 μM
zwf-camR-rev (20 μM)	1.25	0.5 μM
pBBR1MCS1	0.3	Variable
Q5 Polymerase (2 U/μL)	0.5	1 U/50 μL PCR

Table 5.6: PCR programme for *zwf*-camR-*zwf*

Step	Temperature	Time
Initial denaturation	98°C	30 s
30X	98°C 55°C (Anneal) 72°C (Extend)	8 s 30 s 30 s/kb *i.e* 30 s
Final Extension	72°C	10 minutes
Hold	8°C	

5.2.2 λ-Red Recombination protocol

λ-Red-mediated gene inactivation in *E. coli* BW25113 was performed according the protocol by Datsenko and Wanner (2000), with few modifications. Transformation of the λ-Red plasmids was carried out according to the protocol previously discussed (Chapter 3). Overnight cultures of *E. coli* BW25113 λ-Red plasmid transformant strain were inoculated in fresh 2YT media in 5 mL falcon tubes supplemented with antibiotics corresponding to the selection marker on each λ-Red plasmid type. Protein expression cultures of each strain were prepared as previously described (Chapter 3). The test cultures for λ-Red recombination were also supplemented with 0.4 % L-arabinose solution at the start of cultivation, while the control cultures were not. Cultures were cultivated to OD_{600} ~0.6 and pretreated for electroporation according to protocol detailed in Chapter 3. Samples were then transformed via electroporation with appropriate linear dsDNA cassette according to previously detailed protocol.

Outgrowth culture of BW25113 transformed with pKD20 and pKD46 were cultivated at 30°C to allow for sufficient expression of the λ-Red proteins, and recombination event. 300 μL of cells were plated on appropriate TYE agar plates supplemented with antibiotics according to the selectable maker present in the linear dsDNA antibiotics resistance cassette.

For selection of mutant cells possessing the kanR gene, TYE agar plates supplemented to 50 mg/L kanamycin were used. For selection of mutant cells possessing the camR gene, TYE agar plates supplemented to 25 mg/L were used.

Table 5.7: Strains used in this study

Strain	Description	Reference
BWD20	*E. coli* BW25113 with pKD20	Chapter 3
BWD46	*E. coli* BW25113 with pKD46	Chapter 3
BWRed1	*E. coli* BW25113 with pBBR1c-RED1	Chapter 3
BWRed2c	*E. coli* BW25113 with pBBR1c-RED2	Chapter 3
BWRed2k	*E. coli* BW25113 with pBBR1k-RED2	Chapter 3
BWD20K	Kanamycin resistant *E. coli* BW25113 with pKD20 and a genome integrated kanR gene, Δ*zwf*	This study
BWRed1K	Kanamycin resistant *E. coli* BW25113 with pBBR1c-RED1 and a genome integrated kanR gene, Δ*zwf*	This study
BWRed2cK	Kanamycin resistant *E. coli* BW25113 with pBBR1c-RED2, Δ*zwf*	This study
BWRed2kC	Chloramphenicol resistant *E. coli* BW25113 with pBBR1k-RED2, Δ*zwf*	This study

5.2.3 Verification of genomic integration of linear dsDNA cassette

The number of colonies of *E. coli* BW25113 observed on test agar plates were counted and compared to number of colonies observed on control plates from samples without induction of protein expression. A colony count ratio of >10:1 between test plates and control plate was set as an arbitrary standard for preliminary confirmation of successful genomic integration. Transformant colonies of *E. coli* BW25113 after the gene inactivation experiment were re-streaked on TYE agar plates supplemented with appropriate antibiotics according to selectable maker in the linear dsDNA cassette. Re-streaked agar plates were incubated overnight at 37°C. Emerging colonies regrown on new TYE agar plates indicated that the colonies observed were due to genomic integration of dsDNA linear cassette. Further verification of these colonies was performed via colony PCR with the primers used to design the linear dsDNA cassette. Colony PCR was performed with *OneTaq* or *Taq* polymerase by New England Biolabs,

and used according to the manufacturer's instructions. Different primers pairs were used to confirm genomic integration, (Figure 5.1).

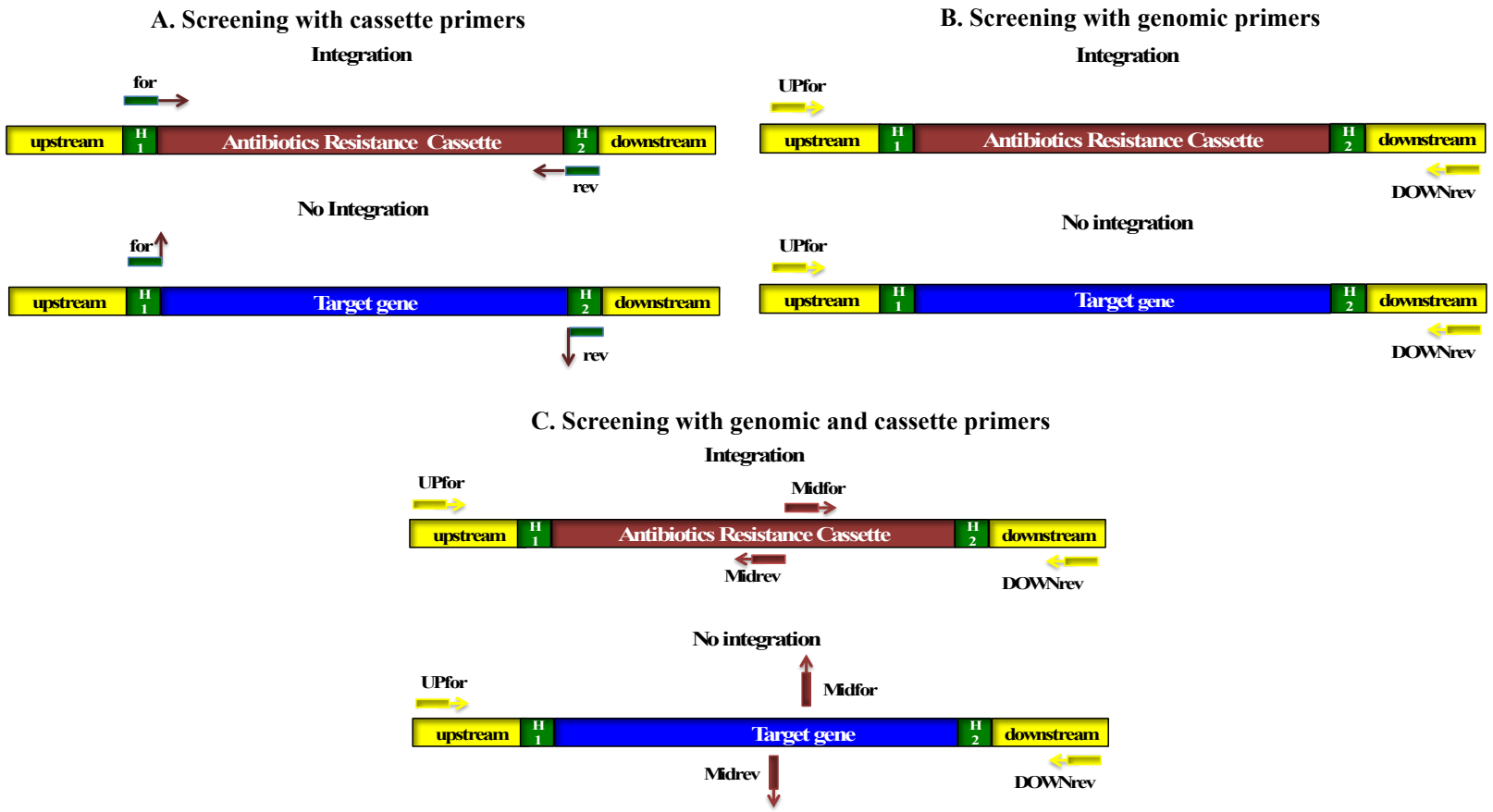

Figure 5.1: Methods of screening for successful genomic integration of antibiotics resistance marker.
(A) Primers used in constructing the cassette will yield corresponding PCR amplicon of the cassette in mutant strains and will not yield PCR amplicon in wild type strains. (B) Primers targeting genomic regions upstream and downstream to the target gene will yield PCR amplicon of the cassette flanked by upstream and downstream genomic regions in mutant strains and will yield PCR amplicons corresponding to the target gene flanked by the upstream and downstream genomic regions in wild type strains. (C) Primers targeting genomic region upstream or downstream of the target gene and the centre of the cassette will yield corresponding PCR amplicon in mutant strains but will not yield corresponding PCR amplicon in wild type strains.

5.2.3.1 Colony PCR verification

Colonies were picked from each TYE agar plates P200 pipette tip under sterile conditions. The colonies on the tips were swirled vigorously in 30 μL of nuclease free water in 200 μL tubes. The liquid colony suspension were used as DNA template for colony PCR using *OneTaq* polymerase from NEB Biolabs as follows:

Table 5.8: Colony PCR protocol with cassette primers

Colony PCR mixture component	**Volume [μL]**	**Final concentration**
Nuclease free water	36	-
5X Standard *OneTaq* Reaction Buffer	10	1X
10 mM dNTPs	1	0.2 mM
20 μM *zwf*-kanR-*for*/ *zwf*-camR-*for*	0.75	300 nM
20 μM *zwf*-kanR-*rev*/ *zwf*-camR-*rev*	0.75	300 nM
Colony suspension	1	-
OneTaq DNA polymerase (5 U/μL)	0.5	2.5 units/50 μL PCR mix

Table 5.9: Colony PCR programme with cassette primers

Step	**Temperature [°C]**	**Time**
Initial denaturation	94	5 mins
30 cycles	94 55 68	30 secs 45 secs 1 minutes/kb *i.e.* 1 minute 20 secs
Final extension	68	5 minutes
Hold	8	-

Table 5.10: Colony PCR protocol with upstream-downstream Primers

Colony PCR mixture component	**Volume [μL]**	**Final concentration**
Nuclease free water	37.25	-
5X Standard *OneTaq* Reaction Buffer	10	1X
10 mM dNTPs	0.5	0.2 mM
20 μM UP*zwf*-for	0.5	200 nM
20 μM DOWN*zwf*-rev	0.5	200 nM
Colony suspension	1	-
OneTaq DNA polymerase (5 U/μL)	0.25	1.25 units/50 μL PCR mix

Table 5.11: Colony PCR programme with upstream-downstream Primers

Step	Temperature [°C]	Time
Initial denaturation	94	5 mins
30 cycles	94 49 68	30 secs 30 secs 1 minutes/kb *i.e.* 1 minute 20 secs
Final extension	68	5 minutes
Hold	8	-

Table 5.12: Colony PCR protocol with upstream-midstream and midstream-downstream Primers (for checking *zwf*-kanR-*zwf* integration)

Colony PCR mixture component	**Volume [μL]**	**Final concentration**
Nuclease free water	37.25	-
5X Standard *OneTaq* Reaction Buffer	10	1X
10 mM dNTPs	0.5	0.2 mM
20 μM UPzwf-for/ zwf-kanR-for	0.5	200 nM
20 μM zwf-kanR-rev/DOWNzwf-rev	0.5	200 nM
Colony suspension	1	-
OneTaq DNA polymerase (5 U/μL)	0.25	1.25 units/50 μL PCR mix

Table 5.13: Colony PCR Programme for 1181 bp UP*zwf*-kanR amplicon using primers UP*zwf*-for and *zwf*-kanR-rev

Step	Temperature [°C]	Time
Initial denaturation	94	5 mins
30 cycles	94 51 68	30 secs 30 secs 1 minutes/kb *i.e.* 1 min 15 seconds
Final extension	68	5 minutes
Hold	8	-

Table 5.14: PCR Programme for 1181 bp kanR-DOWN*zwf* amplicon using primers *zwf*-kanR-for and DOWN*zwf*-rev

Step	Temperature [°C]	Time
Initial denaturation	94	5 mins
30 cycles	94 49 68	30 secs 30 secs 1 minutes/kb *i.e.* 1 minute 15 seconds
Final extension	68	5 minutes
Hold	8	-

Table 5.15: Colony PCR protocol with upstream-midstream and midstream-downstream primers (for checking zwf-camR-zwf integration)

Colony PCR mixture component	**Volume [μL]**	**Final concentration**
Nuclease free water	37.25	-
5X Standard *OneTaq* Reaction Buffer	10	1X
10 mM dNTPs	0.5	0.2 mM
20 μM UP*zwf*-for/ camR-for	0.5	200 nM
20 μM camR-rev/ DOWN*zwf*-rev	0.5	200 nM
Colony suspension	1	-
OneTaq DNA polymerase (5 U/μL)	0.25	1.25 units/50 μL PCR mix

Table 5.16: Colony PCR programme for 600 bp *zwf*-camR amplicon using upstream-midstream primers: UP*zwf*-for and camR-rev

Step	Temperature [°C]	Time
Initial denaturation	94	5 mins
30 cycles	94 51 68	30 secs 30 secs 1 minutes/kb *i.e*. 40 seconds
Final extension	68	5 minutes
Hold	8	-

Table 5.17: Colony PCR programme for 500 bp *zwf*-camR amplicon using upstream-midstream primers: UP*zwf*-for and camR-rev

Step	Temperature [°C]	Time
Initial denaturation	94	5 mins
30 cycles	94 49 68	30 secs 30 secs 1 minutes/kb *i.e*. 30 seconds
Final extension	68	5 minutes
Hold	8	-

5.2.4 λ-Red Recombineering in *E. coli* BW25113 with pKD20

First, the gene inactivation protocol was tested in *E. coli* BW25113 using pKD20 to establish a proof of principle of the protocol. ~300 ng of *zwf*-kanR-*zwf* PCR product or ~180 ng of gel extracted *zwf*-kanR-*zwf* PCR product was transformed into pKD20-transformed *E. coli* BW25113 cultures. All transformation cultures were induced except for the control, which was transformed with 300 ng of PCR product *zwf*-kanR-*zwf* but not induced. All outgrowth cultures were cultivated overnight at 30°C. The experiment was set up in duplicate such that one set of plates were incubated at 30°C and the other at 37°C to observe if curing the plasmid during overnight incubation compromised recombination event and hence genomic integration of the dsDNA cassette.

5.2.5 λ-Red Recombineering in *E. coli* BW25113 with pKD20 and pBBR1c-RED1

Next, to verify the functionality of the pBBR1c-RED1 vector, the same protocol was adapted for gene inactivation in *E. coli* BW25113 by separately using the pKD20 and pBBR1c-RED1 vectors with the ~180 ng of gel extracted *zwf*-kanR-*zwf* cassette. Each plasmid type has a control culture, which was un-induced for protein expression but transformed with the same quantity of *zwf*-kanR-*zwf* cassette as the induced culture. All outgrowth cultures were cultivated for 2 hours. Transformed samples of BWD20 were incubated at 30°C while transformed samples of BWRed1 were incubated at 37°C. A number of colonies observed from on the agar plates from the test cultures were re-streaked on new selection TYE agar plates with 50 mg/L kanamycin. Re-grown colonies on these plates for use for colony PCR verification of the successful recombination.

5.2.6 λ-Red Recombineering in *E. coli* BW25113 with pBBR1c-RED1, pBBR1c-RED2, pBBR1k-RED

The λ-Red recombineering was performed using the pBBR1c-RED1, pBBR1k-RED, pBBR1c-RED2 vectors for gene inactivation in *E. coli* BW25113. ~300 ng of *zwf*-kanR-*zwf* was transformed into BWRed1 and BWRed2c, while ~300 ng of *zwf*-camR-*zwf* was transformed into BWRed2k. To screen for successful insertion of the antibiotics resistance gene in both instances, primers that would amplify genomic regions further upstream and downstream of the insertion loci (Upstream-Downstream Primers) were applied. In this

instance, successful genomic integration was confirmed by size of the ensuing amplicon, which could either include the target gene (in the event of unsuccessful insertion or the antibiotics resistance marker (in the event of successful insertion). Subsequently, upstream-midstream and midstream-downstream were further applied to further confirm successful genomic integration event(s).

5.3 RESULTS AND DISCUSSION

5.3.1 λ-Red recombineering with pKD20

Test samples of BWD20 induced for expression of the λ-Red proteins and transformed with the *zwf*-kanR-*zwf* cassette all produced at least 100 kanamycin resistant colonies when plated on TYE agar plate with 50 mg/L kanamycin. This suggested that the recombination event between the dsDNA cassette and the genomic region the *zwf* gene was successful. The control culture transformed with PCR purified linear dsDNA but was not induced, had only 2 colonies, (Table 6.17). The colonies on the control plate could have been due to kanamycin resistance conferred by presence of residual pBbA8k-RFP plasmid template, which escaped *DpnI* digestion in the *zwf*-kanR-*zwf* PCR product.

Table 5.18: Colony count λ-Red recombineering with pKD20 at different conditions

Induction	***zwf*-kanR-*zwf***	**Incubation Temperature [°C]**	**Colony count**
+	PCR, 300 ng	30	924
+	PCR, 300 ng	37	685
+	Gel extracted, 180 ng	30	486
+	Gel extracted, 180 ng	37	151
-	PCR, 300 ng	30	2

The colony count ratio from induced to un-induced cultures was > 10:1 - confirming that an appreciable number of colonies observed from the test cultures were indeed Δ*zwf* mutant colonies. It is important to note that previous protocol on λ-Red recombineering using dsDNA with antibiotics selection markers suggest lower concentration of antibiotics (20 mg/L for kanamycin) for selecting for recombinant cells. However, using this concentration in preliminary experiments produced lots of *E. coli* BW25113 colonies from the controls samples thus leading to lower colony count ratio of <10:1 (data not shown). As this made screening for actual recombinants difficult, the antibiotics selection was increased to 50 mg/L for kanamycin.

More colonies were observed at 30°C incubation where the pKD20 plasmid was not cured than at 37°C under plasmid curing conditions, Table 6.18. This suggested that extending the expression of the λ-Red proteins by keeping the plasmid uncured during incubation had a positive effect on recombination efficiency. Overall, at both incubation temperatures,

cultures transformed with the PCR product (300 ng) had more colonies than cultures transformed with the gel-extracted product (180 ng), of course owing to higher DNA mass from the former.

5.3.2 λ-Red recombineering in *E. coli* BW25113 with pKD20 and pBBR1c-RED1

Proof of principle of λ-Red recombineering in *E. coli* BW25113 was used to test the pBBR1c-RED1 construct for its recombineering functionality. pBBR1c-RED1 elicited similar results as pKD20 in mediating the knockout of the *zwf* gene in *E. coli* BW25113. From this experimental set-up, the complete absence of colonies from all controls was a good indicator that the colonies obtained from induced samples of BWD20 and BWRed1 were largely deletion strains with the *zwf* gene replaced with a kanR gene. The ~ 1 kb band from colony PCR screening of three colonies per test plate with cassette-specific primers *zwf*-kanR-for and *zwf*-kanR-rev further confirmed genomic integration of the kanR cassette, (Figure 6.2). Additionally, whilst BWD20 produced 75 Δ*zwf* colonies, BWRed1 produced 80 Δ*zwf* colonies, suggesting that the pBBR1c-RED1 plasmid is only marginally more efficient in mediating λ-Red recombineering than pKD20. This further suggests that the more marked expression of the λ-Red proteins observed from BWRed1 compared to BWD20 (Chapter 3) does not create a marked difference in recombination efficiency between pKD20 and pBBR1-RED1. It also supports the position that marked expression (as observed by SDS-PAGE analysis) may not be absolutely definite in comparatively evaluating the performance of pKD20.

Table 5.19: Colony count from λ-Red recombineering with pKD20 and pBBR1c-RED1

Induction	Original strain	Plasmid	Final strain	Colony count
-	BWD20	pKD20	BWD20	0
-	BWRed1	pBBR1c-RED1	BWRed1	0
+	BWD20	pKD20	BWD20K	75
+	BWRed1	pBBR1c-RED1	BWRed1K	80

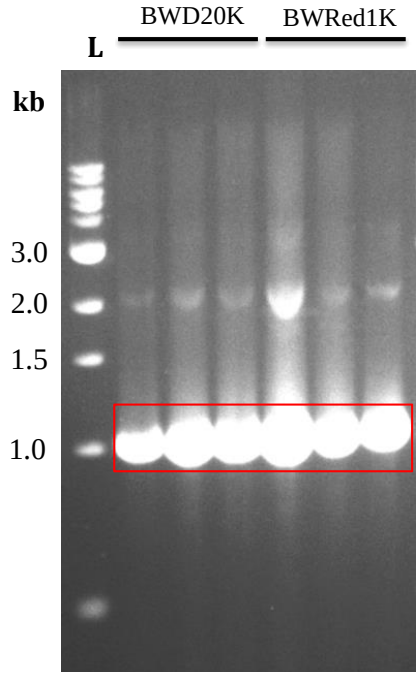

Figure 5.2: Agarose gel electrophoresis image from colony PCR with cassette-specific primers to identify Δ*zwf* BWD20K and BWRed1K strains of *E. coli* BW25113 after λ-Red recombineering.
The ~1.0 kb band from the pKD20/*zwf*-kanR-*zwf* and pBBR1c-RED1/*zwf*-kanR-*zwf* colonies are the *zwf*-kanR-*zwf* amplicon from the genome of selected colonies indicating that all colonies are Δ*zwf* BWD20K and BWRed1K strain, respectively. L – 1 kb DNA ladder.

5.3.3 λ-Red Recombineering in *E. coli* BW25113 with pBBR1c-RED1, pBBR1c-RED2, and pBBR1k-RED

The λ-Red protocol was adapted using the pBBR1c-RED1, pBBR1k-RED, pBBR1c-RED2 vectors for gene inactivation in *E. coli* BW25113. ~300 ng of *zwf*-kanR-*zwf* was separately transformed into BWRed1 and BWRed2c while ~300 ng of *zwf*-camR-*zwf* was transformed into BWRed2k. To screen for successful insertion of the antibiotics resistance gene in both instances, primers that would amplify genomic regions further upstream and downstream of the insertion loci (Upstream-Downstream Primers) were applied. In this instance, successful genomic integration was confirmed by size of the ensuing amplicon, which could either include the target gene (in the event of unsuccessful insertion or the antibiotics resistance marker (in the event of successful insertion). Subsequently, upstream-midstream and midstream-downstream were further applied to further confirm successful genomic integration event(s).

All three plasmid types (pBBR1c-RED1, pBBR1k-RED, pBBR1c-RED2) in combination with appropriate antibiotics resistance cassettes (*zwf*-kanR-*zwf* and *zwf*-camR-*zwf*) effected genomic deletion of the *zwf* gene in *E. coli* BW25113. Strains BWRed1 and BWRed2c with pBBR1c-RED1 and pBBR1c-RED2, respectively produced 1840 and 4000 colonies, respectively on the kanamycin selection plate. Strain BWRed2k with the pBBR1k-RED plasmid produced only 10 colonies. Colony-PCR screening of 5 colonies obtained from BWRed1 and BWRed2c confirmed that all colonies screened were indeed BWRed1K and BWRed2cK mutants as they possessed the screening yielded a ~1.3 kb band indicative of an amplicon from the genomic loci containing the *zwf*-kanR-*zwf* cassette, (Table 6.20, Figure 6.3). On the other hand, of all 4 colonies screened BWRed2k, only one yielded the ~1.1 kb band indicative of an amplicon from the genomic loci containing the *zwf*-camR-*zwf* cassette, (Table 6.20, Figure 6.3). This identified mutant was further confirmed to be a BWRed2kC mutant as screening with the upstream-midstream and midstream-downstream pair of primers produced ~0.6 and ~0.5 kb bands indicative of amplicons of a genomic loci containing part of the *zwf*-camR-*zwf* cassette, (Figure 6.4).

Single colonies of colony-PCR verified Δ*zwf* strains BWRed1K and BWRed2cK were cultivated in 2YT media supplemented with kanamycin (50 mg/L) and chloramphenicol (25 mg/L), respectively. Wild type *E. coli* BW25113 was also cultivated in kanamycin and chloramphenicol media as controls. The Δ*zwf* strains BWRed1cK and BWRed2cK mutants grew to saturation in their respective media after 24 hour of cultivation. However, the wild type *E. coli* BW25113 control did not survive in the kanamycin or chloramphenicol selection pressure in the 2YT media.

pBBR1c-RED2 had a ~2-fold higher recombination efficiency ($3.3*10^{-5}$) relative to pBBR1c-RED1 ($1.5*10^{-5}$). This could be a result of the reportedly higher efficiency of pKD46 (parent plasmid of pBBR1c-RED2) compared to pKD20 (parent plasmid of pBBR1c-RED1), as pKD46 has been previously reported to be more efficient than pKD20 (Datsenko and Wanner, 2000). On the other hand, the significantly lower efficiency of pBBR1k-RED using the camR cassette might be due to unsuitable chloramphenicol selection concentration and/ or insufficient expression of the cat gene from the P_{cat}-camR cassette.

Table 5.20: Colony count from λ-Red recombineering with pBBR1c-RED1, pBBR1c-RED2 and pBBR1k-RED

	Original strain	Linear DNA	Induction	Selection Antibiotics	Colony count	Recombination efficiency	Final strain
1.	BWRed1	*zwf*-kanR-*zwf*	+	50 μg/ml Kan	1840	$1.5*10^{-5}$	BWRed1K
2.	BWRed2k	*zwf*-camR-*zwf*	+	25 μg/ml Cam	10	N/A	BWRed2kC
3.	BWRed2c	*zwf*-kanR-*zwf*	+	50 μg/ml Kan	4000	$3.3*10^{-5}$	BWRed2cK
4.	BWRed1	*zwf*-kanR-*zwf*	-	50 μg/ml Kan	16	N/A	BWRed1
5.	BWRed2k	*zwf*-camR-*zwf*	-	25 μg/ml Cam	0	N/A	BWRed2k
6.	BWRed2c	*zwf*-kanR-*zwf*	-	50 μg/ml Kan	2	N/A	BWRed2c
7.	BWRed2c	*zwf*-kanR-*zwf*	-	25 μg/ml Cam	$1200 *10^{5}$	N/A	BWRed2c

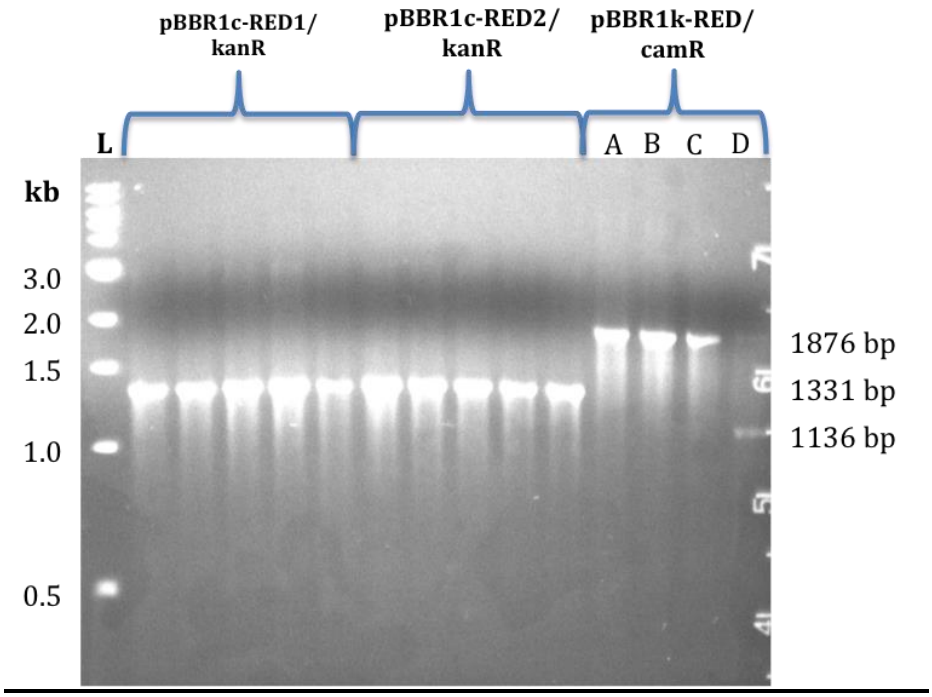

Figure 5.3: Agarose gel electrophoresis from colony PCR screening with upstream-downstream primers to identify Δ*zwf* strains BWRed1K, BWRed2cK and BWRed2kC of *E. coli* BW25113 after λ-Red recombineering.
Colony PCR was performed with primers binding to genomic regions upstream and downstream to the genomic integration site of the antibtiotics resistance cassette. All 5 colonies out of >1000 colonies tested for both BWRed1/*zwf*-kanR-*zwf* and BWRed2c/*zwf*-kanR-*zwf* systems show successful integration, as confirmed by the 1331 bp kanR amplicon. Of all 4 colonies out of 5 colonies tested from the BWRed2k/*zwf*-camR-*zwf* system, only one colony (D) showed gene replacement (1136 bp camR amplicon), while other colonies (A-C) show still possessed the *zwf* gene of *E. coli* BW25113 (1876 bp zwf amplicon). L – 1 kb DNA ladder.

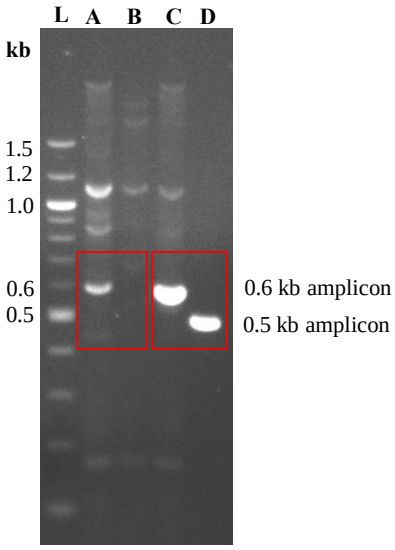

Figure 5.4: Agarose gel electrophoresis of colony PCR screening with upstream-midstream primers to confirm Δ*zwf* strains BWRed2kC *E. coli* BW25113 after λ-Red recombineering. **A** - PCR amplicon of a false positive colony using primers specific to upstream of genomic region and midstream of camR cassette show multiple bands confirming no successful integration. **B** - PCR amplicon of a false positive colony using primers specific to midstream of camR cassette and downstream of genomic region show no band specific to expected PCR amplicon. **C** - PCR amplicon of the identified BWRed2kC mutant colony using primers specific to upstream of genomic region and midstream of camR cassette show a 0.6 kb band confirming successful integration of camR cassette. **D** - PCR amplicon of identified BWRed2kC mutant colony using primers specific to midstream of camR cassette and downstream of genomic region show a 0.5 kb band confirming successful integration of camR cassette successful integration of camR cassette into the genome of BW25113. L -100 bp ladder.

5.4 CONCLUSION

The result herein confirm that the plasmid constructs pBBR1c-RED1, pBBR1c-RED2, and pBBR1k-RED are useful for mediating λ-Red recombineering in *E. coli* BW25113. The observed recombination efficiency, particularly with the pBBR1c-RED1 and pBBR1c-RED2 plasmids strongly suggests that the plasmids should be effective, and thus may be employed as broad host range λ-Red recombineering vectors in other microbial cell factories.

CHAPTER SIX

6 DEVELOPING A λ-RED RECOMBINEERING METHOD OF GENOME EDITING IN R. EUTROPHA H16 (PART II)

6.1 INTRODUCTION

Building on the results obtained from λ-Red recombineering in *E. coli* BW25113, the plasmids pBBR1c-RED1 and pBBR1c-RED2 were tested for mediating λ-Red recombineering in *R. eutropha* H16. The *phaC1* gene encoding the polyhydroxyalkanaote synthase was targeted using a kanamycin resistance (kanR) dsDNA cassette. The 1770 bp *phaC1* gene (H16_A1437) spans the 1557353 and 1559122 nucleotides of chromosome 1 of the genome of *Ralstonia eutropha* H16. Two different kanR genes from pBbA8K-RFP were separately used in designing linear dsDNA cassette for targeting the *phaC1* gene. Successful integration of a kanR resistance marker could not be confirmed, thus suggesting that *Ralstonia eutropha* H16 may not be amenable to λ-Red recombineering.

6.2 METHODS

6.2.1 Linear dsDNA cassettes

Linear dsDNA cassettes carrying the kanR genes from pBbA8k-RFP and pBHR1 designed to target the phaC1 gene. The *phaC1*-nkanR-*phaC1,* 100H.*phaC1*-nkanR-100H.*phaC1,* 1000H.*phaC1*-nkanR-1000H.*phaC1* linear dsDNA cassettes were also designed to target the *phaC1* gene. PCR products of linear dsDNA cassette were incubated with 1 µL *Dpn*I to remove plasmid template where there were no PCR side products. In the presence of PCR side products, the intended PCR products were gel extracted. To improve chances of successful recombination, 5'-phosphorothiolated versions of some of the cassettes were created re-amplying the cassettes with primers with 5'-phosphorothiolated ends (Mosberg et al., 2012).

Table 6.1: Description of dsDNA cassettes for λ-Red recombineering in *R.eutropha* H16

dsDNA cassette	Length of cassette (bp)	Description	Orientation of sense strand of kanR gene
phaC1-nkanR-*phaC1*	1220	A kanR cassette with the kanR from pBHR1 and 50 bp homology arms flanking the *phaC1* gene	Top strand
100H.*phaC1*-nkanR-100H.*phaC1*	1320	A kanR cassette with the kanR from pBHR1 and 100 bp homology arms flanking the *phaC1* gene	Top strand
phaC1-kanR-*phaC1*	1031	A kanR cassette with the kanR from pBbA8k-RFP and 50 bp homology arms flanking the *phaC1* gene	Top strand
phaC1-rckanR-*phaC1*	1031	A kanR cassette with the kanR from pBbA8k-RFP and 50 bp homology arms flanking the *phaC1* gene	Bottom strand
100H.*phaC1*-kanR-100H.*phaC1*	1131	A kanR cassette with the kanR from pBbA8k-RFP and 100 bp homology arms flanking the *phaC1* gene	Top strand
100H.*phaC1-rc*kanR-100H.*phaC1*	1131	A kanR cassette with the kanR from pBbA8k-RFP and 100 bp homology arms flanking the *phaC1* gene	Bottom strand
5'.pT.100H.*phaC1*-kanR-5'.pT. 100H.*phaC1*	1131	A variant of 100H.*phaC1*-kanR-100H.*phaC1* 5'-phosphorothiolated at both ends	Top strand
5'.pT.100H.*phaC1-rc*kanR-5'.pT. 100H.*phaC1*	1131	A variant of 100H.*phaC1-rc*kanR-100H.*phaC1* 5'-phosphorothiolated at both ends	Bottom strand
5'.pT.100H.*phaC1*-kanR-100H.*phaC1*	1131	A variant of 100H.*phaC1*-kanR-100H.*phaC1* 5'-phosphorothiolated at the beginning of the upstream homology arm	Top strand
5'.pT.100H.*phaC1-rc*kanR-100H.*phaC1*	1131	A variant of 100H.*phaC1-rc*kanR-100H.*phaC1* 5'-phosphorothiolated at the beginning of the upstream homology arm	Bottom strand
100H.*phaC1*-kanR-5'.pT.100H.*phaC1*	1131	A variant of 100H.*phaC1*-kanR-100H.*phaC1* 5'-phosphorothiolated at the end of the downstream homology arm	Top strand
100H.*phaC1*-rckanR-5'.pT.100H.*phaC1*	1131	A variant of 100H.*phaC1-rc*kanR-100H.*phaC1* 5'-phosphorothiolated at the end of the downstream homology arm	Bottom strand

Table 6.2: Primers used in this study

PCR product	PCR Template	Primer name	Sequence
1.9 kb NdeI-Gam.Bet.Exo-BamHI	pBBR1c-RED1	*NdeI*-Gam-*for*	5′-GATCCATATGATGGATATTAATACTGAAACTGAGATCAAGCAAAAGC-3′
		BamHI-Exo-*rev*	5′-GATCGGATCCTCATCGCCATTGCTCCCCA-3′
2.2 kb NdeI-Gam.Bet.Exo.λLt - BamHI	pBBR1c-RED2	*NdeI*-Gam-*for*	5′-GATCCATATGATGGATATTAATACTGAAACTGAGATCAAGCAAAAGC-3′
		BamHI-λLt-Exo-*rev*	5′-GATCGGATCCCTACTGGTATTGGCACAAACCTGATT-3′
Segment of *Chr1* containing the *phaC1* gene	*Ralstonia eutropha* H16	*Chr1-for*	5′-CTCGGAATCGCTGACGATTCCCAG-3′
		Chr1-rev	5′-TGGCCCATGATGACTTCGCTCACCTG-3′

Table continues below

PCR product	PCR Template	Primer name	Sequence
1.22 kb *phaC1*-nkanR-*phaC1*	pBHR1	*phaC1*-nkanR-*for*	5′-**GCAATGCCCGGAGCCGGTTCGAATAG TGACGGCAGAGAGACAATCAAATC**TTGTGTCTCAAAATCTCTGATGTTAC ATTGCAC-3′
		phaC1-nkanR-*rev*	5′-**TGCAGGCCTGCCGGCGCCGTGCATGA CGCACGCCGGCACTCATGCAAGCG**GCCACGGTTGATGAGAGCTTTG-3′
1.32 kb 100H.*phaC1*-nkanR-100H.*phaC1*	pBHR1	100H.*phaC1*-nkanR-*for*	5′-**CAAGCCGGGTCCATTCGGATAGCATC TCCCCATGCAAAGTGCCGGCCAGG**GC AATGCCCGGAGCCGGTTCGAATAGTG ACG-3′
		100H.*phaC1*-nkanR-*rev*	5′-**TGACAACGTCAGTCATTGTGTAGTCC TTTCAATGGAAACGGGAGGGAACC**TG CAGGCCTGCCGGCGCCGTG-3′

Table continues below

PCR product	PCR Template	Primer name	Sequence
50H.*phaC1*-kanR-50H.*phaC1*	*zwf*-kanR-*zwf*	50H.phaC1-kanR-*for*	5′-**GCAATGCCCGGAGCCGGTTCGAATAG TGACGGCAGAGAGACAATCAAATC**GG AATTGCCAGCTGG-3′
		50H.phaC1-kanR-*rev*	5′-**TGCAGGCCTGCCGGCGCCGTGCATGA CGCACGCCGGCACTCATGCAAGCG**TC AGAAGAACTCGTCAAGAAGG-3′
phaC1-rckanR-*phaC1*	*zwf*-kanR-*zwf*	50H.phaC1-rckanR-*for*	5′-**GCAATGCCCGGAGCCGGTTCGAATAG TGACGGCAGAGAGACAATCAAATC**TC AGAAGAACTCGTCAAGAAGG-3′
		50H.phaC1-rckanR-*rev*	5′-**TGCAGGCCTGCCGGCGCCGTGCATGA CGCACGCCGGCACTCATGCAAGCG**GG AATTGCCAGCTGG-3′

Table continues below

PCR product	PCR Template	Primer name	Sequence
100H.*phaC1*-kanR-100H.*phaC1*	50H.*phaC1*-kanR-50H.*phaC1*	100H.*phaC1*-nkanR-*for*	5′-**CAAGCCGGGTCCATTCGGATAGCATCTCCCCATGCAAAGTGCCGGCCAGG**GCAATGCCCGGAGCCGGTTCGAATAGTGACG-3′
		100H.*phaC1*-nkanR-*rev*	5′-**TGACAACGTCAGTCATTGTGTAGTCCTTTCAATGGAAACGGGAGGGAACC**TGCAGGCCTGCCGGCGCCGTG-3′
100H.*phaC1-rc*kanR-100H.*phaC1*	50H.*phaC1-rc*kanR-50H.*phaC1*	100H.*phaC1*-nkanR-*for*	5′-**CAAGCCGGGTCCATTCGGATAGCATCTCCCCATGCAAAGTGCCGGCCAGG**GCAATGCCCGGAGCCGGTTCGAATAGTGACG-3′
		100H.*phaC1*-nkanR-*rev*	5′-**TGACAACGTCAGTCATTGTGTAGTCCTTTCAATGGAAACGGGAGGGAACC**TGCAGGCCTGCCGGCGCCGTG-3′
5'.pT.100H.*phaC1*-kanR-5'.pT.100H.*phaC1*	100H.*phaC1*-kanR-100H.*phaC1*	5'.pT.u.phaC1-nkanR-*for*	5′PTO-caagccgggtccattc-3′
		5'.pT.u.phaC1-nkanR-*rev*	5′PTO-tgacaacgtcagtcattg-3′

Table continues below

PCR product	PCR Template	Primer name	Sequence
5'.pT.100H.*phaC1*-*rc*kanR-5'.pT.100H.*phaC1*	100H.*phaC1*-kanR-100H.*phaC1*	5'.pT.u.phaC1-nkanR-*for*	5′PTO-caagccgggtccattc-3′
		5'.pT.u.phaC1-nkanR-*rev*	5′PTO-tgacaacgtcagtcattg-3′
5'.pT.100H.*phaC1*-kanR-100H.*phaC1*	100H.*phaC1*-kanR-100H.*phaC1*	5'.pT.u.phaC1-nkanR-*for*	5′PTO-caagccgggtccattc-3′
		100H.*phaC1*-nkanR-*rev*	5′-tgacaacgtcagtcattg-3′
5'.pT.100H.*phaC1*-*rc*kanR-100H.*phaC1*	100H.*phaC1*-kanR-100H.*phaC1*	5'.pT.u.phaC1-nkanR-*for*	5′PTO-caagccgggtccattc-3′
		100H.*phaC1*-nkanR-*rev*	5′-tgacaacgtcagtcattg-3′
100H.*phaC1*-kanR-5'.pT.100H.*phaC1*	100H.*phaC1*-kanR-100H.*phaC1*	100H.*phaC1*-nkanR-*for*	5′-caagccgggtccattc-3′
		5'.pT.u.phaC1-nkanR-*rev*	5′PTO-tgacaacgtcagtcattg-3′
100H.*phaC1*-*rc*kanR-5'.pT.100H.*phaC1*	100H.*phaC1*-*rc*kanR-100H.*phaC1*	100H.*phaC1*-nkanR-*for*	5′-caagccgggtccattc-3′
		5'.pT.u.phaC1-nkanR-*rev*	5′PTO-tgacaacgtcagtcattg-3′

*Underlined nucleotides are restriction sites. Nucleotides in bold represent 50 bp homology part of the primer, which is not part of PCR DNA template.

6.2.1.1 phaC1-nkanR-phaC1

A 1.22 kb *phaC1*-nkanR-*phaC1* amplicon was amplified using pBHR1 plasmid template as a source of the P_{neokan}-kanR gene. Forward primer: *phaC1*-nkanR-for and reverse primer *phaC1*-nkanR-rev possessed 50 nucleotide sequences at their 5'-ends corresponding to the 5'-upstream and 5'-downstream sequences flanking the *phaC1* gene in *R. eutropha* H16, respectively, Table 6.3.

Table 6.3: PCR protocol for *phaC1*-nkanR-*phaC1*

PCR reaction component	Volume [μL]	Final concentration
Nuclease free Water	35.5	
5X Q5 HF Buffer	10	1X
dNTPs (10mM)	1	0.2 mM
phaC1-nkanR-*for* (20 μM)	1.25	0.5 μM
phaC1-nkanR-*rev* (20 μM)	1.25	0.5 μM
pBHR1	0.5	5 ng
Q5 polymerase (2 U/μL)	0.5	1 U/50μL

Table 6.4: PCR programme for *phaC1*-nkanR-*phaC1*

Step	Temperature	Time
Initial denaturation	98°C	30 s
30X	98°C 70°C (Anneal) 72°C (Extend)	8 s 30 s 30 s/kb *i.e.* 45 s
Final Extension	72°C	2 minutes
Hold	8°C	

6.2.1.2 100H.*phaC1*-nkanR-100H.*phaC1*

A 1.32 kb 100H.*phaC1*-nkanR-100H.*phaC1* amplicon was amplified using the 1.22 kb *phaC1-nkanR-phaC1* amplicon as PCR template. Forward primer: 100H.phaC1.nkanR-for and reverse primer: 100H.phaC1.nkanR-rev possessed 50 nucleotide sequences at their 5'-ends corresponding to the 5'-upstream and 5'-downstream sequences flanking the 50 nucleotides flanking the *phaC1* gene in *R. eutropha* H16, respectively, Table 6.5.

Table 6.5: PCR protocol for 100H.*phaC1*-nkanR-100H.*phaC1*

PCR reaction component	Volume [μL]	Final concentration
Nuclease free Water	35.5	-
5X Q5 HF Buffer	10	1X
dNTPs (10 mM)	1	0.2 mM
100H.phaC1.nkanR-*for* (20 μM)	1.25	0.5 μM
100H.phaC1.nkanR-*rev* (20 μM)	1.25	0.5 μM
phaC1-nkanR-*phaC1*	0.5	5 ng
Q5 polymerase (2 U/μL)	0.5	1 U/50μL

Table 6.6: PCR programme for *phaC1*-nkanR-*phaC1*

Step	Temperature	Time
Initial denaturation	98°C	30 s
30X	98°C 70°C (Anneal) 72°C (Extend)	8 s 30 s 30 s/kb *i.e.* 45 s
Final Extension	72°C	2 minutes
Hold	8°C	

6.2.1.3 50H.*phaC1*-kanR-50H.*phaC1*

A 1.031 kb 50H.*phaC1*-kanR-50H.*phaC1* amplicon was amplified using *zwf*-kanR-*zwf* as a source of the P_{neokan}-kanR gene. Forward primer: 50H.*phaC1*-kanR-for and reverse primer 50H.*phaC1*-nkanR-rev possessed 50 nucleotide sequences at their 5'-ends corresponding to the 5'-upstream and 5'-downstream sequences flanking the *phaC1* gene in *R. eutropha* H16, respectively, (Table 6.7).

Table 6.7: PCR protocol for 50H.*phaC1*-kanR-50H.*phaC1*

PCR reaction component	Volume [μL]	Final concentration
Nuclease free Water	35.5	-
5X Q5 HF Buffer	10	1X
dNTPs (10 mM)	1	0.2 mM
50H.phaC1.kanR-*for* (20 μM)	1.25	0.5 μM
50H.phaC1.kanR-*rev* (20 μM)	1.25	0.5 μM
zwf-kanR-zwf	0.5	5 ng
Q5 polymerase (2 U/μL)	0.5	1 U/50μL

Table 6.8: PCR programme for 50H.*phaC1*-kanR-50H.*phaC1*

Step	Temperature	Time
Initial denaturation	98°C	30 s
30X	98°C 65°C (Anneal) 72°C (Extend)	8 s 30 s 30 s/kb *i.e.* 35 s
Final Extension	72°C	2 minutes
Hold	8°C	

6.2.1.4 50H.*phaC1*-rckanR-50H.*phaC1*

A 1.031 kb 50H.*phaC1-rc*kanR-50H.*phaC1* amplicon was amplified using *zwf*-kanR-*zwf* as a source of the P_{neokan}-kanR gene. Forward primer 50H.*phaC1*-rckanR-for and reverse primer 50H.*phaC1*-rckanR-rev possessed 50 nucleotide sequences at their 5'-ends corresponding to the 5'-upstream and 5'-downstream sequences flanking the *phaC1* gene in *R. eutropha* H16, respectively, (Table 6.9).

Table 6.9: PCR protocol for 50H.*phaC1*-rckanR-50H.*phaC1*

PCR reaction component	Volume [μL]	Final concentration
Nuclease free Water	35.5	-
5X Q5 HF Buffer	10	1X
dNTPs (10 mM)	1	0.2 mM
50H.phaC1.rckanR-*for* (20 μM)	1.25	0.5 μM
50H.phaC1.rckanR-*rev* (20 μM)	1.25	0.5 μM
zwf-kanR-zwf	0.5	5 ng
Q5 polymerase (2 U/μL)	0.5	1 U/50μL

Table 6.10: PCR programme for 50H.*phaC1*-rckanR-50H.*phaC1*

Step	Temperature	Time
Initial denaturation	98°C	30 s
30X	98°C 61°C (Anneal) 72°C (Extend)	8 s 30 s 30 s/kb *i.e.* 35 s
Final Extension	72°C	2 minutes
Hold	8°C	

6.2.1.5 100H.*phaC1*-kanR-100H.*phaC1 and* 100H.*phaC1*-kanR-100H.*phaC1*

The cassettes 100H.*phaC1*-kanR-100H.*phaC1* and 100H.*phaC1*-rckanR-100H.*phaC1* were amplified from their respective 50H.*phaC1*-kanR-100H.*phaC1* and 50H.*phaC1*-rckanR-100H.*phaC1* precursors. Forward primer 100H.*phaC1*-kanR-for and reverse primer 100H.*phaC1*-nkanR-rev possessed 50 nucleotide sequences at their 5'-ends corresponding to the 5'-upstream and 5'-downstream sequences flanking the 50 bp sequences upstream and downstream of the *phaC1* gene in *R. eutropha* H16, respectively, Table 6.11.

Table 6.11: PCR protocol for 100H.*phaC1*-kanR-100H.*phaC1* and 100H.*phaC1*-rckanR-100H.*phaC1*

PCR reaction component	Volume [μL]	Final concentration
Nuclease free Water	35.5	-
5X Q5 HF Buffer	10	1X
dNTPs (10 mM)	1	0.2 mM
100H.phaC1.nkanR-*for* (20 μM)	1.25	0.5 μM
100H.phaC1.nkanR-*rev* (20 μM)	1.25	0.5 μM
50H.phaC1-kanR-50H.phaC1/ 50H.phaC1-rckanR-50H.phaC1	0.5	5 ng
Q5 polymerase (2 U/μL)	0.5	1 U/50μL

Table 6.12: PCR programme for 100H.*phaC1*-kanR-100H.*phaC1* and and 100H.*phaC1*-rckanR-100H.*phaC1*

Step	Temperature	Time
Initial denaturation	98°C	30 s
30X	98°C 72°C (Anneal) 72°C (Extend)	8 s 30 s 30 s/kb *i.e.* 45 s
Final Extension	72°C	2 minutes
Hold	8°C	

6.2.1.6 Phosphorotholated variants of 100H.*phaC1*-kanR-100H.*phaC1* and 100H.*phaC1*-kanR-100H.*phaC1*

The phosphorothiolated variants of the 100H.*phaC1*-kanR-100H.*phaC1* and 100H.*phaC1*-rckanR-100H.*phaC1* were constructed using primers detailed in Table 6.13.

Table 6.13: PCR protocol for phosphorothiolated cassettes

PCR reaction component	Volume [μL]	Final concentration
Nuclease free Water	35.5	-
5X Q5 HF Buffer	10	1X
dNTPs (10 mM)	1	0.2 mM
Forward primer (20 μM)	1.25	0.5 μM
Reverse primer (20 μM)	1.25	0.5 μM
100H.phaC1-kanR-50H.phaC1/ 100H.phaC1-rckanR-50H.phaC1	0.5	5 ng
Q5 polymerase (2 U/μL)	0.5	1 U/50μL

Table 6.14: PCR programme for phosphorothiolated cassettes

Step	Temperature	Time
Initial denaturation	98°C	30 s
30X	98°C 60°C (Anneal) 72°C (Extend)	8 s 30 s 30 s/kb *i.e.* 45 s
Final Extension	72°C	2 minutes
Hold	8°C	

6.2.2 Verification of stability of pBBR1c-RED1 and pBBR1c-RED2 in *Ralstonia eutropha* H16

The λ-Red plasmids pBBR1c-RED1 and pBBR1c-RED2 were transformed into *Ralstonia eutropha* H16 thus creating strains ReRed1 and ReRed2. 5 mL of NB media in a 50 mL falcon tube, supplemented with chloramphenicol and gentamicin was inoculated with transformant colonies of each plasmid. The inoculum was cultivated for up to 30 h to create an overnight culture. The presence and stability of the plasmids in overnight culture was confirmed via colony PCR using the 1 μL of the liquid culture as DNA template, Table 6.15 and 6.16.

Table 6.15: Colony PCR protocol for ReRed1 and ReRed2

Reaction component	Unit volume [μL]	Unit concentration
Nuclease free water	19	
10X Taq Buffer	2.5	1X
20 mM $MgSO_4$	1.875	1X
10 mM dNTP	0.5	1X
20 μM Forward primer [*NdeI*-Gam-for]	0.5	400 nM
20 μM Reverse primer [*BamHI*-Exo-rev/ *BamHI*-Exo-λlt]	0.5	400 nM
Taq polymerase (5 U/μL)	0.125	1.25 units/50 μL

Table 6.16: Colony PCR programme for ReRed1 and ReRed2

Step	Temperature	Time
Initial denaturation	95°C	5 minutes
30 X	95°C 57°C (Anneal) 68°C (Extend)	30 s 1 minute 60s/kb *i.e.* 2 min 15 secs
Final Extension	68°C	5 minutes
Hold	8°C	

6.2.3 Recombineering via λ-Red recombinase proteins in *Ralstonia eutropha* H16

The λ-Red-mediated gene inactivation in *Ralstonia eutropha* H16 was adapted from the protocol used in *E. coli* BW25113 in Chapter 6. Fresh 5 mL of NB media in a 50 mL falcon tube, supplemented with chloramphenicol and gentamicin was inoculated in a 1:50 ratio with 100 μl of overnight cultures of ReRed1 and ReRed2. Cultures meant for λ-Red recombineering were supplemented with L-arabinose (0.1%), while the control cultures were not. The cultures were cultivated at 30°C to OD_{600} value 0.6-1.0 to allow transient expression of the λ-Red proteins. The cultures were then transformed via electroporation with appropriate linear dsDNA cassette according to the protocol already detailed in Chapter 2. Outgrowth culture of *Ralstonia eutropha* strains was cultivated for 4 h at 30°C, 250 rpm. A predefined amount of cells were plated on appropriate NB agar plates supplemented appropriate antibiotics. Some NB agar plates were supplemented to L-arabinose (0.1%) to allow for continued expression for the λ-Red proteins as the colonies grew. In some cases the plates were additionally supplemented with chloramphenicol (25 mg/L) in addition to L-arabinose (0.1%) in order to select for cells that still possessed the λ-Red plasmid.

6.2.4 Verification of successful recombination *Ralstonia eutropha* H16

Colonies observed on test agar plates were counted and the number of colonies is compared to number of colonies observed on control plates from cultures without induction of protein expression or without the addition of dsDNA cassettes. A colony count ratio of >10:1 was set as an arbitrary standard for preliminary confirmation of successful genomic integration. Further verification of these colonies was performed via colony PCR. Colony PCR was performed with *OneTaq* or *Taq* polymerase by New England Biolabs, and used according to the manufacturer's instructions.

6.2.5 λ-Red Recombineering with pBBR1c-RED2 and kanR cassettes from pBbA8k-RFP

A number of kanR linear dsDNA cassettes with the kanR gene in pBbA8k-RFP were used to target the *phaC1* gene in *R. eutropha*. The experiment was set-up as follows, Figure 6.2:

1. 50 mL of NB supplemented with gentamicin (10 mg/L), L-arabinose (0.1%) and chloramphenicol (25 mg/L) was cultivated in a 250 mL flask. The culture was inoculated with ReRed2 overnight culture.
2. 5 mL of NB supplemented with gentamicin (10 mg/L), chloramphenicol (25 mg/L) was cultivated in a 50 mL falcon tube. The culture was inoculated with ReRed2 overnight culture.
3. 5 mL of NB supplemented with gentamicin (10 mg/L) in a 50 mL falcon tube. This was inoculated with overnight culture of *Ralstonia eutropha* H16 (ReH16).

All inoculated cultures were cultivated to OD_{600} of ~1.0. 24 mL of the culture in "1" was aliquoted into fresh 50 mL new falcon tube. 2 mL each of the culture in "B" was inoculated into two fresh 2 mL microfuge tube. 2 mL each of the culture in "C" was aliquoted into 2 fresh 2 mL microfuge tubes. All cultures were pre-treated for electroporation according to the protocol already detailed in Chapter 3. 200 μL each of cell suspension in 0.2 M sucrose of each culture type from "1" was aliquoted into 11 fresh 1.5 mL microfuge tubes labeled A-K. 200 μL each of cell suspension in 0.2 M sucrose of culture from "2" was aliquoted into 2 fresh 2 mL microfuge tubes labeled "L" and "M". 200 μL each of cell suspension in 0.2 M sucrose of culture from "3" was aliquoted into 2 fresh 2 mL microfuge tubes labeled

"M" and "N". 500 ng of the dsDNA linear dsDNA was added to the each cell suspension labeled according to Table 7.17. Cell suspensions K, L, M, N and O were used as controls according to Table 7.18.

Table 6.17: Experimental set-up of λ-Red recombineering using different dsDNA cassettes

Sample	Strain	Culture	Linear dsDNA type added
A	ReRed2	1	50H.phaC1-kanR-50H.phaC1
B	ReRed2	1	50H.phaC1-rckanR-50H.phaC1
C	ReRed2	1	100H.phaC1-kanR-100H.phaC1
D	ReRed2	1	100H.phaC1-rckanR-100H.phaC1
E	ReRed2	1	5'-PTO-100H.phaC1-kanR-100H.phaC1
F	ReRed2	1	5'-PTO-100H.phaC1-rckanR-100H.phaC1
G	ReRed2	1	100H.phaC1-kanR-5'-PTO-100H.phaC1
H	ReRed2	1	100H.phaC1-rckanR-5'-PTO-100H.phaC1
I	ReRed2	1	5'-PTO-100H.phaC1-kanR-5'-PTO-100H.phaC1
J	ReRed2	1	5'-PTO-100H.phaC1-rckanR-5'-PTO-100H.phaC1
K	ReRed2	1	-
L	ReRed2	2	100H.phaC1-kanR-100H.phaC1
M	ReRed2	2	100H.phaC1-rckanR-100H.phaC1
N	ReH16	3	100H.phaC1-rckanR-100H.phaC1
O	ReH16	3	-

Table 6.18: Negative controls for λ-Red recombineering

Sample	Role of control
K	A negative control to ascertain integration of dsDNA kanR cassette in A-J
L	A negative control to ascertain L-arabinose-induced and λ-Red-mediated integration of 100H.phaC1-kanR-100H.phaC1 in A-J
M	A negative control to ascertain L-arabinose-induced and λ-Red-mediated integration of 100H.phaC1-rckanR-100H.phaC1 in A-J
N	A negative control to ascertain that λ-Red-mediated integration of 100H.phaC1-rckanR-100H.phaC1 is *ReRed2*-dependent
O	A negative control to ascertain kanamycin resistance phenotype of mutants with genomic integration of dsDNA kanR cassette

All outgrowth cultures of each transformant were cultivated for up to 5 h. All cells from outgrowth cultures of all cell suspensions apart from B, D, F, G, H, J from were plated on only NB agar plate supplemented with kanamycin (250 mg/L). Cells from outgrowth cultures of cell suspensions B and D were plated in equal volume on NB agar plate supplemented with kanamycin (250 mg/L), NB agar plate supplemented with kanamycin (250 mg/L) and L-arabinose (0.1%), NB agar plate supplemented with kanamycin (250 mg/L) and L-arabinose (0.1%) and chloramphenicol (25 mg/L). All plates were incubated for up to 96 h.

To screen for possible mutants, colonies were selected from the agar plates from the samples A-J, and O as the control. The selected colonies were cultivated in NB media supplemented with 250 mg/L in a 96-well plate to screen for kanamycin resistance colonies, which had possibly integrated the kanR cassettes into the genome.

The liquid culture of the colonies was used as genomic template for the colony PCR-based screening, (Table 6.19 and 6.20). Also, the primers 100H.*phaC1*-nkanR-for and 100H.*phaC1*-nkanR-rev, which are specific to the genomic regions 100 bp upstream and downstream of the *phaC1* gene, were used. This meant that the primers were genomic primers in cases where the cassettes with 50 bp homology arms were used. It also meant that the primers were both genomic and cassette based primers in cases where cassettes with 100 bp homology arms were used. Given this choice of primers, a band of ~ 2.0 kb would be indicative of unsuccessful genomic integration of dsDNA cassette. A band of ~1.1 kb would be indicative of successful genomic integration of dsDNA cassette.

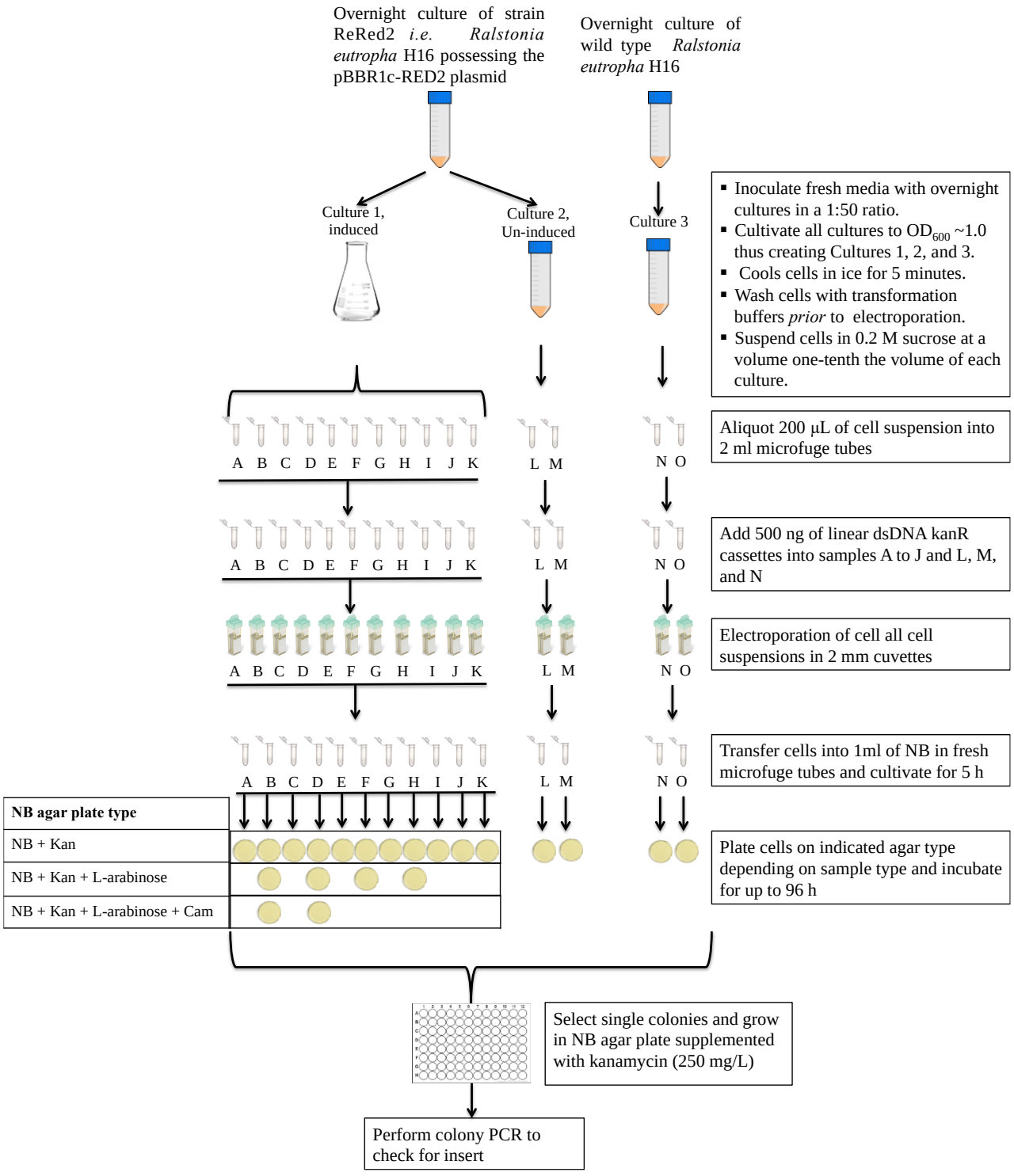

Figure 6.1. Schematic of experimental set-up of λ-Red recombineering in *Ralstonia eutropha* H16 using several variants of the kanR cassette from pBbA8K-RFP and the strain ReRed2 containing the pBBR1c-RED2 λ-Red plasmid.

Table 6.19: Colony PCR protocol for screening for mutant clones

Reaction component	Unit volume [µl]	Unit concentration
Nuclease free water	12.6	
Liquid culture	5.0	
5X *OneTaq* GC Buffer	5.0	1X
50 mM $MgSO_4$	0.75	1X
10 mM dNTP	0.5	1X
20 µM Forward primer [100H.*phaC1*-nkanR-for]	0.5	400 nM
20 µM Reverse primer [100H.*phaC1*-nkanR-rev]	0.5	400 nM
Taq polymerase (5 U/µL)	0.125	1.25 units/50 µL

Table 6.20: Colony PCR programme for screening for mutant clones

Step	Temperature	Time
Initial denaturation	95°C	5 minutes
30 X	95°C 68°C (Anneal) 68°C (Extend)	30 s 1 minute 60 s/kb *i.e.* 2 min 15 secs
Final Extension	68°C	5 minutes
Hold	8°C	

6.3 RESULTS AND DISCUSSION

6.3.1 Transformation of pBBR1c-RED1 and pBBR1c-RED2 into *R. eutropha* H16

Agarose gel electrophoresis of the colony PCR products of the overnight cultures of *ReRed1* and *ReRed2* indicate bands at ~ 1.9 kb and ~2.2 kb, Figure 7.2. This band sizes correspond to the NdeI-pKD20-BamHI and the NdeI-pKD46-BamHI inserts from the λ-Red plasmids pBBR1c-RED1 and pBBR1c-RED2, respectively. This indicated that the plasmids were indeed stably maintained in the cells.

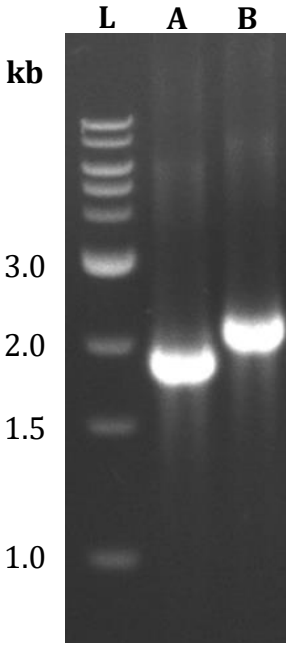

Figure 6.2: Agarose gel electrophoresis of colony PCR amplicons of *Ralstonia eutropha* with pBBR1c-RED1 (ReRed1), and pBBR1c-RED2 (ReRed2) transformants using appropriate primers for the λ-Red operon. (A) 1.905 kb band shows the *Nde*I-pKD20-*BamH*I amplicon from pBBR1c-RED1, (B) 2.2 kb band shows the *Nde*I-pKD46-*BamH*I amplicon from pBBR1c-RED2. L – 1 kb DNA ladder.

6.3.2 λ-Red Recombineering with pBBR1c-RED2 and kanR cassettes from pBbA8k-RFP

The negative control samples K, L M produced 0, 0 and 1 colonies, respectively when plated on NB agar plate supplemented with kanamycin (250 mg/L). This is wide contrast to the number of colonies from samples A-J that had between 10 and 750 total colony count, depending on the type of NB agar plate used. Samples B and H, which were transformed

with the 50H.phaC1-kanR-50H.phaC1 and 100H.phaC1-rckanR-5'-PTO-100H.phaC1 had the highest number of colonies (69 and 70, respectively) when the outgrowth was plated on NB agar supplemented with just kanamycin (250 mg/L). Sample B also had the highest numbers of colonies at 420 colonies when plated on NB agar supplemented with kanamycin (250 mg/L) and L-arabinose (0.1%) and at 750 colonies when plated on NB agar supplemented with kanamycin (250 mg/L) and L-arabinose (0.1%) and chloramphenicol (25 mg/L). Similarly, sample D had a total of 720 colonies when plated on NB agar supplemented with kanamycin (250 mg/L) and L-arabinose (0.1%) and chloramphenicol (25 mg/L).

It was observed that the total number of colonies from sample B was highest (at 750 colonies) when cells were plated on NB agar supplemented with kanamycin (250 mg/L) and L-arabinose (0.1%) and chloramphenicol (25 mg/L). This was lower (at 420 colonies) when the cells were plated on NB agar supplemented with kanamycin (250 mg/L) and L-arabinose (0.1%). This, in turn, is lower compared to the number of cells observed when the outgrowth was plated on NB agar supplemented with just kanamycin (250 mg/L), Table 7.19. The same trend was observed with the outgrowth culture from sample D, Table 7.9. Overall, a ratio of >10:1 was established between the colony count from some of the test samples and the control samples. This suggested that the colonies observed from the test samples might be mutants.

Upon cultivation of selected colonies from the plates, most of the colonies grew in NB media supplemented with kanamycin (250 mg/L). Growth of the selected colonies upon cultivation in 96-well plate might be attributed to native resistance of *Ralstonia eutropha* H16 to kanamycin, Table 7.22. The colonies from sample N (*i.e.* wild type ReH16 transformed with 100H.phaC1-rckanR-100H.phaC1) grew to a higher OD_{600} of ~1.3 compared to the selected colonies from sapmle A-J which grew to OD_{600} 0.5 - 0.9 after 48 h of cultivation. The cell density of *Ralstonia eutropha* H16 outgrowth culture is expected to be higher than the ReRed2 outgrowth cultures given the fact that the latter would have a relatively lower cell growth rate owing to the metabolic burden from replicating the pBBR1c-RED plasmid. Growth of the selected colonies suggested that they might be mutants. However colony PCR screening was primarily requisite for confirming successful integration of the kanR gene/deletion of the *phaC1* gene.

Table 6.21: Colony count for λ-Red recombineering in *R. eutropha* H16

	Total colony count on different NB agar plate types		
Sample	NB+Kan	NB+Kan+L-arabinose	NB+Kan+L-arabinose+Cam
A	20	N/A	N/A
B	69	420	750
C	15	N/A	N/A
D	54	288	720
E	25	N/A	N/A
F	10	20	N/A
G	30	N/A	N/A
H	70	100	N/A
I	20	N/A	N/A
J	20	N/A	N/A
K	0	N/A	N/A
L	0	N/A	N/A
M	1	N/A	N/A
N	10	N/A	N/A
O	8	N/A	N/A

Table 6.22: OD_{600} of cells of selected colonies screened for cell growth against kanamycin selection pressure.

	A	B	C	D	E	F	G	H	I	J	N
1	0.3315[i]	0.2510[i]	0.2629[i]	0.2371[i]	0.3525[i]	0.3008[i]	0.2476[i]	0.3087[i]	0.2278[i]	0.2215[i]	0.2244[i]
2	0.2928[i]	0.3965[i]	0.3711[i]	0.2747[i]	0.3698[i]	0.3705[i]	0.2822[i]	0.4497[i]	0.3831[i]	0.2605[i]	1.3332[i]
3	0.9202[i]	0.2748[i]	0.2760[i]	0.4217[i]	0.3498[i]	0.2995[i]	0.3525[i]	0.4023[i]	0.2947[i]	0.3546[i]	0.3123[i]
4	0.2983[i]	0.4411[ii]	0.2903[i]	0.7638[ii]	0.7348[i]	0.2931[i]	0.5619[i]	0.4125[i]	0.2633[i]	0.3820[i]	1.3642[i]
5	0.5311[i]	0.2205[ii]	0.2584[i]	0.3454[ii]	0.3840[i]	0.3376[ii]	0.4133[i]	0.4518[ii]	0.2795[i]	0.4123[i]	0.2825[i]
6	0.3259[i]	0.2124[ii]	0.3810[i]	0.2378[ii]	0.4225[i]	0.2999[ii]	0.3723[i]	0.3783[ii]	0.4546[i]	0.3943[i]	0.3526[i]
7	0.2428[i]	0.2145[iii]	0.2316[i]	0.2975[iii]	0.3753[i]	0.2547[ii]	0.3963[i]	0.6680[ii]	0.2304[i]	0.6556[i]	0.2316[i]
8	0.3284[i]	0.2240[iii]	0.2135[i]	0.3966[iii]	0.3032[i]	0.2041[ii]	0.5486[i]	0.2150[ii]	0.2609[i]	0.3318[i]	1.2844[i]

(i) Cells on NB+Kan plates, (ii) Cells on NB+Kan+L-arabinose plates, (iii) Cells on NB+Kan+L-arabinose+Cam plates, Red colour – OD_{600} above 0.500

The cultures that grew to optical density >0.5 were selected for colony-PCR based screening. These include cultures in wells A3, D4, E4, G4, H7, J7, N2 and N4, corresponding to cultures from samples A, D, E, G H, J, and N, Table 7.22. Colony PCR evaluation of all selected mutants showed bands at ~2.0 kb which is indicative of a genomic amplicon containing the 1.77 kb phaC1 gene flanked upstream and downstream by 100 bp of homology arms, (Figure 7.4). This indicated that in the colonies, the *phaC1* gene remained undeleted and thus questions if the dsDNA kanR cassettes had not been integrated into the genome. This suggested that the observed colonies from both the test and control samples probably grew as a result of adaptation to selection pressure from kanamycin after a lengthy incubation period of 96 h.

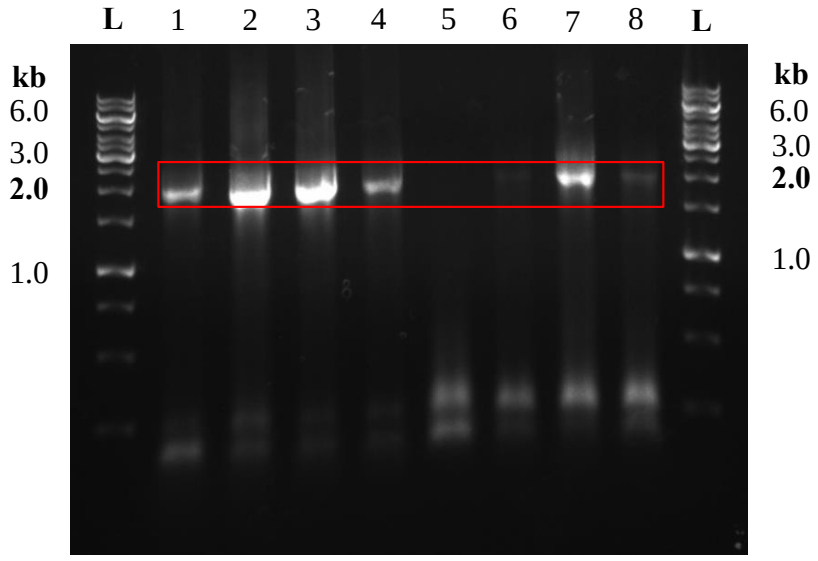

Figure 6.3: Agarose gel electrophoresis of colony PCR from selected colonies which grew above OD_{600} after λ-Red recombineering with pBBR1c-RED2 in *R. eutropha* H16. All 8 screened colonies show band at ~2.0 kb showing that the *phaC1* gene is undeleted and that the linear dsDNA cassettes are not integrated into the genome.

6.4 CONCLUSION

Deletion of the *phaC1* gene *R. eutropha* H16 *via* λ-Red recombineering was not confirmed. This might be attributed to a number of reasons especially the non-detectable levels of expression of the λ-Red proteins Gam, Bet and Exo. Other possible reasons could potentially include the poor compatibility of the λ-Red recombineering tool with native recombination-enabling machineries in *R. eutropha* H16.

CHAPTER SEVEN

7 CONCLUSION

7.1 Contributions of this work

In the quest to expand molecular tools for the metabolic engineering of *R. eutropha* H16, the need for chassis-compatible expression vectors is an essential requirement that has been emphazised in this study. Such vectors must have predictable performance in terms of their transformability into *R. eutropha*, and must offer tunable expression pattern of the genetic elements (biological parts) they encode. The L-arabinose inducible P_{BAD} promoter in the pBBR1c-RFP vector was used to demonstrate tunable protein expression in *Ralstonia eutropha* H16 *via* dose-dependent expression of RFP (Chapter 2). The inducer-response profile of this vector showed high expression maxima at 0.2% L-arabinose. This expression profile has also recently been confirmed in a recent study by Xiong et al. (2018).

The Fatty Acid and Phospholipid Regulator (FapR) protein – a malonyl-CoA-responsive transcriptional regulator is one such biological part requiring controlled expression. To achieve this, the P_{BAD} promoter in the pBBR1c-FapR vector was used to drive expression of the FapR repressor to show that the FapR repressor can be expressed in *Ralstonia eutropha* H16 without negatively imparting on cell viability. This reported expression of the FapR– a vital Gram-positive bacterium fatty acid synthesis regulator is the first ever study demonstrating expression of this transcriptional repressor in *R. eutropha* H16.

In expanding the frontiers of genome editing in *R. eutropha* H16 as a metabolic engineering tool, the genome editing tool - λ-Red recombineering was extensively studied in order to explore how the method might be tailored for use in *R. eutropha* H16. Controlled expression of the λ-Red proteins was identified as a crucial hurdle in engineering this method. To this end, the L-arabinose inducible P_{BAD} expression vectors (pBBR1c-RED1, pBBR1c-RED2, pBBR1k-RED) plasmids for expressing the λ-Red proteins in *R. eutropha* were developed. Firstly, the functionality of these vectors was verified in *E. coli* BW25113. The fact that all three proteins were successfully expressed and detected in *E. coli* BW25113 and not detected in *Ralstonia eutropha* H16 suggests that the proteins may have undergone proteolysis as a cellular mechanism to protect the cell from potential cellular toxicity they might initiate. Although, expression was not detected in *R. eutropha* H16,

there have been no studies till date showing successful expression or detection of expression of the λ-Red proteins in *R. eutropha.*

Whilst the L-arabinose promoter was used to demonstrate and achieve tunable expression in *R. eutropha* H16, the comparative advantage of constitutive promoters over inducible promoter systems was identified. To this end, replacing the L-arabinose inducible P_{BAD} promoter in the pBBR1c-RFP plasmid with a set of 42 constitutive promoters yielded a set of 42 constitutive expression vectors with a 137-fold activity range (Chapter 3). The activities of these constitutive promoters arranged in hierarchical order of promoter strength span and exceed the entire induction range of the L-arabinose inducible P_{BAD} promoter. The unique promoter identifier assigned each promoter in accordance with promoter strength makes the set of promoters readily assessable for pathway optimization in metabolic engineering applications. In engineering this set of 42 constitutive promoters, several strategies to alter promoter activity by tweaking promoter architecture were utilized. The strategies include point mutation, promoter hybridization, promoter length alteration, promoter configuration alteration, and incorporating *cis*-acting transcriptional and translational units. The application of these promoter engineering strategies further shed light on the unique transcriptional behavior/pattern of divergent promoters in back-to-back orientation in *Ralstonia eutropha* H16, a transcriptional pattern which has not been reported about *Ralstonia eutropha* H16 in prior study. This observed transcriptional pattern and promoter behavior could be potentially explored in other biological systems such as mammalian cells where the transcription process is a lot more complex in comparison to prokaryotic cells. The novelty of the promoter engineering strategy "E" (back-to-back orientation of divergent promoters) will thus potentially prove very useful in the engineering of mammalian promoters. This is particularly because transcriptional amplification is largely mediated by upstream elements and/or transcriptional factor binding sites in mammalian promoters (Brown et al., 2017, Brown et al., 2014).

A key knowledge gap in controlling gene expression in *R. eutropha* H16 is the availability of genetic circuits to orchestrate dynamic control over gene expression. Malonyl-CoA-responsive genetic circuits were particularly of interest as malonyl-CoA engineering is the core objective of this study. Whilst already developed for microbial chassis such as *E. coli* and *Saccharomyces cerevisiaie, R. eutropha* H16-compatible malonyl-CoA biosensors has

yet to be reported, prior to the study contained herein. By applying the toolbox of promoters already developed in this study, a set of 6 modular single-plasmid malonyl-CoA biosensors, which are functional in *Ralstonia eutropha* H16 were designed and construction (Chapter 4). Essentially, the novelty in the design of the biosensors lies in the application of the divergent promoter configuration (strategy "E") to achieve structural modularity and optimal functionality of the sensors. The functionality of the best performing biosensor (S1) is achieved through careful selection of the promoters with the right activity levels in order to achieve a desired level of expression of the metabolite-responsive transcriptional factor (FapR). In addition, the response (RFP expression intensities) of the sensors to cerulenin confirmed that cerulenin is indeed a fatty acid inhibitor and a malonyl-CoA up-regulator in *Ralstonia eutropha* H16.

Lastly, the need for facile genome editing tools in consolidating heterologous pathway optimization and gene expression control was identified. For this requirement, the development of a λ-Red recombineering method for *Ralstonia eutropha* H16 was attempted. The expression vectors pBBR1c-RED1, pBBR1c-RED2, pBBR1k-RED, successfully mediated deletion of the *zwf* gene in *E. coli* BW25113 using kanamycin and chloramphenicol resistance cassettes bearing 50 bp long homology arms to the *zwf* gene. Recombination efficiency as high as $3.3*10^{-5}$ was achieved with chloramphenicol-resistant pBBR1c-RED2 vector using a kanamycin resistance cassette *zwf*-kanR-*zwf*. Unsuccessful recombination in *Ralstonia eutropha* using the kanamycin-resistance markers and the chloramphenicol-resistant vectors pBBR1c-RED1 and pBBR1c-RED2 could be attributed to the previously identified poor expression of the λ-Red proteins driven by the L-arabinose inducible P_{BAD} promoter. Other plausible reasons are limited transformation efficiency and/or poor stability of the linear dsDNA resistance markers in the cell prior to possible recombination events. To the best of available knowledge, there has been no other report on successful use of λ-Red recombineering as method of genome editing in *R. eutropha* H16.

7.2 Future work

Achieving malonyl-CoA engineering in *Ralstonia eutropha* H16 in *R. eutropha* will continue to benefit from rapid advancement in the synergistic application of the molecular tools studied and developed in this study *viz* a toolbox of promoters, malonyl-CoA-

responsive genetic circuits, and a facile genome editing method. There remains a vast promoter engineering potential for regulating gene expression in *R. eutropha*, particularly through incorporation of essential genetic elements and exploring varied promoter configurations. This will particularly be useful in the construction of more sophisticated genetic circuits to control gene expression.

With regards to the constructed malonyl-CoA biosensors reported in Chapter 4, these can be immediately leveraged upon in selecting for high malonyl-CoA producers subsequent to engineering *Ralstonia eutropha* H16 for malonyl-CoA production. Such strains could potentially be engineered with the controlled expression of heterologous malonyl-CoA source pathway(s) and/or more promising genome editing methods. The fluorescence intensities produced from the sensors will be used as a read-out to rank the mutants in order of their malonyl-CoA-production phenotype. This will require leveraging on the dynamic range of response of the malonyl-CoA sensors.

In engineering a heterologous malonyl-CoA source pathway, the fold-range of activity of the engineered set of promoters from Chapter 3 will be leveraged in tuning expression levels in the pathway until a high-producer strain is achieved. Possible pathways/gene clusters worthy of experimentation include: (1) the malonyl-CoA synthetase (matB) and malonate carrier protein (matC) using malonate as a substrate and, (2) the acetyl-CoA carboxylase (ACC) genes from *Corynebacterium glutamicum* (Miyahisa et al., 2005).

The first point of call in re-investigating the λ-Red recombineering method in *Ralstonia eutropha* will be optimizing the expression of the λ-Red proteins to levels detectable by SDS-PAGE protein analysis. One way to explore this might be to leverage the set of constitutive promoters reported in Chapter 3 in place of the L-arabinose inducible P_{BAD} promoter used in this study. It is projected that experimenting with the time profile of expression of these promoters and their varied strengths will afford tunable expression of the λ-Red proteins to levels that might support recombineering event. Furthermore, investigation of the presence of, functions and mechanism of function of native recombination machineries, endonuclease and exonuclease enzymes in *R. eutropha* H16

will better help to understand how a functional λ-Red recombineering molecular tool may be better engineered in this microbial host.

7.3 Future perspectives

This work reported in this has successfully expanded the molecular tools for malonyl-CoA engineering in *R. eutropha* H16, particularly in the development of expression vectors and a collection of constitutive promoters for controlling gene expression. Potential metabolic engineering applications of the toolbox of constitutive promoters are: (1) optimizing static control of metabolic pathway(s), (2) optimizing the functionality of other metabolite-responsive genetic circuits, (3) tunable expression of vital genetic elements required for genome editing in *Ralstonia eutropha* H16. These engineered vectors, promoters, and genetic circuits will also be applicable in similar microbial chassis apart from *R. eutropha* H16.

However, the failure of the λ-Red recombineering method in *Ralstonia eutropha* H16 portends that other proven methods of genome editing would continue to be adopted in engineering mutant strains. These methods include the more wildly applied allelic exchange method using suicide vectors, retrohoming (Enyeart et al., 2014) and the more recently developed CRISPR-Cas toolbox for *R. eutropha* H16 (Xiong et al., 2018). Although the λ-Red recombineering method did not work in *Ralstonia eutropha* H16, the fact that all the constructed vectors were functional in *E. coli* BW25113 suggests that they could potentially be utilized in other relevant microbial cell factories where the pKD20 and pKD46 are not be functional.

Overall, the engineered molecular tools *viz*: expression vectors, constitutive promoters, and malonyl-CoA biosensors reported in this study have expanded the collection of molecular tools available for the metabolic engineering of *R. eutropha* H16. This invariably further enables its genetic tractability and enhances its use as a microbial cell factory for the biosynthesis of varied valuable chemicals.

REFERENCES

AGBOR, V. B., CICEK, N., SPARLING, R., BERLIN, A. & LEVIN, D. B. 2011. Biomass pretreatment: Fundamentals toward application. *Biotechnology Advances,* 29**,** 675-685.

AHRENS, W. & SCHLEGEL, H. G. 1972. Carbon dioxide requiring mutants of *Hydrogenomas eutropha* Strain H16. I. Growth and CO2-fixation. *Archiv Fur Mikrobiologie,* 85**,** 142-&.

AIYAR, S. E., GOURSE, R. L. & ROSS, W. 1998. Upstream A-tracts increase bacterial promoter activity through interactions with the RNA polymerase alpha subunit. *Proceedings of the National Academy of Sciences of the United States of America,* 95**,** 14652-14657.

ALBUQUERQUE, M. G. E., MARTINO, V., POLLET, E., AVEROUS, L. & REIS, M. A. M. 2011. Mixed culture polyhydroxyalkanoate (PHA) production from volatile fatty acid (VFA)-rich streams: Effect of substrate composition and feeding regime on PHA productivity, composition and properties. *Journal of Biotechnology,* 151**,** 66-76.

ALPER, H., FISCHER, C., NEVOIGT, E. & STEPHANOPOULOS, G. 2005. Tuning genetic control through promoter engineering. *Proceedings of the National Academy of Sciences of the United States of America,* 102**,** 12678-12683.

ARIKAWA, H. & MATSUMOTO, K. 2016. Evaluation of gene expression cassettes and production of poly(3-hydroxybutyrate-*co*-3-hydroxyhexanoate) with a fine modulated monomer composition by using it in *Ralstonia eutropha*. *Microb Cell Fact,* 15**,** 184.

ASHBY, R. D., SOLAIMAN, D. K. Y., STRAHAN, G. D., ZHU, C., TAPPEL, R. C. & NOMURA, C. T. 2012. Glycerine and levulinic acid: Renewable co-substrates for the fermentative synthesis of short-chain poly(hydroxyalkanoate) biopolymers. *Bioresource Technology,* 118**,** 272-280.

ATSUMI, S., HIGASHIDE, W. & LIAO, J. C. 2009. Direct photosynthetic recycling of carbon dioxide to isobutyraldehyde. *Nature Biotechnology,* 27**,** 1177-U142.

BABA, T., ARA, T., HASEGAWA, M., TAKAI, Y., OKUMURA, Y., BABA, M., DATSENKO, K. A., TOMITA, M., WANNER, B. L. & MORI, H. 2006. Construction of *Escherichia coli* K-12 in-frame, single-gene knockout mutants: the Keio collection. *Molecular Systems Biology,* 2.

BARNARD, G. C., HENDERSON, G. E., SRINIVASAN, S. & GERNGROSS, T. U. 2004. High level recombinant protein expression in *Ralstonia eutropha* using T7 RNA polymerase based amplification. *Protein Expression and Purification,* 38**,** 264-271.

BECK, C. F. & WARREN, R. A. 1988. Divergent promoters, a common form of gene organization. *Microbiol Rev,* 52**,** 318-26.

BI, C., SU, P., MULLER, J., YEH, Y. C., CHHABRA, S. R., BELLER, H. R., SINGER, S. W. & HILLSON, N. J. 2013. Development of a broad-host synthetic biology toolbox for *Ralstonia eutropha* and its application to engineering hydrocarbon biofuel production. *Microb Cell Fact,* 12**,** 107.

BLANK, K., HENSEL, M. & GERLACH, R. G. 2011. Rapid and Highly Efficient Method for Scarless Mutagenesis within the *Salmonella enterica* Chromosome. *Plos One,* 6.

BOWIEN, B. & KUSIAN, B. 2002. Genetics and control of CO2 assimilation in the chemoautotroph *Ralstonia eutropha*. *Archives of Microbiology,* 178**,** 85-93.

BOYLE, N. R., REYNOLDS, T. S., EVANS, R., LYNCH, M. & GILL, R. T. 2013. Recombineering to homogeneity: extension of multiplex recombineering to large-scale genome editing. *Biotechnology Journal,* 8**,** 515-522.

BOZELL, J. J., MOENS, L., ELLIOTT, D. C., WANG, Y., NEUENSCWANDER, G. G., FITZPATRICK, S. W., BILSKI, R. J. & JARNEFELD, J. L. 2000. Production of levulinic acid and use as a platform chemical for derived products. *Resources Conservation and Recycling,* 28**,** 227-239.

BOZELL, J. J. & PETERSEN, G. R. 2010. Technology development for the production of biobased products from biorefinery carbohydrates-the US Department of Energy's "Top 10" revisited. *Green Chemistry,* 12**,** 539-554.

BRAEMER, C. O. & STEINBUECHEL, A. 2001. The methylcitric acid pathway in Ralstonia eutropha: New genes identified involved in propionate metabolism. *Microbiology (Reading),* 147**,** 2203-2214.

BRIGHAM, C. J., BUDDE, C. F., HOLDER, J. W., ZENG, Q., MAHAN, A. E., RHA, C. & SINSKEY, A. J. 2010. Elucidation of beta-Oxidation Pathways in *Ralstonia eutropha* H16 by Examination of Global Gene Expression. *Journal of Bacteriology,* 192**,** 5454-5464.

BRIGHAM, C. J., ZHILA, N., SHISHATSKAYA, E., VOLOVA, T. G. & SINSKEY, A. J. 2012. Manipulation of *Ralstonia eutropha* carbon storage pathways to produce useful bio-based products. *Subcell Biochem,* 64**,** 343-66.

BROCKMAN, I. M. & PRATHER, K. L. 2015. Dynamic metabolic engineering: New strategies for developing responsive cell factories. *Biotechnol J,* 10**,** 1360-9.

BROWN, A. J., GIBSON, S. J., HATTON, D. & JAMES, D. C. 2017. In silico design of context-responsive mammalian promoters with user-defined functionality. *Nucleic Acids Research,* 45**,** 10906-10919.

BROWN, A. J., SWEENEY, B., MAINWARING, D. O. & JAMES, D. C. 2014. Synthetic Promoters for CHO Cell Engineering. *Biotechnology and Bioengineering,* 111**,** 1638-1647.

BYROM, D. 1987. Polymer Synthesis by Micro-organisms - Technology and Economics. *Trends in Biotechnology,* 5**,** 246-250.

BYROM, D. 1992. Production of poly-beta-hydroxybutyrate-poly-beta-hydroxyvalerate copolymers. *Fems Microbiology Letters,* 103**,** 247-250.

CAMERON, D. C., ALTARAS, N. E., HOFFMAN, M. L. & SHAW, A. J. 1998. Metabolic engineering of propanediol pathways. *Biotechnology Progress,* 14**,** 116-125.

CARTER, D. M. & RADDING, C. M. 1971. Role of Exonuclease and Beta Protein of Phage Lambda in Genetic Recombination .2. Substrate Specificity and Mode of Action of Lambda Exonuclease. *Journal of Biological Chemistry,* 246**,** 2502-&.

CASSUTO, E., LASH, T., SRIPRAKA.KS & RADDING, C. M. 1971a. Role of Exonuclease and Beta Protein of Phage Lambda in Genetic Recombination .5. Recombination of Lambda DNA *In vitro* - (Single-Strans Assimilation/Mechanism of Arrest). *Proceedings of the National Academy of Sciences of the United States of America,* 68**,** 1639-&.

CASSUTO, E., LASH, T., SRIPRAKA.KS & RADDING, C. M. 1971b. Role Of Exonuclease And Beta Protein Of Phage Lambda In Genetic Recombination .5. Recombination Of Lambda Dna In-Vitro - (Single-Strand Assimilation/Mechanism Of Arrest). *Proceedings of the National Academy of Sciences of the United States of America,* 68**,** 1639-&.

CHAVEROCHE, M.-K., GHIGO, J.-M. & D'ENFERT, C. 2000. A rapid method for efficient gene replacement in the filamentous fungus Aspergillus nidulans. *Nucleic Acids Research,* 28.

CHEN, J. S., COLON, B., DUSEL, B., ZIESACK, M., WAY, J. C. & TORELLA, J. P. 2015. Production of fatty acids in *Ralstonia eutropha* H16 by engineering beta-oxidation and carbon storage. *PeerJ,* 3**,** e1468.

CHOI, J. C., SHIN, H. D. & LEE, Y. H. 2003. Modulation of 3-hydroxyvalerate molar fraction in poly(3-hydroxybutyrate-3-hydroxyvalerate) using *Ralstonia eutropha* transformant co-amplifying phbC and NADPH generation-related *zwf* genes. *Enzyme and Microbial Technology,* 32**,** 178-185.

CHOI, J. I. & LEE, S. Y. 1997. Process analysis and economic evaluation for poly(3-hydroxybutyrate) production by fermentation. *Bioprocess Engineering,* 17**,** 335-342.

CHU, S. 2009. Carbon Capture and Sequestration. *Science,* 325**,** 1599-1599.

COPELAND, N. G., JENKINS, N. A. & COURT, D. L. 2001. Recombineering: A powerful new tool for mouse functional genomics. *Nature Reviews Genetics,* 2**,** 769-779.

COSTANTINO, N. & COURT, D. L. 2003. Enhanced levels of lambda red-mediated recombinants in mismatch repair mutants. *Proceedings of the National Academy of Sciences of the United States of America,* 100**,** 15748-15753.

CRAMM, R. 2009. Genomic View of Energy Metabolism in *Ralstonia eutropha* H16. *Journal of Molecular Microbiology and Biotechnology,* 16**,** 38-52.

CRÉPIN, L., LOMBARD, E. & GUILLOUET, S. E. 2016. Metabolic engineering of *Ralstonia eutropha* for heterotrophic and autotrophic alka(e)ne production. *Metab Eng,* 37**,** 92-101.

CRESS, B. F., TRANTAS, E. A., VERVERIDIS, F., LINHARDT, R. J. & KOFFAS, M. A. 2015. Sensitive cells: enabling tools for static and dynamic control of microbial metabolic pathways. *Curr Opin Biotechnol,* 36**,** 205-14.

DAHL, R. H., ZHANG, F., ALONSO-GUTIERREZ, J., BAIDOO, E., BATTH, T. S., REDDING-JOHANSON, A. M., PETZOLD, C. J., MUKHOPADHYAY, A., LEE, T. S., ADAMS, P. D. & KEASLING, J. D. 2013. Engineering dynamic pathway regulation using stress-response promoters. *Nature Biotechnology,* 31**,** 1039-1046.

DANTAS, T. L. P., RODRIGUES, A. E. & MOREIRA, F. P. M. 2012. Separation of Carbon Dioxide from Flue Gas Using Adsorption on Porous Solids. *In:* (ED), D. G. L. (ed.) *Greenhouse Gases - Capturing, Utilization and Reduction.*

DATSENKO, K. A. & WANNER, B. L. 2000. One-step inactivation of chromosomal genes in *Escherichia coli* K-12 using PCR products. *Proceedings of the National Academy of Sciences of the United States of America,* 97**,** 6640-6645.

DATTA, S., COSTANTINO, N. & COURT, D. L. 2006. A set of recombineering plasmids for gram-negative bacteria. *Gene,* 379**,** 109-115.

DAVIS, J. H., RUBIN, A. J. & SAUER, R. T. 2011. Design, construction and characterization of a set of insulated bacterial promoters. *Nucleic Acids Research,* 39**,** 1131-1141.

DAVIS, M. S., SOLBIATI, J. & CRONAN, J. E. 2000. Overproduction of acetyl-CoA carboxylase activity increases the rate of fatty acid biosynthesis in *Escherichia coli*. *Journal of Biological Chemistry,* 275**,** 28593-28598.

DEKKER, L. & POLIZZI, K. M. 2017. Sense and sensitivity in bioprocessing-detecting cellular metabolites with biosensors. *Curr Opin Chem Biol,* 40**,** 31-36.

DENNIS, D., MCCOY, M., STANGL, A., VALENTIN, H. E. & WU, Z. 1998. Formation of poly(3-hydroxybutyrate-co-3-hydroxyhexanoate) by PHA synthase from *Ralstonia eutropha*. *Journal of Biotechnology,* 64**,** 177-186.

DERBISE, A., LESIC, B., DACHEUX, D., GHIGO, J. M. & CARNIEL, E. 2003. A rapid and simple method for inactivating chromosomal genes in *Yersinia*. *Fems Immunology and Medical Microbiology,* 38**,** 113-116.

DIETRICH, J. A., MCKEE, A. E. & KEASLING, J. D. 2010. High-throughput metabolic engineering: Advances in small-molecule screening and selection. *Annual Review of Biochemistry,* 79**,** 563-590.

DIETRICH, J. A., SHIS, D. L., ALIKHANI, A. & KEASLING, J. D. 2013. Transcription factor-based screens and synthetic selections for microbial small-molecule biosynthesis. *ACS Synthetic Biology,* 2**,** 47-58.

DIRUSSO, C. C., METZGER, A. K. & HEIMERT, T. L. 1993. Regulation of transcription of genes required for fatty-acid transport and unsaturated fatty-acid biosynthesis in *Escherichia coli* by FadR. *Molecular Microbiology,* 7**,** 311-322.

DOI, Y., TAMAKI, A., KUNIOKA, M. & SOGA, K. 1987. Biosynthesis of Terpolyesters of 3-Hydroxybutyrate, 3-Hydroxyvalerate, and 5-Hydroxyvalerate in *Alcaligenes eutrophus* from 5-Chloropentanoic and Pentanoic Acids. *Makromolekulare Chemie-Rapid Communications,* 8**,** 631-635.

DRUMMOND, M. L., CUNDARI, T. R. & WILSON, A. K. 2012. Protein-based carbon capture: progress and potential. *Greenhouse Gases-Science and Technology,* 2**,** 223-238.

DU, G. C., CHEN, J., YU, J. & LUN, S. Y. 2001a. Continuous production of poly-3-hydroxybutyrate by *Ralstonia eutropha* in a two-stage culture system. *Journal of Biotechnology,* 88 59-65.

DU, G. C. C., CHEN, J., YU, J. & LUN, S. Y. 2001b. Feeding strategy of propionic acid for production of poly(3-hydroxybutyrate-co-3-hydroxyvalerate) with *Ralstonia eutropha*. *Biochemical Engineering Journal,* 8**,** 103-110.

DUCAT, D. C., WAY, J. C. & SILVER, P. A. 2011. Engineering cyanobacteria to generate high-value products. *Trends in Biotechnology,* 29**,** 95-103.

ELLIS, H. M., YU, D. G., DITIZIO, T. & COURT, D. L. 2001. High efficiency mutagenesis, repair, and engineering of chromosomal DNA using single-stranded oligonucleotides. *Proceedings of the National Academy of Sciences of the United States of America,* 98**,** 6742-6746.

ELLIS, J. M. & WOLFGANG, M. J. 2012. A genetically encoded metabolite sensor for malonyl-CoA. *Chemistry & Biology,* 19**,** 1333-1339.

ENYEART, P. J., MOHR, G., ELLINGTON, A. D. & LAMBOWITZ, A. M. 2014. Biotechnological applications of mobile group II introns and their reverse transcriptases: gene targeting, RNA-seq, and non-coding RNA analysis. *Mobile DNA,* 5.

ESVELT, K. M. & WANG, H. H. 2013. Genome-scale engineering for systems and synthetic biology. *Molecular Systems Biology,* 9.

EWERING, C., HEUSER, F., BENOELKEN, J. K., BRAEMER, C. O. & STEINBUECHEL, A. 2006. Metabolic engineering of strains of *Ralstonia eutropha* and *Pseudomonas putida* for biotechnological production of 2-methylcitric acid. *Metabolic Engineering,* 8**,** 587-602.

EZEJI, T. C., QURESHI, N. & BLASCHEK, H. P. 2007. Bioproduction of butanol from biomass: from genes to bioreactors. *Current Opinion in Biotechnology,* 18**,** 220-227.

FARMER, W. R. & LIAO, J. C. 2000. Improving lycopene production in *Escherichia coli* by engineering metabolic control. *Nature Biotechnology,* 18**,** 533-537.

FEHER, T., LIBIS, V., CARBONELL, P. & FAULON, J.-L. 2015. A sense of balance: Experimental investigation and modeling of a malonyl-CoA sensor in *Escherichia coli*. *Frontiers in bioengineering and biotechnology,* 3**,** 1-14.

FOLMES, C. D. L. & LOPASCHUK, G. D. 2007. Role of malonyl-CoA in heart disease and the hypothalamic control of obesity. *Cardiovascular Research,* 73**,** 278-287.

FOSTER, D. W. 2012. Malonyl-CoA: the regulator of fatty acid synthesis and oxidation. *Journal of Clinical Investigation,* 122**,** 1958-1959.

FOWLER, Z. L., GIKANDI, W. W. & KOFFAS, M. A. G. 2009. Increased malonyl coenzyme A biosynthesis by tuning the *Escherichia coli* metabolic network and Its application to flavanone production. *Applied and Environmental Microbiology,* 75**,** 5831-5839.

FRANZ, A., REHNER, R., KIENLE, A. & GRAMMEL, H. 2012. Rapid selection of glucose-utilizing variants of the polyhydroxyalkanoate producer *Ralstonia eutropha* H16 by incubation with high substrate levels. *Letters in Applied Microbiology,* 54**,** 45-51.

FUCHTENBUSCH, B., FABRITIUS, D. & STEINBUCHEL, A. 1996. Incorporation of 2-methyl-3-hydroxybutyric acid into polyhydroxyalkanoic acids by axenic cultures in defined media. *Fems Microbiology Letters,* 138 153-160.

FUJITA, Y., MATSUOKA, H. & HIROOKA, K. 2007. Regulation of fatty acid metabolism in bacteria. *Molecular Microbiology,* 66**,** 829-839.

FUKUI, T., ABE, H. & DOI, Y. 2002. Engineering of Ralstonia eutropha for production of poly(3-hydroxybutyrate-*co*-3-hydroxyhexanoate) from fructose and solid-state properties of the copolymer. *Biomacromolecules,* 3**,** 618-624.

FUKUI, T., MUKOYAMA, M., ORITA, I. & NAKAMURA, S. 2014. Enhancement of glycerol utilization ability of *Ralstonia eutropha* H16 for production of polyhydroxyalkanoates. *Applied Microbiology and Biotechnology,* 98**,** 7559-7568.

FUKUI, T., OHSAWA, K., MIFUNE, J., ORITA, I. & NAKAMURA, S. 2011. Evaluation of promoters for gene expression in polyhydroxyalkanoate-producing *Ralstonia eutropha* H16. *Appl Microbiol Biotechnol,* 89**,** 1527-36.

GAI, C. S., LU, J., BRIGHAM, C. J., BERNARDI, A. C. & SINSKEY, A. J. 2014. Insights into bacterial CO2 metabolism revealed by the characterization of four carbonic anhydrases in *Ralstonia eutropha* H16. *AMB Express,* 4**,** 2-2.

GAY, P., LECOQ, D., STEINMETZ, M., BERKELMAN, T. & KADO, C. I. 1985. Positive Selection Procedure for Entrapment of Insertion-Sequence Elements in Gram-negative Bacteria. *Journal of Bacteriology,* 164**,** 918-921.

GENTZ, R. & BUJARD, H. 1985. Promoters recognized by *Escherichia coli* RNA polymerase selected by function: highly efficient promoters from bacteriophage T5. *J Bacteriol,* 164**,** 70-7.

GHERMAN, A., WANG, R. & AVRAMOPOULOS, D. 2009. Orientation, distance, regulation and function of neighbouring genes. *Hum Genomics,* 3**,** 143-56.

GOH, E.-B., BAIDOO, E. E. K., KEASLING, J. D. & BELLER, H. R. 2012. Engineering of Bacterial Methyl Ketone Synthesis for Biofuels. *Applied and Environmental Microbiology,* 78**,** 70-80.

GREEN, P. R., KEMPER, J., SCHECHTMAN, L., GUO, L., SATKOWSKI, M., FIEDLER, S., STEINBUCHEL, A. & REHM, B. H. A. 2002. Formation of short chain length/medium chain length polyhydroxyalkanoate copolymers by fatty acid beta-oxidation inhibited *Ralstonia eutropha*. *Biomacromolecules,* 3**,** 208-213.

GROTHE, E., MOO-YOUNG, M. & CHISTI, Y. 1999. Fermentation optimization for the production of poly(beta-hydroxybutyric acid) microbial thermoplastic. *Enzyme and Microbial Technology,* 25**,** 132-141.

GRUBER, S., HAGEN, J., SCHWAB, H. & KOEFINGER, P. 2014. Versatile and stable vectors for efficient gene expression in *Ralstonia eutropha* H16. *J Biotechnol,* 186**,** 74-82.

GRUBER, S., SCHWENDENWEIN, D., MAGOMEDOVA, Z., THALER, E., HAGEN, J., SCHWAB, H. & HEIDINGER, P. 2016. Design of inducible expression vectors for improved protein production in *Ralstonia eutropha* H16 derived host strains. *J Biotechnol,* 235**,** 92-9.

GUO, Y., DONG, J., ZHOU, T., AUXILLOS, J., LI, T., ZHANG, W., WANG, L., SHEN, Y., LUO, Y., ZHENG, Y., LIN, J., CHEN, G. Q., WU, Q., CAI, Y. & DAI, J. 2015. YeastFab: the design and construction of standard biological parts for metabolic engineering in *Saccharomyces cerevisiae*. *Nucleic Acids Res,* 43**,** e88.

BROWN, A. J., GIBSON, S. J., HATTON, D. & JAMES, D. C. 2017. In silico design of context-responsive mammalian promoters with user-defined functionality. *Nucleic Acids Research,* 45**,** 10906-10919.

BROWN, A. J., SWEENEY, B., MAINWARING, D. O. & JAMES, D. C. 2014. Synthetic Promoters for CHO Cell Engineering. *Biotechnology and Bioengineering,* 111**,** 1638-1647.

DATSENKO, K. A. & WANNER, B. L. 2000. One-step inactivation of chromosomal genes in *Escherichia coli* K-12 using PCR products. *Proceedings of the National Academy of Sciences of the United States of America,* 97**,** 6640-6645.

ENYEART, P. J., MOHR, G., ELLINGTON, A. D. & LAMBOWITZ, A. M. 2014. Biotechnological applications of mobile group II introns and their reverse transcriptases: gene targeting, RNA-seq, and non-coding RNA analysis. *Mobile DNA,* 5.

GUZMAN, L. M., BELIN, D., CARSON, M. J. & BECKWITH, J. 1995. Tight Regulation, Modulation, and High-level expression by Vectors Containing the Arabinose PBAD Promoter. *Journal of Bacteriology,* 177**,** 4121-4130.

JOHNSON, A. O., GONZALEZ-VILLANUEVA, M., TEE, K. L. & WONG, T. S. 2018. An Engineered Constitutive Promoter Set with Broad Activity Range for *Cupriavidus necator* H16. *ACS Synthetic Biology*.

JOHNSON, A. O., V.M., G., WONG, L., STEINBÜCHEL, A., TEE, K. L., XU, P. & WONG, T. S. 2017. Design and application of genetically-encoded malonyl-CoA biosensors for metabolic engineering of microbial cell factories. *Metab Eng,* 44**,** 253-264.

KOVACH, M. E., PHILLIPS, R. W., ELZER, P. H., ROOP, R. M. & PETERSON, K. M. 1994. pBBR1MCS - A Broad-Host-Range Cloning Vector. *Biotechniques,* 16**,** 800-&.

TEE, K. L., GRINHAM, J., OTHUSITSE, A. M., GONZALEZ-VILLANUEVA, M., JOHNSON, A. O. & WONG, T. S. 2017. An Efficient Transformation Method for the Bioplastic-Producing "Knallgas" Bacterium *Ralstonia eutropha* H16. *Biotechnol J,* 12.

XIONG, B., LI, Z., LIU, L., ZHAO, D., ZHANG, X. & BI, C. 2018. Genome editing of Ralstonia eutropha using an electroporation-based CRISPR-Cas9 technique. *Biotechnology for Biofuels,* 11.

HANKO, E. K. R., MINTON, N. P. & MALYS, N. 2017. Characterisation of a 3-hydroxypropionic acid-inducible system from *Pseudomonas putida* for orthogonal

gene expression control in *Escherichia coli* and *Ralstonia eutropha*. *Sci Rep,* 7**,** 1724.

HARRISON, M. E. & DUNLOP, M. J. 2012. Synthetic feedback loop model for increasing microbial biofuel production using a biosensor. *Frontiers in Microbiology,* 3**,** 1-9.

HATTI-KAUL, R., TORNVALL, U., GUSTAFSSON, L. & BORJESSON, P. 2007. Industrial biotechnology for the production of bio-based chemicals - a cradle-to-grave perspective. *Trends in Biotechnology,* 25**,** 119-124.

HATZIMANIKATIS, V., LI, C. H., IONITA, J. A., HENRY, C. S., JANKOWSKI, M. D. & BROADBELT, L. J. 2005. Exploring the diversity of complex metabolic networks. *Bioinformatics,* 21**,** 1603-1609.

HENDERSON, R. A. & JONES, C. W. 1997 Poly-3-hydroxybutyrate production by washed cells of *Alcaligenes eutrophus*; purification, characterisation and potential regulatory role of citrate synthase. *Archives of Microbiology,* 168**,** 486-492.

HENRY, C. S., BROADBELT, L. J. & HATZIMANIKATIS, V. 2010. Discovery and Analysis of Novel Metabolic Pathways for the Biosynthesis of Industrial Chemicals: 3-Hydroxypropanoate. *Biotechnology and Bioengineering,* 106**,** 462-473.

HOLTZ, W. J. & KEASLING, J. D. 2010. Engineering static and dynamic control of synthetic pathways. *Cell,* 140**,** 19-23.

ISHIZAKI, A., TAGA, N., TAKESHITA, T., SUGIMOTO, T., TSUGE, T. & TANAKA, K. 1997. Microbial production of biodegradable plastics from carbon dioxide and agricultural waste material. *Fuels and Chemicals from Biomass,* 666**,** 294-306.

ISHIZAKI, A., TANAKA, K. & TAGA, N. 2001. Microbial production of poly-D-3-hydroxybutyrate from CO2. *Applied Microbiology and Biotechnology,* 57**,** 6-12.

JAIN, A. & SRIVASTAVA, P. 2013. Broad host range plasmids. *Fems Microbiology Letters,* 348**,** 87-96.

JAJESNIAK, P., OMAR ALI, H. E. M. & WONG, T. S. 2014. Carbon dioxide capture and utilization using biological systems: Opportunities and challenges. *J Bioprocess Biotech,* 4**,** 155.

JAMES, E. S. & CRONAN, J. E. 2003. Never fat or gaunt. *Developmental Cell,* 4**,** 610-611.

JIANG, W., BIKARD, D., COX, D., ZHANG, F. & MARRAFFINI, L. A. 2013. RNA-guided editing of bacterial genomes using CRISPR-Cas systems. *Nature Biotechnology,* 31**,** 233-239.

JOHNSON, A. O., GONZALEZ, V. M., TEE, K. L. & WONG, T. S. 2018. An engineered constitutive promoter set with broad activity range for *Cupriavidus necator* H16. *ACS Synth Biol*.

JOHNSON, A. O., GONZALEZ-VILLANUEVA, M., WONG, L., STEINBÜCHEL, A., TEE, K. L., XU, P. & WONG, T. S. 2017. Design and application of genetically-encoded malonyl-CoA biosensors for metabolic engineering of microbial cell factories. *Metab Eng,* 44**,** 253-264.

JONES, J. P., KIERLIN, M. N., COON, R. G., PERUTKA, J., LAMBOWITZ, A. M. & SULLENGER, B. A. 2005. Retargeting mobile group II introns to repair mutant genes. *Molecular Therapy,* 11**,** 687-694.

JUNG, Y.-M. & LEE, Y.-H. 2000. Utilization of oxidative pressure for enhanced production of poly-β-hydroxybutyrate and poly(3-hydroxybutyrate-3-hydroxyvalerate) in *Ralstonia eutropha*. *Journal of Bioscience and Bioengineering,* 90**,** 266-270.

JUNG, Y. M., PARK, J. S. & LEE, Y. H. 2000. Metabolic engineering of *Alcaligenes eutrophus* through the transformation of cloned phbCAB genes for the investigation

of the regulatory mechanism of polyhydroxyalkanoate biosynthesis. *Enzyme and Microbial Technology.* , 26 201-208.

KAHAR, P., TSUGE, T., TAGUCHI, K. & DOI, Y. 2004. High yield production of polyhydroxyalkanoates from soybean oil by *Ralstonia eutropha* and its recombinant strain. *Polymer Degradation and Stability,* 83**,** 79-86.

KARAKOUSIS, G., YE, N., LI, Z., CHIU, S. K., REDDY, G. & RADDING, C. M. 1998. The beta protein of phage lambda binds preferentially to an intermediate in DNA renaturation. *Journal of Molecular Biology,* 276**,** 721-731.

KATASHKINA, J. I., HARA, Y., GOLUBEVA, L. I., ANDREEVA, I. G., KUVAEVA, T. M. & MASHKO, S. V. 2009. Use of the lambda Red-recombineering method for genetic engineering of *Pantoea ananatis*. *Bmc Molecular Biology,* 10.

KEASLING, J. D. 2012. Synthetic biology and the development of tools for metabolic engineering. *Metab Eng,* 14**,** 189-95.

KELL, D. B., SWAINSTON, N., PIR, P. & OLIVER, S. G. 2015. Membrane transporter engineering in industrial biotechnology and whole cell biocatalysis. *Trends in Biotechnology,* 33**,** 237–246.

KESSLER, B. & WITHOLT, B. 2001. Factors involved in the regulatory network of polyhydroxyalkanoate metabolism. *Journal of Biotechnology,* 86**,** 97-104.

KHALIL, A. S. & COLLINS, J. J. 2010. Synthetic biology: applications come of age. *Nature Reviews Genetics,* 11**,** 367-379.

KIM, B. S., LEE, S. C., LEE, S. Y., CHANG, H. N., CHANG, Y. K. & WOO, S. I. 1994. Production of Poly(3-Hydroxybutyric Acid) By Fed-Batch Culture Of *Alcaligenes eutrophus* With Glucose-Concentration Control. *Biotechnology and Bioengineering,* 43.

KIM, H. Y., PARK, J. S., SHIN, H. D. & LEE, Y. H. 1995. Isolation of glucose utilizing mutant of *Alcaligenes eutrophus*, its substrate selectivity, and accumulation of poly-beta-hydroxybutyrate. *Journal of Microbiology,* 33**,** 51-58.

KOUTINAS, M., KIPARISSIDES, A., PISTIKOPOULOS, E. N. & MANTALARIS, A. 2012. Bioprocess systems engineering: transferring traditional process engineering principles to industrial biotechnology. *Computational and structural biotechnology journal,* 3**,** e201210022-e201210022.

KOVACH, M. E., ELZER, P. H., HILL, D. S., ROBERTSON, G. T., FARRIS, M. A., ROOP, R. M. & PETERSON, K. M. 1995. 4 New Derivatives of the Broad-Host-Range Cloning vector pBBR1MCS, Carrying Different Antibiotic-Resistance Cassettes. *Gene,* 166**,** 175-176.

KOVACH, M. E., PHILLIPS, R. W., ELZER, P. H., ROOP, R. M. & PETERSON, K. M. 1994. pBBR1MCS - A Broad-Host-Range Cloning Vector. *Biotechniques,* 16**,** 800-&.

KROLL, J., KLINTER, S., SCHNEIDER, C., VOSS, I. & STEINBUCHEL, A. 2010. Plasmid addiction systems: perspectives and applications in biotechnology. *Microbial Biotechnology,* 3**,** 634-657.

KUNIOKA, M., KAWAGUCHI, Y. & DOI, Y. 1989. Production of Biodegradable Copolyesters of 3-Hydroxybutyrate and 4-Hydroxybutyrate by *Alcaligenes eutrophus*. *Applied Microbiology and Biotechnology,* 30 569-573.

KUSIAN, B., SULTEMEYER, D. & BOWIEN, B. 2002. Carbonic anhydrase is essential for growth of *Ralstonia eutropha* at ambient CO2 concentrations. *Journal of Bacteriology,* 184**,** 5018-5026.

KUTUZOVA, G. I., FRANK, G. K., MAKEEV, V., ESIPOVA, N. G. & POLOZOV, R. V. 1997. [Fourier analysis of nucleotide sequences. Periodicity in *E. coli* promoter sequences]. *Biofizika,* 42**,** 354-62.

LAMBOWITZ, A. M. 2011. Mobile Group II Introns: Site-Specific DNA Integration and Applications in Gene Targeting. *Faseb Journal,* 25.

LAMBOWITZ, A. M. & ZIRNMERLY, S. 2004. Mobile group II introns. *Annual Review of Genetics,* 38**,** 1-35.

LEE, I. Y., KIM, G. J., SHIN, Y. C., CHANG, H. N. & PARK, Y. H. 1995. Production of Poly(beta-hydroxybutyrate-*co*-beta-hydroxyvalerate) by 2-Stage Fed-Batch Fermentation of *Alcaligenes eutrophus*. *Journal of Microbiology and Biotechnology,* 5**,** 292-296.

LEE, J. W., NA, D., PARK, J. M., LEE, J., CHOI, S. & LEE, S. Y. 2012. Systems metabolic engineering of microorganisms for natural and non-natural chemicals. *Nature Chemical Biology,* 8**,** 536-546.

LEE, S. Y. 1996. Plastic bacteria? Progress and prospects for polyhydroxyalkanoate production in bacteria. *Trends in Biotechnology,* 14**,** 431-438.

LEE, T. S., KRUPA, R. A., ZHANG, F., HAJIMORAD, M., HOLTZ, W. J., PRASAD, N., LEE, S. K. & KEASLING, J. D. 2011. BglBrick vectors and datasheets: A synthetic biology platform for gene expression. *J Biol Eng,* 5**,** 12.

LEONARD, E., LIM, K. H., SAW, P. N. & KOFFAS, M. A. G. 2007. Engineering central metabolic pathways for high-level flavonoid production in *Escherichia coli*. *Applied and Environmental Microbiology,* 73**,** 3877-3886.

LESIC, B. & RAHME, L. G. 2008. Use of the lambda Red recombinase system to rapidly generate mutants in *Pseudomonas aeruginosa*. *Bmc Molecular Biology,* 9.

LEWIS, N. E., NAGARAJAN, H. & PALSSON, B. O. 2012. Constraining the metabolic genotype-phenotype relationship using a phylogeny of *in silico* methods. *Nature Reviews Microbiology,* 10**,** 291-305.

LI, H. & LIAO, J. C. 2015. A Synthetic Anhydrotetracycline-Controllable Gene Expression System in *Ralstonia eutropha* H16. *ACS Synthetic Biology,* 4**,** 101-106.

LI, H., OPGENORTH, P. H., WERNICK, D. G., ROGERS, S., WU, T.-Y., HIGASHIDE, W., MALATI, P., HUO, Y.-X., CHO, K. M. & LIAO, J. C. 2012. Integrated Electromicrobial Conversion of CO2 to Higher Alcohols. *Science,* 335**,** 1596-1596.

LI, S. J., SI, T., WANG, M. & ZHAO, H. M. 2015. Development of a Synthetic Malonyl-CoA Sensor in *Saccharomyces cerevisiae* for Intracellular Metabolite Monitoring and Genetic Screening. *ACS Synthetic Biology,* 4**,** 1308-1315.

LI, Z., KARAKOUSIS, G., CHIU, S. K., REDDY, G. & RADDING, C. M. 1998. The beta protein of phage lambda promotes strand exchange. *Journal of Molecular Biology,* 276**,** 733-744.

LIAO, J. C. & OH, M. K. 1999. Toward predicting metabolic fluxes in metabolically engineered strains. *Metabolic Engineering,* 1**,** 214-223.

LIM, S. I., MIN, B. E. & JUNG, G. Y. 2008. Lagging Strand-Biased Initiation of Red Recombination by Linear Double-Stranded DNAS. *Journal of Molecular Biology,* 384**,** 1098-1105.

LINDE, M., GALBE, M. & ZACCHI, G. 2008. Bioethanol production from non-starch carbohydrate residues in process streams from a dry-mill ethanol plant. *Bioresource Technology,* 99**,** 6505-6511.

LINDENKAMP, N., VOLODINA, E. & STEINBUECHEL, A. 2012. Genetically Modified Strains of *Ralstonia eutropha* H16 with beta-Ketothiolase Gene Deletions for

Production of Copolyesters with Defined 3-Hydroxyvaleric Acid Contents. *Applied and Environmental Microbiology,* 78**,** 5375-5383.
LIU, D., EVANS, T. & ZHANG, F. Z. 2015a. Applications and advances of metabolite biosensors for metabolic engineering. *Metabolic Engineering,* 31**,** 35-43.
LIU, D., XIAO, Y., EVANS, B. S. & ZHANG, F. 2015b. Negative feedback regulation of fatty acid production based on a malonyl-CoA sensor-actuator. *ACS Synthetic Biology,* 4**,** 132-140.
LOO, C.-Y. & SUDESH, K. 2007. Polyhydroxyalkanoates: Bio-based microbial plastics and their properties. *Malaysian Polymer Journal,* 2**,** 31-57.
LOO, C. Y., LEE, W. H., TSUGE, T., DOI, Y. & SUDESH, K. 2005. Biosynthesis and characterization of poly(3-hydroxybutyrate-*co*-3-hydroxyhexanoate) from palm oil products in a *Wautersia eutropha* mutant. *Biotechnology Letters,* 27**,** 1405-1410.
LU, J., BRIGHAM, C. J., GAI, C. S. & SINSKEY, A. J. 2012. Studies on the production of branched-chain alcohols in engineered *Ralstonia eutropha*. *Appl Microbiol Biotechnol,* 96**,** 283-97.
LUETTE, S., POHLMANN, A., ZAYCHIKOV, E., SCHWARTZ, E., BECHER, J. R., HEUMANN, H. & FRIEDRICH, B. 2012. Autotrophic Production of Stable-Isotope-Labeled Arginine in *Ralstonia eutropha* Strain H16. *Applied and Environmental Microbiology,* 78**,** 7884-7890.
LUTKE-EVERSLOH, T., BERGANDER, K., LUFTMANN, H. & STEINBUCHEL, A. 2001. Biosynthesis of poly(3-hydroxybutyrate-*co*-3-mercaptobutyrate) as a sulfur analogue to poly(3-hydroxybutyrate) (PHB). *Biomacromolecules,* 2**,** 1061-1065.
LUTKE-EVERSLOH, T., KAWADA, J., MARCHESSAULT, R. H. & STEINBUCHEL, A. 2002. Characterization of microbial polythioesters: Physical properties of novel copolymers synthesized by *Ralstonia eutropha*. *Biomacromolecules,* 3**,** 159-166.
LUTKE-EVERSLOH, T. & STEINBÜCHEL, A. 2003. Novel precursor substrates for polythioesters (PTE) and limits of PTE biosynthesis in *Ralstonia eutropha*. *FEMS Microbiol Lett,* 221**,** 191-6.
MADDEN, L. A., ANDERSON, A. J., ASRAR, J., BERGER, P. & GARRETT, P. 2000. Production and characterization of poly(3-hydroxybutyrate-co-3-hydroxyvalerate-co-4-hydroxybutyrate) synthesized by *Ralstonia eutropha* in fed-batch cultures. . *Polymer,* 41**,** 3499-3505.
MAGNUSON, K., JACKOWSKI, S., ROCK, C. O. & CRONAN, J. E. 1993. Regulation of fatty-acid biosynthesis in *Escherichia coli*. *Microbiological Reviews,* 57**,** 522-542.
MAINGUET, S. E. & LIAO, J. C. 2010. Bioengineering of microorganisms for C-3 to C-5 alcohols production. *Biotechnology Journal,* 5**,** 1297-1308.
MARC, J., GROUSSEAU, E., LOMBARD, E., SINSKEY, A. J., GORRET, N. & GUILLOUET, S. E. 2017. Over expression of GroESL in *Ralstonia eutropha* for heterotrophic and autotrophic isopropanol production. *Metab Eng,* 42**,** 74-84.
MARRAKCHI, H., PATEL, D. & ROCK, C. 2001. Regulation of fatty acid biosynthesis and degradation in *Escherichia coli*. *Faseb Journal,* 15**,** A192-A192.
MCNERNEY, M. P., WATSTEIN, D. M. & STYCZYNSKI, M. P. 2015. Precision metabolic engineering: The design of responsive, selective, and controllable metabolic systems. *Metab Eng,* 31**,** 123-31.
MEDEMA, M. H., VAN RAAPHORST, R., TAKANO, E. & BREITLING, R. 2012. Computational tools for the synthetic design of biochemical pathways. *Nature Reviews Microbiology,* 10**,** 191-202.
MIYAHISA, I., KANEKO, M., FUNA, N., KAWASAKI, H., KOJIMA, H., OHNISHI, Y. & HORINOUCHI, S. 2005. Efficient production of (2S)-flavanones by *Escherichia*

coli containing an artificial biosynthetic gene cluster. *Applied Microbiology and Biotechnology,* 68**,** 498-504.

MOHRLE, V., STADLER, M. & EBERZ, G. 2007. Biosensor-guided screening for macrolides. *Analytical and Bioanalytical Chemistry,* 388**,** 1117-1125.

MOSBERG, J. A., GREGG, C. J., LAJOIE, M. J., WANG, H. H. & CHURCH, G. M. 2012. Improving Lambda Red Genome Engineering in *Escherichia coli* via Rational Removal of Endogenous Nucleases. *Plos One,* 7.

MOSBERG, J. A., LAJOIE, M. J. & CHURCH, G. M. 2010. Lambda Red Recombineering in *Escherichia coli* Occurs Through a Fully Single-Stranded Intermediate. *Genetics,* 186**,** 791-U59.

MUELLER, J., MACEACHRAN, D., BURD, H., SATHITSUKSANOH, N., BI, C., YEH, Y.-C., LEE, T. S., HILLSON, N. J., CHHABRA, S. R., SINGER, S. W. & BELLER, H. R. 2013. Engineering of *Ralstonia eutropha* H16 for Autotrophic and Heterotrophic Production of Methyl Ketones. *Applied and Environmental Microbiology,* 79**,** 4433-4439.

MUNOZ-LOPEZ, M. & GARCIA-PEREZ, J. L. 2010. DNA Transposons: Nature and Applications in Genomics. *Current Genomics,* 11**,** 115-128.

MURPHY, K. C. 1991. Lambda-Gam Protein Inhibits The Helicase And Chi-Stimulated Recombination Activities of *Escherichia coli* RECBCD Enzyme. *Journal of Bacteriology,* 173**,** 5808-5821.

MURPHY, K. C. 1998. Use of bacteriophage lambda recombination functions to promote gene replacement in Escherichia coli. *Journal of Bacteriology,* 180**,** 2063-2071.

MURPHY, K. C. & CAMPELLONE, K. G. 2003. Lambda Red-mediated recombinogenic engineering of enterohemorrhagic and enteropathogenic E-coli. *Bmc Molecular Biology,* 4.

NAKASHIMA, N. & MIYAZAKI, K. 2014. Bacterial Cellular Engineering by Genome Editing and Gene Silencing. *International Journal of Molecular Sciences,* 15**,** 2773-2793.

NIELSEN, J. & KEASLING, J. D. 2016. Engineering Cellular Metabolism. *Cell,* 164**,** 1185-1197.

NUNN, W. D., KELLY, D. L. & STUMFALL, M. Y. 1977. Regulation of fatty-acid synthesis during cessation of phospholipid biosynthesis in *Escherichia coli*. *Journal of Bacteriology,* 132**,** 526-531.

ODA, T., ODA, K., YAMAMOTO, H., MATSUYAMA, A., ISHII, M., IGARASHI, Y. & NISHIHARA, H. 2013. Hydrogen-driven asymmetric reduction of hydroxyacetone to (R)-1,2-propanediol by *Ralstonia eutropha* transformant expressing alcohol dehydrogenase from *Kluyveromyces lactis*. *Microbial Cell Factories,* 12.

OPPENHEIM, A. B., RATTRAY, A. J., BUBUNENKO, M., THOMASON, L. C. & COURT, D. L. 2004. In vivo recombineering of bacteriophage lambda by PCR fragments and single-strand oligonucleotides. *Virology,* 319**,** 185-189.

OVERHAGE, J., STEINBUCHEL, A. & PRIEFERT, H. 2002. Biotransformation of eugenol to ferulic acid by a recombinant strain of *Ralstonia eutropha* H16. *Applied and Environmental Microbiology,* 68**,** 4315-4321.

PARDELHA, F., ALBUQUERQUE, M. G. E., REIS, M. A. M., DIAS, J. M. L. & OLIVEIRA, R. 2012. Flux balance analysis of mixed microbial cultures: Application to the production of polyhydroxyalkanoates from complex mixtures of volatile fatty acids. *Journal of Biotechnology,* 162**,** 336-345.

PARIKH, M. R., GREENE, D. N., WOODS, K. K. & MATSUMURA, I. 2006. Directed evolution of RuBisCO hypermorphs through genetic selection in engineered *E. coli*. *Protein Engineering Design & Selection,* 19**,** 113-119.

PARK, H. C., LIM, K. J., PARK, J. S., LEE, Y. H. & HUH, T. L. 1995. High-Frequency Transformation of *Alcaligenes eutrophus* producing Poly-Beta-Hydroxybutyric Acid by Electroporation. *Biotechnology Techniques,* 9**,** 31-34.

PARK, J. M., JANG, Y. S., KIM, T. Y. & LEE, S. Y. 2010. Development of a gene knockout system for *Ralstonia eutropha* H16 based on the broad-host-range vector expressing a mobile group II intron. *FEMS Microbiol Lett,* 309**,** 193-200.

PARK, J. M., KIM, T. Y. & LEE, S. Y. 2011. Genome-scale reconstruction and in silico analysis of the *Ralstonia eutropha* H16 for polyhydroxyalkanoate synthesis, lithoautotrophic growth, and 2-methyl citric acid production. *Bmc Systems Biology,* 5.

PARK., J. S., HUH., T. L. & LEE., Y. H. 1997. Characteristics of cell growth and poly-β-hydroxybutyrate biosynthesis of *Alcaligenes eutrophus* transformants harboring cloned phbCAB genes.

PAULUS, M., HASLBECK, M. & WATZELE, M. 2004. RNA stem-loop enhanced expression of previously non-expressible genes. *Nucleic Acids Research,* 32.

PEPLOW, M. 2015. Industrial biotechs turn greenhouse gas into feedstock opportunity. *Nat Biotechnol,* 33**,** 1123-5.

PERETTI, S. W. & BAILEY, J. E. 1987. Simulations of host-plasmid interactions in *Escherichia coli* - copy number, promoter strength, and ribosome binding-site strength effects on metabolic-activity and plasmid gene-expression. *Biotechnology and Bioengineering,* 29**,** 316-328.

PERUTKA, J., WANG, W. J., GOERLITZ, D. & LAMBOWITZ, A. M. 2004. Use of computer-designed group II introns to disrupt *Escherichia coli* DExH/D-box protein and DNA helicase genes. *Journal of Molecular Biology,* 336**,** 421-439.

PHARKYA, P., BURGARD, A. P. & MARANAS, C. D. 2004. OptStrain: A computational framework for redesign of microbial production systems. *Genome Research,* 14**,** 2367-2376.

PHELAN, R. M., SACHS, D., PETKIEWICZ, S. J., BARAJAS, J. F., BLAKE-HEDGES, J. M., THOMPSON, M. G., REIDER APEL, A., RASOR, B. J., KATZ, L. & KEASLING, J. D. 2017. Development of Next Generation Synthetic Biology Tools for Use in Streptomyces venezuelae. *ACS Synth Biol,* 6**,** 159-166.

POHLMANN, A., FRICKE, W. F., REINECKE, F., KUSIAN, B., LIESEGANG, H., CRAMM, R., EITINGER, T., EWERING, C., PÖTTER, M., SCHWARTZ, E., STRITTMATTER, A., VOSS, I., GOTTSCHALK, G., STEINBÜCHEL, A., FRIEDRICH, B. & BOWIEN, B. 2006. Genome sequence of the bioplastic-producing "Knallgas" bacterium *Ralstonia eutropha* H16. *Nat Biotechnol,* 24**,** 1257-62.

POSFAI, G., PLUNKETT, G., FEHER, T., FRISCH, D., KEIL, G. M., UMENHOFFER, K., KOLISNYCHENKO, V., STAHL, B., SHARMA, S. S., DE ARRUDA, M., BURLAND, V., HARCUM, S. W. & BLATTNER, F. R. 2006. Emergent properties of reduced-genome *Escherichia coli*. *Science,* 312**,** 1044-1046.

POTEETE, A. R. 2001. What makes the bacteriophage lambda Red system useful for genetic engineering: molecular mechanism and biological function. *Fems Microbiology Letters,* 201**,** 9-14.

PRIES, A., STEINBUCHEL, A. & SCHLEGEL, H. G. 1990. Lactose-utilizing and Galactose-utilizing Strains of Poly(Hydroxyalkanoic Acid)-Accumulating

Alcaligenes eutrophus and *Pseudomonas saccharophila* obtained by Recombinant-DNA Technology. *Applied Microbiology and Biotechnology,* 33**,** 410-417.

QUANDT, J. & HYNES, M. F. 1993. Versatile suicide vectors which allow direct selection for gene replacement in Gram-negative bacteria. *Gene,* 127**,** 15-21.

RABERG, M., HEINRICH, D. & STEINBÜCHEL, A. 2015. Analysis of phb metabolism applying Tn5 mutagenesis in *Ralstonia eutropha*. *In:* MCGENITY, T., TIMMIS, K. & NOGALES, B. (eds.) *Hydrocarbon and Lipid Microbiology Protocols. Springer Protocols Handbooks.* Berlin, Heidelberg: Springer.

RABERG, M., PEPLINSKI, K., HEISS, S., EHRENREICH, A., VOIGT, B., DOERING, C., BOEMEKE, M., HECKER, M. & STEINBUECHEL, A. 2011. Proteomic and Transcriptomic Elucidation of the Mutant *Ralstonia eutropha* G(+)1 with Regard to Glucose Utilization. *Applied and Environmental Microbiology,* 77**,** 2058-2070.

RAUCH, R., HRBEK, J. & HOFBAUER, H. 2014. Biomass gasification for synthesis gas production and applications of the syngas. *Wiley Interdisciplinary Reviews-Energy and Environment,* 3**,** 343-362.

REED, D. C., BARNARD, G. C., ANDERSON, E. B., KLEIN, L. T. & GERNGROSS, T. U. 2006. Production and purification of self-assembling peptides in *Ralstonia eutropha*. *Protein Expression and Purification,* 46**,** 179-188.

REHM, B. H. A. 2010. Bacterial polymers: biosynthesis, modifications and applications. *Nature Reviews Microbiology,* 8**,** 578-592.

REINECKE, F. & STEINBUECHEL, A. 2009. *Ralstonia eutropha* Strain H16 as Model Organism for PHA Metabolism and for Biotechnological Production of Technically Interesting Biopolymers. *Journal of Molecular Microbiology and Biotechnology,* 16**,** 91-108.

REZNIKOFF, W. S. 1993. The Tn5 Transposon. *Annual Review of Microbiology,* 47**,** 945-963.

REZNIKOFF, W. S. 2003. Tn5 as a model for understanding DNA transposition. *Molecular Microbiology,* 47**,** 1199-1206.

RIEDEL, S. L., BADER, J., BRIGHAM, C. J., BUDDE, C. F., YUSOF, Z. A. M., RHA, C. & SINSKEY, A. J. 2012. Production of poly(3-hydroxybutyrate-*co*-3-hydroxyhexanoate) by *Ralstonia eutropha* in high cell density palm oil fermentations. *Biotechnology and Bioengineering,* 109**,** 74-83.

ROCHELLE, G. T. 2009. Amine Scrubbing for CO2 Capture. *Science,* 325**,** 1652-1654.

ROGERS, J. K. & CHURCH, G. M. 2016. Genetically encoded sensors enable real-time observation of metabolite production. *Proceedings of the National Academy of Sciences of the United States of America,* 113**,** 2388-2393.

ROGERS, J. K., GUZMAN, C. D., TAYLOR, N. D., RAMAN, S., ANDERSON, K. & CHURCH, G. M. 2015. Synthetic biosensors for precise gene control and real-time monitoring of metabolites. *Nucleic Acids Research,* 43**,** 7648-7660.

ROGERS, J. K., TAYLOR, N. D. & CHURCH, G. M. 2016. Biosensor-based engineering of biosynthetic pathways. *Curr Opin Biotechnol,* 42**,** 84-91.

SCHALLMEY, M., FRUNZKE, J., EGGELING, L. & MARIENHAGEN, J. 2014. Looking for the pick of the bunch: high-throughput screening of producing microorganisms with biosensors. *Curr Opin Biotechnol,* 26**,** 148-54.

SCHLEGEL, H. G. & GOTTSCHA.G 1965. Verwertung Von Glucose Durch Eine mutante Von *Hydrogenomas* H16. *Biochemische Zeitschrift,* 341**,** 249-&.

SCHLEGEL, H. G., KALTWASSER, H. & GOTTSCHALK, G. 1961. [A submersion method for culture of hydrogen-oxidizing bacteria: growth physiological studies]. *Arch Mikrobiol,* 38**,** 209-22.

SCHLEGEL, H. G., LAFFERTY, R. & KRAUSS, I. 1970. Isolation of Mutants Not Accumulating Poly-beta-hydroxybutyric acid. *Archiv Fur Mikrobiologie,* 71**,** 283-&.
SCHRAG, D. P. 2007. Preparing to capture carbon. *Science,* 315**,** 812-813.
SCHUJMAN, G. E., ALTABE, S. & DE MENDOZA, D. 2008. A malonyl-CoA-dependent switch in the bacterial response to a dysfunction of lipid metabolism. *Molecular Microbiology,* 68**,** 987-996.
SCHUJMAN, G. E., GUERIN, M., BUSCHIAZZO, A., SCHAEFFER, F., LLARRULL, L. I., REH, G., VILA, A. J., ALZARI, P. M. & DE MENDOZA, D. 2006. Structural basis of lipid biosynthesis regulation in Gram-positive bacteria. *EMBO Journal,* 25**,** 4074-4083.
SCHUJMAN, G. E., PAOLETTI, L., GROSSMAN, A. D. & DE MENDOZA, D. 2003. FapR, a bacterial transcription factor involved in global regulation of membrane lipid biosynthesis. *Developmental Cell,* 4**,** 663-672.
SCHWARTZ, E., HENNE, A., CRAMM, R., EITINGER, T., FRIEDRICH, B. & GOTTSCHALK, G. 2003. Complete nucleotide sequence of pHG1: A *Ralstonia eutropha* H16 megaplasmid encoding key enzymes of H-2-based lithoautotrophy and anaerobiosis. *Journal of Molecular Biology,* 332**,** 369-383.
SERGUEEV, K., YU, D. G., AUSTIN, S. & COURT, D. 2001. Cell toxicity caused by products of the p(L) operon of bacteriophage lambda. *Gene,* 272**,** 227-235.
SHI, S. B., CHEN, Y., SIEWERS, V. & NIELSEN, J. 2014. Improving production of malonyl coenzyme A-derived metabolites by abolishing Snf1-dependent regulation of Acc1. *Mbio,* 5**,** 1-8.
SICHWART, S., HETZLER, S., BROEKER, D. & STEINBUECHEL, A. 2011. Extension of the Substrate Utilization Range of *Ralstonia eutropha* Strain H16 by Metabolic Engineering To Include Mannose and Glucose. *Applied and Environmental Microbiology,* 77**,** 1325-1334.
SOLAIMAN, D. K. Y., SWINGLE, B. M. & ASHBY, R. D. 2010. A new shuttle vector for gene expression in biopolymer-producing Ralstonia eutropha. *Journal of Microbiological Methods,* 82**,** 120-123.
SONG, C. W., LEE, J. & LEE, S. Y. 2015. Genome engineering and gene expression control for bacterial strain development. *Biotechnology Journal,* 10**,** 56-68.
SOUCAILLE, P. 2002. Metabolic pathway engineering for the production of 1,3-propanediol from glucose. *Abstracts of Papers American Chemical Society,* 224**,** 129-BIOT 129.
STEINBUCHEL, A. & LUTKE-EVERSLOH, T. 2003. Metabolic engineering and pathway construction for biotechnological production of relevant polyhydroxyalkanoates in microorganisms. *Biochemical Engineering Journal,* 16**,** 81-96.
STEINBUCHEL, A. & PIEPER, U. 1992. Production of a Copolymer of 3-Hydroxybutyric Acid and 3-Hydrovaleric Acid From Single Unrelated Carbon-Sources by a Mutant of *Alcaligenes eutrophus*. *Applied Microbiology and Biotechnology,* 37 1-6.
STEINBÜCHEL, A. & PIEPER, U. 1992. Production of a copolyester of 3-hydroxybutyric acid and 3-hydroxyvaleric acid from single unrelated carbon sources by a mutant of *Alcaligenes eutrophus*. *Appl Microbiol Biotechnol,* 37**,** 1-6.
SUGIMOTO, T., TSUGE, T., TANAKA, K. & ISHIZAKI, A. 1999. Control of acetic acid concentration by pH-Stat continuous substrate feeding in heterotrophic culture phase of two-stage cultivation of *Alcaligenes eutrophus* for production of P(3HB) from CO2, H-2, and O2 under non-explosive conditions. *Biotechnology and Bioengineering,* 62**,** 625-631.

TAGA, N., TANAKA, K. & ISHIZAKI, A. 1997. Effects of rheological change by addition of carboxymethylcellulose in culture media of an air-lift fermentor on poly-D-3-hydroxybutyric acid productivity in autotrophic culture of hydrogen-oxidizing Bacterium, *Alcaligenes eutrophus*. *Biotechnology and Bioengineering,* 53**,** 529-533.

TAKAMURA, Y., KITAYAMA, Y., ARAKAWA, A., YAMANAKA, S., TOSAKI, M. & OGAWA, Y. 1985. Malonyl-CoA-acetyl-CoA cycling - A new micromethod for determination of acyl-CoAs with malonate decarboxylase. *Biochimica Et Biophysica Acta,* 834**,** 1-7.

TAKAMURA, Y. & NOMURA, G. 1988. Changes in the intracellular concentration of acetyl-CoA and malonyl-CoA in relation to the carbon and energy-metabolism of *Escherichia coli*-K12. *Journal of General Microbiology,* 134**,** 2249-2253.

TANAKA, K., ISHIZAKI, A., KANAMARU, T. & KAWANO, T. 1995. Production of Poly(D-3-hydroxybutyrate) from CO2, H2, and O2 by High Cell density Autotrophc Cultivation of *Alcaligenes eutrophus*. *Biotechnology and Bioengineering,* 45**,** 268-275.

TCHERKEZ, G. G. B., FARQUHAR, G. D. & ANDREWS, T. J. 2006. Despite slow catalysis and confused substrate specificity, all ribulose bisphosphate carboxylases may be nearly perfectly optimized. *Proceedings of the National Academy of Sciences of the United States of America,* 103**,** 7246-7251.

TEE, K. L., GRINHAM, J., OTHUSITSE, A. M., GONZALEZ-VILLANUEVA, M., JOHNSON, A. O. & WONG, T. S. 2017. An Efficient Transformation Method for the Bioplastic-Producing "Knallgas" Bacterium *Ralstonia eutropha* H16. *Biotechnol J,* 12.

TEE, K. L. & WONG, T. S. 2013. Polishing the craft of genetic diversity creation in directed evolution. *Biotechnology Advances,* 31**,** 1707-1721.

TEE, K. L. & WONG, T. S. 2014. Directed Evolution: A Powerful Algorithm for Advancing Synthetic Biology. *In:* SINGH, V. (ed.) *Advanced Synthetic Biology.* USA: Studium Press LLC.

THOMASON, L. C., SAWITZKE, J. A., LI, X., COSTANTINO, N. & COURT, D. L. 2014. Recombineering: genetic engineering in bacteria using homologous recombination. *Current protocols in molecular biology / edited by Frederick M. Ausubel ... [et al.],* 106**,** 1.16.1-1.16.39.

TOKIWA, Y. & UGWU, C. U. 2007. Biotechnological production of (R)-3-hydroxybutyric acid monomer. *Journal of Biotechnology,* 132**,** 264-272.

VALENTIN, H. E., SCHONEBAUM, A. & STEINBUCHEL, A. 1992. Identification of 4-Hydroxyvaleric Acid as a Constituent of Biosynthetic Polyhydroxyalkanoate Acids from Bacteria. *Applied Microbiology and Biotechnology,* 36 507-514.

VALENTIN, H. E. & STEINBUCHEL, A. 1994. Application of Enzymatically Synthesized Short-Chain-Length hydroxy Fatty-Acid Coenzyme-A Thioesters For Assay of Polyhydroxyalkanoic acid Synthases. *Applied Microbiology and Biotechnology,* 40**,** 699-709.

VALENTIN, H. E., ZWINGMANN, G., SCHÖNEBAUM, A. & STEINBÜCHEL, A. 1995. Metabolic pathway for biosynthesis of poly(3-hydroxybutyrate-co-4-hydroxybutyrate) from 4-hydroxybutyrate by *Alcaligenes eutrophus*. *Eur J Biochem,* 227**,** 43-60.

VAN DER MEER, J. R. & BELKIN, S. 2010. Where microbiology meets microengineering: design and applications of reporter bacteria. *Nature Reviews: Microbiology,* 8**,** 511-522.

VOLODINA, E., RABERG, M. & STEINBÜCHEL, A. 2016. Engineering the heterotrophic carbon sources utilization range of *Ralstonia eutropha* H16 for applications in biotechnology. *Crit Rev Biotechnol,* 36**,** 978-991.

VOSS, I. & STEINBUCHEL, A. 2006. Application of a KDPG-aldolase gene-dependent addiction system for enhanced production of cyanophycin in *Ralstonia eutropha* strain H16. *Metabolic Engineering,* 8**,** 66-78.

WANG, H. H. & CHURCH, G. M. 2011. Multiplexed Genome Engineering And Genotyping Methods: Applications For Synthetic Biology And Metabolic Engineering. *Synthetic Biology, Pt B: Computer Aided Design and DNA Assembly,* 498**,** 409-426.

WANG, H. H., ISAACS, F. J., CARR, P. A., SUN, Z. Z., XU, G., FOREST, C. R. & CHURCH, G. M. 2009. Programming cells by multiplex genome engineering and accelerated evolution. *Nature,* 460**,** 894-U133.

WARNER, J. R., REEDER, P. J., KARIMPOUR-FARD, A., WOODRUFF, L. B. A. & GILL, R. T. 2010. Rapid profiling of a microbial genome using mixtures of barcoded oligonucleotides. *Nature Biotechnology,* 28**,** 856-U138.

WATTANACHAISAEREEKUL, S., LANTZ, A. E., NIELSEN, M. L. & NIELSEN, J. 2008. Production of the polyketide 6-MSA in yeast engineered for increased malonyl-CoA supply. *Metabolic Engineering,* 10**,** 246-254.

WILLIAMS, T. C., PRETORIUS, I. S. & PAULSEN, I. T. 2016. Synthetic evolution of metabolic productivity using biosensors. *Trends in Biotechnology,* 34**,** 371-381.

WONG, T. S., ZHURINA, D. & SCHWANEBERG, U. 2006. The diversity challenge in directed protein evolution. *Combinatorial Chemistry & High Throughput Screening,* 9**,** 271-288.

WU, J. J., ZHOU, T. T., DU, G. C., ZHOU, J. W. & CHEN, J. 2014. Modular optimization of heterologous pathways for *de novo* synthesis of (2S)-naringenin in *Escherichia coli*. *PLoS One,* 9**,** 1-9.

XU, P., GU, Q., WANG, W. Y., WONG, L., BOWER, A. G. W., COLLINS, C. H. & KOFFAS, M. A. G. 2013. Modular optimization of multi-gene pathways for fatty acids production in *E. coli*. *Nature Communications,* 4**,** 1-8.

XU, P., LI, L., ZHANG, F., STEPHANOPOULOS, G. & KOFFAS, M. 2014a. Improving fatty acids production by engineering dynamic pathway regulation and metabolic control. *Proceedings of the National Academy of Sciences of the United States of America,* 111**,** 11299-11304.

XU, P., RANGANATHAN, S., FOWLER, Z. L., MARANAS, C. D. & KOFFAS, M. A. G. 2011. Genome-scale metabolic network modeling results in minimal interventions that cooperatively force carbon flux towards malonyl-CoA. *Metabolic Engineering,* 13**,** 578-587.

XU, P., WANG, W., LI, L., BHAN, N., ZHANG, F. & KOFFAS, M. A. 2014b. Design and kinetic analysis of a hybrid promoter-regulator system for malonyl-CoA sensing in *Escherichia coli*. *ACS Chem Biol,* 9**,** 451-8.

YANG, Y. P., LIN, Y. H., LI, L. Y., LINHARDT, R. J. & YAN, Y. J. 2015. Regulating malonyl-CoA metabolism via synthetic antisense RNAs for enhanced biosynthesis of natural products. *Metabolic Engineering,* 29**,** 217-226.

YAO, J. & LAMBOWITZ, A. A. 2007. Gene targeting in gram-negative bacteria by use of a mobile group II intron ("targetron") expressed from a broad-host-range vector. *Applied and Environmental Microbiology,* 73**,** 2735-2743.

YAO, Z. Z., DAVIS, R. M., KISHONY, R., KAHNE, D. & RUIZ, N. 2012. Regulation of cell size in response to nutrient availability by fatty acid biosynthesis in *Escherichia*

coli. *Proceedings of the National Academy of Sciences of the United States of America,* 109**,** E2561-E2568.

YIM, H., HASELBECK, R., NIU, W., PUJOL-BAXLEY, C., BURGARD, A., BOLDT, J., KHANDURINA, J., TRAWICK, J. D., OSTERHOUT, R. E., STEPHEN, R., ESTADILLA, J., TEISAN, S., SCHREYER, H. B., ANDRAE, S., YANG, T. H., LEE, S. Y., BURK, M. J. & VAN DIEN, S. 2011. Metabolic engineering of *Escherichia coli* for direct production of 1,4-butanediol. *Nature Chemical Biology,* 7**,** 445-452.

YU, B. J., KANG, K. H., LEE, J. H., SUNG, B. H., KIM, M. S. & KIM, S. C. 2008. Rapid and efficient construction of markerless deletions in the Escherichia coli genome. *Nucleic Acids Research,* 36.

YU, D. G., ELLIS, H. M., LEE, E. C., JENKINS, N. A., COPELAND, N. G. & COURT, D. L. 2000. An efficient recombination system for chromosome engineering in Escherichia coli. *Proceedings of the National Academy of Sciences of the United States of America,* 97**,** 5978-5983.

YU, J. 2014. Bio-based products from solar energy and carbon dioxide. *Trends in Biotechnology,* 32**,** 5-10.

ZAREI, M., ATAEI, S. A. & FAZAELIPOOR, M. H. 2013. Regulation of Metabolic Pathway of Polyhydroxyalkanoates Production Using Reducing Agents. *World Applied Sciences Journal,* 21**,** 244-249.

ZHA, W. J., RUBIN-PITEL, S. B., SHAO, Z. Y. & ZHAO, H. M. 2009. Improving cellular malonyl-CoA level in *Escherichia coli* via metabolic engineering. *Metabolic Engineering,* 11**,** 192-198.

ZHANG, J., JENSEN, M. K. & KEASLING, J. D. 2015. Development of biosensors and their application in metabolic engineering. *Curr Opin Chem Biol,* 28**,** 1-8.

ZHANG, Y. M., BUCHHOLZ, F., MUYRERS, J. P. P. & STEWART, A. F. 1998. A new logic for DNA engineering using recombination in Escherichia coli. *Nature Genetics,* 20**,** 123-128.

ZHANG, Y. M., WHITE, S. W. & ROCK, C. O. 2006. Inhibiting bacterial fatty acid synthesis. *J Biol Chem,* 281**,** 17541-4.

ZHONG, J., KARBERG, M. & LAMBOWITZ, A. M. 2003. Targeted and random bacterial gene disruption using a group II intron (targetron) vector containing a retrotransposition-activated selectable marker. *Nucleic Acids Research,* 31**,** 1656-1664.